Impact of Hyperbilirubinaemia on Cholesterol Metabolism and Bioenergetics

Author

Vidimce, Josif

Published

2020

Thesis Type

Thesis (PhD Doctorate)

School

School of Medical Science

DOI

10.25904/1912/542

Impact of Hyperbilirubinaemia on Cholesterol Metabolism and Bioenergetics

Josif Vidimce

BPharmSci (Hons)

School of Medical Science

Griffith Health

Griffith University

Submitted in fulfilment of the requirements of the degree of Doctor of Philosophy

March 2020

Dedicated to my loving mother and father, Jagoda and Mihail Vidimce. Thank you for your unconditional love and support throughout my life.

General Abstract

Bilirubin is a haem catabolite that is excreted through the hepatobiliary pathway and is therefore, commonly used as a biomarker of hepatic dysfunction and haemolysis in the clinical setting [1]. Although, bilirubin has been considered toxic [2], recent evidence suggests that mildly elevated circulating bilirubin concentrations may be protective against obesity, cardiovascular diseases (CVDs) and all-cause mortality [3–5]. Generally, the protective effects of bilirubin are attributed to its antioxidant potential [6–8], however, recent studies demonstrate that bilirubin modulates lipid metabolism and reduces adiposity, which could partly contribute to CVD protection [5,9–12]. However, a shortage of studies have examined the precise mechanisms of cholesterol metabolism and adiposity that could be affected by bilirubin. The main aims of this thesis were to: 1) determine whether hyperbilirubinaemia affects cholesterol synthesis, transport, and excretion; 2) explore bilirubin's impact on body composition and bioenergetics including mitochondrial function in liver/skeletal muscle and changes in mitochondrial density and quality; 3) determine the effectiveness of oral Legalon® ingestion on circulating bilirubin concentrations, to investigate whether inducing mild hyperbilirubinaemia could impact circulating lipid concentrations in human participants.

The first study measured the effect of hyperbilirubinaemia in mutant Gunn rats on circulating lipid concentrations, cholesterol synthesis, lipid excretion, and expression of hepatic genes/proteins involved in cholesterol metabolism. Female hyperbilirubinaemic (Gunn) rats had reduced serum cholesterol concentrations (0.60 ± 0.12 vs 1.56 ± 0.34 mM, $P<0.001$), elevated cholesterol synthesis (33.8 ± 3.77 vs 28.4 ± 5.73 % [^{13}C]-cholesterol, $P<0.05$), enhanced LDL receptor (LDLr; $P<0.01$) expression, and increased biliary cholesterol excretion (232 ± 32.7 vs 141 ± 42.1 nmol hr^{-1} $100g^{-1}$ bodyweight, $P<0.001$) compared to female normobilirubinaemic littermate (control) rats. These results indicate that female hyperbilirubinaemic Gunn rats have reduced circulating cholesterol in association with elevated LDLr expression. Increased LDLr expression and cholesterol synthesis is typical when hepatic cholesterol concentrations are

decreased [13,14]. Therefore, increased cholesterol synthesis and LDLr expression observed in female Gunn rats may represent a counter-regulatory mechanism to maintain hepatic cholesterol content in the presence of elevated biliary cholesterol excretion [13,14].

The underlying mechanism explaining increased biliary lipid excretion in female Gunn rats remains unknown. However, this observation could be partly explained by greater relative biliary lipid (cholesterol+phospholipid) to bile acid excretion (0.33 ± 0.06 vs 0.24 ± 0.03 mol:mol, lipid:bile acids, $P<0.01$) in female Gunn rats. Previous studies have established that organic anions including bilirubin glucuronides disrupt the capacity of bile acid micelles to excrete lipids in the bile [15]. Biliary excretion of bilirubin conjugates was decreased in female (13.1 ± 2.92 vs 33.5 ± 5.09 nmol hr^{-1} $100g^{-1}$ bodyweight, $P<0.001$) and male (11.0 ± 2.43 vs 43.2 ± 12.8 nmol hr^{-1} $100g^{-1}$ bodyweight, $P<0.001$) Gunn rats compared to controls, due to UGT1A1 dysfunction and the inability to conjugate bilirubin. Therefore, decreased biliary excretion of bilirubin conjugates, as observed in Gunn rats, may potentially facilitate the greater coupled excretion of biliary lipids to bile acids as demonstrated in this study.

It should be noted that this conclusion does not completely explain the results reported here because Gunn rats demonstrated significant sexual dimorphism in cholesterol metabolism. Male Gunn rats exhibited a non-significant reduction in circulating cholesterol concentrations (1.41 ± 0.15 vs 1.56 ± 0.23, $P=0.14$) and increased biliary lipid:bile acid excretion (0.31 ± 0.07 vs 0.25 ± 0.04 mol:mol, lipid:bile acid, $P=0.08$) compared to male normobilirubinaemic littermate (control) rats, indicating that additional mechanisms, beyond bilirubin excretion, are involved. For example, UGT1A1, which conjugates bilirubin also conjugates and facilitates the excretion of sex hormones including oestrogen. Therefore, oestrogen concentrations may be elevated in female hyperbilirubinaemic rats and synergistically impact lipid metabolism [16,17].

The second study examined the effect of hyperbilirubinaemia *in vitro* and *in vivo* on mitochondrial function and body composition. Dual X-ray absorptiometry (DEXA) analysis revealed that female Gunn rats had significantly reduced fat mass (9.94 ± 5.35 vs 16.1 ± 6.65 g,

P<0.05) and lean mass (140 ± 12.1 vs 160 ± 16.0 g, P<0.05) compared to littermate controls. Female Gunn rats consumed fewer calories per day (54.1 ± 6.38 vs 63.3 ± 6.95 kcal day^{-1}, P<0.01). However, weight gain relative to calories consumed was reduced (8.09 ± 5.75 vs 14.9 ± 5.10 mg $kcal^{-1}$, P<0.05) in female Gunn rats indicating that they are less energetically efficient. This led to the analysis of mitochondrial function in liver and skeletal muscle using high-resolution respirometry to ascertain the cause of reduced energetic efficiency. This analysis revealed that female Gunn rats exhibited increased oxidative phosphorylation (OXPHOS) relative to maximal noncoupled mitochondrial respiration (ETS) in hepatic mitochondria (0.78 ± 0.16 vs 0.62 ± 0.09 OXPHOS:ETS, P<0.05).

The above findings were consistent with the effect of exogenous addition of unconjugated bilirubin (UCB) to control hepatic mitochondria, with 31.3 and 62.5 µM UCB increasing the OXPHOS: ETS ratio. However, exogenous UCB addition produced this effect by inhibiting ETS without affecting OXPHOS, indicating that UCB induces mitochondrial dysfunction at high concentrations. Conversely, no change in ETS (1130 ± 217 vs 1290 ± 373 pmol s^{-1} ng^{-1} citrate synthase (CS), P=0.16) or OXPHOS (901 ± 222 vs 796 ± 259 pmol s^{-1} ng^{-1} CS, P=0.36) was observed between female Gunn rats and controls. These data indicate that the greater OXPHOS:ETS ratios are a combination of increased OXPHOS and decreased ETS in female Gunn rats. Analysis of mitochondrial respiratory complexes revealed greater hepatic mitochondrial complex IV (CIV; P<0.01) expression in female Gunn rats. These findings support a conclusion that hepatic mitochondria have increased quality in female Gunn rats [18,19]. At present it remains unknown how this change in mitochondrial quality relates to reduced fat mass and energetic efficiency, however, the changes observed in female Gunn rats could represent an adaptation to bilirubin mediated inhibition of CIV as reported *in vitro* [20,21]. Otherwise, alterations in reproductive hormone metabolism in Gunn rats could also partially explain altered energetic states, as speculated in study one.

Considering that hyperbilirubinaemia induced perturbed lipid metabolism and body composition in chapters one and two, study three sought to determine whether increasing bilirubin could alter circulating lipid profile in humans. The effect of Legalon®, containing the active ingredient silymarin, supplementation on circulating bilirubin concentrations and lipid status was investigated in a placebo controlled, single blind crossover clinical trial in healthy individuals (ACTRN12619001296123). Legalon® capsules containing 140 mg of silymarin were supplemented thrice daily (total dose of 420 mg silymarin) in a cohort of healthy males for two weeks. Two weeks of Legalon® supplementation did not change UCB concentrations compared to baseline (Legalon®: 12.5 ± 7.63 vs Baseline: 11.4 ± 4.14 μM, P=0.79). Secondary outcomes including lipid concentrations, inflammation, and total antioxidant status were also reported. Two weeks of Legalon® supplementation did not change serum cholesterol (4.80 ± 1.00 vs 4.88 ± 1.00 mM, P=0.19), triglyceride (1.07 ± 0.63 vs 1.04 ± 0.54 mM, P=0.79), C-reactive protein concentrations (1.74 ± 1.88 vs 0.92 ± 0.87 mg L^{-1}, P=0.23) or serum antioxidant capacity (1194 ± 182 vs 1183 ± 201 mmol Fe^{2+} L^{-1}, P=0.19) compared to baseline. Several clinical trials evaluating the impact of silymarin have reported changes to bilirubin concentrations following treatment [22–24]. However, these studies were conducted in patients with hepatic disease, which confounded bilirubin results, and with greater doses or different formulations of silymarin to that reported in this thesis. Although the results of this study demonstrated a negative finding, they are important because they represent the first attempt to use an orally administered, commercially approved, nutraceutical compound to increase bilirubin. These results provide important guidance to future studies that could utilise different doses or commercial preparations to induce a transient unconjugated hyperbilirubinaemia and test the impact on circulating cholesterol concentrations.

In conclusion, this thesis contains three novel investigations that aimed to determine the impact of unconjugated hyperbilirubinaemia on cholesterol metabolism, synthesis and hepatic excretion; in addition to its effect on mitochondrial metabolism and body composition in Gunn rats. To determine whether these effects could be induced in humans, a nutraceutical with

documented effects on circulating bilirubin was administered in a clinical trial, utilising a randomised, single-blind, crossover design. The results of this thesis suggest that bilirubin has the potential to modulate lipid and whole-body metabolism, particularly in female animals and provides the groundwork for additional studies that seek to reveal the mechanisms responsible for bilirubin's effects. In addition, this thesis will support the discovery of more effective orally administered compounds that can modulate circulating bilirubin and lipid profile for protection against CVD.

Statement of Originality

This work has not previously been submitted for a degree or diploma in any university. To the best of my knowledge and belief, the thesis contains no material previously published or written by another person except where due reference is made in the thesis itself.

(Signed)_____ 16th March 2020

Josif Vidimce
PhD Candidate
School of Medical Science, Griffith University

Table of Contents

List of Figures

List of Tables

List of Abbreviations

ABC	ATP binding cassette
ACAT1	acyl-CoA:cholesterol acyltransferase 1
ADP	adenosine diphosphate
AHA	American Heart Association
Ahr	aryl hydrocarbon receptor
AKR1D1	Δ4–3-oxosteroid-5β-reductase
AMP	adenosine monophosphate
AMPK	adeonsine monophosphate-activated protein kinase
ANGII	Angiotensin 2
Apo	Apolipoprotein
ApoE -/-	Apolipoprotein E knockout
ASBT	apical sodium bile acid transporter
ATP	adenosine triphosphate
BAAT	*N*-acyltransferase
BMI	body mass index
BMR	Basal metabolic rate
BRDT	Bilirubin ditaurate
BSEP	bile salt export pump
BSTFA	N,O-Bis (trimethylsilyl) trifluoroacetamide
BV	Biliverdin
BVR	Biliverdin reductase
CA	cholic acid
CAD	Coronary artery disease
CDCA	Chenodeoxycholic acid
CETF	electron-transferring flavoprotein complex
CETP	cholesteryl ester transfer protein
cGPDH	glycerol-3-phosphate dehydrogenase
CHD	Coronary heart disease
CI	NADH-CoQ oxidoreductase
CII	succinate CoQ oxidoreductase
CIII	$CoQH_2$-cytochrome c oxidoreductase
CIV	cytochrome c oxidase
CM	chylomicron
CMR	chylomicron remnant
CO	Carbon Monoxide
CoQ	coenzyme Q
CV	ATP synthase
CVD	Cardiovascular disease
CYP27A1	sterol 27-hydrolase
CYP7A1	Cholesterol 7 alpha-hydroxylase
CYP7B1	oxysterol 7α-hydroxylase
CYP8B1	sterol 12-alpha-hydroxylase
DAP	dihydroxyacetone phosphate
DNP	2,4-dinitrophenol
E3S	estrone-3-sulfate
EDL	Extensor digitorum longus
eNOS	Endothelial-type NO synthase

ER	oestrogen receptor
ETC	electron transport chain
ETF	electron transfer flavoprotein
$FADH_2$	flavin adenine dinucleotide
Fe2+	Iron
FGF15	fibroblast growth factor 15–JUN N-terminal kinase
FH	Familial hypercholesterolemia
G3P	glycerol-3-phosphate
GGOH	isoprenoid geranylgeraniol
GS	Gilbert's Syndrome
GS/MS	gas chromatography mass spectrometry
Gunn	Rats with genetic unconjugated hyperbilirubinaemia
hCG	human chorionic gonadotropin
HCV	hepatitis C viral infections
HDL	High-density lipoprotein
HFD	high fat diet
HMGCR	3-hydroxy-3-methylglutaryl coenzyme A reductase
HNF-4α	hepatocyte nuclear factor-4α
HO-1	Haem-Oxygenase-1
i.p.	intraperitoneal injection
ICAM	intercellular adhesion molecule
IDL	intermediate density lipoprotein
IHD	Ischemic heart disease
IL-10	Interleukin 10
IMT	Intima-media thickness
iNOS	Inducible nitric oxide synthase
INSIG	insulin-induced gene protein
IR	Ischemia reperfusion
KLF2	Kruppel-like factor 2
LCAT	lecithin-cholesterol acyltransferase
LDL	Low density lipoprotein
LDL-C	Low density lipoprotein cholesterol
LDLr	Low density lipoprotein receptor
LDLr -/-	Low density lipoprotein receptor knockout
LDs	lipid droplets
LPL	lipoprotein lipase
LRH-1	liver receptor homolog 1
LRP	lipoprotein receptor-related proteins
LXR	liver X receptor
MCP-1	monocyte chemoattractant protein-1
MCSF	Macrophage colony stimulating factor
Mdr	multidrug resistance P-glycoprotein
MI	Myocardial infarct
MRP2	multidrug resistance-related protein-2
MTTP	microsomal triglyceride transfer protein
NADH	nicotinamide adenine dinucleotide
NF-kB	Nuclear factor kB
NOX	NADPH oxidase
NPC1L1	Niemann–Pick C1-like 1
NPC2	Niemann-Pick C2

Nrf2	Nuclear factor erythroid 2-related factor-2
NTCP	Na^+/taurocholate co-transporting polypeptide
O_2	molecular oxygen
OR	odds ratio
oxLDL	Oxidatively modified LDL
PGC-1α	peroxisome proliferator-activated receptor gamma coactivator 1-alpha
pmf	protonmotive force
PPAR	Peroxisome proliferator-activated receptor
RBCs	Red Blood Cells
RCT	reverse cholesterol transport
ROS	Reactive oxygen species
RR	Relative risk
RT	Room temperature
RXR	retinoid X receptor
SCAP	SREBP cleavage activating protein
SHP	small heterodimer partner
SR-B1	scavenger receptor B1
SREBP	Sterol regulatory element-binding protein
statins	HMG CoA reductase inhibitors
T2DM	Type 2 diabetes mellitus
TCA	taurocholic acid
TCA cycle	tricarboxylic acid cycle
TGFβ	transforming growth factor beta
TICE	transintestinal cholesterol efflux
TLR	Toll-like receptors
TR	thyroid hormone receptor
UCB	unconjugated bilirubin
UCP	family of uncoupling proteins
UGT1A1	UDP-glycosyltransferase 1A1
VCAM-1	Vascular cell adhesion molecule 1
VLDL	very low-density lipoprotein
VO_{2max}	maximal aerobic capacity
VSMCs	Vascular smooth muscle cells

Acknowledgements

I would first like to sincerely thank my primary supervisor Associate Professor Andrew Bulmer. Thank you for your encouragement, guidance, and training throughout my candidature. Thank you also for providing research funding for the studies conducted in this thesis. Without your support I would not have been able to complete my PhD and I am very thankful. Throughout your supervision I have gained invaluable skills and knowledge on how to be scientist and a professional. I am very appreciative for your mentorship and for always trying to be the best supervisor that you can be. So, once again thank you everything and I wish you and your lab group much more success for the future.

Next, I want to thank other academics that have played a significant part in my candidature. I would like to thank Professor Henkjan Verkade, Onne Ronda and Dr. Theo H. van Dijk for all their support and assistance around the research conducted on cholesterol metabolism, their involvement has been critical to this area of the thesis. I would like to thank Dr. Olivia Holland and Dr. Lan-feng Dong for their training and guidance around mitochondrial function, their help has been invaluable to my success in this area. I would like to thank Dr. Christina Bursill for her external support particularly in the area of atherosclerosis. I would like to thank Professor John Headrick for his co-supervision for this thesis. Finally, I would like to thank Associate Professor Eugene Du Toit and Associate Professor Jason Peart for always being approachable and providing guidance along the way.

To Mr Ryan Shiels, your friendship has been a big positive part of my PhD experience. I want to thank you for always being there for me when I needed your support and for your genuine care and encouragement. You have truly been like a big brother to me throughout this experience and I will forever appreciate our friendship. Moreover, I want to thank you for always offering to help with my research problems regardless whether you were busy or not in the mood, and I really appreciate it. Lastly, I want to commend your creativity as a scientist. Throughout your PhD you have thought of and utilised many creative solutions beyond what I have seen from

anyone else. Even though I often make fun of you for doing this, I think that this is one of your strongest qualities and you should continue cultivating this ability as the world needs more creative people.

To Mr Yaman Tayyar, one of the highlights of my PhD has been meeting you and becoming friends. Even though we know each other for a short time, I feel like we have been friends for a lifetime. I feel this way because you have been a great friend with a great sense of humour who is always supportive and willing to help. I also want to compliment your ability to think about things deeply, I think it's a very important quality for science and I think you have the ability to become a great scientist. So, I want to sincerely thank you for being a great friend and being part of my PhD experience and wish you all the best in your PhD journey.

To Mr Evan Pennell, it has been great doing our PhDs as part of the same research group and sharing the same office. I personally admire your work ethic, you have put in a lot of work and have done a great job throughout your PhD. I also want to thank you for being a great friend and research colleague. You have always been very kind and helpful both scientifically and as a friend. Together with Ryan you guys have made my PhD experience easier and much more pleasant so I would like to wish you all the best for the future.

To Miss Johara Pillay, it was a pleasure working together during my PhD. Your great sense of humour and kindness made it easy to work together and made my experience much more pleasurable. Also, your assistance was critical to the successful completion of our projects and I appreciate all your hard work. So, I want to thank you for being a friend and part of my PhD experience, and I wish you all the very best in the future.

A special thank you also goes to friends and colleagues that have played a part in my PhD thesis. I would like to thank Carlo Alimboyong, Mylee Suarna, Maddy Dallow, Marko Simunovic, Ally Hawthorn, Wenu, Jarrod Horobin, Lana Bivol, Emiri, Tessa, Sura, and Calvin for their support, help, and encouragement throughout my PhD.

To my girlfriend Iuliia Ri, thank you for being the most amazing girlfriend anyone could ask for. I know that I am not always easy nor pleasant to be around especially when I have been stressed because of this PhD. Yet you were always there for me unconditionally trying to help in whatever way that you can. So, from the bottom of my heart I want to thank you and tell you that I really appreciate everything you have done for me. Love you moje bebće!

Finally, I want to thank my family for their unconditional support during my PhD. I would like to thank my brother Stefan Vidimce for being the best big brother I can hope for. Thank you for putting up with all my complaining and being supportive at the same time. I could always rely on you to give me words of encouragement and support whenever I needed it. You are a great role model and I am thankful to have you as my brother and I will always appreciate the things you have done for me. I also want to thank my parents Jagoda and Mihail Vidimce, for always caring and supporting me throughout this process, your love is all a son can ask for. Love you!

Publications During Candidature

Published studies as a co-author

Shiels, RG, **Vidimce, J**, Pearson, AG, Matthews, B, Wagner, KH, Battle, AR, Sakellaris, H, and Bulmer, AC. Unprecedented Microbial Conversion of Biliverdin into Bilirubin-10-sulfonate. *Sci Rep* **9,** 2988 (2019).

Pennell EN, Shiels R, **Vidimce J**, Wagner KH, Shibeeb S, and Bulmer AC. The impact of bilirubin ditaurate on platelet quality during storage. *Platelets* 00, 1–13 (2019).

Manuscripts under review at the time of thesis submission

Vidimce J, Pennell EN, Foo M, Shiels RG, Shibeeb S, Watson M, and Bulmer AC. The effect of Legalon®(Silymarin) treatment on circulating bilirubin concentrations and markers of cardiovascular disease in healthy men: randomised crossover single blind clinical trial. Submitted to journal of *Complementary Therapies in Medicine*.

Shiels, RG, Hewage, W, **Vidimce, J**, Pearson, AG, Wagner, K-H, and Bulmer, AC. Pharmacokinetics of bilirubin-10-sulfonate and biliverdin: unlocking the therapeutic potential of a novel antioxidant formed by the enteric microbiome. Submitted to *European Journal of Pharmaceutical Science.*

Shiels, RG, Hewage, W, Pennell, EN, **Vidimce, J**, Grant, G, Pearson, AG, Wagner, K-H, Morgan, M, and Bulmer, AC. Biliverdin and bilirubin sulfonate inhibit monosodium urate induced sterile inflammation in the rat. Submitted to *European Journal of Pharmaceutical Science.*

Conference abstracts

Vidimce, **J**, Pillay, J, Dong, L, Neuzil, J, Holland, OJ, and Bulmer, AC. Hyperbilirubinaemia is associated with perturbed mitochondrial function and reduced fat mass. *9th meeting of the International Conference for The Society for Free Radical Research Australasia (SFRRA)*, Sydney (2019).

Vidimce, J, Pillay, J, Ronda, O, Boon, AC, Dijk, TH, Wagner, KH, Verkade, HJ, and Bulmer, AC. Hyperbilirubinaemia in female Gunn rats is associated with lower circulating cholesterol, increased LDL receptor expression and biliary cholesterol excretion. *Annual Conference of the Australian Atherosclerosis Society*, *ASM*, Melbourne (2019).

Boon, AC, **Vidimce, J**, and Bulmer, AC. Hepatic gene expression analysis reveals perturbed cholesterol metabolism in the hyperbilirubinaemic Gunn rat. *Annual Health and Medical Research Conference*, Gold Coast (2015).

ALL PAPERS INCLUDED ARE CO-AUTHORED

Acknowledgement of Papers included in this Thesis

Section 9.1 of the Griffith University Code for the Responsible Conduct of Research ("Criteria for Authorship"), in accordance with Section 5 of the Australian Code for the Responsible Conduct of Research, states:

To be named as an author, a researcher must have made a substantial scholarly contribution to the creative or scholarly work that constitutes the research output, and be able to take public responsibility for at least that part of the work they contributed. Attribution of authorship depends to some extent on the discipline and publisher policies, but in all cases, authorship must be based on substantial contributions in a combination of one or more of:

- conception and design of the research project
- analysis and interpretation of research data
- drafting or making significant parts of the creative or scholarly work or critically revising it so as to contribute significantly to the final output.

Section 9.3 of the Griffith University Code ("Responsibilities of Researchers"), in accordance with Section 5 of the Australian Code, states:

Researchers are expected to:

- Offer authorship to all people, including research trainees, who meet the criteria for authorship listed above, but only those people.
- accept or decline offers of authorship promptly in writing.
- Include in the list of authors only those who have accepted authorship
- Appoint one author to be the executive author to record authorship and manage correspondence about the work with the publisher and other interested parties.
- Acknowledge all those who have contributed to the research, facilities or materials but who do not qualify as authors, such as research assistants, technical staff, and advisors on cultural or community knowledge. Obtain written consent to name individuals.

Included in this thesis are papers in *Chapter 5* which are co-authored with other researchers. My contribution to each co-authored paper is outlined at the front of the relevant chapter. The bibliographic details (if published or accepted for publication)/status (if prepared or submitted for publication) for these papers including all authors, are outlined at the start of each chapter.

(Where a paper(s) has been published or accepted for publication, you must also include a statement regarding the copyright status of the paper(s).

Chapter 5: Submitted to journal of *Complementary Therapies in Medicine* as an original research manuscript. I, the primary and corresponding author, retain the right to include under Personal Use copyrights.

Appropriate acknowledgements of those who contributed to the research but did not qualify as authors are included in each paper.

(Signed) _____ (Date)__19th March 2020_

PhD Candidate
Josif Vidimce

(Countersigned) _____ (Date)_19th March 2020_

Primary Supervisor
Associate Professor Andrew Bulmer

Chapter 1: General Introduction

1.1 Background and Project Significance

Cardiovascular diseases (CVDs) are the leading cause of death globally and are responsible for 31% of all deaths, equating to 17.9 million in 2016 [World Health Organisation; WHO]. CVDs comprise several different conditions of which, coronary heart disease (CHD), heart failure and cerebrovascular disease (stroke) have the greatest impact in terms of incidence, prevalence, quality of life, and fiscal costs [WHO] [25,26]. Similarly, obesity is one of the main public health challenges of the 21st century with more than a third of all adults around the world classified as overweight or obese, and this is expected to increase [WHO]. Obese individuals are much more likely to suffer from chronic diseases including CVDs, therefore, the increasing prevalence of obesity threatens to increase morbidity and mortality, globally [27]. While obesity is largely preventable through lifestyle changes, public health measures have been unsuccessful in curbing the rise in obesity prevalence [28]. Therefore, pharmacological interventions are essential to aid public health measures in fighting the obesity epidemic [28]. One major risk factor associated with obesity is the development of metabolic syndrome, which includes multiple co-morbidities that promote atherogenesis and the risk of death from CVDs [27].

A critical underlying pathology that leads to many cardiovascular fatalities, is atherosclerosis. Atherosclerosis is a slowly progressing, chronic inflammatory disease characterised by a gradual build-up of lipid laden plaques in the intimal lining of large and medium-sized arteries, which can lead to major adverse cardiac events [29,30]. High circulating cholesterol represents a critical precursor to the initiation and progression of atherosclerosis [31,32], with systemic inflammation also intricately linked to the progression of this condition [33]. Obesity has the potential to increase circulating cholesterol concentrations and promote systemic inflammation, therefore, predisposing individuals to atherosclerosis [34]. Most clinically available treatments that slow or aim to treat atherosclerosis reduce cholesterol production and the circulating low-density lipoprotein (LDL) cholesterol concentration. The hallmark of the cholesterol-reducing class of drugs are the 3-hydroxy-3-methylglutaryl coenzyme A reductase (HMGCR) inhibitors

(statins), which inhibit HMGCR, the rate-limiting enzyme of cholesterol synthesis [35]. Despite their impressive capacity to lower circulating LDL cholesterol, several problems with statins exist as they are only moderately (20-40%) effective in reducing the clinical manifestations of atherosclerosis [36], and can induce side effects, including myopathy, in 10-15% of patients [37]. Although, elevated LDL cholesterol likely represents a critical factor that initiates atherosclerosis, the generation of reactive oxygen species (ROS) and inflammation are also intricately involved in the progression of this disease [38–41]. This observation may provide an explanation for why lipid-reducing treatments do not completely prevent CVD, because they do not directly affect ROS production or inflammation.

Therefore, an important need remains for a treatment that improves upon the efficacy of cholesterol-lowering therapeutics by inhibiting ROS production and inflammation. A treatment that could target the triad (cholesterol, ROS and inflammation) of atherosclerosis would potentially yield far greater effectiveness in preventing the clinical manifestations of CVD and could save millions of lives globally [40–42]. One such molecule with therapeutic potential is bilirubin. Bilirubin is a haem catabolite that is primarily excreted through the hepatobiliary route [43]. A growing body of evidence suggests that bilirubin is a potent antioxidant with lipid reducing and anti-obesogenic potential [3,8]. For instance, several cross-sectional studies report that mildly elevated circulating bilirubin is associated with reduced body mass index (BMI), cholesterol, and protection against CVD and all-cause mortality [3–5,12,44]. However, very little is understood concerning the mechanisms underlying these relationships. Therefore, this thesis aimed to determine the effects of bilirubin on cholesterol metabolism, body composition, and bioenergetics in hyperbilirubinaemic rats; and aimed to test the effectiveness of oral Legalon® supplementation on circulating bilirubin, lipid, and inflammatory biomarker concentrations in a human clinical trial, to determine whether bilirubin's effects in rodents could be translated into humans.

1.2 Aims and Hypotheses

Study 1

This study aimed to measure and compare the *in vivo* rate of cholesterol synthesis, biliary lipid excretion, and gene/protein expression of molecules involved in cholesterol metabolism between hyperbilirubinaemic Gunn and normobilirubinaemic (control) rats. Animals' drinking water was supplemented with [^{13}C]-acetate, a metabolic precursor to cholesterol, and analysis of isotopomer distribution of [^{13}C]-cholesterol species was conducted to determine the rate of *in vivo de* novo cholesterol synthesis. Biliary lipid excretion was determined by cannulating the common bile duct and collecting bile for 30 mins. Statistically significant changes in these measurements were supported by gene (PCR array) and protein (Western Blot) expression analysis of liver tissue, targeting the mevalonate pathway of cholesterol synthesis. It was hypothesised that hyperbilirubinaemic animals would demonstrate reduced cholesterol synthesis and elevated biliary lipid excretion.

Study 2

The aim of this study was to examine the effect of hyperbilirubinaemia on body composition and bioenergetics in rats. Body composition was assessed using dual energy X-ray absorptiometry (DEXA) and by dissecting and weighing different organs and muscle from adult hyperbilirubinaemic Gunn and normobilirubinaemic control rats. Bioenergetics were assessed by measuring mitochondrial function of liver tissue and skeletal muscle using high-resolution respirometry and by measuring bodyweight change and food consumption over 20 days. Any changes in bioenergetics were supported by protein expression of hepatic pAMPK:AMPK and mitochondrial respiratory complexes. Overall, these measurements allowed for an evaluation of body composition and whether this was associated with parameters of mitochondrial function. It was hypothesised that hyperbilirubinaemic Gunn rats would have reduced fat mass and greater rate of uncoupled mitochondrial respiration.

Study 3

The aim of this study was to examine the effects of an oral milk thistle extract, silymarin (Legalon®; 420 mg daily for two weeks), on circulating bilirubin concentrations, plasma antioxidant capacity, inflammation, and lipid concentrations in healthy male human participants. The study design was a prospective, single blind, randomised crossover placebo-controlled clinical trial. Circulating unconjugated bilirubin (UCB) concentrations were measured after one and two weeks of oral supplementation with Legalon® or placebo, using high performance liquid chromatography (HPLC). Additional biochemistry analyses were conducted using commercially available kits on the COBAS Integra 400+. Antioxidant capacity was assessed using the ferric reducing ability of plasma (FRAP) assay while Inflammation was assessed by measuring serum C-reactive protein concentration. Finally, total cholesterol, high-density lipoprotein cholesterol (HDL-C), low-density lipoprotein cholesterol (LDL-C), and triglyceride concentrations were measured to assess lipid status. Collectively, these measurements established whether Legalon® supplementation affected circulating bilirubin concentrations and whether any changes in this parameter was associated with serum lipid concentrations, inflammation, and antioxidant capacity. It was hypothesised that Legalon® supplementation would increase circulating bilirubin concentrations (by >5 μM) and reduce lipid concentrations, inflammatory biomarkers, and increase antioxidant capacity compared to baseline and placebo.

1.3 Thesis structure

This thesis includes six chapters. Chapters 3, 4 and 5 each represent original experimental studies and are presented in manuscript format for future publication or are currently considered for publication.

Chapter 1

This chapter gives a general introduction of the thesis topic and the rationale, including aims and hypothesis, for the experimental studies conducted in this thesis.

Chapter 2

This chapter provides a review of the literature on mitochondrial function and its role in obesity, the pathophysiology of atherosclerosis and its relation to cholesterol metabolism. Additionally, this chapter reviews aspects of bilirubin biology and how bilirubin could impact cholesterol metabolism, obesity, and atherosclerosis. Finally, this chapter reviews pharmacological agents and nutraceuticals that affect bilirubin metabolism.

Chapter 3 – Study 1

This chapter presents the first experimental study: the impact of hyperbilirubinaemia on cholesterol metabolism. The rate of *in vivo* cholesterol synthesis, biliary lipid excretion, and the hepatic expression of genes/proteins involved in cholesterol metabolism were compared between hyperbilirubinaemic Gunn (mutated/dysfunctional UGT1A1 gene) and littermate normobilirubinaemic control (UGT1A1 competent) rats. The study demonstrated a strong sexually dimorphic effect of UGT1A1 function/hyperbilirubinaemia on cholesterol metabolism with female hyperbilirubinaemic rats demonstrating reduced circulating cholesterol concentrations, elevated cholesterol synthesis, and increased biliary lipid excretion.

Chapter 4 – Study 2

This chapter presents the second experimental study: the impact of hyperbilirubinaemia on body composition and bioenergetics. Body composition was evaluated using DEXA while mitochondrial function, pAMPK:AMPK ratios, and food consumption were measured to explore changes in bioenergetics utilising Gunn rats as conducted in Chapter 3. This study also discovered prominent sexually dimorphic effects with female hyperbilirubinaemic rats demonstrating reduced fat mass and improved mitochondrial quality.

Chapter 5 – Study 3

This chapter presents the final experimental study of this thesis: the impact of oral Legalon® supplementation on circulating bilirubin concentrations (primary outcome) in a single blind crossover placebo controlled clinical trial in healthy men. This study also reported circulating lipid status, markers of inflammation and serum antioxidant capacity (secondary outcomes). The impact of Legalon® was assessed after one and two weeks of supplementation, with results compared to baseline and placebo measurements. Legalon® supplementation failed to affect bilirubin, lipids, inflammation, or antioxidant capacity.

Chapter 6

This chapter discusses the overall findings from this thesis and how they impact the current understanding of this field. Additionally, this chapter provides suggestions for future studies that can add to the novel findings of this thesis.

1.4 Author Contributions to Experimental Chapters

Chapter 3

Mr Josif Vidimce:

- Study design, method development, and writing of ethics application
- Animal work including daily measurements and interventions and terminal procedures
- Planned, optimised and conducted all western blot experiments (exception CYP7A1)
- Provided training for the Western Blot measurement of CYP7A1
- Biochemistry analysis (bile, blood, and faecal samples)
- Conducted calculations on the rate of biliary lipid excretion
- Developed method for lipid extraction from liver and faecal samples
- Validated method and conducted the measurements for faecal cholesterol excretion
- Wrote the research chapter, conducted all final statistical analysis, and designed tables and figures

Associate Professor Andrew Bulmer contribution:

- Provided supervision of the research chapter
- Contributed to study design, method development, and writing of ethics application
- Critically reviewed research chapter and provided suggestions for the overall structure
- Assisted in interpretation of results and provided guidance on statistical methods

Assisted in terminal procedures and biochemical analysis Miss Johara Pillay contribution:

- Assisted in animal work (daily measurements, interventions and terminal procedures)
- Conducted troubleshooting and final Western Blot measurement of CYP7A1
- Validated method and measured hepatic lipid concentrations
- Assisted in biochemistry analysis

Professor Henkjan Verkade and Mr Onne Ronda (University of Groningen) contribution:

- Assisted in the planning of study design and method development
- Measured and calculated cholesterol synthesis and measured biliary bile acid species and biliary cholesterol concentrations.

Dr Ai-Ching Boon contribution:

- Conducted PCR array and calculated relative gene expression

Professor Karl-Heinz Wagner contribution:

- Provided funding for the research project

Professor John Headrick contribution:

- Critically reviewed the study chapter

Chapter 4

Mr Josif Vidimce contribution:

- Study design, method development, and writing of ethics application
- Animal work including daily measurements and interventions and terminal procedures
- Planned, optimised, and conducted all Western Blot measurements of mitochondrial respiratory complexes and citrate synthase activity
- Provided training for the Western Blot measurement of AMPK
- Conducted biochemistry analysis on blood
- Conducted all measurements of mitochondrial function using high-resolution respirometry
- Developed method and provided training for lipid extraction from liver tissue
- Wrote the research chapter, conducted all final statistical analysis, and designed tables and figures

Associate Professor Andrew Bulmer contribution:

- Provided supervision of the research chapter
- Contributed to study design, method development, and writing of ethics application
- Critically reviewed research chapter and provided suggestions for the overall structure
- Conducted DEXA scan measurements
- Assisted in interpretation of results and provided guidance on statistical methods
- Assisted in terminal procedures and biochemical analysis

Miss Johara Pillay contribution:

- Assisted with tissue collection and measurements using metabolic cages
- Conducted troubleshooting and Western Blot measurement of AMPK
- Validated method and measured hepatic lipid concentrations
- Assisted in biochemistry analysis

Dr Olivia Holland contribution:

- Provided training and guidance for the assessment of mitochondrial function and citrate synthase activity
- Provided general guidance and ideas to study design
- Critically reviewed aspects of study chapter

Dr Lan-feng Dong contribution:

- Provided training and guidance for the assessment of mitochondrial function
- Critically reviewed aspects of study chapter

Professor Jiri Neuzil contribution:

- Critically reviewed aspects of study chapter

Professor John Headrick contribution:

- Critically reviewed the study chapter

Chapter 5

Mr Josif Vidimce contribution:

- Assisted in study design and ethical approval
- Analytical experimental design, planning, development, and validation of analytical methods including COBAS Integra 400+ and HPLC
- Participant recruitment, screening and follow up
- Participant sample processing
- Conducted biochemistry analysis on COBAS Integra 400+ and HPLC
- Wrote the manuscript, conducted all final statistical analysis, and designed tables and figures and prepared for submission

Associate Professor Andrew Bulmer contribution:

- Provided supervision of the research chapter
- Study design, method development, and writing of ethics application
- Critically reviewed manuscript and provided suggestions for the overall structure
- Assisted in interpretation of results and provided guidance on statistical methods

Dr Mike Watson contribution:

- Study design and writing of ethics application
- Critically reviewed manuscript

Mr Evan Pennell contribution:

- Assisted in analytical experimental design, planning, development, and validation of analytical methods
- Acquisition of participant blood samples
- Assisted in acquisition of analytical data and statistical analysis
- Participant recruitment, screening and follow up
- Critically reviewed manuscript

Mr Maximillian Foo contribution:

- Assisted in acquisition of analytical data
- Acquisition of participant blood samples
- Participant recruitment, screening and follow up
- Critically reviewed manuscript

Dr Sapha Shibeeb contribution:

- Assessed screening data of participants and provided final approval
- Critically reviewed manuscript

Mr Ryan Shiels contribution:

- Method development of bilirubin measurement via HPLC
- Assisted in data acquisition of bilirubin measurement
- Critically reviewed manuscript

Chapter 2: Literature Review

This chapter provides an overall review of the literature regarding the epidemiology and causes of obesity and atherosclerosis. This is followed by an overview of mitochondrial physiology and cholesterol metabolism and how these aspects of biology impact obesity and atherosclerosis. Additionally, this chapter reviews the relationship between bilirubin and obesity/cardiovascular diseases and how bilirubin specifically impacts mitochondrial function, lipid metabolism, inflammation, and oxidative stress. Finally, a review of literature concerning existing medicines and nutraceuticals that impact bilirubin metabolism is provided.

2.1 Obesity and the Role of Mitochondria

2.1a Epidemiology and causes of obesity

Obesity is considered as one of the primary public health challenges of the 21st century. Over the last four decades the prevalence of obesity has rapidly grown and it is expected to continue growing into the future. Globally in 2016, 39% of people were classified as overweight which equates to almost 2 billion people with half a billion being obese worldwide [WHO]. The percentage is even greater in the developed world; in the US more than 68% of adults are overweight with 35% classified as obese [45]. This is a major health concern since obesity greatly increases risk of chronic disease including type 2 diabetes mellitus (T2DM), depression, dyslipidaemia, cancer, and atherosclerosis [27]. Consequently, the rise in obesity is leading to higher rates of mortality and morbidity, and threatens to reverse the upward trend in life expectancy around the world [27]. Therefore, urgent attention is needed from policy makers and the medical community to combat the obesity epidemic.

Obesity is simply classified as excess weight relative to height which is determined by the body mass index (BMI) [WHO]. Clinically, individuals with BMI of ≥30.0 kg/m^2 are classified as obese, however, this is only an indirect and imperfect measure of body fatness [46,47]. Obesity is the accumulation of excess adiposity that can also manifest itself as metabolic dysfunction. Long-term excess in energy consumption relative to energy expenditure (resting metabolic rate and physical activity) leads to obesity [46,48]. The aetiology of obesity is multifactorial and can be influenced, to varying degrees, by genetics, diet, physical activity, psychological wellbeing, social and economic factors. According to twin studies, genetics accounts for 40-70% of body fat, yet most of the global increase in the prevalence of obesity has occurred in the last four decades, a timespan too short for genetics to change [46,49]. Therefore, the most plausible explanation for the obesity epidemic is a change in the environment. Indeed, the recent decades has seen major technological upheaval that has made access to food cheaper while simultaneously reducing the need for physical activity [50]. In particular, calorie-dense food rich in fats and simple sugars has

drastically become cheaper while healthier alternatives have become more expensive in relative terms [50]. Consequently, a diet high in calorie-dense food and low fibre leads to overeating and a greater daily calorie intake for the average individual. Combined with decreasing physical activity, the difference between energy intake and energy expenditure has become positive for many individuals in the modern world [51,52]. The obvious approach to preventing obesity is to reduce calorie intake while increasing energy expenditure. Lifestyle changes such as calorie restriction and increasing physical activity can address both of these factors, however, these approaches will not be discussed further, and the reader is referred to several excellent reviews on this topic [28,53,54]. This review will evaluate the role of mitochondrial function in obesity and how pharmacological approaches can exploit this organelle to combat obesity.

2.1b The role of mitochondrial function in obesity

As mentioned previously, excessive adiposity is a result of excess energy consumption that is not compensated by increased energy expenditure. Energy expenditure is a function of physical activity, basal metabolic rate (BMR) and adaptive thermogenesis [50,55]. The oxidative phosphorylation capacity of mitochondria is a major determinant of daily energy expenditure and metabolic health. VO_{2max} is a measure of cardiorespiratory fitness which is determined by O_2 delivery mechanisms and the efficiency of O_2 utilisation by mitochondria in peripheral tissues, in particular, skeletal muscle [56]. The importance of mitochondrial capacity is highlighted by the negative relationship of cardiorespiratory fitness (e.g. VO_{2max}) and the risk for CVD, and all-cause mortality [57,58].

Indeed, mitochondrial dysfunction is a hallmark of metabolic diseases including obesity, and metabolic syndrome. For instance, mitochondrial content of white adipose tissue and oxidative phosphorylation capacity is reduced in obese subjects [59,60]. This is consistent with findings that demonstrate increased mitochondrial biogenesis and improved oxidative phosphorylation following exercise and calorie restriction [61,62]. Nevertheless, it remains controversial as to

whether mitochondrial dysfunction leads to obesity or whether excessive adiposity induces mitochondrial dysfunction [63].

2.1c Mitochondrial physiology

Mitochondria are the powerhouse of the cell where the majority of adenosine triphosphate (ATP) synthesis takes place. Beyond energy production, mitochondria are also vital for thermogenesis, fatty acid synthesis, Ca^{2+} homeostasis, and haem and iron-sulphur protein synthesis [55]. Food is decomposed to its smallest components, glucose, amino acids and fatty acids, prior to aerobic or anaerobic metabolism. Mitochondria are the functional and structural units of aerobic metabolism where metabolic energy and electrons from nutrient oxidation are used to produce ATP and to reduce molecular oxygen (O_2) into water (H_2O), respectively [64]. The electron transport chain (ETC) is composed of four membrane-bound complexes in the inner mitochondrial membrane and it carries out the function of aerobic respiration (Fig. 2.1). Electron donating molecules, nicotinamide adenine dinucleotide (NADH) and flavin adenine dinucleotide ($FADH_2$), produced from glycolysis, β-oxidation, and the tricarboxylic acid cycle (TCA cycle) transfer electrons to O_2 through a range of sequential oxidation-reduction reactions catalysed by the mitochondrial complexes [64]. The first complex, NADH-CoQ oxidoreductase (CI) and the second complex, succinate CoQ oxidoreductase (CII) oxidise NADH and succinate, respectively, and transfer these electrons to coenzyme Q (CoQ), producing a reduced form, $CoQH_2$. CII has a function in both the TCA cycle and the ETC. As part of the TCA cycle, CII oxidises succinate to produce fumarate and $FADH_2$, then $FADH_2$ is oxidised by CII as part of the ETC to reduce CoQ into $CoQH_2$ [64].

Additional electron-donating pathways to CoQ are mediated through the electron-transferring flavoprotein complex (CETF) and the glycerophosphate shuttle [65,66]. The CETF pathway constitutes an electron acceptor, electron transfer flavoprotein (ETF), and membrane-bound ETF:ubiquinone oxidoreductase found in the inner mitochondrial membrane. ETF accepts electrons from the first step of β-oxidation of fatty acids catalysed by acyl-CoA dehydrogenases

while ETF:ubiquinone oxidoreductase catalyses the transfer of electrons from ETF to CoQ to form $CoQH_2$ [65]. The glycerophosphate shuttle begins with oxidation of NADH by cytosolic glycerol-3-phosphate dehydrogenase (cGPDH) and the conversion of dihydroxyacetone phosphate (DAP) into glycerol-3-phosphate (G3P). G3P then translocates to the mitochondria where membrane-bound mitochondrial GPDH (mGPDH) converts G3P back to DAP and in the process generating $FADH_2$ from FAD. The electrons from $FADH_2$ are then transferred to CoQ to produce $CoQH_2$ [66]. Collectively, electron transfer to CoQ can originate from four independent pathways: CI, CII, CETF, and the glycerophosphate shuttle. Convergent electron flow into CoQ is known as the Q-junction of the ETC, consequently, many have argued that the ETC is better described as an electron transfer system because electron flow is not linear (from a single origin) as would be indicated by a chain [67].

$CoQH_2$ is a mobile membrane soluble carrier that transports electrons to the third complex, $CoQH_2$-cytochrome c oxidoreductase (CIII). CIII oxidises $CoQH_2$ back into CoQ and in this way CoQ is recycled and can participate again as an electron acceptor in the Q-junction [64,67]. The electrons from CIII are passed onto another membrane-soluble carrier, cytochrome c. Cytochrome c is a single electron carrier, hence, two molecules are needed for each CIII-mediated oxidation of $CoQH_2$ [64]. Complex four, cytochrome c oxidase (CIV), catalyses the final steps of the ETC by oxidising two cytochrome c molecules and reducing O_2 into H_2O, completing the electron transfer. The free energy produced by the electron transfer through the ETC, drives CI, CIII, and CIV, to transport protons (H^+) from the mitochondrial matrix and out into the intermembrane space [64]. The membrane is relatively impermeable to ions, thus, this process produces an electrochemical gradient that is known as the protonmotive force (pmf) [67,68].

The pmf arises from a difference in proton concentration (ΔpH) and charge (or membrane potential) between the mitochondrial intermembrane space and the matrix [67]. Under physiological conditions only a small proportion of protons re-enter the matrix via different uncoupling mechanisms while the rest cross the membrane through ion channels provided by

ATP synthase (CV). CV is bound to the inner mitochondrial membrane and in addition to its ion channel capacity, catalyses the phosphorylation of adenosine diphosphate (ADP) into ATP [64]. Therefore, while the protons flow down their electrochemical gradient through CV they release energy that is utilised for the phosphorylation of ADP into ATP [64]. This process is known as oxidative phosphorylation. Electron transfer through the ETC is an exergonic process that is highly coupled, though not completely, to oxidative phosphorylation (ATP synthesis; an endergonic process) [67].

During low demand and high supply of ATP, the rate of ATP synthesis is reduced leading to a rise in the pmf [55]. A high pmf attenuates electron transfer because the ETC has insufficient energy to pump protons against a stronger electrochemical force [68]. Conversely, when ATP synthesis increases, the pmf begins to dissipate inducing electron transfer in order to maintain the pmf. Therefore, the pmf exerts control on the rate of nutrient oxidation, electron transfer, and O_2 consumption. While the pmf is affected by various factors, in particular the rate of ATP synthesis (supply and demand of ATP) and the rate of uncoupled respiration [68].

A small proportion of protons re-enter the mitochondrial matrix through mechanisms that do not involve CV and ATP synthesis. This is an energy dissipative process that reduces pmf and produces heat as a by-product. This process is known as uncoupled mitochondrial respiration and it comprises several independent mechanisms: 1) Proton leak through the inner mitochondrial membrane and into the matrix through unregulated and inducible pathways. 2) Uncompensated cation movement into the matrix via ion channels, such as K^+ or Ca^{2+} can dissipate the electric gradient of the pmf. 3) Decoupling caused by proton slip through the proton pumps (CI, CIII, and CIV) due to ineffective function of the proton pumps. 4) Electron leak during electron transfer in the ETC causing univalent reduction of O_2 to superoxide ($O_2^{\cdot-}$) [67–69].

2.1d Pharmacological targets of mitochondrial respiration to treat obesity

Of the different uncoupling mechanisms, proton leak is the largest contributor to uncoupled mitochondrial respiration [69]. Indeed, in rats proton leak accounts for 20-30% of BMR [70]. Perfect coupling of mitochondrial respiration (O_2 consumption) to ATP synthesis would constitute a coupling efficiency of 100%, however, all cells and tissues have some degree of uncoupling. For instance, hepatocytes of various organisms consistently demonstrate ~80% of coupling efficiency, indicating that uncoupling is an evolutionary conserved mechanism [71].

Proton leak can be subdivided into basal (unregulated) and inducible-proton leak by endogenous uncoupling molecules [72]. Unregulated proton leak occurs by diffusion of protons across the inner mitochondrial membrane in the downhill direction of the pmf. Consequently, unregulated proton leak is non-linearly dependent on the pmf [69]. On the contrary, inducible uncoupling is a physiologically regulated process mediated through the family of uncoupling proteins (UCP) [73]. UCP1 plays an important role for non-shivering thermogenesis in mammals. It is highly expressed in brown adipose tissue where it induces energy dissipation as heat and the uncoupling of mitochondrial respiration from ATP synthesis [73]. Transgenic mice overexpressing UCP1 and UCP3 are resistant to weight gain and show improved insulin sensitivity when fed a high fat diet (HFD) [74–76]. The benefits of uncoupling are also seen with pharmacological treatment using small molecule uncouplers such as 2,4-dinitrophenol (DNP) [77]. A controlled-release formulation of DNP, that has improved safety and therapeutic index, enhances insulin sensitivity and reduces ectopic lipid storage in diabetic Zucker rats fed a HFD [78]. Therefore, pharmacologically induced uncoupling of mitochondrial respiration may be beneficial for weight control and prevention of chronic disease by reducing aerobic metabolic efficiency.

An alternative approach to combating obesity is to increase BMR by inducing mitochondrial biogenesis. Tissue-specific oxidative phosphorylation capacity of athletic individuals is approximately 3-fold greater compared to sedentary individuals [79]. Similarly, maximal O_2

consumption and mitochondrial volume per bodyweight is 2.5-fold greater between athletic and sedentary animals [80]. Exercise elicits mitochondrial adaptations that result in greater mitochondrial density and increased cardiorespiratory capacity. Various intracellular pathways are activated by exercise which directly or indirectly activate the master regulator of mitochondrial biogenesis, peroxisome proliferator-activated receptor gamma coactivator 1-alpha (PGC-1α) [81]. PGC-1α is a transcription factor that regulates genes encoding mitochondrial proteins and activation of this molecule leads to increased mitochondrial biogenesis [82]. Pharmacological treatment that enhances mitochondrial biogenesis by activating PGC-1α or a related mechanism can increase BMR and protect against obesity [63,81]. Taken together, mild uncoupling and/or enhancement of mitochondrial density are potential targets for pharmacological intervention against obesity and metabolic disorders [63,73,81,83].

Figure 2.1. Aerobic respiration mediated by the electron transport chain (system) in mitochondria. Aerobic respiration begins with the oxidation of electron donating molecules such as NADH and $FADH_2$ by CI, CII, CETF or the glycerophosphate shuttle. The electrons received from these molecules are passed onto CoQ to produce $CoQH_2$. $CoQH_2$ is membrane soluble and transports the electrons to CIII which subsequently transfers the electrons to another membrane soluble electron acceptor, cytochrome c. CIV catalyses the final step of the electron transfer chain by oxidising cytochrome c and reducing O_2 into H_2O. During electron transfer, CI, CIII, and CIV, export out protons (H^+) into the intermembrane space creating a proton gradient. The protons flow down their concentration gradient through an ion channel in ATP synthase (CV) and the energy produced is used to phosphorylate ADP into ATP. TCA, tricarboxylic acid cycle; AAO, amino acid oxidation; CI-IV, mitochondrial respiratory chain complexes; Q or CoQ, coenzyme Q; CGpDH, glycerophosphate shuttle; FAO CETF, electron-transferring flavoprotein complex; F1, ATP synthase (adapted from [67]).

2.2 Aetiology of Atherosclerosis

2.2a Structure and function of healthy arteries

The circulatory system has a vital role in distributing molecules (nutrients, O_2, ions, etc.) to organs, and removing toxic substances including carbon dioxide (CO_2). Collectively, normal functioning of these processes are critical to survival [84]. Cardiovascular function is carried out by the connection of the heart with the arterial and venous systems, which through cyclical contractions and relaxations, propels and delivers blood to organs around the body [84].

Arteries and veins are composed of three layers, known as the intima, media and adventitia, from closest to the lumen to the most superficial layer, respectively (Fig. 2.2). Although arteries and veins are composed of the same layers, these layers differ in size and composition and within different sized vessels of the same type, e.g. small arteries are structurally different to large arteries [85]. Discussion of veins, small arteries and arterioles are beyond the scope of this review, therefore, all structural reference will be based upon medium to large-sized arteries given their susceptibility to atherosclerosis (e.g. aorta, carotid and coronary arteries) [86]. The adventitia is the outer most layer of the blood vessel and lies superficial to the media. The adventitia is composed of loose connective tissue woven with nerve fibres and the vasa vasorum (small vessels that supply the outer walls of blood vessels), and it is separated from the media by an external elastic lamina [85]. The media, or middle layer, is composed of several concentric rings of vascular smooth muscle cells (VSMCs) endowed with high elastin content which allows vessels to expand and contract during systole (heart contraction) and diastole (heart relaxation), respectively [85]. This dilation and contraction of blood vessels (particularly in medium sized arteries and arterioles) is important in regulating vessel diameter, blood pressure and blood flow distribution throughout the body [85]. The final layer, which is adjacent to the vessel lumen, is the intima. The intima is composed of a single layer of endothelial cells which is exposed to direct contact with the blood and it is separated from the media by an internal elastic lamina [85].

Endothelial cells serve a multifunctional role important for vessel homeostasis [87]. They serve as mechano-sensors of blood flow induced shear stress, metabolise hormones such as angiotensin, modulate vascular tone through paracrine signals that prompt VSMCs to relax or contract, affect the growth of other cells, and regulate inflammation. Endothelial cells induce vessel dilation by secreting nitric oxide (NO), which induces VSMCs of the media to relax by activating guanylate cyclase, on the contrary, they also produce vasoconstrictive molecules including endothelin [87]. In comparison, VSMCs directly modulate vascular tone by contracting or dilating in response to chemical stimuli [88]. They are also important in vascular injury and repair. For example, in response to injury, VSMCs proliferate and locomote to the site of injury and synthesise extracellular matrix constituents including collagen, elastin, proteoglycans, and secrete growth factors and cytokines [88]. Together, endothelial cells and VSMCs act in synchrony to maintain vascular homeostasis [85].

Figure 2.2. Generalised structure of arteries [84].

2.2b Initiation of atherosclerosis

Atherosclerosis is a chronic inflammatory disease of the blood vessels, which involves both innate and adaptive immune responses, and is most often associated with hypercholesterolemia, hypertension, and/or several other risk factors [89]. Development of this disease is a gradual process generally progressing over several decades to become symptomatic and potentially life-threatening [90]. Interestingly, the presence of fatty streaks within arteries, which is representative of early atherosclerosis, can be observed as early as adolescence (10-14 years) [89]. Atherosclerosis typically affects large elastic arteries (e.g. aorta, carotid and iliac arteries) and medium to large muscular arteries (e.g. coronary and popliteal arteries), moreover, it develops in a non-random pattern which correlates with arterial branch points and areas of altered haemodynamics [29,30]. Central to atherosclerosis is the microscopic appearance of lipid deposits within and around an infiltration of blood-borne leucocytes in the sub-endothelial space of arteries – a pathologic manifestation known as atherosclerotic plaques [89]. Atherosclerotic plaques become larger and more complex over time with a potential to culminate in a clinically significant manifestation, notably, ischemic occlusion, thrombosis, or embolism secondary to their rupture [36,91]. Despite the study of atherosclerosis for over 100 years, debate remains concerning the key process that initiate this disease. Several competing hypotheses for the initiation of atherosclerosis exist with the strongest evidence to support the shear-stress, and the response-to-retention hypotheses as described below [30,31,33,89].

Shear-stress hypothesis

Regions exposed to turbulent/disturbed laminar blood flow, as opposed to uniform laminar flow, causes endothelial activation and dysfunction that initiates atherogenesis [92]. This hypothesis is supported by the development of early atherosclerotic lesions at distinct, non-random, regions associated with branching points, bifurcations, and major curvatures of arterial vessels that are exposed to altered haemodynamics [86,92]. Such regions are subject to disturbed laminar flow patterns that produce significant temporal and spatial gradients of wall shear stresses over relatively short distances that culminate in a high oscillatory index and a low

time-averaged wall shear stress (atheroprone waveforms) [86,93]. In contrast, atheroresistant regions are found at non-branching portions of the vasculature and they are subject to uniform laminar flows (atheroprotective waveforms) [86,93]. Haemodynamic flow alters the structure and function of the endothelium, at a cellular level, with atheroresistant waveforms inducing an ellipsoidal nuclear and cellular morphology of the exposed endothelial cells with coaxial alignment in the primary flow direction, while atheroprone waveforms disrupt this orderly cellular structure [39]. At a molecular level, undisturbed laminar flow induces endothelial expression of two important atheroprotective transcription factors, zinc finger transcription factor, Kruppel-like factor 2 (KLF2) and nuclear factor erythroid 2-related factor-2 (Nrf2) [39]. Studies show that KLF2 promotes an anti-inflammatory and anti-thrombotic endothelial phenotype in addition to regulating endothelial barrier function and metabolism, implicated in atherogenesis [30]. The atheroprotective effects of KLF2 are explained in part by antagonism of cellular nuclear factor kB (NF-kB), which causes downregulation of cell-surface adhesion molecules such as vascular cell adhesion molecule 1 (VCAM-1) and toll-like receptor 2 (TLR2), with overall attenuation of inflammation [30]. KLF2 expression also stimulates the production of vascular tone modulating agents, NO and C-type natriuretic peptide, which are important in conserving endothelial function [39]. Interestingly, flow-mediated expression of KLF2 and Nrf2 have independent effects on downstream genes involved in atheroprotection, however, KLF2 expression is required for maximal Nrf2 activity [94]. Nrf2 transcriptional activity regulates the expression of genes involved in antioxidant defences and cellular resistance to oxidative stress including haem-oxygenase-1 (HO-1), which is both a transcription factor and an enzyme involved in haem catabolism and bilirubin formation [30]. Together, KLF2 and Nrf2 are responsible for regulating ~70% of the flow-mediated gene expression of the atheroprotective endothelial phenotype [94].

On the contrary, exposure to disturbed laminar flow produces an atheroprone endothelial phenotype which has increased permeability, amplified cell turnover and senescence, and elevated markers of chronic endoplasmic reticulum stress that are suggestive of greater

apoptosis, in comparison to atheroresistant regions [39]. Atheroprone waveforms activate the NF-kB pathway and down-stream induction of atherogenic genes, including expression of cell-surface receptors, VCAM-1 and TLR2, pro-inflammatory chemokines and cytokines, micro-RNAs, extracellular matrix proteins, and growth factors [33,39]. Ultimately, it is suggested that this phenotype is critical to the initiation of atherosclerosis as it allows greater apolipoprotein B (ApoB) lipoprotein diffusion through increased inter-junctional permeability and expression of surface adhesion receptors, and subsequent retention, promotes ROS production, and initiates recruitment of blood-borne monocytes [39]. Collectively, these phenomena start a feed-forward cycle that promotes greater ApoB lipoprotein retention and inflammation that leads to the formation of atherosclerotic plaques.

Response-to-retention hypothesis

The competing response-to-retention hypothesis, postulates that elevation of circulating cholesterol, and not atheroprone waveforms, is the key factor for the initiation of atherosclerosis [31]. The hypothesis postulates that ApoB lipoproteins, most notably the low-density lipoprotein (LDL), accumulate within the vascular wall of susceptible arterial regions, only once systemic cholesterol concentrations are above a range that is subject to debate [31]. Susceptible, as opposed to resistant regions, to ApoB lipoprotein retention, are classified based on the type of lipoprotein-retaining molecules found in the extracellular matrix of the subendothelial space [32]. Several lipoprotein-retaining molecules have been identified, including the family of proteoglycans. Extracellular proteoglycans are composed of a core protein attached with sulphated sugar polymers [95]. One possible mechanism of lipoprotein retention is through the interaction of the negatively charged sulphate groups of proteoglycans with the positively charged ApoB group of lipoproteins [96]. Consequently, retained ApoB lipoproteins induce the endothelium to transform into an atheroprone phenotype as described in the shear-stress hypothesis, which via a feed-forward mechanism further enhances inflammation and ApoB lipoprotein accumulation [31,32].

2.2c Initiation and progression of atherosclerosis

For the purpose of this thesis which focuses on cholesterol metabolism, the response-to-retention hypothesis will be assumed as the initiating step of atherosclerosis when describing the sequential progression of atherosclerosis from hereon. The pathophysiology of atherosclerosis is documented to occur in five sequential stages: 1. Subendothelial ApoB lipoprotein retention, endothelial activation, and VSMCs proliferation and migration into the intima 2. Intimal infiltration of blood-borne monocytes and their differentiation into macrophages 3. Intracellular accumulation of cholesterol and formation of foam cells 4. Extensive lipid accumulation resulting in lipid core formation with accrual of necrotic debris 5. Necrotic cores, fibrous-cap thinning, and destabilisation (Fig. 2.3).

Figure 2.3. Progression of an atherosclerotic lesion (from left to right) [97].

In the presence of dyslipidaemia, with or without other risk factors, ApoB lipoproteins accumulate in the sub-endothelial space within the intima of susceptible regions found in middle to large sized arteries [32]. Apolipoprotein B lipoproteins become attached to the sub-endothelial matrix by ionic interaction with the negatively charged sulphate groups of proteoglycans [98]. Consequently, this interaction increases the retention period of ApoB lipoproteins and leaves them more susceptible to oxidation and other chemical modification [31]. Compared to the serum, the sub-endothelial space is deficient in antioxidant defences, therefore, the combination of an increased retention period, susceptibility, and lower

antioxidant protection, causes the accumulation of oxidatively modified atherogenic ApoB lipoproteins, such as oxidised LDL (oxLDL) [99,100].

Sub-endothelial ROS, responsible for oxidative modification of LDL, is produced by endothelial cells, leucocytes and VSMCs, primarily through NADPH oxidase (NOX), inducible NO synthase (iNOS), dysfunctional endothelial NO synthase (eNOS) and myeloperoxidase (MPO) activation [38,100]. Collectively, they cause protein oxidation and peroxidation of fatty acid residues in phospholipids, cholesteryl esters and triglycerides contained in ApoB lipoproteins [38,100]. Progression of atherosclerosis is then advanced by the innate and adaptive immune response [40]. In early atherosclerosis, oxLDL and other modified ApoB lipoproteins are viewed by the immune system as foreign invaders which therefore, trigger the adaptive immune response [40]. Adaptive immunity begins through the activation of VSMCs and the overlying endothelial cells (also known as endothelial dysfunction) by oxLDL [30,40]. Consequently, VSMCs begin to proliferate and migrate from the media to the intima where they begin to secrete extracellular matrix proteoglycans, collagen and elastic fibres [88]. The combined accrual of VSMCs and the secretion of extracellular matrix proteins progressively causes pathological intimal thickening, manifesting as a thick fibrous cap that overlays the underlying lipid/necrotic core [88,101].

On the other hand, activated endothelial cells begin to: express cell-specific adhesion molecules such as E-selectin and VCAM-1 on their surface; secrete chemokines including monocyte chemoattractant protein-1 (MCP-1); and together with VSMCs, secrete lipoprotein-specific adhesion molecules [30,36]. Chemokines attract blood-borne mononuclear cells to the area - in particular, monocytes and lymphocytes – while endothelial surface adhesion molecules adhere these cells to the endothelium. Together, they direct the diapedesis of mononuclear cells into the intima [30]. Furthermore, an activated endothelium facilitates the entry of additional ApoB lipoproteins and their subsequent oxidation. Within the intima, the recruited monocytes, under the influence of macrophage colony-stimulating factor (MCSF) produced in the inflamed endothelium, differentiate into activated macrophages that exhibit an augmented expression of

pathogen and danger-associated, pattern-recognising receptors for innate immunity, including TLRs and scavenger receptors [102].

Monocytes can differentiate into two types of macrophages, either a pro-inflammatory phenotype, M1, or an anti-inflammatory phenotype, M2 [103]. M1-type macrophages appear to outnumber M2 in atherosclerotic lesions and this imbalance may account, in part, for the impaired resolution of inflammation within growing lesions [103]. Scavenger receptors, expressed by macrophages, serve to recognise and phagocytose apoptotic and necrotic cells, which also identify similar ligands expressed on oxLDL particles [41]. Of the family of scavenger receptors, type A scavenger receptor and CD36 account for the majority of binding and degradation of oxLDL [104]. Although, native LDL can also be taken up by macrophages, this process is very slow and does not contribute to the formation of atherogenic foam cells, once LDL is modified to oxLDL there is an increase in uptake which causes pathological lesion formation [104]. Once internalised within macrophages, oxLDL aggregates are degraded, releasing cholesterol.

Cholesterol is metabolised, stored, or transferred out into lipoproteins by a number of sterol transporters, notably, ATP binding cassette (ABC) A1 (ABCA1) and ABCG1 – a process described as reverse-cholesterol transport (see *Sec. 2.3d*) [105]. Free cholesterol is cytotoxic, therefore, intracellularly it is esterified in the endoplasmic reticulum by acyl-CoA:cholesterol acyltransferase 1 (ACAT1) and subsequently stored in cytoplasmic lipid droplets, while the remaining cholesterol is transferred to the outer membrane where it is exported by ABCA1 and ABCG1 into ApoA1 and HDL, respectively [105,106]. Cholesterol efflux is the major mechanism through which cholesterol is eliminated from macrophages and consequently it plays a major role in atherosclerosis [105]. Contrary to the LDL receptor (LDLr), scavenger receptors do not downregulate in response to cellular accumulation of cholesterol, thus, when cholesterol uptake surpasses the rate of cholesterol efflux, it begins to accumulate as cytosolic lipid droplets transforming the appearance of macrophages into foam cells [107]. Impaired ACAT1 function or

cholesterol efflux results in an accumulation of intracellular free cholesterol, which consequently, leads to cytotoxicity and apoptosis, and the exacerbation of atherosclerosis [106].

Macrophages have an important role in controlling sub-endothelial cholesterol accumulation and inflammation. As mentioned earlier, macrophages uptake and degrade retained ApoB lipoproteins and subsequently remove cholesterol via lipoprotein-mediated efflux [105]. Furthermore, macrophages and foam cells undergo apoptosis in atherosclerotic lesions, both early and throughout the progression of the disease [106]. Several factors can induce apoptosis, including high concentrations of oxLDL, tumour necrosis factor alpha (TNFα), NO, oxidative stress, and intracellular accumulation of free cholesterol [106]. Interestingly, studies that investigated the effects of induction or inhibition of macrophage apoptosis, demonstrated that induction of apoptosis was associated with smaller lesions and attenuated plaque progression [108–112]. Apoptosis of macrophages seems to be atheroprotective in early lesions because apoptotic debris is rapidly cleared by neighbouring macrophages (efferocytosis), resulting in fewer inflammatory cells within lesions than if apoptosis did not occur [106].

The phagocytosis of apoptotic cells has a number of additional, potentially favourable consequences including the initiation of anti-inflammatory pathways through the induction of transforming growth factor beta (TGFβ), interleukin-10 (IL-10), and other cytokines which supress inflammation [97]. In addition, efferocytosis prevents the accumulation apoptotic cells and their potential evolution into necrotic cells. Necrotic cells demonstrate additional features such as swelling and disrupted membranes which lead to the release of pro-inflammatory and pro-thrombotic intracellular contents [106]. Phagocytosis of necrotic cells, contrary to apoptotic cells, results in induction of pro-inflammatory processes [97]. An increase in the number of necrotic cells is observed in advanced lesions, which coalesce into pools that contain lipid crystals to form well delineated pro-inflammatory and pro-thrombotic, necrotic cores [102]. The increase in necrosis in late stage lesions, indicates that either the extent of apoptosis exceeds the capacity of efferocytosis or that this mechanism becomes defective [106]. Under normal

conditions, lesional efferocytosis has a high-capacity in animal studies which have demonstrated that induction of apoptosis does not increase the number of apoptotic cells in early atherosclerotic lesions [108,113]; thus, saturation of this mechanism in advanced lesions is unlikely.

On the other hand, evidence points towards defective efferocytosis in late stage atherosclerosis as the main culprit of necrosis [97,106]. Several studies suggest a number of possibilities regarding why clearance becomes defective in late stage atherosclerosis, such as poorer expression of efferocytosis ligands, receptors, or bridging molecules, or an increase in M1/M2 ratio of macrophages, since the M1 phenotype is less efficient at phagocytosis than M2 [97,106]. Alternatively, recent lineage tracing studies suggest that cells formerly identified as macrophages in advanced lesions, may in fact be VSMC-derived macrophage-like cells, which express some of the same markers observed in macrophages but have a reduced phagocytic capacity [88]. Regardless of the mechanism, defective clearance of apoptotic macrophages plays a major role in plaque necrosis.

Plaque stability is a critical determinant of the clinically significant manifestation of luminal thrombosis [114]. Vulnerable plaques, known as unstable lesions that are prone to rupture, contain a thin overlying fibrous cap (≤65 μm in thickness) and an underlying necrotic core associated with inflammation [115,116]. It is now established that necrotic cores destabilise plaques and contribute to the ongoing inflammation observed in atherosclerosis. Virmani et al. [115] reported that 70% of lesions responsible for vascular events were associated with plaque rupture, and the great majority of these ruptures were in close proximity to an underlying necrotic core. In plaques that contain a large number of apoptotic and necrotic cells, macrophages secrete less TGFβ, depriving intimal VSMCs of an important activator of collagen synthesis [97]. Furthermore, the secretion of macrophage-derived metalloproteinases (MMPs) is also increased within necrotic cores. The MMPs are a family of protease-activated enzymes that degrade a variety of extracellular matrix proteins including collagen [97]. Collectively, these

two mechanisms contribute to plaque destabilisation through fibrous-cap thinning, which can lead to rupture and thrombosis (Fig. 2.3).

2.2d Clinical complications of atherosclerosis – sudden coronary death

In the adult population, coronary heart disease (CHD) is the most common cause of sudden death accounting for 80% of all cases. CHD manifests when the lumen of coronary arterial vessels narrow and reduce or completely prevent blood supply to the myocardium. Consequently, the heart either stops beating or beats in an irregular, ineffective rhythm known as ventricular fibrillation, which in either case can lead to sudden death [117]. The overwhelming underlying cause of CHD is atherosclerosis. More specifically, CHD is the result of clinical complications of advanced atherosclerotic lesions which more broadly can be separated in two categories, sudden coronary death due to thrombosis or stenosis [36,114,117]. Thrombosis is the formation of a blood clot in a blood vessel which may or may not cause occlusion [118]. On the other hand, stenosis is the narrowing of a vessel lumen caused by the thickening/outgrowth of the vessel wall [36,119]. Together, thrombosis and stenosis account for the majority of atherosclerosis related mortality [36,118,119]. Given that elevated cholesterol concentrations are critical in the development of atherosclerosis, tight regulation of cholesterol concentrations are essential for preventing mortality from cardiovascular diseases (CVDs) as discussed in the following section.

2.3 Cholesterol Metabolism

Cholesterol is a lipid with a sterol chemical structure that is specific to mammals and it is the most ubiquitous among the steroid molecules [64]. The abundance of cholesterol is a measure of its importance in mammalian biology. It is an indispensable structural component of cell membranes due to its role in membrane dynamics, signal transduction, and structural integrity [120]. Furthermore, it serves as a precursor for the biosynthesis of many biologically important steroids, such as bile acids, vitamin D, adrenocortical hormones (aldosterone and cortisone) and sex hormones (oestrogen, progesterone, androsterone, and testosterone) [120,121]. Excess

cholesterol is cytotoxic and it leads to atherosclerosis and CVDs (see Sec. 2.2), therefore, tight physiological regulation of the cholesterol pool is necessary in order to maintain homeostasis [120].

2.3a Regulation of the cholesterol pool

Circulating cholesterol concentrations are determined by diet, lifestyle, endogenous *de novo* synthesis, transport, metabolism, and the rate of clearance. The contribution of dietary cholesterol to total body cholesterol varies between species [122–124], however, it is estimated that relative to *de novo* synthesis, diet contributes approximately 30% of total cholesterol in humans [125]. In reality there is great variation in the relative impact dietary cholesterol has on cholesterol concentrations and this is determined by the diet and genetic predisposition, such as the capacity to downregulate endogenous cholesterol synthesis when cholesterol absorption increases [120,126]. Therefore, the proficiency of the various aspects of cholesterol metabolism including *de novo* synthesis, transport, excretion, and cholesterol reabsorption are vital in determining the cholesterol pool, and disease risk, in mammals [123,126].

The liver plays the primary role of maintaining a steady cholesterol pool as it is the most active site of cholesterol synthesis and uptake [127]. Moreover, the liver is the only organ capable of converting cholesterol to bile acids and it is the site of hepatobiliary sterol excretion [128]. Hepatocytes regulate cholesterol metabolism by sensing internal changes to the cholesterol pool which are induced by variations in nutrient exchange with blood [127]. For instance, when intestinal cholesterol absorption increases, greater amounts of cholesterol are delivered to the liver via the portal vein causing an acute elevation to hepatic intracellular cholesterol concentrations [129]. In response, hepatocytes down regulate cholesterol synthesis, lipoprotein uptake, and increase cholesterol output in order to reduce cholesterol concentrations [127,129]. Consequently, the system achieves a new equilibrium to normalise the body cholesterol pool where the contribution of *de novo* synthesis is reduced relative to dietary sources of cholesterol [120,126].

2.3b Regulation of cholesterol synthesis

Cholesterol is endogenously synthesised through the mevalonate pathway and as mentioned previously, it is the major contributor to the overall cholesterol pool in mammals [120]. Consequently, tight regulation of cholesterol synthesis is essential to maintain a constant pool, ensuring that it meets but does not exceed cellular requirements in the presence of changing dietary and/or environmental circumstances. The mevalonate pathway includes 20 different enzymes that sequentially convert acetyl-CoA into cholesterol with 3-hydroxy-3-methylglutaryl coenzyme A reductase (HMGCR) serving as the sole rate-limiting enzyme of cholesterol synthesis (Fig. 2.4). Therefore, change in HMGCR activity affects the overall rate of cholesterol synthesis making this enzyme a primary importance for regulatory control [130]. HMGCR resides in the endoplasmic reticulum and several molecules can regulate its activity including sterol and non-sterol metabolites of the mevalonate pathway such as cholesterol. HMGCR is regulated at a transcriptional level by modulating gene expression and at a post-translation level by affecting activity and/or the rate of protein degradation [131].

Transcriptional regulation of HMGCR

Sterols reduce the rate of cholesterol synthesis by inhibiting the translocation of membrane bound transcription factors, the sterol regulatory binding proteins (SREBPs). SREBPs are genetically conserved from fission yeast and are master regulators that control the expression of more than 30 genes involved in uptake and synthesis of cholesterol, phospholipids, and triglycerides [132,133]. In mammals, inactive SREBPs are embedded in the membrane of the endoplasmic reticulum by existing in a heterodimeric complex with SREBP cleavage activating protein (SCAP) that is bound to endoplasmic reticulum-retention membrane proteins such as insulin-induced gene 1 protein (INSIG1) and INSIG2 [134]. INSIGs require sterols to stabilise and to bind to the SREBP-SCAP complex. For instance, cholesterol directly binds to the membrane-bound region of SCAP to induce a conformational change that stimulates INSIG binding [135]. In addition, oxysterols bind directly to INSIG2 to induce SREBP-SCAP-INSIG formation [136].

Together, sterols promote INSIG binding to the SREBP-SCAP complex and prevent the activation and nuclear translocation of SREBP2 [134].

In sterol depleted cells, INSIGs are ubiquitylated and rapidly degraded allowing free movement of the SREBP-SCAP complex to the Golgi [137]. SCAP functions as an escort protein that guides the SREBP-SCAP complex to the Golgi where SREBPs are proteolytically activated. Proteolysis disintegrates the SREBP-SCAP complex and produces a transcriptionally active fragment of the original SREBP molecule which is approximately half the original size. The cleaved SREBP2 molecule transports to the nucleus with the aid of importin β and modulates gene expression [137]. Three main SREBP proteins exist and these are transcribed by two genes: one gene encodes for both SREBP-1a and SREBP-1c while the other for SREBP2. Of the three variants SREBP2 preferentially affects expression of genes involved in cholesterol metabolism and has the most important role in regulating cholesterol levels [132]. In the nucleus, SREBP2 induces gene expression of HMGCR and the low-density lipoprotein (LDL) receptor (LDLr), resulting in greater hepatic uptake of LDL cholesterol (LDL-C) and increased cholesterol synthesis. While SREBP-1c has no effect on cholesterol synthesis and transport, SREBP-1a moderately upregulates these processes, albeit, less significantly than SREBP2 [132].

Apart from post-translational regulation by sterols, SREBP2 is modulated at a transcriptional level via a feedforward mechanism or by thyroid hormones [138,139]. In sterol depleted conditions, endoplasmic reticulum-bound SREBP2 migrates to the nucleus where it induces its own expression in addition to genes involved in lipid metabolism [139]. Additionally, thyroid hormones stimulate SREBP2 gene expression via the thyroid hormone receptor (TR). When activated, the TR forms a complex with retinoid X receptor (RXR) that binds to the DR-4 site on the 5'-flanking sequence of the SREBP2 gene, directly stimulating its expression [138]. Secondary to increasing SREBP2 expression, thyroid hormones increase cholesterol synthesis and LDLr expression [138]. Overall, a decrease in intracellular sterol concentrations and/or an increase in thyroid hormone levels induce SREBP2 gene expression, proteolysis and translocation of SREBP2

to the nucleus, culminating in enhanced cholesterol synthesis and uptake, due to elevated HMGCR and LDLr expression, respectively [132,134,137–139].

Post-translational regulation of HMGCR

Sterols and an isoprenoid product of the mevalonate pathway, isoprenoid geranylgeraniol (GGOH), accelerate the rate of degradation of HMGCR protein in a INSIG-dependent manner [131,140]. In sterol-replete intracellular environments INSIGs bind to the NH_2-terminal of HMGCR and recruit enzymes that ubiquitinate the K89 and K248 amino acid regions of HMGCR leading to proteasomal degradation [130]. The proteasomal degradation pathway is very rapid, therefore, sterols have a striking effect on the half-life of HMGCR which is reduced from >12 hrs in sterol-deprived cells to <1 hr in sterol-replete cells [137]. This is further illustrated in mice with insufficient capacity to ubiquitinate HMGCR due to the absence of INSIG1, who have 85-fold greater HMGCR activity [141]. During sterol-depleted conditions, INSIG proteins are preferentially ubiquitinated over HMGCR and are rapidly degraded. In contrast, sterols induce binding of INSIG proteins to either HMGCRs or the SREBP-SCAP complexes preventing further ubiquitination and proteasomal degradation of INSIG proteins [130]. In contrast, GGOH does not induce ubiquitination of HMGCR instead it enhances sterol-induced proteasomal degradation, potentially by stimulating the transport of ubiquitinated HMGCR to the proteasome [140]. Therefore, accelerated proteasomal degradation of HMGCR is dependent on the intracellular concentrations of sterols and GGOH, and it is mediated by the INSIG proteins in the endoplasmic reticulum [130,131,137,140].

HMGCR activity is also regulated in an INSIG-independent manner by adenosine monophosphate (AMP)-activated protein kinase (AMPK) during metabolic stress [131]. AMPK is a molecular sensor of the cellular energy state and has a vital role in regulating metabolism. Specifically, AMPK detects shifts in AMP/ADP:ATP ratios and under reduced ATP levels, AMP or ADP, binds to the regulatory γ-subunit of AMPK, stimulating conformational change that promotes phosphorylation and activation of AMPK [142]. Activated AMPK phosphorylates the

catalytic site of HMGCR, inhibiting its activity. While it's not yet determined how phosphorylation inhibits HMGCR activity, it may decrease affinity for NADPH or interfere with closure of the COOH-terminal flap at the active site [131]. In summary, HMGCR is regulated post-translationally through sterol-INSIG mediated proteasomal degradation or via direct inhibition of enzymatic activity by AMPK induced phosphorylation [130,131,137,140,142].

Figure 2.4. The mevalonate pathway and its transcriptional regulation by the SREBP pathway. A) The mevalonate pathway is initiated by the conversion of Acetyl-CoA into HMG-CoA by HMG-CoA synthase (HMGCS) which is subsequently metabolised by a cascade of enzymes into cholesterol. HMG-CoA reductase (HMGCR) is the rate-limiting enzyme of the mevalonate pathway and it is the pharmacological target of the cholesterol reducing agents, statins. B) The sterol regulatory element-binding proteins (SREBPs) are sterol sensing molecules that regulate the expression of HMGCR and the rate of cholesterol synthesis. When endoplasmic reticulum (ER) sterol concentrations decrease, SREBP2-SCAP complex is freed from the family of membrane-retaining proteins, insulin-induced gene (INSIG), to be packaged and transported in COPII vesicles to the golgi. In the golgi, the SREBP2-SCAP complex is cleaved to produce a transcriptionally active fragment from SREBP2 that translocates to the nucleus and upregulates the gene transcription of HMGCR, HMGCS, and low density lipoprotein receptor (LDLr) which results in increased cholesterol synthesis and uptake (adapted from [143,144] for A) and B), respectively).

2.3c Cholesterol absorption

Cholesterol absorption occurs in the intestine with the greatest flux located in the proximal section of the small intestine. Cholesterol in the intestine originates either from the diet or from endogenous pools secreted into the gut lumen such as bile [129]. In western societies, humans consume between 0.3-0.5 g day^{-1} of cholesterol through the diet with an additional 1 g day^{-1} secreted into the gut lumen from endogenous sources. Of the total intestinal cholesterol, approximately 50% is absorbed with the remaining removed through faecal excretion [145]. Bile acids, the breakdown products of cholesterol, are essential for efficient absorption of cholesterol and lipids [128]. The liver produces bile acids and secretes them into bile and into the intestine. In the bile, bile acids are present in the form of mixed micelles that contain phospholipids and cholesterol [146]. When bile enters the small intestine, the mixed micelles are enzymatically modified by pancreatic and gastric juices to increase their capacity for absorbing dietary lipids [147].

As cholesterol and dietary lipids are hydrophobic, they need to be solubilised in order to be absorbed in the intestine. Bile acid mixed micelles emulsify and solubilise free cholesterol and lipids in the intestinal lumen, consequently, their presence is essential for effective lipid absorption [128]. The importance of bile acids for lipid absorption is highlighted in conditions of severe cholestasis where absorption of dietary fats is greatly reduced while cholesterol absorption is non-existent [129]. It is important to note that the composition of the bile acid species secreted into the intestine is an important determinant of the rate of cholesterol absorption [129]. In particular, the hydrophobic:hydrophillic balance affects the capacity of bile acids to solubilise cholesterol for absorption [129]. As such, hydrophobic bile acids more potently absorb cholesterol than hydrophilic bile acids because of their superior capacity to solubilise cholesterol [148–150]. For instance, feeding mice with various bile acids in order to change the biliary hydrophobic:hydrophillic bile acid balance induced a proportional increase in cholesterol absorption as the hydrophobic index increased (r=0.95) [151].

Once cholesterol is solubilised in mixed micelles it is taken up by the membrane-bound transporter Niemann–Pick C1-like 1 (NPC1L1) found on the surface of enterocytes that line the intestinal wall. NPC1L1 is the primary target for the inhibition of cholesterol absorption by the clinically approved cholesterol reducing agent, ezetimibe [152]. NPC1L1 deficiency in mice causes a striking reduction in cholesterol absorption (i.e. by ~70%), and in these animals ezetimibe is ineffective at inhibiting cholesterol absorption [153]. Humans with a heterozygote null mutation of NPC1L1 have a reduction of 0.31 mM in LDL-C and a 54% reduction in CVD risk. The expression of NPC1L1 is greatest in the proximal region of the small intestine which is consistent with the highest rate of cholesterol absorption in that section [152,153]. Inside the enterocytes, cholesterol can be excreted back into the gut lumen through the heterodimer ATP binding cassette (ABC) G5/G8 or it is packed with other lipids into chylomicrons (CMs) and secreted into the systemic circulation for delivery to the liver [129].

2.3d Cholesterol transport

Cells enhance uptake of extracellular cholesterol during sterol deprived conditions, and conversely, increase cholesterol efflux under sterol-replete environments [143]. As cholesterol is insoluble in aqueous compartments it is packaged in lipoproteins for transport in the systemic circulation [154]. Therefore, both processes of uptake and efflux require lipoproteins to deposit or accept cholesterol, respectively. Six major lipoproteins exist in mammals, very low-density lipoprotein (VLDL), intermediate-density lipoprotein (IDL), LDL, high-density lipoprotein (HDL), CMs, and chylomicron remnants (CMRs) [154]. The first four lipoproteins mediate endogenous forward and reverse transport of cholesterol in the systemic circulation while the latter two deliver exogenous cholesterol and lipids from the intestine to the liver [154].

Exogenous lipoprotein pathway – delivery of dietary lipids and cholesterol to the systemic circulation

CMs serve a vital role in delivering nutrients to muscle and adipose tissue by functioning as a carrier for dietary lipids and cholesterol that are absorbed from the intestine. Intestinal and pancreatic lipases hydrolyse dietary lipids into free fatty acids and monoglycerides which are

absorbed with cholesterol as mixed micelles from the intestine into enterocytes where they are packaged into CMs [154]. The formation of CMs is initiated by the synthesis of triglycerides from free fatty acids and esterification of cholesterol by lecithin-cholesterol acyltransferase (LCAT) [138]. Cholesteryl esters, triglycerides, and phospholipids are fused with apolipoprotein B-48 (ApoB-48) proteins by microsomal triglyceride transfer protein (MTTP) to form nascent CMs [138]. Apolipoprotein B-48 proteins are an essential structural component of CMs and are a truncated (48% of original length) version of the original ApoB (ApoB-100) protein. In humans, the truncated ApoB-48 protein is only synthesised in enterocytes and it occurs due to a post-transcriptional modification that results into a premature stop codon [155]. On the contrary, the liver synthesises full length ApoB-100 and it is used for the formation of VLDL [155].

Nascent CMs are secreted into the lymphatic system and are delivered to the systemic circulation where they develop into mature CMs after acquiring ApoC2 and ApoE from HDL particles [138]. The ApoC2 surface proteins on CMs activate the extracellular protein, lipoprotein lipase (LPL), found on the luminal surface of the capillary endothelium from muscle and adipose tissue. LPL utilises ApoC2 as a cofactor in order to hydrolyse triglycerides into free fatty acids which are taken up by neighbouring adipocytes and muscle cells via CD36 and fatty acid transport proteins for energy production or storage [154]. Deficiency in ApoC2 significantly hampers LPL activity and leads to hypertriglyceridaemia and hyperchylomicronaemia [156]. Metabolism of triglycerides leads to degradation of CMs into CMRs which are enriched with ApoE and cholesteryl esters but are depleted of ApoC2 and lipids [154]. During this process CMs /CMRs transfer phospholipids and ApoC2 to HDL and other lipoproteins, which in turn inhibits further hydrolysis of triglycerides by LPL [154]. Finally, CMRs are rapidly taken up by the liver via ApoE mediated uptake through the LDL, lipoprotein receptor-related proteins (LRP), and heparan sulphate proteoglycan (HSPG) receptors [157–159].

The necessity of ApoE for efficient removal of CMRs is demonstrated in familial ApoE deficiency who demonstrate type 3 hyperlipoproteinaemia and elevated plasma concentrations of

cholesterol and triglycerides [160]. Once CMRs are picked up by surface receptors on hepatocytes they undergo endocytosis and catabolism, completing the delivery of intestinal (dietary origin or excreted cholesterol) cholesterol to the liver. In the liver, cholesterol may be stored, used for VLDL and bile acid synthesis, or simply excreted via the hepatobiliary route depending on the metabolic demands of the cells [129,154]. Since intestinal cholesterol originates from biliary/transepithelial excretion and from the diet, the exogenous lipoprotein pathway is essential for enterohepatic recycling of cholesterol [129]. Therefore, the exogenous lipoprotein pathway effectively recycles the body's cholesterol pool and supplies adipose tissue and skeletal muscle with dietary lipids for energy production [129,154].

Endogenous pathway - forward cholesterol transport

The forward cholesterol transport pathway enables the liver to deliver lipids and cholesterol to the periphery for various cellular demands [154,161]. This process begins with the synthesis of VLDL particles which is primarily regulated by the availability of triglycerides and to a lesser extent, cholesterol. Increasing triglyceride and/or cholesterol concentrations in the liver stimulates the production of VLDL particles while depletion of lipids induces decomposition of nascent VLDLs [161–163]. Hepatic triglyceride concentrations are dependent on three main sources including dietary lipids delivered via the exogenous lipoprotein pathway, *de novo* synthesis, and free fatty acids secreted from adipose tissue [154,161]. VLDL synthesis is akin to CM formation; in the endoplasmic reticulum, MTTP catalyses the lipidation of the full length ApoB-100 to form nascent VLDL particles. Nascent VLDLs undergo further metabolism to produce mature VLDLs by a secondary lipidation step that occurs during their migration from the endoplasmic reticulum to the Golgi; VLDLs merge with triglyceride rich particles found in the cytosol and acquire additional amounts of cholesterol and phospholipids [154,161].

In lipid deprived environments, ApoB-100s are poorly lipidated and are prone to degradation by the proteasome and by proteasome-independent mechanisms leading to unsuccessful VLDL assembly [162]. Mature VLDL particles are secreted to the systematic circulation by a

mechanism that is yet to be determined [162]. In the systemic circulation VLDLs acquire ApoC2 and ApoE from HDL particles during the process of delivering triglycerides to the peripheral tissues [154]. Furthermore, in humans, VLDL particles are potent acceptors of cholesteryl esters from HDL and LDL particles via a cholesteryl ester transfer protein (CETP) dependent transport, which is not found in some species like the rat [164]. In an analogous way to CM metabolism, LPL hydrolyses triglycerides to free fatty acids and produces IDL particles rich in cholesteryl esters and ApoE proteins. Consequently, CMs and VLDLs compete for LPL hydrolysis and under elevated concentrations of CMs, VLDL clearance is attenuated [154].

IDLs are either removed by the liver through LRP and LDLr mediated uptake or by further lipase activity which transforms IDLs into LDLs. During metabolism of IDLs into LDLs, ApoE is lost, leaving LDL particles with just ApoB-100 proteins that are rich with cholesteryl esters [154]. Due to the smaller size of LDL particles they can diffuse through the vascular endothelium, apart from the blood brain barrier, in order to supply peripheral tissues with cholesterol [165]. The central nervous system (CNS) supplies its own cholesterol through ApoE rich HDL particles [165]. Consequently, LDL particles are prone to accumulating in the vascular endothelium and initiating atherosclerosis as discussed in *Sec. 2.2*. LDL concentrations are controlled by the rate of VLDL synthesis in the liver and the whole-body receptor-dependent clearance. Catabolism of LDL particles is primarily dependent on the liver (80-90% of whole-body metabolism) through LDLr mediated endocytosis via ApoB-100 interaction, with the remaining taken up by extrahepatic tissues [166]. Overall, the liver plays an important role in supplying cholesterol and triglycerides to peripheral tissues by synthesising lipid rich VLDL particles. These VLDL particles distribute endogenous triglycerides to extrahepatic tissue and in the process are metabolised by lipases to produce small dense LDL particles that can diffuse through the vascular endothelium and deliver cholesterol to the peripheral tissues [154,161].

Endogenous pathway - reverse cholesterol transport

The two main sources of cellular cholesterol are derived from d*e novo* synthesis or by receptor-mediated uptake of circulating lipoproteins that contain free cholesterol or cholesteryl esters [127]. However, most extrahepatic cells do not have an effective means of decomposing cholesterol and rely on the reverse cholesterol transport (RCT) pathway to effectively remove excess cholesterol in order to maintain homeostasis [167]. RCT is loosely described as the process of transporting excess cholesterol from peripheral tissue to the liver for hepatobiliary excretion or by trans-intestinal cholesterol efflux (TICE) (see *Sec. 2.3d*) [167]. HDL is the primary acceptor of cholesterol which transports excess cholesterol from peripheral tissue for disposal in the RCT pathway. In addition to its role in RCT, HDL also delivers cholesterol to steroidogenic tissue for steroid hormone synthesis [168]. The liver and intestine synthesise nascent HDL particles that are constituted primarily of ApoA1 with small amounts of lipids and other apolipoproteins. ApoA1 constitutes ~70% of apolipoprotein content in HDL particles and in addition to serving as a structural component of HDL, acts as a cholesterol acceptor. ApoA1 is recognised by various important proteins involved in RCT such as LCAT, ATP binding cassette A1 (ABCA1) and scavenger receptor B1 (SR-B1) [169]. As such, human studies evaluating mutations of proteins involved in RCT determined that mutations in ApoA1 accounts for a significant variation in HDL levels and atherosclerosis risk [164].

Cholesterol efflux to HDL particles is mediated through ABCA1, ABCG1, SR-B1 and aqueous diffusion across the cell plasma membrane. ABCA1 facilitates early lipidation of lipid-poor ApoA1 particles and it is a major regulator of HDL concentrations [170]. Individuals with Tangier disease are homozygous for an ABCA1 mutation which causes loss of functional ABCA1 protein and a near absence of plasma HDL cholesterol and ApoA1 protein [171]. Parallel observations are reported in ABCA1 knockout mice, corroborating the importance of ABCA1 in determining HDL concentrations. Of particular importance to circulating HDL concentrations is hepatic ABCA1 expression since liver specific knockouts demonstrate a 80% reduction in plasma HDL cholesterol, indicating that the liver is the major source of HDL [172]. The primary function of

ABCA1 is to mobilise and export intracellular stores of cholesterol and phospholipids to extracellular lipid-poor ApoA1 molecules. Lipidation of lipid-poor ApoA1 particles is the rate-limiting step of HDL formation, therefore, the cell membrane concentration of active ABCA1 protein determines the rate of formation of nascent disc-shaped HDL molecules [173]. In the bloodstream, free cholesterol in nascent HDLs are esterified by a HDL-associated enzyme, LCAT, to produce mature spherical HDL molecules. The cholesteryl esters can then be transferred to VLDL or LDL in exchange for triglycerides by CETP to form triglyceride-rich HDL [173].

On the other hand, it remains controversial whether ABCG1 affects HDL concentrations even though it is vital in facilitating cholesterol efflux [174]. Unlike ABCA1 efflux, lipid-poor ApoA1 is a poor acceptor of cellular cholesterol via the ABCG1 pathway and does not stimulate cholesterol efflux in the absence of ABCA1 [175]. In contrast, the disc-shaped or mature HDL particles formed by ABCA1-induced lipidation of ApoA1 are effective acceptors of ABCG1-mediated cholesterol efflux. Therefore, the early lipidation step of ApoA1 particles by ABCA1 is crucial for effective ABCG1 efflux as supported by several studies that demonstrate that ABCG1 acts synergistically with ABCA1 to enhance cholesterol efflux [175,176]. The precise mechanism of ABCG1-mediated cholesterol efflux is not understood, however, there is no evidence of direct interaction with ApoA1 or HDL. Preliminary findings suggest that ABCG1 mobilises intracellular stores of lipids to the outer leaflet of the plasma membrane where they are picked up by extracellular HDL [174]. Therefore, tight regulation of ABCA1 and ABCG1 is essential for effective RCT and maintenance of a constant cellular cholesterol pool [167].

ABCA1 and ABCG1 expression is regulated by the nuclear hormone transcription factor, liver X receptor (LXR), while post-transcriptionally they are targeted for degradation by a micro RNA, miR-33, which is part of the SREBP2 gene [177,178]. LXR is activated by oxysterols in cholesterol rich environments and this leads to increased ABCA1 and ABCG1 expression. As mentioned previously (see *Sec. 2.3b*), sterol-replete conditions inhibit SREBP2 transcription along with cholesterol synthesis and uptake, resulting in reduced miR-33 expression and decreased

degradation of ABCA1 and ABCG1 mRNA [134,178]. Together, this leads to reduced cholesterol synthesis and uptake, with enhanced cholesterol efflux [134,177,178].

Another important pathway for RCT is mediated by the SR-B1 receptor. The importance of SR-B1 for RCT is demonstrated by hepatic SR-B1 overexpression reducing atherosclerosis while whole body knockout increasing atherosclerosis in mice [179,180]. Paradoxically, hepatic overexpression of SR-B1 reduces circulating HDL cholesterol concentrations despite providing protection against atherosclerosis. As will be discussed shortly, this is a consequence of selective depletion of cholesteryl esters from HDL particles via a SR-B1-mediated process without affecting the rate of HDL decomposition [168,181].

SR-B1 is widely expressed in various cell types, however, it is most abundant in steroidogenic tissues (adrenal glands, placenta, ovary, and testis) and the liver [168]. Interestingly, the SR-B1 receptor is unique as it participates in bi-directional cholesterol transport between HDL and the cell plasma membrane and this is dependent on the cholesterol gradient [168]. In macrophages, SR-B1 facilitates the export of free cholesterol to mature HDL particles and this is driven by the high free cholesterol:phospholipid ratio in the plasma membrane relative to the lower cholesterol:phospholipid ratio in HDL. It is presumed that SR-B1-mediated efflux occurs by passive diffusion of membrane localised cholesterol through a hydrophobic tunnel created by the binding of SR-B1 with lipoproteins [168,182].

Conversely, in the liver and steroidogenic tissue, SR-B1 primarily facilitates the selective uptake of cholesteryl esters from HDL particles. In contrast to the LDLr-mediated endocytosis of lipoproteins, this occurs without catabolism of the HDL particles [181]. HDL binds to the extracellular domain of SR-B1 creating a hydrophobic tunnel where cholesteryl esters move down their concentration gradient into the plasma membrane [168]. The rate of SR-B1-mediated uptake of cholesteryl esters is dependent on the initial cholesteryl ester concentrations of the receptor bound HDL. Furthermore, lipid uptake through the SR-B1 pathway is coupled to the rate of HDL binding and this is proportional to the HDL concentration

and the size of the HDL particles [170]. Indeed, SR-B1 has markedly greater affinity for larger lipid-rich HDL particles. Therefore, greater HDL concentrations or larger HDL particles lead to greater uptake of cholesteryl esters [170]. In addition to cholesteryl esters, free cholesterol, triglycerides and phospholipids can move down their concentration gradient via the SR-B1 pathway, although, transport of polar lipids is considerably slower [183].

Similar to the LDLr, SR-B1 expression is upregulated during sterol-depleted environments via SREBP-1a. Lopez and Mclean demonstrated that depletion of intracellular sterol through inhibition of cholesterol synthesis with a statin, or by inducing steroidogenesis with human chorionic gonadotropin (hCG), SREBP-1 translocates to the nucleus and enhances SR-B1 expression [184]. As such, expression of SR-B1 is positively enhanced by trophic hormones (follicle-stimulating hormone, luteinising hormone, and hCG) by inducing steroidogenesis and sterol depletion [168]. Several other transcription factors also regulate SR-B1 gene expression independent of SREBP-1 [168,185–187]. Peroxisome proliferator-activated receptor alpha (PPARα)/RXR heterodimer induces SR-B1 expression by binding to the PPRE motif within the promoter region of the SR-B1 gene [185]. Comparably, the oestrogen receptor (ER) α and β, and the liver receptor homolog 1 (LRH-1) bind to response elements on the gene promoter of SR-B1 and enhance SR-B1 expression [186,187]. In contrast, SR-B1 expression is repressed by nuclear receptor DAX-1, transcription factor Ying Yang 1, and pregnane X receptor [168].

Taken together, SR-B1 expressed in hepatic and steroidogenic tissue mediates uptake of cholesteryl esters from mature HDL particles and produces lipid-poor HDL particles that are ready to repeat the RCT process. In this way the body removes excess cholesterol from peripheral tissue by using HDL to transport it to the liver for conversion to bile acids and hepatobiliary excretion, or to steroidogenic tissue for metabolism into steroid hormones [154,168,170]. Additional breakdown of mature HDL can occur in the blood where it is metabolised by lipases into lipid-poor ApoA1. Lipid-poor ApoA1s are recycled in the RCT

pathway or taken up by a membrane-bound protein, cubulin, found on epithelial cells of the renal tubules where they become degraded by megalin [188].

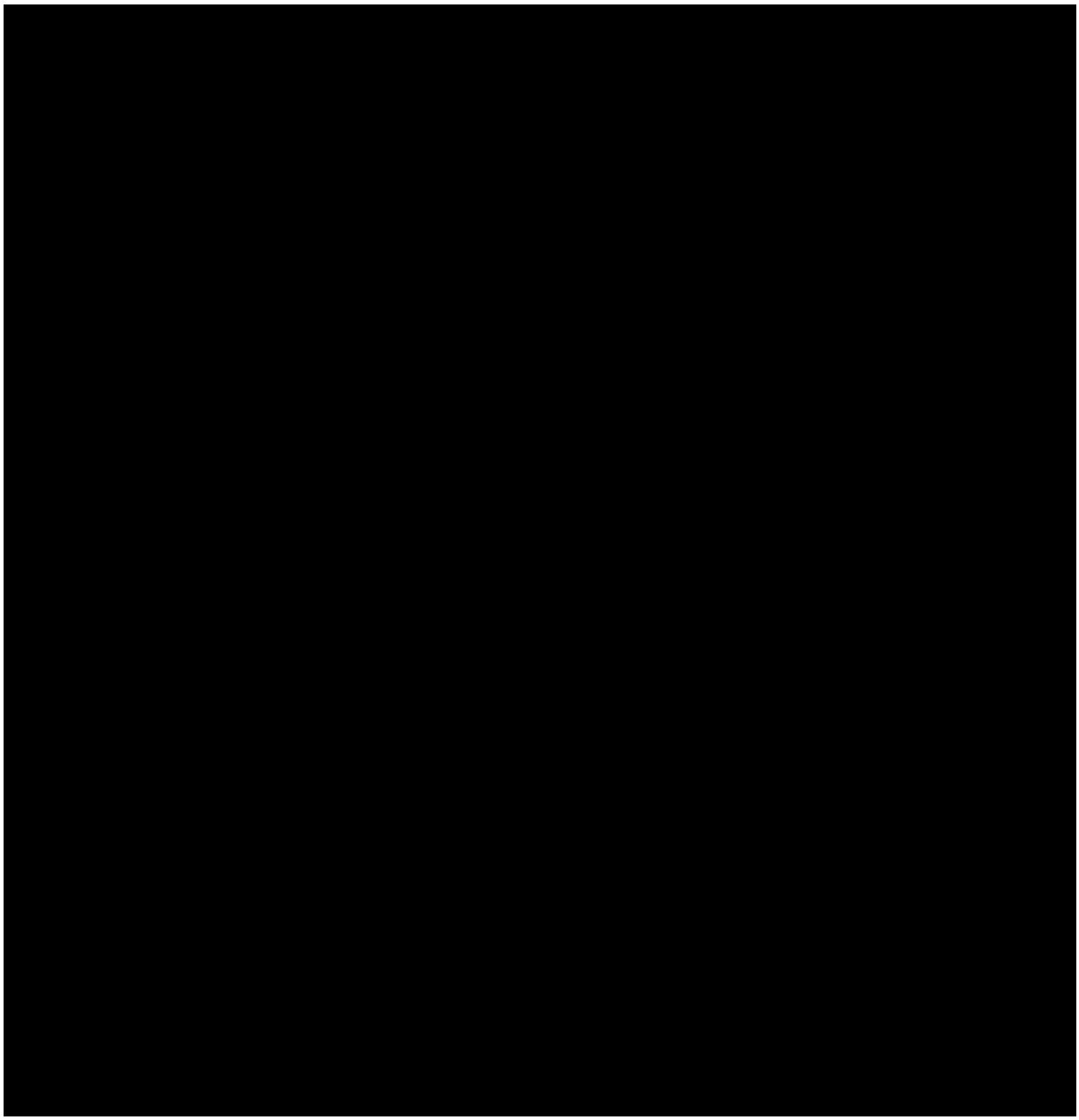

Figure 2.5. Metabolism of HDL. Biosynthesis of HDL begins with unidirectional ABCA1-mediated lipidation of lipid-poor ApoA1 molecules to form discoidal HDL particles that later accept FC from ABCG1 or SR-B1. In blood FC in discoidal HDL particles is converted to CE by LCAT to form mature spherical HDLs. Furthermore, mature HDL can exchange CE for triglycerides with VLDL/LDL via CETP. Mature HDL is decomposed by hepatic uptake via SR-B1 or by lipases in the plasma into lipid-poor ApoA1. Subsequently, cholesterol derived from HDL is excreted via the hepatobiliary route and ApoA1 is degraded by lysosomes in the liver and kidneys. HDL, high-density lipoproteins; ABCA1, adenosine triphosphate-binding cassette sub-family A member 1; Apo, apolipoprotein; FC, free cholesterol; PL, phospholipid; CE, cholesteryl esters; SR-B1, scavenger receptor class B type 1; LCAT, lecithin cholesterol acyltransferase; CETP, cholesterol ester transfer protein; VLDL, very low-density lipoprotein; EL, endothelial lipase; HL, hepatic lipase; BA, bile acid [168].

2.3e Cholesterol breakdown and clearance

Since most cells are unable to significantly catabolise cholesterol, it must be disposed intact or converted to bile acids with subsequent faecal excretion. Small amounts of cholesterol are removed through the skin or intestinal shedding, however, the majority is cleared via the hepatobiliary and transintestinal cholesterol efflux (TICE) pathways [189]. It was generally considered that the main route for cholesterol excretion occurred through HDL-mediated RCT to the liver for biliary excretion (see *Sec. 2.3d*) [189]. Cholesterol transported by lipoproteins to the liver is taken up on the basolateral side of hepatocytes by various surface-bound receptors and either secreted directly or after conversion to bile acids on the apical side into the bile canaliculus [167]. However, it is now evident that the small intestine is similarly important for cholesterol clearance by actively excreting plasma-derived cholesterol via TICE [129]. In mice, TICE is responsible for one-third of the total faecal excretion of cholesterol and this can be upregulated to as much as two-thirds [190]. The existence of TICE was established in light of persistent faecal cholesterol excretion in models of biliary cholesterol insufficiency such as hepatic NPC1L1 overexpression [191]. Since the initial discovery of TICE, its existence has been firmly established in humans, dogs, rats, and mice, strongly supporting the universal importance of this pathway for cholesterol homeostasis in mammals [192]. Discussion of cholesterol clearance will be limited to the hepatobiliary route and TICE as they are by far the most significant routes for cholesterol excretion in mammals [127,146].

Hepatobiliary route

Cholesterol delivered to the liver through the RCT pathway (see *Sec. 2.3d*) or via LDLr-mediated endocytosis of cholesterol rich lipoproteins (CMRs, VLDL, IDL and LDL) are stored as lipid droplets, secreted back into the bloodstream in VLDL or nascent lipid-poor ApoA1 particles, or are excreted through bile depending on the cellular metabolic demands [127,154,167]. Since the hepatobiliary route is one of the main pathways for excess body cholesterol excretion, there is a large flux of cholesterol in the liver that amounts to 108% of daily turnover of the hepatic cholesterol pool [193]. Therefore, effective excretion through the biliary route is essential to

counterbalance the daily cholesterol influx from the rest of the body in order to prevent accumulation of cholesterol in the liver. Dysfunction of hepatobiliary excretion has been linked to non-alcoholic steatohepatitis because it can lead to toxicity from cholesterol accumulation [194].

Bile formation and biliary lipid transport

In the liver a significant portion of cholesterol is metabolised into bile acids prior to biliary excretion. As such bile acid synthesis and excretion accounts for a major fraction of total daily cholesterol turnover [193,195]. Bile acid secretion into the bile canaliculus provides the primary stimulus for bile flow and biliary excretion of hepatic cholesterol and phospholipids [195]. Bile acids are osmotically active solutes that attract water and smaller molecules into the canaliculus forming bile, also known as bile acid-dependent bile flow. Consequently, bile flow is linearly proportional to bile acid concentration and as bile acid secretion increases, bile flow increases [146]. Apart from bile acids, unesterified cholesterol and phospholipids constitute the majority of lipids secreted in bile [146]. Phosphatidylcholine is the primary phospholipid excreted accounting for ~95% of the total phospholipids excreted through bile [196]. Transport of bile acids into the bile canaliculus is primarily mediated through the bile salt export pump (BSEP) located on the canalicular membrane. Interestingly, genetic knockout of BSEP does not completely inhibit biliary bile acid excretion in mice, since multidrug resistance P-glycoprotein 1a (Mdr1a) and Mdr1b are bile acid exporters that compensate for BSEP deficiency. Only a triple knockout of BSEP, Mdr1a and Mdr1b ends in complete inhibition of biliary bile acid excretion, indicating that they collectively mediate bile acid transport into the canalicular lumen [197].

The precise mechanism of cholesterol export into the biliary canalicular lumen remains elusive, however, it requires transport via the heterodimer ABCG5/G8 and the presence of bile acids [198]. Indeed ABCG5/G8 knockout mice or lack of biliary bile acid secretion dramatically reduces biliary cholesterol excretion [197,199]. Bile acids induce biliary cholesterol excretion likely through forming mixed micelles that aid solubilisation of membrane localised cholesterol [200].

Importantly, formation of mixed micelles is also dependent on the presence of phospholipids since lack of biliary phospholipid secretion in animals deficient in Mdr2 demonstrate almost complete absence of cholesterol excretion [201,202]. Elevated bile acid concentrations are toxic to cells, therefore, the liver tightly regulates biliary excretion in order to eliminate excess bile acids [203]. FXR is commonly referred to as the nuclear bile acid receptor because bile acids are endogenous agonists, and this receptor mediates bile acid synthesis, biliary excretion, and reabsorption from the intestine [204]. FXR regulates the rate of biliary lipid excretion directly by modulating the gene expression of BSEP, Mdr2, and ABCG5. Therefore, increasing hepatic bile acid concentrations leads to FXR activation and upregulation of biliary lipid exporters resulting in elevated biliary lipid excretion [204].

In addition to bile acids, Niemann-Pick C2 (NPC2) also stimulates biliary cholesterol secretion. NPC2 is a hepatic protein secreted in bile which is a potent acceptor of non-esterified sterols that promotes cholesterol efflux through a ABCG5/G8 dependent mechanism [205]. Conversely, NPC1L1 reduces biliary cholesterol excretion by increasing reuptake of cholesterol from the biliary canalicular lumen and attenuating NPC2 expression by inhibiting the maturation of NPC2 protein [206]. Overall, cholesterol is secreted into bile either intact by the ABCG5/G8 heterodimer or after conversion to bile acids. Bile flows into the small intestine where approximately 95% and 80% of secreted bile acids and cholesterol, respectively, are reabsorbed by apical sodium bile acid transporter (ASBT) and NPC1L1, respectively [207,208]. The reabsorbed sterols undergo enterohepatic circulation; cholesterol is packed into CMs inside enterocytes and are secreted into the systemic circulation where they eventually return to the liver (see *Sec. 2.3d*).While bile acids travel through the hepatic portal vein back to the liver where they are taken up by Na^+/taurocholate co-transporting polypeptide (NTCP) and are excreted through bile once again [128]. In the intestine, bile acids are essential for absorption of dietary fats and cholesterol by acting as detergents that form micelles around intestinal lipids which enhances absorption [129]. Collectively, bile acids are primary regulators of bile flow and in addition to phospholipids are essential for effective biliary cholesterol excretion [146].

Therefore, close regulation of bile acid synthesis and biliary lipid excretion is vital to maintain cholesterol homeostasis in the body.

Bile acid synthesis

Bile acids are synthesised from cholesterol through a cascade of reactions that take place in various locations in a cell such as the cytosol, microsomes, mitochondria, and peroxisomes. The complete synthesis of bile acids takes place exclusively in the liver [128]. Synthesis of bile acids occurs through two main pathways known as the "classical" and "alternative" pathways (Fig. 2.6). The classical pathway produces neutral sterol intermediates and consequently is also known as the "neutral" pathway of bile acid synthesis [209]. In humans, the classical pathway accounts for the majority of bile acid synthesis (~85%) producing cholic acid (CA) and chenodeoxycholic acid (CDCA) as the primary bile acid species [210]. Cholesterol 7 alpha-hydroxylase (CYP7A1) is the rate-limiting enzyme of the classical pathway and it initiates bile acid synthesis by hydroxylation of cholesterol at C-7. The next critical point of metabolism occurs to 7α-hydroxy-4-cholesten-3-one which is either metabolised by Δ4–3-oxosteroid-5β-reductase (AKR1D1) leading to CDCA formation or by sterol 12-alpha-hydroxylase (CYP8B1) leading to CA synthesis. Therefore, CYP8B1 expression is an essential determinant of the CA:CDCA bile acids ratio [210].

On the other hand, the alternative pathway is also known as the acidic pathway because it produces acidic intermediate metabolites. The acidic pathway only contributes up to 10% of total bile acid synthesis in humans, however, it can become the primary driver of bile acid production in hepatic dysfunction [211]. Bile acid synthesis through this pathway is initiated in the mitochondria by sterol 27-hydrolase (CYP27A1), which oxidises cholesterol into 27-hydroxycholesterol, followed by transformation into 7α,27-dihydroxycholesterol by oxysterol 7α-hydroxylase (CYP7B1). Unlike CYP7A1, CYP27A1 is not the rate-limiting enzyme of the acidic pathway as it is controlled by the rate of cholesterol transport into the mitochondria via the LXR induced steroidogenic acute regulatory protein [212,213]. Furthermore, while CYP7A1 is

localised exclusively in the liver, CYP27A1 and CYP7B1 are expressed in many tissues, therefore, any oxysterol metabolites produced extrahepatically by CYP27A1 and CYP7B1 must be transported to the liver to complete their conversion into bile acids [128,211]. In the liver, oxysterols are metabolised by several sequential enzymatic reactions to produce CDCA as the main product of the acidic pathway. Although in humans this completes the synthesis of free bile acids, rodents express an additional metabolic step where CDCA is rapidly converted to α-muricholic acid and β-muricholic acid [214]. Finally, the majority of the bile acids produced by the two pathways (primarily CA and CDCA or α/β-muricholic acid) are conjugated with glycine or taurine amino acids on the terminal side-chain carboxylic acid by *N*-acyltransferase (BAAT) prior to secretion into bile by BSEP [128]. Bile acid conjugation reduces toxicity, increases aqueous solubility while minimising reabsorption, prevents Ca^{2+} precipitation, and provides resistance against cleavage from pancreatic carboxypeptidases [128].

Figure 2.6. The two main pathways of bile acid synthesis. The classical (neutral) pathway is initiated by cholesterol 7α-hydroxylase (CYP7A1) in the endoplasmic reticulum (ER) of the liver which is also the rate-limiting enzyme for this pathway. Sterol 12α-hydroxylase (CYP8B1) determines the ratio of cholic acid (CA) to chenodeoxycholic acid (CDCA) production in the classical pathway. Conversely, the alternative pathway is initiated by sterol 24-hydroxylase (CYP46A1) in the brain and sterol 27-hydroxylase (CYP27A1) in other tissues producing oxysterols that must be transported to the liver in order to produce CDCA. In the final step, cytosolic or peroxisomal bile acid: amino-acid transferase (BAAT) catalyses conjugation of amino acids, glycine or taurine to the carboxyl group of cholyl-CoA and chenodeoxycholyl-CoA to form tauro- or glycol-conjugated CA or CDCA [209].

Regulation of bile acid synthesis and excretion

Bile acid synthesis undergoes diurnal variation and it is regulated by diet, cholesterol, and bile acid concentrations. Cholesterol modulates bile acid synthesis indirectly through the accumulation of oxysterols which activate LXRα leading to increased CYP7A1 expression and enhanced bile acid synthesis [209]. Mice fed a high cholesterol diet demonstrate elevated bile acid synthesis which is abolished in the absence of LXRα [215]. However, oxysterols do not appear to affect CYP7A1 expression in humans because the human CYP7A1 gene promoter lacks a LXRα-response element, indicating that regulation of bile acid synthesis by LXRα is species-specific [216,217]. On other hand, bile acids regulate bile acid synthesis through a negative feedback mechanism. For instance, tauro-CA (TCA) intraduodenal infusion in rats with a biliary fistula inhibits CYP7A1 activity and bile acid synthesis [218]. The negative feedback inhibition of bile acid synthesis is mediated through the activation of nuclear receptor FXR. However, unlike the direct FXR-mediated regulation of biliary lipid exporters, FXR indirectly modulates bile acid synthesis by enhancing the expression of small heterodimer partner (SHP) [209]. SHP inhibits LRH-1 and hepatocyte nuclear factor-4α (HNF-4α) from binding to response elements on the promoter regions of the CYP7A1 and CYP8B1 genes, culminating in repressed gene expression and bile acid synthesis [128]. Additionally, FXR inhibits bile acid synthesis in a SHP-independent manner by inducing intestinal secretion of mouse fibroblast growth factor 15–JUN N-terminal kinase (FGF15; FGF19 in humans). FGF15 is reabsorbed from the intestine and travels to the liver where it binds to FGF receptor 4 to inhibit bile acid synthesis [204].

PPARα affects bile acid synthesis in a similar way to FXR/SHP pathway. Fibrate treatment (i.e. a PPARα agonist) reduces CYP7A1 expression and biliary bile acid excretion while increasing biliary cholesterol elimination in humans, with parallel findings in rodents [219,220]. Mechanistic studies revealed that PPARα modulates bile acid synthesis by reducing HNF-4α levels, thus, repressing CYP7A1 gene expression [221]. Nevertheless, the presence of PPARα does not appear critical under normal physiology since PPARα knockout animals have unaltered CYP7A1 expression [220]. Interestingly, insulin and thyroid hormones can also affect bile acid synthesis.

Insulin attenuates expression of CYP7A1 and CYP27A1 in several species, however, the effect in humans is less clear [128]. Similarly, there are contradicting findings on the effect of thyroid hormones on bile acid synthesis in humans, however, in rats they enhance CYP7A1 expression [222–224].

Transintestinal cholesterol efflux (TICE)

In the classical view of faecal cholesterol excretion, cholesterol originates from the diet, intestinal shedding, or bile. However, recent studies have challenged this view with strong evidence showing that plasma-derived cholesterol can be transported across the intestinal wall into the lumen by mechanisms that are not yet completely understood [129,192,225]. This process is now known as TICE and occurs throughout the intestine with the greatest flux occurring in the proximal region of the small intestine [226]. Under normal physiological conditions this pathway accounts for 20-30% of faecal neutral sterol excretion in humans and rodents and can be greatly enhanced with dietary or pharmacological intervention [14,190,225]. The importance of TICE is emphasised in conditions of biliary obstruction or genetically induced cholestasis where faecal neutral sterol loss is unchanged or even increased, despite lack of biliary lipid excretion [227–229]. Since stimulation of biliary cholesterol excretion raises the risk of gallstone formation, TICE is potentially an exciting alternative for pharmacological intervention in hypercholesterolaemia and atherosclerosis [192]. Indeed, growing evidence suggests that pharmacological upregulation of TICE protects against atherosclerosis in animals by increasing non-biliary RCT. TICE can be induced through several pathways including activation of LXR, FXR or PPARδ [129].

At present there are many unanswered questions regarding the intestinal cholesterol efflux mechanisms and even less is known about the lipoproteins that transport plasma cholesterol to the intestine [129]. Naturally the HDL particle was initially hypothesised to transport cholesterol to the enterocytes for excretion via TICE since it mediates RCT through the hepatobiliary route [129]. However, this lipoprotein was eliminated as being critical for TICE because double ABCA1

and SR-B1 gene knockout animals that lack HDL do not demonstrate changes in the rate of TICE [230]. Other authors have proposed that ApoB containing lipoproteins mediate cholesterol transport to the intestine via the LDLr pathway, however, a lack of conclusive evidence exists and more studies are needed to confirm this theory [129,225,231].

Conversely, the mechanisms involved in cholesterol efflux from the enterocyte and into the gut lumen are better understood. Several studies have provided strong evidence that the heterodimer ABCG5/G8 mediates cholesterol efflux from enterocytes into the gut lumen [127,129,192]. Mice with double gene knockout of ABCG5/G8 have substantially reduced TICE, however, there is residual activity suggesting the presence of additional transporters including ABCB1a/b [129,190,232,233]. Nevertheless, it is yet to be demonstrated whether ABCB1a/b functions complementary to the ABCG5/G8 heterodimer in mediating cholesterol efflux in the intestine [129]. Overall, while it is evident that the TICE pathway plays a significant role in cholesterol excretion many questions remain unanswered. Its importance warrants further study to better understand the mechanisms regulating this pathway and its therapeutic value in treating hypercholesterolaemia and atherosclerosis.

2.4 Therapeutic Potential of Bilirubin against Obesity and Atherosclerosis

2.4a Bilirubin biology

Bilirubin is a metabolic end product of haem catabolism from senescent red blood cells (RBCs) and haemoproteins in mammals [234]. Due to a lack of nuclei and organelles, RBCs can't self-repair and have a life-span of ~120 days before being degraded by macrophages of the reticulo-endothelial system (i.e. in liver, spleen and lymph nodes) [235]. Following degradation, haemoglobin is released and rapidly metabolised by macrophages [236]. The degradation of haemoglobin liberates haem which is further metabolised by inducible Haem-Oxygenase-1 (HO-1) [1]. Haem Oxygenase-1 catalyses the breakdown of haem to produce biliverdin (BV), carbon monoxide (CO) and iron (Fe^{2+}). The C10 bridge of BV is then chemically reduced to unconjugated bilirubin (UCB) by cytosolic, biliverdin reductase (BVR; Fig. 2.7) [1].

Figure 2.7. The oxidation of haem catalysed by haem-oxygenase to produce biliverdin, Fe2+ and CO, followed by the conversion of biliverdin to bilirubin IXα [1].

Bilirubin is water insoluble, therefore, once it diffuses out of macrophages and into the circulation it becomes albumin bound and it is transported to the liver for metabolism and excretion [1]. In the liver, bilirubin dissociates from albumin and passively diffuses across the sinusoidal endothelium [237,238]. Unbound bilirubin is then transported across the apical membrane of the hepatocyte by facilitated diffusion [237]. Within the cytosol of hepatocytes, bilirubin binds to glutathione-S-transferase or fatty acid binding protein-1 (FABP1), temporarily

solubilising bilirubin [237]. This complex, serves to prevent the reflux of bilirubin back to the systemic circulation and to facilitate transport of bilirubin to the endoplasmic reticulum [237,238]. Bilirubin is then conjugated to glucuronic acid by UDP-glucuronosyltransferase 1A1 (UGT1A1). Individuals diagnosed with Gilbert's syndrome (GS) possess a mutation in the gene promoter of UGT1A1, and thus express ~60% reduced hepatic activity of UGT1A1 [239]. Therefore, GS individuals have impaired capacity to conjugate bilirubin leading to reduced bilirubin excretion and mild accumulation of unconjugated bilirubin (UCB) in the blood (>17.1 μM) [239]. Glucuronidation of bilirubin makes the molecule water soluble, allowing for effective biliary excretion of the compound by multidrug resistance-related protein 2 (MRP2) mediated export of bilirubin conjugates into the bile canaliculus [237,238]. The biliary tree then directs bilirubin conjugates to the gall bladder and duodenum [237]. Within the intestine, a proportion of bilirubin conjugates are deconjugated by intestinal flora. UCB is reabsorbed back into the systemic circulation and undergoes entero-hepatic recycling [240]. Remaining bilirubin conjugates metabolised within the intestine are excreted in the stool [240].

2.4b The relationship between bilirubin and body composition – the anti-obesogenic effects of bilirubin

There is growing evidence to support a beneficial function for bilirubin in protecting against chronic diseases including metabolic syndrome and CVDs. Individuals with GS who have mildly elevated levels of UCB (17 – 80 μM in serum) are protected against CVDs, metabolic syndrome, type 2 diabetes mellitus (T2DM), and all-cause mortality [12,241–243]. Generally, this protection in GS is attributed to the antioxidant effects of UCB [6,8,244,245]. However, emerging evidence suggests that UCB may contain additional anti-obesogenic properties and this could explain the protective association of UCB against chronic diseases.

In line with this notion, several clinical studies demonstrate that circulating UCB concentrations are inversely associated with body mass index (BMI) and abdominal obesity [5,246–250]. For instance, a cross-sectional analysis of U.S. children and adolescents (n=4723) reported that individuals in the highest quartile of total bilirubin concentration (>13.7 μmol/L) compared to

the lowest quartile (<8.6 µmol/L) had a 77% (OR, 0.23; 95% CI: 0.08-0.65) reduced odds of having metabolic syndrome and 65% (OR, 0.35; 95% CI: 0.18-0.67) reduced odds of abdominal obesity, corrected for usual risk factors [250]. Similarly, a cross-sectional study in Korean adults (n=12342) reported that individuals in the high total bilirubin group (mean = 19.1 ± 5.3 µmol/L) had 26% (OR, 0.74; CI: 0.64-0.86) reduced risk of having metabolic syndrome compared to individuals with low total bilirubin (mean = 10.7 ± 2.1 µmol/L). Furthermore, individuals in the high total bilirubin group had significantly lower BMI and waist circumference compared to the low total bilirubin group [249]. Accordingly, Rodriguez et al. reported an inverse correlation between BMI and total bilirubin concentrations and a trend towards reduced fat mass in females with greater total bilirubin [247]. GS individuals (>17 µmol/L total bilirubin) compared to a healthy control group have reduced BMI, waist circumference, and fat mass. Interestingly, this effect was most pronounced in individuals ≥35 years of age [5]. Parallel observations are also apparent in female hyperbilirubinaemic rats who demonstrate substantially reduced bodyweight compared to normobilirubinaemic controls [246]. However, the same effect is not observed in male rats. On the contrary, others have reported no significant association between bilirubin and body composition [251,252]. Therefore, further controlled studies are required to clearly establish the impact of UCB on metabolic function.

2.4c Potential anti-obesogenic mechanisms of bilirubin

Several possible mechanisms could explain the anti-obesogenic effects associated with bilirubin such as direct effects on mitochondrial function or through activation of PPARα (see *Sec. 2.4f* for PPARα) [10,253,254]. Early investigations of bilirubin-induced encephalopathy revealed profound alterations to the morphology of neuronal mitochondria leading to extensive study in the structure-function relationship of bilirubin and mitochondria [255]. Mustafa et al. illustrated that UCB exhibits a U-shape relationship with respect to uncoupled mitochondrial respiration (state 4 respiration) in rat liver mitochondria. UCB dose-dependently stimulated O_2 flux with at peak at 20 µM, while further increases in UCB concentration led to a gradual decline in its stimulatory effects [253]. Conversely, there was a parallel decrease in ADP stimulated oxidative

phosphorylation (state 3 respiration). Therefore, the data suggests that UCB uncouples mitochondrial respiration from ATP synthesis [253].

Indeed, subsequent studies reported that UCB depolarizes the mitochondrial membrane potential confirming the uncoupling potential of UCB. For example, incubation of primary rat neurons with UCB, at 1:1, 2:1, or 3:1 UCB to albumin ratios, dose-dependently decreased membrane potential (5, 15, 50% decrease, respectively) and induced apoptosis at all UCB to albumin ratios. Furthermore, UCB treatment led to increased mitochondrial membrane permeability, cytochrome c release, and change to membrane lipid polarity [256]. Similarly, 20 μM UCB (0.2 UCB:albumin ratio) induced mitochondrial swelling and dissipated the mitochondrial membrane potential of isolated rat liver mitochondria [257]. Investigations into the potential uncoupling mechanism of UCB revealed that UCB associates superficially with membrane lipids which induces phospholipid packing near the membrane surface while increasing permeability of inner regions. The increased membrane permeability may allow greater proton leak and dissipation (uncoupling) of the mitochondrial membrane potential [258–260]. Collectively, the *in vitro* data suggests that UCB is an endogenous uncoupler of mitochondrial respiration.

Additionally, it has been reported that UCB can specifically inhibit CIV activity in mouse brain and liver mitochondria [261,262]. These findings suggest that UCB potentially reduces oxidative phosphorylation by inhibiting CIV function. However, CIV activity has not yet been studied in mitochondria from hyperbilirubinaemic animals, thus, it is unknown whether these findings are relevant to the *in vivo* condition.

A paucity of studies have evaluated mitochondrial function in hyperbilirubinaemic animals with published studies reporting inconsistent results [263–265]. For example, Celier et al. reported no difference in state 3 respiration or respiratory control ratios (state 3 to state 4 ratio of O_2 consumption) of hepatic mitochondria between male hyperbilirubinaemic (Gunn) rats and Wistar controls [263]. Conversely, Fritz-Niggli demonstrated a reduction in P/O (measure of ATP

synthesis relative to oxygen consumption) ratios in Gunn rats compared to Sprague-Dawley controls in hepatic mitochondria, indicating that aerobic ATP synthesis is dysfunctional in Gunn rats [264]. On the other hand, Zelenka et al. demonstrated that hepatic mitochondria from aged Gunn rats had a greater maximal O_2 flux compared to normobilirubinaemic siblings, and attributed this improvement due to the antioxidant effects of bilirubin [265]. The results of these investigations are difficult to interpret because each study used different methods to measure mitochondrial respiration and each study reported differing parameters. Therefore, more studies are needed that comprehensively evaluate mitochondrial function including uncoupled mitochondrial respiration, rate of ATP synthesis, and mitochondrial membrane potential in hyperbilirubinaemic animals, in order to support or disprove an *in* vivo effect of bilirubin on mitochondrial function.

2.4d Association of bilirubin with cardiovascular disease protection

Several studies have demonstrated a strong and inverse relationship between bilirubin and development of CVD. For instance, Schwertner et al. [266] reported in middle-aged men, that a 50% *decrease* in circulating bilirubin concentration was associated with an *increase* of 47% (OR, 1.47; 95% CI: 1.06-2.05) in the odds of having severe CAD, independent of other CVD risk factors. The strength of this association was similar to that of smoking and systolic blood pressure. The inverse association of bilirubin with CAD was reinforced by Hopkins et al. [267] who in addition to men, also included women in their investigation. Hopkins et al. [267] reported that an *increase* of 17 µM of bilirubin was associated with a significant *decrease* of 75% (OR, 0.25; 95% CI: 0.11-0.59) in the odds of having early CAD, independent of other risk factors. The strength of this association was similar to that of HDL cholesterol. Another cross-sectional case control study, Hunt et al. [268] reported a significant inverse relationship between bilirubin and CHD in males but not in females. The lack of association in females could be confounded by an unexpected inverse association between bilirubin and HDL cholesterol, whereby females in the CHD group had significantly lower HDL cholesterol than the females in the non-CHD group. Gender specific CVD protection was also reported by Endler et al. [269] who reported a 40%

reduction in CAD risk in male subjects with bilirubin >8.0 µM, while similar protection was not observed in females [269]. On the other hand, in male and female patients with familial hypercholesterolemia, Nolting et al. [270] documented a 73% (OR, 0.27; 95% CI: 0.08-0.73) *decrease* in the odds of having CVD in individuals with mildly elevated bilirubin levels (>17 µM) compared to those with bilirubin levels of <17 µM, which existed independent of classical risk factors. Similarly, Amor et al. [271] reported a decrease of 60% (OR, 0.40; 95 CI, 0.18-0.89) in risk for developing a carotid plaque for every increase of 8.6 µM of serum total bilirubin after adjustment for LDL, HDL and total cholesterol. These studies provide evidence that bilirubin may also provide protection from CVD independent of lipid status in humans.

Bilirubin is also inversely associated with intima-media thickness (IMT), an early, pre-clinical marker of atherosclerosis [272]. Ishizaka et al. [273] reported that an *increase* of 17.1 µM of bilirubin was associated with a significant *decrease* of 63% (OR, 0.37; 95% CI, 0.28 – 0.49; P<0.05) in the odds of individuals presenting with pathological carotid IMT. The inverse relationship between bilirubin and IMT is also supported by Erdogan et al. [274] who demonstrated that bilirubin concentrations of ≥17.1 µM, when compared to ≤8.55 µM, were associated with significantly *reduced* IMT. Similarly, in a cross-sectional study of participants aged ≥40 years, elevated total bilirubin concentrations of ≥12.3 µM compared to <12.3 µM *reduced* odds by 47% (OR, 0.53; 95% CI, 0.34 – 0.83; P<0.01) for suffering from moderate-severe asymptomatic intracranial atherosclerosis [275]. Furthermore, bilirubin was positively associated with endothelium-dependent vasodilation, a measure of endothelial function which is inversely associated with CVD risk. This association has been confirmed in a double blind cross-over experimental study where hyperbilirubinaemia was induced by retroviral therapy (atazanavir) in T2DM patients [276]. Participants administered with atazanavir for three days developed hyperbilirubinaemia with a mean of 64 µM and demonstrated improved endothelial function [276].

In prospective cohort studies a similar relationship between bilirubin and CVD is observed. Interestingly, in a study of 7685 men (mean age of 50 years) with a follow up period of 11.5 years, a U-shape relationship between circulating bilirubin concentration and relative risk (RR) of a major ischemic heart disease (IHD) event was presented [277]. The U-shape relationship indicated that the highest RR for suffering a major IHD event was associated with the lowest and highest bilirubin quintiles, <7 μM and ~12 μM, respectively. In comparison, the middle bilirubin quintile had a 29% (RR, 0.71; 95% CI, 0.53-0.93) *reduction* in RR of IHD when compared to the lowest quintile. A U-shape relationship between serum bilirubin and CHD risk was also reported in a prospective study of CHD incidence in Northern Ireland and France, investigating both men and women [278]. In another prospective study, a trend suggesting a U-shape relationship between bilirubin and CVD in men, but not in women was reported [279]. In men, the middle three quintiles (9.40-11.10, 11.11-14.52, and 14.53-17.94 μM) of total bilirubin were associated with the lowest risk of CVD, followed by the highest (17.95-66.69 μM) and then the lowest (0.17-9.39 μM) quintile [279]. It is important to note that similar U-shape relationships between bilirubin and CVD endpoints are often reported in studies that fail to control for underlying hepatic disorders. For example, liver disease is known to elevate both bilirubin levels and increase risk of CVD [280], therefore, care must be taken to screen and exclude patients with hepatic conditions, which can confound the potential protection of bilirubin from CVD.

Additionally, a weak but significant inverse linear relationship (r = -0.31) between serum bilirubin levels and severity of atherosclerosis was also established by a meta-analysis investigating male subjects (females were excluded due to a lack of studies) by Novotny and Vitek [281]. Finally, an inverse relationship between serum bilirubin levels and CVD is further supported by a comprehensive meta-analysis that examined 12 studies containing a total of 173 325 participants. The study documented a reduction of 7% in RR per 1-SD increase in serum bilirubin concentration after adjustment for typical CVD risk factors [44].

In summary, an inverse association exists between serum bilirubin concentration and risk of CVD. Although a small number of studies show no association or a U-shape relationship between these variables, the greater majority point towards a linear inverse association between serum bilirubin and CVD, with meta-analyses supporting this conclusion. These findings suggest that serum bilirubin is either directly involved in protection or serves as a surrogate marker for CVD risk. Considering that bilirubin has anti-inflammatory, antioxidant, anti-obesogenic and hypolipidaemic effects in experimental studies *in vitro* [7,8,289,290,99,282–288] and *in vivo* [9,10,297–301,11,285,291–296], it is probable that bilirubin protects against CVD. The following sections will examine the anti-inflammatory, antioxidant and hypolipidaemic potential of bilirubin.

2.4e Haem oxygenase and bilirubin: an atheroprotective pathway?

Accumulating body of evidence indicates an important role for the haem catabolic pathway in modulating oxidative stress and inflammation in mammals [302–304]. Three isoforms of haem oxygenase (HO) have been characterised, including inducible HO-1 and constitutively expressed HO-2 and HO-3 [305]. HO-2 and HO-3 are believed to regulate normal physiological function whilst HO-1 is induced in response to various cellular stressors, and is associated with cytoprotection [305]. Nevertheless, HO-1 has been studied more comprehensively due to its active and adaptive role in acute and chronic inflammatory disease.

It is well established that disruption of haem metabolism through HO-1 inhibition exacerbates inflammatory disease [306]. For instance, in an atherosclerotic mouse model of familial hypercholesterolaemia (FH), inhibition of HO-1 enhanced atherosclerosis and increased plasma lipid hydroperoxide levels in LDLr knockout ($LDLr^{-/-}$) mice [307]. Additionally, HO-1 inhibition and induction reduced and increased, respectively, relative fibrous cap thickness in ApoE-/- mice, suggesting a role for HO-1 in preserving plaque stability [308]. Several other studies also report that HO-1 induction exerts protection by upregulating antioxidant and anti-inflammatory mechanisms. Although the mechanisms underlying the protection observed with HO-1 induction

aren't completely understood, it is suspected that the by-products of haem catabolism - CO and BV/bilirubin - play an important role, and may have evolved to counteract the extremely cytotoxic effects of unbound-haem [309]. For the purpose of this review, CO exists outside the scope of interest, thus, will not be further discussed.

In the past, BV and bilirubin were assumed to represent waste products of haem catabolism. It was not until 1987 when a landmark study published by Stocker et al. [8] revealed that BV and bilirubin, possessed potent antioxidant capacity. For example, Stocker et al. [8] demonstrated that bilirubin at a physiological oxygen concentration (2%) more potently scavenged peroxyl radicals than α-tocopherol, which is a highly efficient lipid-soluble serum antioxidant in humans [310]. Since then, BV and bilirubin administration has been shown to protect against oxidative stress/inflammatory disorders including, ischemia reperfusion (IR) injury [291–294,298,300,311–314], endotoxemia [295,315–318], diabetes [9,301,319], obesity [9–11], and atherosclerosis [3,284,320] independent of HO-1 induction and other haem catabolites [317,321].

Ischemia reperfusion injury consists of two stages, initially, tissues experience ischemia and metabolic stress, and this is followed by re-introduction of blood flow and oxygen supply termed 'reperfusion'. During reperfusion an excessive production of ROS occurs, in addition to activation of cytotoxic enzymes including calcium-dependent proteases, which ultimately cause cellular necrosis and apoptosis. Several experimental studies show that bilirubin administration protects the kidney [298], liver [300,311,312], intestine [291], and heart [244,293,313,314] from IR injury. Kirkby et al. [298] reported that bilirubin treatment preserved proximal tubule histology post kidney IR injury. Likewise, in IR injury of the heart, a model representing myocardial infarction (MI), exogenous bilirubin infusion [293,313] and endogenous hyperbilirubinaemia [314] reduces infarct size, prevents mitochondrial disruption, and preserves haemodynamic function when compared to untreated controls. Importantly, infusion of a water-soluble analogue of bilirubin, bilirubin ditaurate (BRDT), into *ex vivo* rat hearts was more effective when administered

immediately upon reperfusion when compared to delivery pre-ischemia or to control hearts [244]. This finding is consistent with bilirubin's antioxidant potential in that bilirubin appears most efficacious when present at the time (reperfusion) of maximal ROS production [322]. Similarly, exogenous bilirubin administration protects against IR injury of the liver [300,311,312] and intestine [291].

Although strong evidence exists for bilirubin protection against IR injury, the underlying mechanisms of BV/bilirubin protection are not completely elucidated. Nevertheless, it is likely that BV and bilirubin offer cytoprotection through their capacity to scavenge ROS [290], inhibit leucocyte infiltration [287,323,324], and/or reduce inflammation [325]. The following paragraphs will review experimental studies regarding the potential mechanisms of protection induced by BV and bilirubin in the context of atherosclerosis.

2.4f Anti-atherogenic effects of biliverdin and bilirubin

The vascular endothelium serves an important role in cardiovascular homeostasis by acting as a transducer and modulator between blood and organs [87]. Endothelial dysfunction is strongly implicated in the initiation and progression of atherosclerosis. It induces the expression of adhesion molecules (VCAM, ICAM, E-selectin) and generation of ROS - primarily through NADPH oxidase (NOX) - which consequently encourages the infiltration of circulating monocytes and lymphocytes, production of proteoglycans, and the proliferation of VSMCs to the site of lipid accumulation or vascular injury [30]. Correspondingly, this process propagates vascular injury and over time can develop into clinically symptomatic atherosclerosis (see *Sec. 2.2*). Increased ROS also depletes atheroprotective nitric oxide (NO) and contributes to hypertension and impaired vasodilation [30].

Currently, only a single study has investigated the impact of exogenous bilirubin treatment on atherosclerosis in mice. Male $LDLr^{-/-}$ mice fed a western diet were treated i.p. with 30 mg kg^{-1} $bodyweight^{-1}$ UCB daily for 8 weeks [320]. At the end of treatment, UCB treated mice had significantly reduced area of atherosclerotic plaques with decreased extracellular matrix and

VSMC proliferation. Furthermore, the aortic lesions of UCB treated mice contained fewer macrophages and T lymphocytes and reduced markers of tissue oxidation. It is suspected that UCB reduced the extent of atherosclerotic plaques by scavenging ROS. This conclusion was supported by *in vitro* results showing that UCB inhibits monocyte migration across monolayers of endothelial cells by scavenging ROS produced via ICAM-1 and VCAM-1-mediated pathways [320]. Therefore, this study provides the first preliminary evidence that bilirubin treatment may be effective in attenuating atherosclerotic development, by reducing oxidative stress [320]. These findings are consistent with several studies reporting antioxidant effects for bilirubin. However, bilirubin also affects other pathophysiological mechanisms involved in atherosclerosis including chemotaxis, cellular proliferation, and cholesterol concentrations, which could explain the above observations. The next sections will review the impact of bilirubin on these mechanisms to provide insight into the protective relationship between bilirubin and CVD.

Bilirubin and protection against oxidative stress

NADPH oxidase (NOX) is a multi-subunit enzyme complex and an important contributor to ROS production within the vascular wall. Four isoforms of NOX exist within the vascular wall including NOX1, NOX2, NOX4 and NOX5, and are differentially expressed in VSMCs, endothelial cells, fibroblasts, and infiltrating immune cells [326]. The primary function of NOX is to produce superoxide ($O_2^{-\cdot}$) from molecular oxygen (O_2) using NADPH as an electron donor. While NOX4 may be atheroprotective, NOX1 and NOX2 are atherogenic, with NOX2 expression being elevated in atherosclerotic plaques [326]. In addition to NOX, as a consequence of endothelial dysfunction, endothelial NO synthase (eNOS) becomes uncoupled and produces superoxide by metabolising NO [327]. The subsequent increase in superoxide production further depletes local NO concentrations and promotes atherogenesis. Since bilirubin is a potent antioxidant, it could contribute to atheroprotection by affecting the redox balance within the vascular wall through scavenging of superoxide, NOX inhibition, reducing oxidative modification, and increasing NO bioavailability.

Thus far, *in vitro* studies have demonstrated that bilirubin inhibits the formation of superoxide from porcine [328] and human [329,330] neutrophils and directly scavenges superoxide produced by mitochondria [331]. Pflueger et al. [332] incubated bilirubin with angiotensin-2 (ANGII; inducer of superoxide formation) in cultured VSMCs, and demonstrated dose-dependent inhibition of NOX-dependent superoxide formation. In the same study, ANGII administration to hyperbilirubinaemic rats (Gunn rats) compared to wild-type (WT) controls, resulted in lower systolic blood pressure, aortic oxidative damage and superoxide levels [332]. Likewise, in mice, mildly elevated hyperbilirubinaemia induced by partial UGT1A1 inhibitors, indinavir [333] and anti-sense vivo morpholino [299], prevented ANGII driven hypertension, in part by inhibiting superoxide production. Surprisingly, hyperbilirubinaemia was more effective at attenuating hypertension than direct NOX inhibition by apocynin, suggesting that bilirubin acts both in a NOX dependent and independent manner to normalise blood pressure [299]. The effects of bilirubin on blood pressure could also be attributed to its NO preserving effects. NO is a vasodilator which normalises blood pressure and in the aforementioned mouse study [333], mildly hyperbilirubinaemic mice had greater NO levels which, could have contributed to prevention of hypertension. Considering that superoxide interacts with NO to produce peroxynitrite, bilirubin could preserve NO by reducing superoxide concentrations [334].

A recent study provides further insight on this topic showing that bilirubin is a membranous scavenger of mitochondrially produced superoxide [331]. These findings indicate that reduced superoxide concentrations reported in models of hypertension and could have been induced by scavenging of superoxide by bilirubin. However, the rate of reaction between bilirubin and superoxide is slower than the reaction between superoxide and NO [331]. Therefore, it is unlikely that bilirubin outcompetes NO for chemical interaction with superoxide. Conversely, *in vitro* studies demonstrate that bilirubin directly scavenges NO (which is also a radical species), which contradicts elevated NO concentrations reported in hyperbilirubinaemic mice [288,333]. However, this reaction is slow in comparison to oxyhaemoglobin and NO, and is unlikely to affect plasma NO levels *in vivo* [335]. Interestingly, in a physiologically relevant *in vitro* model,

incubation of bilirubin with oxidised LDL (oxLDL) in cultured human aortic endothelial cells partially conserved eNOS expression compared to oxLDL alone treated cells, with a similar effect observed in hypercholesteraemic mice treated with bilirubin [336]. Unfortunately, this study did not measure the NO concentration in blood, therefore, a potential NO preserving effect of bilirubin cannot be confirmed. Collectively, the evidence provides support for an anti-hypertensive role for bilirubin which appears to be mediated by preserving NO concentrations. However, further studies are needed to confirm this conclusion and to determine the mechanism by which bilirubin preserves NO concentrations.

Anti-chemotactic effects of bilirubin

Another means by which bilirubin may attenuate atherogenesis is by inhibiting leucocyte recruitment, attachment, and transmigration into injured vessels. Monocyte and lymphocyte infiltration are an established process in the propagation of atherogenesis, whereby their transmigration further increases inflammation/damage, and foam cell formation. Several studies demonstrate that HO-1 expression is augmented in plaques, agreeing with the hypothesised role of HO-1 as an adaptive modulator of vascular injury [303].

In a rabbit model of atherosclerosis, HO-1 was expressed in endothelial, VSMCs, and foam cells of atherosclerotic lesions but not in healthy vessels [337]. HO-1 expression was associated with a corresponding increase in bilirubin within the same foam cells, suggesting that HO-1 induced atheroprotection may occur by the accumulation of bilirubin [337]. The contribution of bilirubin in HO-1 mediated atheroprotection is evidenced in several studies. For instance, both HO-1 induction and exogenous bilirubin administration reduced oxLDL-induced monocyte chemotaxis *in vitro* [324]. In a later study, HO-1 induction and exogenous bilirubin, but not CO administration, attenuated MCP-1, MCSF and VCAM-1 expression, providing a possible mechanism by which HO-1 and bilirubin inhibit chemotaxis. Notably, endothelium dependent vasodilation in *ex vivo* aortic rings from hypercholesterolaemic mice was improved by HO-1 induction and bilirubin treatment but not with CO treatment [336]. This finding is in accordance

with a human study that reported an improvement in endothelium-dependent vasodilation following transient hyperbilirubinaemia (see *Sec. 2.4d*) [276]. Several studies corroborate the finding that bilirubin inhibits VCAM-1 expression and endothelial transmigration of leucocytes [283,287,338]. In these studies physiological concentrations of bilirubin inhibited trans-endothelial leucocyte migration *in vitro* in murine axillary and cervical high endothelial venule cells [338]; murine heart endothelial cells [283,287]; human umbilical vein endothelial cells [283] and *in vivo* in murine lung tissue [338]. Although all three studies demonstrate that bilirubin reduces VCAM-1 mediated leucocyte endothelial transmigration, the mechanism implicated within each is different. For example, in axillary and cervical endothelial cells, bilirubin reduces leucocyte diapedesis without affecting VCAM-1 expression [338]. Instead, it was proposed that bilirubin inhibits transmigration by disrupting downstream VCAM-1 signalling through inhibition of NOX driven formation of ROS [338].

In murine heart endothelial cells, bilirubin administration inhibited TNFα induced VCAM-1 expression, likely mediated via inhibition of nuclear translocation of NF-kB [283,287]. It is possible that bilirubin only affects VCAM-1 expression under inflammatory conditions as seen in TNFα-mediated induction of adhesion molecules [283], in which bilirubin prevents stress induced expression; or the effect varies with the origin and/or type of cells. Interestingly, it seems that even in the absence of an effect on VCAM-1 expression, bilirubin suppresses leucocyte transmigration, suggesting an effect on downstream VCAM-1 signalling. Collectively, these studies support the results of reduced infiltration of monocytes in atherosclerotic plaques of bilirubin treated $LDLr^{-/-}$ mice [320], and provide compelling evidence that bilirubin might provide atheroprotection by inhibiting leucocyte chemotaxis and endothelial transmigration.

Anti-proliferative effects of bilirubin

In addition to affecting superoxide formation/abundance and leucocyte transmigration, bilirubin can inhibit VSMC proliferation. For instance, bilirubin is protective in a model of *in vivo* arterial balloon injury that mimics restenosis and early-intermediate progression of

atherosclerosis. Ollinger et al. [325,339] revealed that untreated Gunn and WT rats pre-treated with BV, were protected from neointimal formation following balloon injury in contrast to untreated WT rats that exhibited profound VSMC proliferation and luminal narrowing. *In vitro*, bilirubin and BV dose-dependently inhibited rat and mouse VSMC proliferation through inducing cell cycle arrest at late phase of G_1 in the absence of apoptosis [325,339]. Bilirubin and BV induced cell cycle arrest by inhibiting p38 MAPK phosphorylation in a p53 mediated manner [325]. Consistent with the findings in mouse and rat cell lines, bilirubin also inhibited proliferation of human VSMCs, suggesting that bilirubin has an anti-proliferative role in humans, which is supported by reduced IMT thicknesses in individuals with mildly elevated bilirubin [274]. Likewise, bilirubin incubation was associated with cell cycle arrest at the G_0/G_1 phase by inhibiting G1 cyclins, D1 and A, which are imperative for cell progression from G_1 to the S phase of the cell-cycle [285]. Cell cycle arrest was also accompanied by attenuated migration of VSMCs after scratch wounding [285]. Together, these studies provide significant evidence to suggest that bilirubin inhibits VSMC proliferation in the absence of apoptosis. VSMC proliferation is critical to pathological intimal thickening observed in early to intermediate stages of atherosclerosis, thus, it is possible that bilirubin would be atheroprotective if the inhibitory effects on VSMC proliferation translate into the *in vivo* human condition [89,90]. However, in advanced lesions where fibrous-cap thinning - a hall-mark of thrombosis-prone unstable plaques – is in part due to VSMC apoptosis, inhibiting VSMC proliferation may contribute and accelerate thinning and lead to a major cardiac adverse event [33]. Thus, it is conceivable that bilirubin administration might not be atheroprotective in advanced-stage atherosclerosis.

Lipid reducing potential of bilirubin

Elevated circulating cholesterol concentrations are a cardinal risk factor - and potentially a necessity - for the initiation and progression of atherosclerosis [31]. Therefore, therapy targeting synthesis, transport, absorption and/or removal of lipids represents a vital therapeutic strategy in treating atherosclerosis. Interestingly, serum bilirubin levels are negatively associated with circulating triglycerides, LDL, oxLDL, and total cholesterol in humans [12]. This relationship is

also corroborated in hyperbilirubinaemic (Gunn) rats when compared to their congenic, normobilirubinaemic counterparts, who also demonstrate marked reductions in circulating total cholesterol concentrations [246]. Although the mechanism inducing reduced circulating cholesterol levels in hyperbilirubinaemic animals remains unclear, two mechanistic hypotheses have been proposed: namely 1. Activation of Aryl hydrocarbon receptor; and 2. Activation of PPARα, both leading to reduced cholesterol synthesis [12].

The aryl hydrocarbon receptor (Ahr) has pleiotropic constitutive roles in mammalian physiology and modulates the mevalonate pathway of cholesterol synthesis. Ligand-activation of Ahr suppresses several genes involved in cholesterol synthesis including HMGCR, while the absence of this receptor causes greater basal expression of these genes, indicating that endogenous ligands might alter cholesterol synthesis [340]. Potential endogenous modulators of Ahr-mediated regulation of cholesterol synthesis include BV and bilirubin, in addition to kynurenic acid, 3-indoxyl sulphate, and indirubin [341]. Nonetheless, there is no direct evidence to implicate bilirubin as mediating circulating cholesterol concentrations by activation of this receptor. Future studies need to determine whether increasing systemic bilirubin concentrations induces Ahr activation and consequently, attenuates cholesterol synthesis, and reduces circulating cholesterol levels.

Peroxisome proliferator-activated receptors (PPAR) are ligand-activated transcription factors which, among other metabolic processes, regulate lipid and glucose metabolism. PPARα is one of three PPAR isoforms – PPARα, PPARβ and PPARγ – and is abundantly expressed in highly metabolic tissues including the liver, heart, brown adipose tissue and skeletal muscle [342]. In these tissues, PPARα serves as a lipid sensor that controls lipid homeostasis, whereby activation of this receptor by endogenous or exogenous ligands causes it to heterodimerize with DNA sequence elements in DNA promoter regions which induce fatty acid metabolism including β-oxidation and ketogenesis [342]. Recently, Stec et al. [10] demonstrated that bilirubin is an endogenous ligand of PPARα of equivalent potency as a clinically approved synthetic agonist,

fenofibrate. Interestingly, bilirubin was much more effective than fenofibrate at reducing lipid accumulation *in vitro*. These lipid reducing effects were confirmed *in vivo*, where mice fed a high fat diet (HFD) and treated with UCB for one week exhibited significantly reduced adiposity and bodyweight, compared to controls [10]. This effect was not observed in UCB treated PPARα KO mice, suggesting that the lipid decreasing effects with UCB treatment may be PPARα mediated [10].

Consistent with these results, PPARα was also activated in chronically hyperbilirubinaemic male mice with an inserted humanised GS gene (UGT1A1*28) [11]. Compared to normobilirubinaemic controls, hyperbilirubinaemic mice had significantly reduced bodyweight, fat mass and body fat (%) after consuming a HFD for 29-33 weeks. Furthermore, hyperbilirubinaemic mice had reduced hepatic cholesterol and triglyceride concentrations and were protected from hepatic steatosis compared to controls [11]. Unfortunately, neither of these studies reported circulating cholesterol concentrations, therefore, it remains unknown whether the association of reduced circulating cholesterol concentrations with elevated serum bilirubin are also PPARα mediated. Interestingly, an additional study provides preliminary evidence that cholesterol concentrations are reduced following UCB treatment [9]. Fourteen weeks of UCB treatment to mice fed a HFD induced a reduction in bodyweight, epididymal fat, circulating cholesterol concentrations, and hepatic triglyceride concentrations. These effects were associated with restored hepatic PPARγ expression and insulin sensitivity [9]. Therefore, these findings provide evidence that exogenous bilirubin treatment reduces circulating cholesterol concentrations, however, whether this effect was mediated through PPARα was not assessed and requires confirmation [9]. Considering that PPARα activation reduces cholesterol concentrations in humans and mice, strengthens the possibility that human hyperbilirubinaemia is sufficient to activate PPARα and contribute to changes in circulating cholesterol [343]. Together, these studies suggest that bilirubin decreases cholesterol concentrations and reduces adiposity, and these effects appear to be mediated through PPARα or Ahr. However, further studies are required to confirm this conclusion and could include investigations of the rate of cholesterol synthesis rate and body composition in

hyperbilirubinaemic animals in WT, PPARα KO, and Ahr KO animals. The results of these studies would help to determine the impact of physiological hyperbilirubinaemia on PPARα, Ahr, cholesterol synthesis, and adiposity.

The physiological importance of BVR

Of noteworthy importance when considering BV, and not bilirubin, as a therapeutic molecule or a means of elevating bilirubin levels, are the physiological roles of BVR. As mentioned earlier, endogenous or exogenous administration of BV is rapidly converted into bilirubin by BVR [234]. Wegiel et al. discovered that the anti-inflammatory effects of BV administration can in part be explained by its metabolism by BVR [37]. Binding of BV to BVR on the cell surface of macrophages stimulates the phosphorylation of the BVR tyrosine 198 residue which is crucial in order for BVR to bind to phosphatidylinositol 3-kinase (PI3K) and activate protein kinase B (also known as Akt) phosphorylation [37]. The phosphorylation of Akt increases the expression of IL-10, hence, elucidating a mechanism of BV induced anti-inflammatory effects [37]. In a similar fashion, phosphorylation of BVR causes nuclear translocation where it binds to AP-1 sites that either induce HO-1 transcription or inhibit pro-inflammatory toll-like receptor-4 (TLR4) [344]. Interestingly, bilirubin may indirectly activate BVR, due to its oxidation to BV [345], which is then chemically reduced back to bilirubin by BVR, leading to a cycle of BVR activation. Notwithstanding, it is yet to be demonstrated that elevated bilirubin levels are associated with greater basal activation of BVR *in vivo*, and thus, currently the bilirubin associated protection against atherosclerosis cannot be attributed to BVR.

2.5 Summary of the Therapeutic Potential of Bilirubin

Taken together, there is plethora of evidence to suggest that bilirubin is a powerful antioxidant with anti-obesogenic, anti-chemotactic, anti-proliferative, and lipid modulating effects. Considering the importance of these factors in the initiation and progression of atherosclerosis, it is likely that bilirubin is an endogenous protectant against CVD. Although, several studies have established that pharmacological induction of HO-1 is protective against atherosclerosis, it is difficult to determine whether bilirubin or other by-products of haem catabolism are responsible. Furthermore, there is a clear lack of studies to explain lower BMI and circulating cholesterol concentrations observed in hyperbilirubinaemic animals and humans. Therefore, it is imperative to test whether altering circulating bilirubin concentrations affects mitochondrial function and cholesterol synthesis. Finally, this thesis will be the first to explore novel means to increase bilirubin in humans, which is expected to reduce circulating cholesterol concentration and inflammation and increase circulating antioxidant defences.

2.6 Strategies to Increase Circulating Bilirubin

Given that there is strong epidemiological evidence and animal studies to suggest that bilirubin is protective against CVDs, it is important to determine whether a safe and effective treatment can increase bilirubin in human clinical trials. Protection from atherosclerosis is associated with UCB levels above 17 µM as found in Gilbert's syndrome (GS). Therefore, any treatment must increase UCB concentrations chronically to a similar level in the average individual with minimal side-effects and dosing frequency, preferably as an oral supplement. An obvious option would include oral UCB or biliverdin supplementation. While these would minimise off-target effects, poor bioavailability (<3%) [346], and short half-lives (<45 mins) [347] preclude these options as viable means to chronically elevate UCB concentrations .

Considering that UCB is primarily excreted through the hepatobiliary route (see *Sec. 2.4a*), inhibition of hepatic transport and/or conjugation could also represent a suitable means to increase UCB concentrations, similar to that observed in GS. Several compounds inhibit UGT1A1 and increase plasma UCB concentrations. For example, two anti-retroviral medications, indinavir and atazanavir, inhibit UGT1A1 activity [348]. UCB conjugation was inhibited by indinavir in human liver microsomes with a IC_{50} of 68 µM [348]. HIV-infected men treated with indinavir for a minimum of 4-weeks at 800 mg thrice per day increased serum total bilirubin by more than 18 µM on average [349]. Unsurprisingly, the change in serum total bilirubin was almost 5-fold greater in individuals with partial UGT1A1 (6/7 or 7/7 polymorphism) impairment compared to individuals with complete UGT1A1 (6/6) activity [349]. On the other hand, atazanavir is a more potent inhibitor of UGT1A1-mediated UCB conjugation with a IC_{50} of 2.4 µM [348]. Moreover, atazanavir was the first drug used in a human clinical trial with the purpose of inducing iatrogenic GS. As mentioned previously, individuals with T2DM were enrolled in a double-blind randomised cross-over trial where they received atazanavir (300 mg twice daily) for three days. Serum total bilirubin concentrations increased from 7 µM to 64 µM [276]. Both anti-retroviral medications are potentially suitable options for increasing serum UCB concentrations in humans, however,

they induce side-effects in a proportion of patients. A more economical and possibly safer alternative with a potential to increase serum UCB concentrations is the Milk thistle extract [282].

Milk thistle (S*ilybum marianum)* is a fruit native to the Mediterranean that has been used historically for medicinal purposes to treat various hepatic ailments [350]. Milk thistle is comprised of various active ingredients, including a mixture of three flavonolignan compounds, silibinin, silydianin, and silychristine, collectively referred to as silymarin [351]. The most common silymarin preparation is Legalon® and this preparation was recommended by the US National Centre for Complementary and Alternative Medicine for use in future clinical investigations in order to improve consistency and comparability between clinical trials investigating silymarin [352]. Legalon® is a patented formulation of milk thistle extract standardised to contain 140 mg of silymarin in each capsule [353]. A single Legalon® capsule contains silibinin A (21.2 mg), silibinin B (29.5 mg), isosilibinin A (11.4 mg), isosilibinin B (8.2 mg), silichristin (31.5 mg), silidianin (36.4 mg) and taxifolin (5.9 mg) [353].

2.6a Mechanisms of UCB metabolism affected by silymarin

Silymarin can affect UCB metabolism by inhibiting its hepatic uptake, glucuronidation, and biliary transport [354–356]. The major biologically active constituent of silymarin is silibinin and is used as the first line of treatment for *Amanita phalloides* mushroom poisoning [357]. Silibinin hinders hepatic uptake of the *Amanita phalloides* toxin by competitively inhibiting OATP transporters that are also critical for serum UCB uptake into the liver [358,359]. Silibinin inhibits OATP1B3 and OATP2B1 in the presence of estrone-3-sulfate (E3S) with K_i values of 5 and 3.6 µM, respectively. Conversely, up to 1 µM of silibinin stimulates OATP1B1-mediated hepatic uptake of E3S, while greater silibinin concentrations inhibit OATP1B1 activity [354]. Therefore, silymarin and/or silibinin have the potential to inhibit hepatocellular uptake of UCB and prevent subsequent hepatobiliary excretion. Additionally, silibinin competitively inhibits MRP2 in the presence of 17β-estradiol-glucuronide with an IC_{50} of 6.8 µM [354]. These findings are consistent

with the fact that hepatobiliary excretion of silibinin conjugates is dependent on MRP2 transport [360,361]. Genetic MRP2 deficiency in humans leads to conjugated hyperbilirubinaemia, also known as Dubin-Johnson syndrome, because of an impaired ability to excrete bilirubin conjugates through the biliary route [362]. Therefore, silibinin treatment could potentially increase conjugated bilirubin concentrations by decreasing biliary excretion of bilirubin conjugates by competing for MRP2 transport.

Finally, silymarin has the potential to increase serum UCB concentrations by inhibiting UGT1A1 activity and UCB conjugation. Incubation of silymarin constituents with a range of recombinant UGT enzymes in the presence of 7-Hydroxy-4-(trifluoromethyl)coumarin demonstrated that silibinin a potent inhibitor of UGT1A1 with an IC_{50} of 1.4 µM [355]. In contrast, silibinin had a markedly lower potency towards UGT1A1 inhibition in rat and human microsomes isolated from hepatic tissue with 41.5 µM of silibinin attenuating UCB glucuronidation by 40% [356]. The underlying mechanism of discrepancy between these studies remains unknown, however, it could be explained by differences in the source of UGT1A1 protein (i.e. pure recombinant UGT1A1 protein vs microsomal UGT1A1). Interestingly, the conjugated form of silibinin (33 µg mL^{-1}) was the most potent inhibitor of UGT1A1 while the other flavonolignan constituents of silymarin had no effect on UGT1A1 activity [356]. Collectively, these findings strongly support the potential for silibinin to inhibit uptake, conjugation, and excretion of UCB and they explain the association of silymarin therapy with asymptomatic unconjugated hyperbilirubinaemia as described in the following section [22,23,363].

2.6b Clinical evidence of silymarin induced hyperbilirubinemia

In line with the *in vitro* and *ex vivo* findings of silymarin perturbation of enzymes involved in UCB metabolism, several clinical studies have reported increased bilirubin concentrations following silymarin treatment. Consumption of silymarin can induce jaundice [23] and this is reflected by the manufacturers product insert of Legalon® which warns against hyperbilirubinaemia as a potential side-effect of silymarin supplementation. Silymarin has been extensively trialled as a

treatment for various hepatic ailments some of which have reported serum bilirubin concentrations as a secondary outcome.

Flaig et al. assessed the pharmacokinetics and toxicity threshold of a commercial silibinin-phytosome formulation (Siliphos^{R}). Thirteen patients with prostate adenocarcinoma were treated with a range of doses of Siliphos^{R} (2.5 to 20 g daily) with 13 g per day determined to be the threshold for toxicity. At a dose of 13 g per day, the average C_{max} of silibinin was ~75 µM and 50% of courses led to grade 1 (17.1-25.7 µM total bilirubin) and 6% to grade 2 (25.7-51.3 µM total bilirubin) hyperbilirubinaemia [23]. Conversely, the 10 g per day dose of silibinin resulted in 25% of courses ending in grade 1 and 4% in grade 2 hyperbilirubinaemia. Doses below 10 g per day of silibinin did not lead to hyperbilirubinaemia [23]. Importantly, in this study Siliphos^{R} therapy specifically induced unconjugated hyperbilirubinaemia without concurrent increase in conjugated bilirubin which is consistent with silibinin-mediated inhibition of UCB conjugation [23,354–356]. Similar results are observed with intravenous (IV) formulations of silibinin [357,364–367].

Silibinin is hydrophobic and consequently unsuitable for IV administration, thus, silibinin-C-2',3-dihydrogen succinate disodium (Legalon®-SIL) is a hydrophilic analogue for IV administration [357]. Considering that silibinin is a potent antiviral agent, it has been tested in patients with recurrent hepatitis C viral infections (HCV) [368]. HCV patients receiving liver transplant were treated with Legalon®-SIL (20 mg kg^{-1} day^{-1}) for ≥14 days which led to a significant increase in average serum total bilirubin concentrations compared to baseline (80.4 vs 65µM, respectively) [24]. Comparably, Legalon®-SIL (20 mg kg^{-1} day^{-1}) therapy for 14 days in patients with HCV post liver transplant induced a gradual rise in serum total bilirubin concentrations with a peak of ~74 µM on the final day of treatment compared to ~14 µM at baseline [22]. Similarly, in a phase II trial, patients that are non-responding to traditional antiviral therapy received Legalon®-SIL (IV; 20 mg kg^{-1} day^{-1}) as an adjunct treatment to pegylated interferon-2a and ribavirin combination therapy, for 14-21 days [363]. Legalon®-SIL treatment significantly increased serum total

bilirubin concentrations from 16.8 μM at baseline to 36 μM [363]. Collectively, these reports provide strong evidence that silymarin/silibinin treatment has the potential to increase circulating UCB concentrations. Considering the protective effects associated with mildly elevated UCB concentrations, it is important to test whether pharmacological increases in serum total bilirubin could lead to reduced risk of obesity and CVDs.

Legalon® has an excellent safety profile and has the potential to increase serum UCB concentrations. However, no clinical trials in healthy participants have evaluated the effectiveness of Legalon® to increase serum UCB concentrations. The studies evaluated above were all conducted in cohorts with underlying hepatic pathology that influences the metabolism of silymarin and bilirubin. Therefore, it is difficult to determine whether silymarin would have a similar impact on bilirubin concentrations in healthy humans. Future studies in healthy cohorts are critical to establishing the effectiveness of Legalon® treatment to increase serum UCB concentrations and potentially reduce cardiovascular risk.

2.7 Conclusion

Bilirubin is a haem catabolite that is primarily removed from the body via the hepatobiliary route. Although, historically, bilirubin has been classified as toxic, accruing evidence supports a protective role for bilirubin against CVDs. Epidemiological data and animal studies suggest that bilirubin modulates lipid concentrations and prevents obesity. However, these findings are based on associations without mechanistic insight regarding the impact of bilirubin on cholesterol metabolism (i.e. synthesis, transport, or excretion) or bioenergetics (i.e. mitochondrial function). Therefore, it is important to determine whether bilirubin affects cholesterol metabolism and mitochondrial function, to determine whether bilirubin has the potential to reduce the incidence of obesity and CVDs.

Chapter 3: Hypocholesterolaemia in hyperbilirubinaemic rats is associated with increased LDLr expression and elevated biliary lipid excretion

The literature reviewed in Chapter 2 provides strong rationale for the need to study the effects of bilirubin on lipid metabolism. Currently our understanding of bilirubin's effects on cholesterol metabolism are limited to associations from human observational studies and hyperbilirubinaemic animals. Therefore, this study aimed to determine the impact of hyperbilirubinaemia on cholesterol synthesis, transport, and excretion in a rat model of genetic hyperbilirubinaemia. This is the first study to demonstrate that hyperbilirubinaemic female Gunn rats exhibit elevated cholesterol synthesis and biliary lipid excretion and that this occurred along with reduced circulating cholesterol and increased hepatic LDL receptor expression.

3.1 Introduction

Cardiovascular diseases (CVDs) cause the greatest number of deaths globally, taking 17.9 million lives in 2016 [World Health Organisation], with atherosclerosis contributing importantly to CVD mortality. Atherosclerosis is a chronic inflammatory condition that is initiated by subendothelial accumulation of cholesterol which can gradually progress to the formation of large cholesterol rich plaques pervaded with inflammatory cells [33]. The development of atherosclerosis is dependent on the complex interplay between rising plasma cholesterol concentrations and systemic inflammation, thus, elevated cholesterol concentrations are a critical risk factor for CVD mortality [33]. Consequently, medications such as statins have been developed to reduce cholesterol concentrations. Despite the effectiveness of statins to reduce plasma cholesterol concentrations, they are only 20-40% successful at reducing clinical manifestations of atherosclerosis. Moreover, statin related side-effects limit their use in a significant proportion of patients [36]. Therefore, there is an important need for new and more effective medications to prevent and treat CVDs.

Although formerly considered a toxic breakdown product of haem catabolism, growing evidence supports a protective role for unconjugated bilirubin (UCB) against CVDs [243,369]. Individuals with Gilbert's syndrome (GS) have mildly elevated serum concentrations of UCB and are protected from coronary artery disease, ischemic heart disease, atherosclerosis and all-cause mortality [241,267,281,369]. Initially, UCB was demonstrated to possess potent antioxidant activity based on its capacity to scavenge peroxyl radicals [8]. This observation sparked numerous investigations concerning whether UCB could protect against low density lipoprotein (LDL) oxidation, which is hypothesised to initiate atherosclerosis [369]. UCB was shown to function as a co-antioxidant with α-tocopherol to inhibit LDL lipid peroxidation, providing an explanation for how UCB may protect from the development of atherosclerosis [6]. This antioxidant mediated protection extended to inhibition of copper induced lipid peroxidation in individuals with GS [370].

Interestingly, Boon et al. reported that GS individuals demonstrate reduced serum concentrations of oxidised LDL (oxLDL) and total LDL cholesterol (LDL-C) [371]. Therefore, it is unclear whether the antioxidant properties of UCB reduce the formation of oxLDL or whether reduced oxLDL concentrations are a secondary effect due to overall reduction in LDL-C in association with increasing UCB. Recent epidemiological studies show an inverse relationship of UCB with total cholesterol and LDL-C, indicating that UCB potentially functions both as an antioxidant and as a lipid reducing agent [12]. Parallel findings are observed in hyperbilirubinaemic (Gunn) rats who possess a ~50% reduction in serum cholesterol concentrations compared to normobilirubinaemic controls [246]. These data suggest that UCB may induce hypocholesterolaemic effects in addition to its antioxidant potential [12].

Indeed, recent studies demonstrate that UCB is an agonist of peroxisome proliferator activated receptor alpha (PPARα) with equivalent potency to clinically utilised fenofibrate [10]. Additionally, UCB is an atypical agonist of the Aryl hydrocarbon receptor (Ahr) [341]. PPARα and Ahr are ligand-activated transcription factors that regulate genes involved in lipid metabolism, and their activation reduces circulating cholesterol and/or triglyceride concentrations [340,372]. The capacity of UCB to activate these receptors may help to explain the hypocholesterolaemic effects observed in GS and hyperbilirubinaemic animals, however, the *in vivo* activation of these pathways remains poorly described [12].

Hereditary hyperbilirubinaemia is associated with mutations in the UDP-glucuronosyltransferase 1A1 (UGT1A1) gene that result in defective UGT1A1 activity [373]. UGT1A1 is the primary enzyme responsible for UCB conjugation, which is necessary for efficient clearance of UCB. Therefore, impaired UGT1A1 activity leads to elevated plasma UCB concentrations. Gunn rats are a mutant strain of Wistar rats which lack UGT1A1 activity, consequently, they exhibit circulating concentrations of UCB in the upper range of GS making them a suitable model to study the effects of hyperbilirubinaemia on cholesterol metabolism [374]. Several studies have reported reduced plasma concentrations of cholesterol in Gunn rats,

however, it is unknown whether hypocholesterolaemia is caused by decreased *de novo* synthesis or increased clearance of cholesterol [12]. The aim of this study was to investigate the synthesis, clearance, and hepatic transport of cholesterol, and to evaluate whether these effects are sex-dependent in Gunn rats.

3.2 Methods

Chemicals and reagents

All chemicals and reagents were purchased from Sigma Aldrich (Australia) unless otherwise stated.

Animals

Breeding pairs of heterozygote Gunn rats on a Wistar background were imported from the Rat Research and Resource Centre (Columbia, MO, USA) and cross bred to produce either homozygote (jaundiced) or heterozygote (non-jaundiced) Gunn rats. Rats were determined to be homozygote Gunn rats based on the presence of jaundice in the days after birth and were ear-tagged. The hyperbilirubinaemic phenotype was then confirmed by measuring serum bilirubin concentrations. From herein, animals expressing hyperbilirubinaemia are phenotypically defined as "Gunn" rats while those possessing normal bilirubin levels are termed as "wild-type or normobilirubinaemic controls". Animals were housed in the G26 animal house facility at Griffith University, Gold Coast, at constant temperature (20^{o}C) and humidity (60%), with a 12 hr light:dark cycle with usual housing enrichment. All animals were provided a standard rodent diet (18% Protein Rodent Diet, 18% protein, 6.2% fat, cholesterol-free; TEKLAD Standard Global, USA) and water *ad libitum.* All procedures were approved by the Griffith University Animal Ethics Research Committee (MSC/02/17/AEC) prior to experimentation.

Experimental protocol

Adult rats

In total, 36 age-matched animals (~10 weeks and 5 days old) from four litters entered the protocol (Day -1; Table 3.1). At days -1, 10, 14, and 18, animals were housed individually in metabolic cages (see "*Metabolic cages"*). Bodyweight was recorded every 2 days for the duration of the study and was measured before and after each metabolic cage day. Blood samples (approx. 1 mL) were collected at Day 1 and Day 8, after a 6-7 hour fast, via tail bleed (see "*Blood collection*"). During the final four days of the study, drinking water was

supplemented with [1-^{13}C]-acetate (2% w/v) and blood spots were collected bidaily from nonfasted animals (see "*Blood collection*") to determine *in vivo* cholesterol synthesis. On the final day of the study, animals underwent terminal day procedures (see "*Bile duct cannulation and terminal procedures*") and were euthanised via removal of the heart under anaesthesia. In order to control for interventions within future studies, several additional control procedures were conducted. For example, animals were administered 400 µL of drinking water via oral gavage daily and sterile phosphate buffered saline (Gibco®, United Kingdom) was administered every 2 days via intraperitoneal injection (i.p.) from day 1 to day 20.

Juvenile rats

Juvenile (3-4 weeks of age) hyperbilirubinaemic and normobilirubinaemic littermates were fasted for 6 hrs prior to tissue collection. They were anaesthetised using sodium pentobarbital (Lethabarb, Australia) at an initial dosage based on the animal weight (heterozygous 1.3 µL g^{-1}, homozygous 1 µL g^{-1}). Pedal reflexes were checked to ensure the animals were non-responsive to pain. Blood was then collected via the inferior vena cava and animals were euthanised by removal of the heart. Blood was centrifuged (2000 g, 10 mins, 21°C) and the serum was flash frozen in liquid N_2 and stored at -80°C for later analysis.

Metabolic cages

Animals (10 weeks of age) were gradually acclimatised to metabolic cages (2, 5, and 24 hrs, respectively) before entering protocol. In total, animals were housed in metabolic cages 4 times (Day -1, 10, 14, and 18) for a period of 24 hrs each time. Food and water were freely available and were weighed before and after each animal was housed in the metabolic cage to determine daily food and water consumption. Additionally, urine and faeces were collected, weighed, and stored after each metabolic cage day, and the average weight of the 4 individual metabolic cage days was used to report daily food and water consumption, and faecal and urine outputs. Faeces were air-dried for at least 48 hrs prior to weighing.

Blood collection

Animals were anaesthetised with 2-5% isofluorane (Lyppard, Australia) in 100% oxygen via inhalation (1-2 L min^{-1}). Pedal reflexes were tested to ensure the animals were not pain responsive. The tip of the tail (1-2mm) was removed using a sterile scalpel blade and blood was drawn via gentle massage of the tail. The first drop of blood was discarded before collecting 1 mL of blood in a 1.5 mL microtube (Sarstedt, Australia) or ~20 µL (~6 mm in diameter) on a filter paper (Sartorius, France). Blood was then left to coagulate for at least 10 min before centrifuging (2000 g, 10 mins at 21°C), while blood spots were left to air-dry for at least 24 hrs prior to storage. Serum was flash frozen and stored at -80°C for later analysis.

Bile duct cannulation and terminal procedures

On day 20 of the protocol, rats were anaesthetised using a ketamine (50 mg kg^{-1}) and xylazine (3 mg kg^{-1}) mixture in a 50:30 ratio via intraperitoneal injection. Additional anaesthetic was administered as necessary in order maintain a surgical plane of anaesthesia. Pedal reflexes were routinely checked prior to and during the procedure. Body temperature was maintained using a heating pad and the temperature was monitored with a rectal probe. A midline laparotomy allowed access to and identification of the common bile duct, with the aid of a dissecting microscope. The bile duct was cannulated with 0.78 OD x 0.32 ID mm tubing (Microtube Extrusions, Australia) and secured in place with a drop of superglue and sutures. Once the bile duct was secured, the abdomen was closed and secured with sutures to maintain body temperature. In total, bile was collected for 35 mins, the first 5 mins of which was discarded with the following 30 mins of bile flow collected into pre-weighed 1.5 mL microtubes on ice. During the procedure, bile was protected from light by covering the collection tube with foil. Immediately after bile collection, tubes were weighed, and flash frozen in liquid N_2 and stored at -80°C. Bile flow was determined gravimetrically assuming a density of 1 g mL^{-1}. Rates of lipid excretion were calculated using bile flow and biliary lipid concentrations. After surgery, blood was collected from the inferior vena cava and centrifuged (2000 g, 10 mins, 4°C). The supernatant was flash frozen in liquid N_2 and stored at -80°C. Liver tissue was rinsed with cold

dPBS (Gibco®, United Kingdom) and one section was flash frozen with liquid N_2 while another added to RNAlater solution (Invitrogen, Australia) prior to flash freezing in liquid N_2. All samples were subsequently stored at -80^{o}C for later analysis.

Biochemistry analysis

Analysis of serum, bile, liver, and faecal biochemistry were conducted using enzymatic, colorimetric assays, via the COBAS Integra 400+ (Roche Diagnostics, Australia) or using gas chromatography mass spectrometry (GS/MS) as described later (see "*Gas chromatography mass spectrometry analysis*"). Lipid concentrations were assessed using total cholesterol (CHOL Gen. 2, Roche Diagnostics), high density lipoprotein cholesterol (HDL-C Gen. 3, Roche Diagnostics), triglycerides (TRIGL, Roche Diagnostics), total bile acids (Total Bile Acids #BI3863, RANDOX, Australia) and phospholipids (Phospholipids C #997-01801, Wako, Japan). Additionally, total bilirubin (BIL-T Gen. 3, Roche Diagnostics), direct bilirubin (BIL-D Gen. 2, Roche Diagnostics), and albumin (ALB Gen. 2, Roche Diagnostics) were measured to differentiate between hyperbilirubinaemic and normobilirubinaemic phenotypes. All biochemical analysis kits were verified with their appropriate calibrators and quality controls prior to sample analysis.

Gas chromatography mass spectrometry analysis

Cholesterol label enrichment, biliary cholesterol concentration and biliary bile acid species were measured as previously published [375]. Briefly, cholesterol was extracted from blood spots or bile and derivatised with N,O-Bis (trimethylsilyl) trifluoroacetamide (BSTFA) containing 1% trimethylchlorosilane before analysis with GS/MS (Agilent 7890A and 5975c, respectively; Netherlands). Isotope ratios were determined by selected ion monitoring mode on m/z 458 (M0) to 465 (M7). The rate of cholesterol synthesis was calculated as previously published [375]. Biliary bile acids were extracted and derivatised with BSTFA-pyridine-trimethylchlorosilane (5:5:0.1) and were quantified using GC/MS. Samples that contained biliary bile acid species below the quantification limit were calculated by dividing the limit of quantification by square

root of two as previously published [376]. Hydrophobicity index of biliary bile acid composition was calculated according to Heuman et al. [377].

Lipid extraction

Frozen liver tissue (~100 mg) was homogenised while frozen (liquid N_2) using a mortar and pestle and stored at -80°C for later lipid extraction. Similarly, dried faeces were homogenised using a mortar and pestle and stored at room temperature (RT) for later lipid extraction. Lipids were extracted from homogenised liver and faecal samples by three sequential solvent extractions with isopropyl-alcohol at a 50:1 mg:mL ratio of sample (liver or faeces) to isopropyl-alcohol as previously published [378] with method validation provided in Appendix 4. During each extraction, homogenates were vortexed vigorously and sonicated at RT for 10 mins and then centrifuged (43000 g, 20°C, 10 mins). The three supernatant fractions were collected in a separate tube and evaporated using a rotary evaporator (Maxivac, Labogene, Australia) at 35°C. Dry pellets were reconstituted in 250 µL of isopropanol and analysed for cholesterol and/or triglycerides (see "*Biochemistry analysis*"). Isopropanol was tested for assay interference and was determined not to affect cholesterol or triglyceride measurements.

PCR array

Liver samples preserved in RNAlater were homogenised in TRIzol® reagent (Invitrogen, Australia), and the total RNA was isolated with RNA extraction kits (Qiagen, Australia) as previously published [379]. The concentration and purity of RNA was analysed using spectrophotometry (NanoDrop, Thermo Scientific, Australia). First-strand cDNA synthesis kits (Qiagen) were used to synthesise cDNA from total RNA according to the manufacturer's protocol and synthesised cDNA was stored at -20°C for later analysis. The rat lipoprotein signalling and cholesterol metabolism RT² Profiler PCR Arrays (Qiagen) were utilised to measure expression of 84 key genes using the CFX96 Real-Time PCR Detection System (Bio-Rad, Australia). All data acquisition was performed with CFX Manager 2.0 software (Bio-Rad). Relative mRNA expression

was calculated using the web-based GeneGlobe Data Analysis Centre (Qiagen) and normalised to β-actin expression.

Western blot

Frozen liver samples were homogenised mechanically by passing tissue sequentially through 18-23G needles in CelLytic MT Cell Lysis buffer (#C3228) in the presence of protease inhibitor (P8340) and phosphatase inhibitor (#ab201114, Abcam, USA) as per manufacturer's protocol. The tissue supernatant was generated by centrifugation (4000 g for 10 mins, 4°C) and standardised based on protein concentration using the Pierce BCA Protein Assay Kit (ThermoFisher Scientific, Australia) as per manufacturer's protocol. Standardised samples were prepared in Laemmli 2X buffer (#S3401) at 1:1 ratio and were heated for 5 mins at 95°C or unheated (ABCA1 protein), prior to loading. Proteins (10-30 µg) were separated on SDS-PAGE (7.5, 10, or 12%) using TGX™ FastCast™ acrylamide kits (#1610171, #1610173, and #1610175, Bio-Rad). After electrophoresis, proteins were transferred onto 0.45 µm polyvinylidene fluoride membranes (PVDF; #IPFL0010, Millipore, Australia) for 1-2 hrs on ice, in Towbin buffer (25 mM Tris, 192 mM glycine, and 20% v/v methanol). Following transfer, membranes were blocked with Odyssey Blocking Buffer (Millenium Science, Australia) and incubated with primary antibodies (HMGCR, #ab174830; SREBP2, #ab30682; B-actin, #ab8226; GAPDH, #sc-32233; CYB5R3, #ab109620; LDLr, #ab30532; CYP7A1, #ab65596; ABCA1, #ab18180) overnight at 4°C with gentle agitation. Finally, membranes were incubated with secondary antibodies (#IRDye 680 or #IRDye 800CW, LI-COR, Australia) for 1 hr with gentle agitation at room temperature and visualised using Odyssey CLX Infrared Imaging System (LI-COR). Densitometric analysis of target proteins were normalised to GAPDH or B-actin. The linear range of detection was determined for each target and housekeeping (GAPDH and B-actin) proteins prior to analysis, as described in Appendix 4. All densitometric analyses were conducted using 5.2 Image Studio Lite (LI-COR). Validation of the analysed target protein bands are presented in Appendix 1.

Statistical analysis

All values are expressed as mean ± standard deviation (SD). Data was tested for normality and homogeneity of variance with Kolmogorov-Smirnov and Spearman tests, respectively. Comparisons between phenotype from the same sex was performed using unpaired t-tests. However, in cases where data was not normally distributed or variance differed between groups nonparametric Mann-Whitney test and Welch's correction were used, respectively. Statistical analysis was performed in GraphPad PRISM (v8.2) and a $P<0.05$ was considered statistically significant.

Table 3.1. Detailed protocol for the timing of procedures.

Procedures	**-1**	**0**	**1**	**2**	**3**	**4**	**5**	**6**	**7**	**8**	**9**	**10**	**11**	**12**	**13**	**14**	**15**	**16**	**17**	**18**	**19**
Bodyweight (all groups)	↑	↑	↑		↑		↑		↑		↑		↑		↑		↑		↑		↑
Metabolic cage (food intake, faeces/urine collection)	↑											↑				↑				↑	
Blood samples (above)/blood spots (below)		↑							↑												
																	↑	↑↑	↑↑	↑↑	↑
Vehicle i.p. injections			↑		↑		↑		↑		↑		↑		↑		↑		↑		↑
H_2O oral gavage			↑	↑	↑	↑	↑	↑	↑	↑	↑	↑	↑	↑	↑	↑	↑	↑	↑	↑	↑
[^{13}C]-acetate																		↑	↑	↑	↑
Terminal procedures and bile-duct cannulation																					↑

Note: arrow (↑) indicates on which day a selected procedure is performed. Double arrow (↑↑) indicates that the procedure was performed twice (12 hrs apart).

3.3 Results

Perturbed serum lipid concentrations in adult female Gunn rats

A total of 19 adult (14 weeks old) homozygote hyperbilirubinaemic Gunn rats and 17 adult heterozygote normobilirubinaemic littermates (controls) were assessed for circulating lipid concentrations (see Table 3.2). Hyperbilirubinaemia was confirmed in male and female Gunn rats as indicated by elevated serum total bilirubin concentrations compared to controls ($P<0.001$; Table 3.2). Total cholesterol and HDL-C were significantly reduced in female Gunn rats compared to controls ($P<0.001$; Table 3.2). Male Gunn rats tended to have reduced total cholesterol ($P=0.14$) with negligible difference in HDL-C versus controls (Table 3.2). Conversely, serum triglyceride concentrations were not different in either group (Table 3.2). However, phospholipids were significantly reduced, while bile acids were increased in female Gunn rats compared to controls ($P<0.01$, $P<0.05$, respectively; Table 3.2). In male Gunn rats, phospholipids and bile acids were not different compared to controls (Table 3.2).

Circulating lipid concentrations in juvenile Gunn rats

The sex-dependent effect on lipid concentrations in Gunn rats suggests that sex hormones potentially affect the impact of hyperbilirubinaemia. Therefore, to minimise the effects of hormones, lipid concentrations were assessed in juvenile animals that had not reached reproductive maturity (3-4 weeks of age; Table 3.2). Circulating total cholesterol and HDL-C concentrations were not different in females, in contrast, they were significantly reduced in male Gunn rats compared to controls ($P<0.01$, $P<0.05$, respectively; Table 3.2). Finally, triglycerides and bile acids were not different across groups, while phospholipids were significantly reduced in male Gunn rats ($P<0.05$) with a similar trend observed in female Gunn rats versus controls ($P=0.10$; Table 3.2).

Table 3.2. Serum biochemistry of juvenile and adult rats.

Variable	Juvenile[a]		Adult[b]		P value
	Control	Gunn	Control	Gunn	
Albumin (g L^{-1})					
• Males	30.7 (3.25)	27.1 (7.66)	40.2 (2.87)	43.4 (3.30)	0.21[a], 0.05[b]
• Females	30.5 (1.72)	34.5 (8.86)	44.7 (5.08)	44.1 (3.32)	0.29[a], 0.77[b]
Total bilirubin (µmol L^{-1})					
• Males	2.29 (1.53)	72.6 (32.0)	2.29 (1.02)	109 (15.0)	**<0.001[a], <0.001[b]**
• Females	2.28 (0.54)	83.9 (34.2)	2.13 (1.54)	64.8 (13.8)	**<0.001[a], <0.001[b]**
Direct bilirubin (µmol L^{-1})					
• Males	1.80 (1.29)	11.3 (3.66)	1.24 (0.62)	8.04 (0.99)	**<0.001[a], <0.001[b]**
• Females	1.44 (0.31)	10.9 (5.25)	1.50 (1.08)	7.11 (1.40)	**<0.01[a], <0.001[b]**
Total cholesterol (mmol L^{-1})					
• Males	1.79 (0.51)	1.21 (0.30)	1.56 (0.23)	1.41 (0.15)	**<0.01[a],** 0.14[b]
• Females	1.45 (0.32)	1.17 (0.34)	1.56 (0.34)	0.60 (0.12)	0.18[a], **<0.001[b]**
HDL-C (mmol L^{-1})					
• Males	1.23 (0.43)	0.89 (0.25)	1.33 (0.22)	1.37 (0.16)	**<0.05[a],** 0.70[b]
• Females	0.99 (0.24)	0.82 (0.32)	1.39 (0.25)	0.20 (0.09)	0.35[a], **<0.001[b]**
Triglycerides (mmol L^{-1})					
• Males	0.93 (0.27)	0.88 (0.32)	1.04 (0.56)	1.19 (0.52)	0.72[a], 0.59[b]
• Females	0.89 (0.08)	1.04 (0.55)	0.87 (0.66)	0.98 (0.37)	0.51[a], 0.68[b]
Phospholipids (mg dL^{-1})					
• Males	156 (38.0)	120 (21.6)	128 (18.1)	129 (12.9)	**<0.05[a],** 0.93[b]
• Females	141 (17.9)	115 (26.7)	130 (29.2)	94.0 (11.9)	0.10[a], **<0.01**[b]
Total bile acids (µmol L^{-1})					
• Males	100 (72.7)	93.2 (61.3)	16.0 (11.0)	14.2 (4.47)	0.82[a], 0.71[b]
• Females	157 (86.0)	134 (69.3)	16.3 (7.35)	41.7 (27.1)	0.63[a], **<0.05[b]**

Note: Control group represents normobilirubinaemic heterozygote littermates. Gunn group represents hyperbilirubinaemic homozygote littermates. Juveniles were 3-4 weeks of age (females: control n=5, Gunn n=7; males: control n=8, Gunn n=10). Adult rats were 14 weeks of age (females: control n=9, Gunn n=10; males: control n=8, Gunn n=9). Abbreviations: HDL-C, high-density lipoprotein cholesterol. Values are represented as mean (standard deviation). All comparisons are made between phenotype of the same age group and within the same sex.

Adult female Gunn rats have reduced bodyweight and consume fewer calories

Adult rats were housed in metabolic cages for 24 hrs on four different days to assess daily food and water intake, and faecal and urine output (Table 3.3). Female Gunn rats had reduced bodyweight compared to controls ($P<0.001$), with a similar trend observed in male Gunn rats ($P=0.07$; Table 3.3). Similarly, food intake was reduced in female Gunn rats ($P<0.01$), however, there was no difference in male Gunn rats compared to controls (Table 3.3). No difference in daily urine and faecal excretion existed across all groups (Table 3.3).

Table 3.3. Terminal bodyweight, daily food and water intake, and excretion of urine and faeces in adult rats.

Variable	Phenotype		P value
	Control	Gunn	
Bodyweight (g)			
• Males	416 (42.7)	382 (27.4)	0.07
• Females	246 (16.2)	191 (12.8)	**<0.001**
Food intake (kcal day^{-1})			
• Males	80.6 (13.1)	79.2 (6.12)	0.78
• Females	61.9 (5.72)	52.5 (5.25)	**<0.01**
Water intake (g day^{-1})			
• Males	33.3 (8.95)	32.5 (7.13)	0.86
• Females	32.0 (9.04)	28.3 (7.41)	0.34
Urine output (g day^{-1})			
• Males	21.3 (6.59)	21.0 (5.92)	0.91
• Females	20.8 (10.2)	17.7 (7.85)	0.47
Faecal output (g day^{-1})			
• Males	5.20 (0.53)	4.75 (0.81)	0.20
• Females	4.11 (1.02)	4.33 (0.58)	0.57

Note: Control group represents normobilirubinaemic heterozygote littermates. Gunn group represents hyperbilirubinaemic homozygote littermates. Adult rats were 14 weeks of age (females: control n=9, Gunn n=10; males: control n=8, Gunn n=9). Daily measures are an average of 4 separate days measured during the study. Values are represented as mean (standard deviation). All comparisons are made between phenotype within the same sex.

Adult female Gunn rats demonstrate elevated fractional cholesterol synthesis

To investigate cholesterol synthesis *in vivo*, acetate pools were enriched with [1-^{13}C]-acetate supplementation in the diet. Fractional cholesterol synthesis reflects the *in vivo* rate of cholesterol synthesis determined by the fractional contribution of newly synthesised [^{13}C]-enriched cholesterol ([^{13}C]-cholesterol) to the overall circulating pool of cholesterol at steady state. Female Gunn rats had a significantly greater rate of serum fractional cholesterol synthesis compared to normobilirubinaemic female controls (33.8 ± 3.77 vs 28.4 ± 5.73%, respectively; P<0.05), while male Gunn and control rats showed no difference (18.1 ± 5.98% vs 21.3 ± 4.40%, Gunn vs controls, respectively; ns; Fig. 3.1A). Considering that circulating levels of total cholesterol were reduced despite an increased fractional rate of cholesterol synthesis in female Gunn rats, cholesterol storage in the liver was assessed. However, no difference in hepatic cholesterol content existed between groups (Fig. 3.1B).

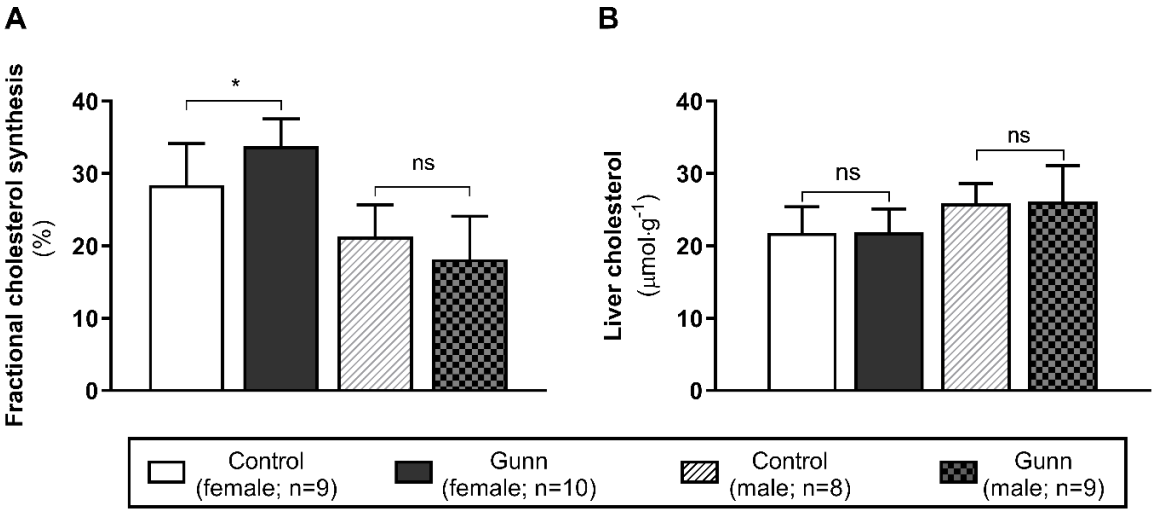

Figure 3.1. De novo fractional cholesterol synthesis and hepatic cholesterol content of adult Gunn (hyperbilirubinaemic) and control (normobilirubinaemic) rats. A) The rate of serum fractional cholesterol synthesis measured as a percentage (%) of newly formed ^{13}C-cholesterol at steady state B) Total cholesterol content per gram of liver tissue. Data are presented as means (standard deviation). Significant differences are presented as P<0.05*, <0.01**, <0.001*** compared to controls of the same sex. Nonsignificant differences are presented as "ns".

Increased biliary and total cholesterol output in adult female Gunn rats

Since hepatic cholesterol content was not different between Gunn and control female rats, it was hypothesised that lipid excretion was enhanced in female Gunn rats. Therefore, biliary and faecal lipid output was assessed. Female Gunn rats demonstrated a significant increase in bile flow (0.67 ± 0.13 vs 0.47 ± 0.06 mL hr^{-1} $100g^{-1}$ BW; P<0.01), biliary cholesterol excretion (232 ± 32.7 vs 141 ± 42.1 nmol hr^{-1} $100g^{-1}$ BW; P<0.001), and biliary phospholipid output (1.69 ± 0.30 vs 0.97 ± 0.36 mg hr^{-1} $100g^{-1}$ BW; P<0.01) compared to controls. Additionally, a trend towards increased biliary bile acid output (7.34 ± 1.75 vs 5.50 ± 1.67 µmol hr^{-1} $100g^{-1}$ BW; P=0.11; Fig. 3.2) occurred in female Gunn rats. Conversely, male Gunn rats demonstrated increased biliary phospholipid excretion (0.75 ± 0.18 vs 0.61 ± 0.16 mg hr^{-1} $100g^{-1}$ BW; P<0.05) versus controls (Fig. 3.2). Biliary lipid (cholesterol+phospholipid) excretion relative to bile acid output was significantly increased in female Gunn rats compared to controls (0.33 ± 0.06 vs 0.24 ± 0.03 mol:mol, lipid:bile acids; P<0.01) with a similar trend observed in male Gunn rats (0.31 ± 0.07 vs 0.25 ± 0.04 mol:mol, lipid:bile acids, Gunn vs controls; P=0.08; Fig. 3.2F). Gunn rats exhibited reduced biliary bilirubin excretion compared to controls (P<0.001; Fig. 3.2E). Daily faecal cholesterol output was significantly greater in female Gunn rats compared to controls (18.1 ± 1.73 vs 13.4 ± 4.28 µmol day^{-1} $100g^{-1}$ BW; P<0.05; Fig. 3.3).

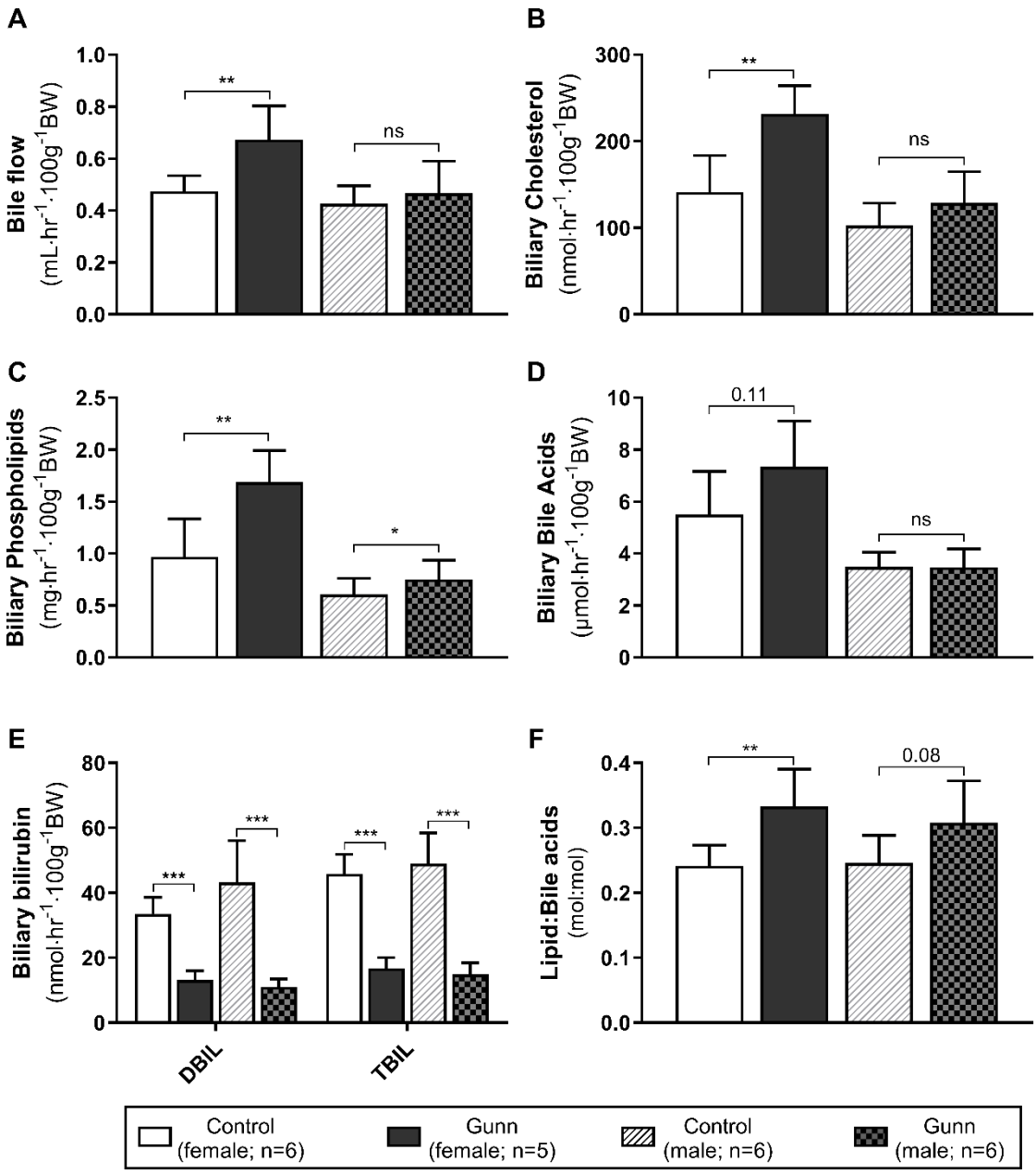

Figure 3.2. Biliary lipid and faecal cholesterol output of adult Gunn (hyperbilirubinaemic) and control (normobilirubinaemic) rats. A) Bile flow rate normalised for bodyweight. B-E) Total cholesterol, phospholipids, bile acids, and bilirubin excreted through bile normalised for bodyweight. F) Biliary lipid (cholesterol+phospholipid) relative to bile acid excretion (mol:mol). DBIL, direct bilirubin; TBIL, total bilirubin. Data are presented as means (standard deviation). Significant differences are presented as P<0.05*, <0.01**, <0.001*** compared to controls of the same sex. Nonsignificant differences are indicated as "ns".

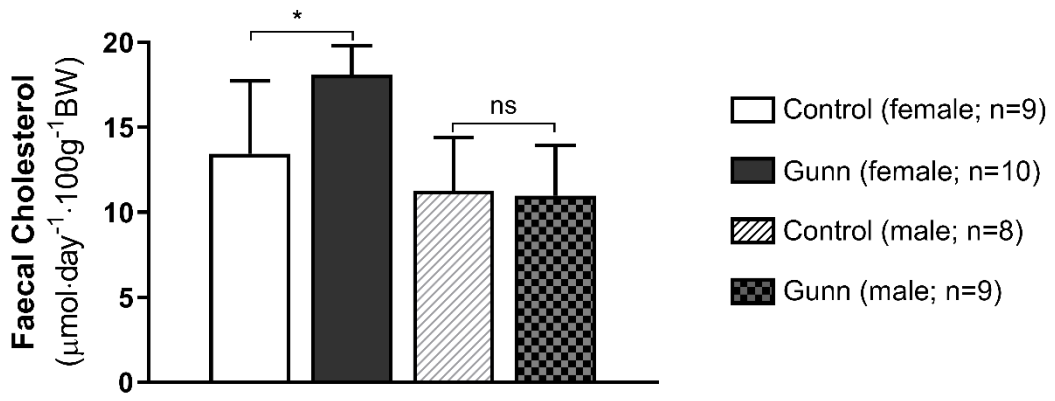

Figure 3.3. Daily faecal cholesterol excreted normalised for bodyweight of adult Gunn (hyperbilirubinaemic) and control (normobilirubinaemic) rats. Data are presented as means (standard deviation). Significant differences are presented as P<0.05*, <0.01**, <0.001*** compared to controls of the same sex. Nonsignificant differences are indicated as "ns".

Altered bile acid composition in bile of adult female Gunn rats

The biliary excretion of individual bile acid species was analysed from adult rats. Biliary excretion of tauro-ursodeoxycholic acid (TUDCA; $P<0.05$), glyco-chenodeoxycholic acid (GCDCA; $P<0.01$), and glycol-hyodeoxycholic acid (GHDCA; $P<0.05$), was significantly greater while tauro-cholic acid (TCA; $P<0.05$) was significantly reduced in female Gunn rats compared to controls (Table 3.4). In contrast, no significant differences in the excretion of individual bile acids were observed in male Gunn rats and controls (Table 3.4). Relative excretion of individual bile acid species were expressed as a percentage of total bile acid excretion. Relative excretion of glyco-UDCA (GUDCA; $P<0.05$), TUDCA ($P<0.01$), GCDCA ($P<0.001$), glyco-deoxycholic acid (GDCA; $P<0.05$), beta-muricholic acid (β-MCA; $P<0.05$), omega-MCA (O-MCA; $P<0.05$), tauro-β-MCA (Tβ-MCA; $P<0.05$) and GHDCA ($P<0.05$) were significantly increased while TCA ($P<0.01$) output was decreased in female Gunn rats versus controls (Table 3.4 and Fig. 3.4). Relative excretion of glycine conjugated bile acids (Gly-BAs) were significantly greater ($P<0.01$) in female Gunn rats with a corresponding significant decrease ($P<0.05$) in taurine conjugated BAs (Tau-BAs) versus controls (Table 3.4). In male rats, only relative TA-MCA output was significantly increased in Gunn rats compared to controls ($P<0.05$; Table 3.4 and Fig. 3.4). Other data that were not significantly different between groups are listed in Table 3.4 and Fig. 3.4.

Table 3.4. Biliary bile acid species of adult Gunn (hyperbilirubinaemic) and control (normobilirubinaemic) rats.

		Females[a]		Males[b]		
Variable		Control	Gunn	Control	Gunn	**P value**
CA	µmol	0.13 (0.09)	0.26 (0.25)	0.14 (0.09)	0.10 (0.04)	0.27[a], 0.41[b]
	µmol (%)	1.51 (0.74)	3.11 (2.44)	1.01 (0.68)	0.82 (0.26)	0.16[a], 0.54[b]
GUDCA	µmol	0.04 (0.01)	0.08 (0.05)	0.06 (0.01)	0.06 (0.02)	0.09[a], 0.77[b]
	µmol (%)	0.54 (0.09)	1.08 (0.48)	0.46 (0.13)	0.53 (0.24)	**<0.05[a]**, 0.55[b]
GCA	µmol	0.39 (0.12)	0.41 (0.20)	0.57 (0.50)	0.33 (0.13)	0.86[a], 0.29[b]
	µmol (%)	5.00 (0.98)	5.55 (1.66)	4.06 (3.40)	2.65 (1.23)	0.51[a], 0.36[b]
TUDCA	µmol	0.07 (0.03)	0.30 (0.18)	0.30 (0.10)	0.26 (0.12)	**<0.05[a]**, 0.53[b]
	µmol (%)	0.85 (0.30)	3.81 (1.57)	2.13 (0.58)	1.96 (0.39)	**<0.01[a]**, 0.56[b]
TCA	µmol	3.41 (1.43)	1.54 (0.48)	5.74 (1.48)	5.76 (2.67)	**<0.05[a]**, 0.99[b]
	µmol (%)	43.3 (9.74)	21.9 (5.97)	40.4 (5.64)	42.9 (8.46)	**<0.01[a]**, 0.56[b]
CDCA	µmol	0.04 (0.01)	0.04 (0.01)	0.06 (0.01)	0.06 (0.02)	0.52[a], 0.77[b]
	µmol (%)	0.54 (0.09)	0.65 (0.20)	0.46 (0.13)	0.53 (0.24)	0.28[a], 0.55[b]
GCDCA	µmol	0.10 (0.05)	0.26 (0.10)	0.10 (0.05)	0.10 (0.05)	**<0.01[a]**, 0.90[b]
	µmol (%)	1.31 (0.59)	3.57 (0.90)	0.72 (0.36)	0.89 (0.50)	**<0.001[a]**, 0.51[b]
GDCA	µmol	0.04 (0.01)	0.05 (0.01)	0.08 (0.05)	0.06 (0.02)	0.12[a], 0.36[b]
	µmol (%)	0.54 (0.09)	0.73 (0.13)	0.58 (0.32)	0.53 (0.24)	**<0.05[a]**, 0.77[b]
TCDCA	µmol	0.92 (0.47)	1.20 (0.62)	0.92 (0.22)	1.22 (0.40)	0.42[a], 0.14[b]
	µmol (%)	11.2 (2.88)	16.6 (7.00)	6.65 (1.70)	10.2 (4.47)	0.11[a], 0.10[b]
TDCA	µmol	0.10 (0.04)	0.07 (0.03)	0.41 (0.14)	0.37 (0.25)	0.26[a], 0.78[b]
	µmol (%)	1.29 (0.46)	1.04 (0.41)	3.09 (1.30)	2.65 (1.32)	0.38[a], 0.57[b]
TLCA	µmol	0.04 (0.01)	0.04 (0.01)	0.06 (0.01)	0.06 (0.02)	0.52[a], 0.77[b]
	µmol (%)	0.54 (0.09)	0.65 (0.20)	0.46 (0.13)	0.53 (0.24)	0.28[a], 0.55[b]
GLCA	µmol	0.04 (0.01)	0.04 (0.01)	0.06 (0.01)	0.06 (0.02)	0.52[a], 0.77[b]
	µmol (%)	0.54 (0.09)	0.65 (0.20)	0.46 (0.13)	0.53 (0.24)	0.28[a], 0.55[b]
α-MCA	µmol	0.05 (0.02)	0.19 (0.18)	0.06 (0.01)	0.06 (0.02)	0.11[a], 0.77[b]
	µmol (%)	0.68 (0.24)	2.26 (1.95)	0.46 (0.13)	0.53 (0.24)	0.08[a], 0.55[b]
β-MCA	µmol	0.04 (0.01)	0.09 (0.06)	0.06 (0.01)	0.06 (0.02)	0.09[a], 0.77[b]
	µmol (%)	0.54 (0.09)	1.16 (0.61)	0.46 (0.13)	0.53 (0.24)	**<0.05[a]**, 0.55[b]
O-MCA	µmol	0.04 (0.01)	0.09 (0.07)	0.06 (0.01)	0.06 (0.02)	0.09[a], 0.77[b]
	µmol (%)	0.54 (0.09)	1.23 (0.69)	0.46 (0.13)	0.53 (0.24)	**<0.05[a]**, 0.55[b]
Tα-MCA	µmol	1.34 (0.50)	1.29 (0.39)	1.39 (0.27)	1.59 (0.34)	0.87[a], 0.29[b]
	µmol (%)	17.2 (5.58)	17.6 (1.47)	9.92 (1.28)	12.6 (1.70)	0.89[a], **<0.05[b]**
Tβ-MCA	µmol	0.24 (0.11)	0.42 (0.22)	2.49 (2.41)	1.29 (0.95)	0.10[a], 0.28[b]
	µmol (%)	3.08 (0.88)	5.58 (1.71)	15.9 (10.7)	9.13 (3.95)	**<0.05[a]**, 0.17[b]
HDCA	µmol	0.04 (0.01)	0.05 (0.01)	0.06 (0.01)	0.06 (0.02)	0.14[a], 0.77[b]
	µmol (%)	0.54 (0.09)	0.69 (0.14)	0.46 (0.13)	0.53 (0.24)	0.06[a], 0.55[b]
GHDCA	µmol	0.11 (0.05)	0.20 (0.10)	0.14 (0.09)	0.12 (0.06)	0.07[a], 0.65[b]
	µmol (%)	1.46 (0.76)	2.76 (0.85)	1.01 (0.64)	1.02 (0.60)	**<0.05[a]**, 0.97[b]
THDCA	µmol	0.67 (0.20)	0.68 (0.21)	1.60 (0.82)	1.34 (0.40)	0.91[a], 0.50[b]
	µmol (%)	8.75 (2.50)	9.34 (1.20)	10.8 (2.97)	10.4 (1.77)	0.64[a], 0.82[b]
Gly-BAs	µmol	0.72 (0.21)	1.05 (0.39)	1.02 (0.69)	0.74 (0.23)	0.11[a], 0.37[b]
	µmol (%)	9.39 (2.11)	14.3 (2.39)	7.29 (4.70)	89.4 (5.71)	**<0.01[a]**, 0.62[b]
Tau-BAs	µmol	6.77 (2.27)	5.55 (1.53)	12.9 (4.36)	11.9 (4.33)	0.33[a], 0.69[b]
	µmol (%)	86.3 (2.52)	76.6 (7.30)	6.16 (2.55)	90.4 (3.62)	**<0.05[a]**, 0.73[b]
Hydrophobicity index		-0.12 (0.04)	-0.12 (0.06)	-0.18 (0.10)	-0.14 (0.03)	0.90[a], 0.28[b]

Note: Bile was collected over 30 mins, however, total output was adjusted for an hour of bile excretion. Percentage (%) excretion of individual bile acid species was calculated relative to total bile acid excretion. Abbreviations: CA, cholic acid; DCA, deoxycholic acid; CDCA,

chenodeoxycholic acid; UDCA, ursodeoxycholic acid; HDCA, hyodeoxycholic acid; α/β/O-MCA, alpha/beta/omega-muricholic acid; T and G prefixes represent taurine and glycine conjugated bile acids, respectively; Gly-BAs, glycine conjugated bile acids; Tau-BAs, taurine conjugated bile acids. Data are presented as means (standard deviation). [a] and [b] are P values of comparisons between female and male groups, respectively.

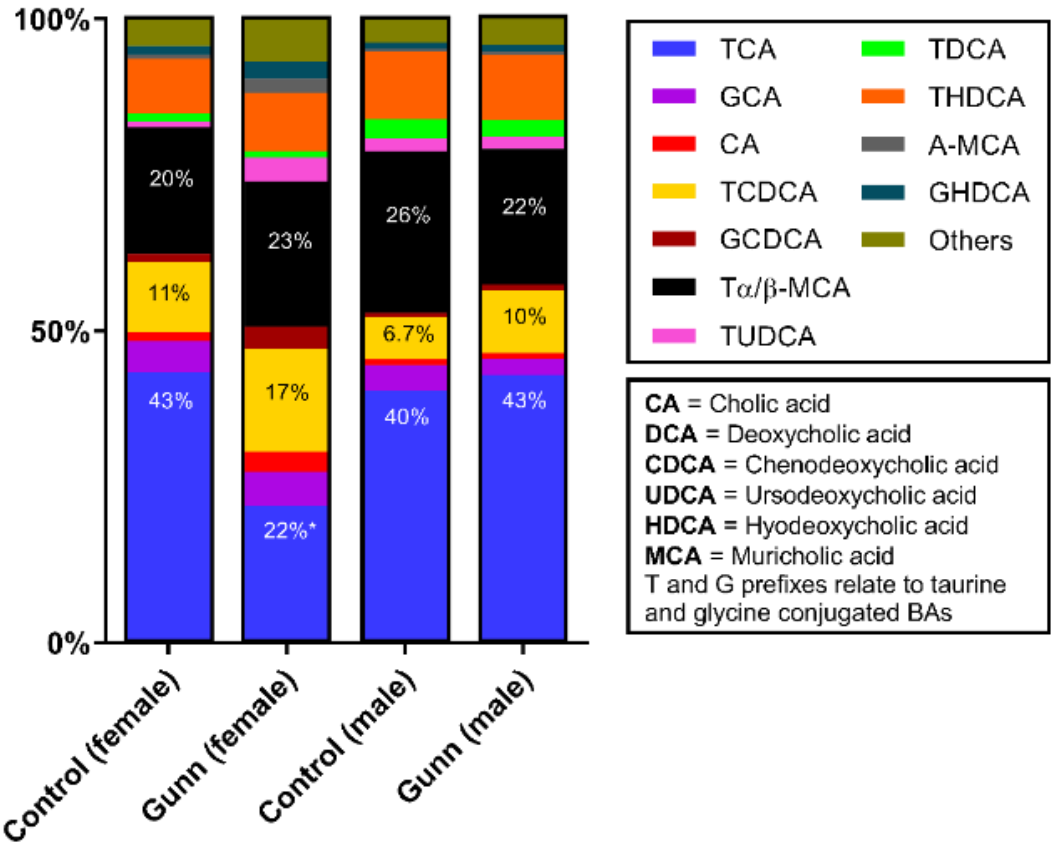

Figure 3.4. Relative composition of biliary bile acid species of adult Gunn (hyperbilirubinaemic) and control (normobilirubinaemic) rats. Bile acid species are presented as a mole percentage (%) of total bile acids excreted over an hour. "Others" represents the sum contribution of GUDCA, CDCA, GDCA, TLCA, GLCA, β-MCA, O-MCA and HDCA. Significant differences are presented as P<0.05* compared to control of the same gender.

Perturbed expression of genes involved in cholesterol metabolism in female Gunn rats

In order to ascertain whether differences in circulating lipid concentrations and biliary/faecal lipid excretion were associated to the expression of genes regulating lipid metabolism and transport, PCR analysis was performed in liver tissue of female adult rats (Fig. 3.5). The expression of genes regulating several enzymes within the cholesterol synthesis pathway including PMVK and CYB5R3 were significantly decreased ($P<0.05$; Fig. 3.5A) while expression of HMGCR, the rate-limiting enzyme of cholesterol synthesis, was not different between groups (1.14-fold increase in female Gunn rats vs controls; NS; Appendix 1, Table S3.1). Furthermore, several genes involved in lipoprotein transport were different between groups. The expression of LRP6 and lipoprotein associated proteins, Colec12 and Apof, were significantly reduced, while LDLr was significantly upregulated in female Gunn rats versus controls ($P<0.05$; Fig. 3.5A). Additionally, the gene responsible for cholesterol esterification (Soat2) was significantly increased in female Gunn rats compared to controls ($P<0.05$; Fig. 3.5A). Finally, genes that tended to differ between groups ($P<0.10$) are shown in Fig. 3.5B, while the remaining genes that were not significantly affected are provided in Appendix 1, Table S3.1.

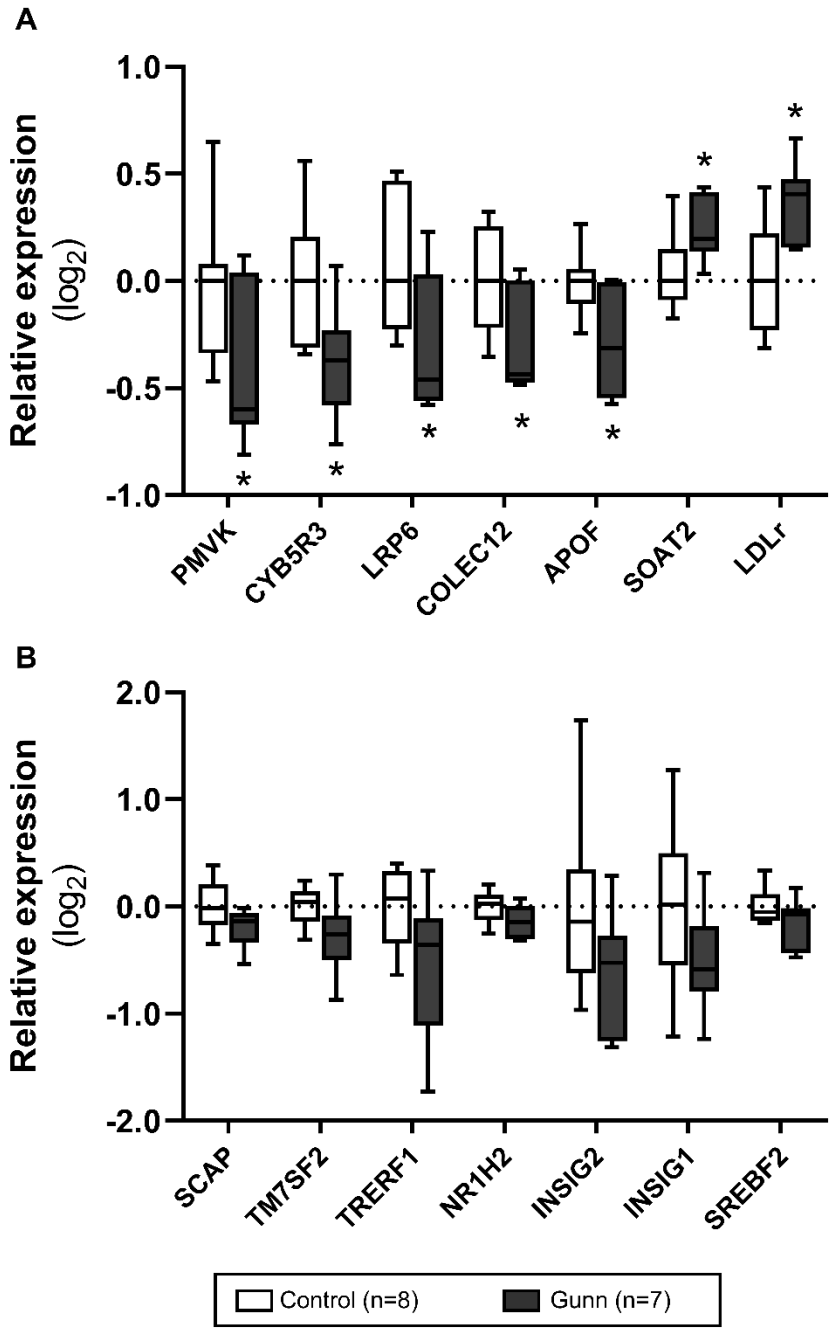

Figure 3.5. Hepatic gene expression of female adult Gunn (hyperbilirubinaemic) and control (normobilirubinaemic) rats. A) Genes that were significantly different between groups (P<0.05). B) Genes that tended (P<0.10) to demonstrate differences. *P<0.05 versus control group. Abbreviations: PMVK, phosphomevalonate kinase; CYB5R3, NADH- cytochrome b5 reductase 3; LRP6, low-density lipoprotein receptor-related protein 6; COLEC12, collectin12; APOF, apolipoprotein F; SOAT2, sterol O-acyltransferase 2; LDLr, low-density lipoprotein receptor; SCAP, Srebf cleavage activating protein; TM7SF2, transmembrane 7 subfamily member 2; TRERF1, transcriptional regulating factor 1; NR1H2, nuclear receptor subfamily 1, group H, member 2; INSIG1-2, insulin-induced gene 1-2; SREBF2, sterol regulatory element-binding factor 2. Data are presented as median ± range as a relative change compared controls.

Perturbed expression of proteins involved in cholesterol metabolism in female Gunn rats

To determine whether differences in gene expression were related to changes in protein expression Western blot analysis was undertaken on key proteins involved in cholesterol metabolism and lipoprotein transport. Expression of CYB5R3 ($P<0.05$) was reduced while HMGCR expression was non-significantly elevated ($P=0.08$) in female Gunn rats versus controls. No difference in the expression of these proteins were observed in male animals (Fig. 3.6A-B). CYP7A1 expression, the rate limiting enzyme of the classical pathway of bile acid synthesis, was significantly greater in male Gunn rats versus controls ($P<0.05$) with a similar trend in female Gunn rats (NS; Fig. 3.6C). Conversely, expression of LDLr was significantly upregulated in female Gunn rats compared to controls ($P<0.01$) with no difference in male rats (Fig. 3.6D). On the other hand, ABCA1 expression was not affected across groups (Fig. 3.6E). The nuclear form of SREBP2, a master regulator of genes that regulate cholesterol metabolism was significantly greater in female Gunn rats compared to controls ($P<0.01$; Fig. 3.7). SREBP2 was not measured in male rats because there was no difference in downstream targets including the fractional rate of cholesterol synthesis and LDLr expression between groups.

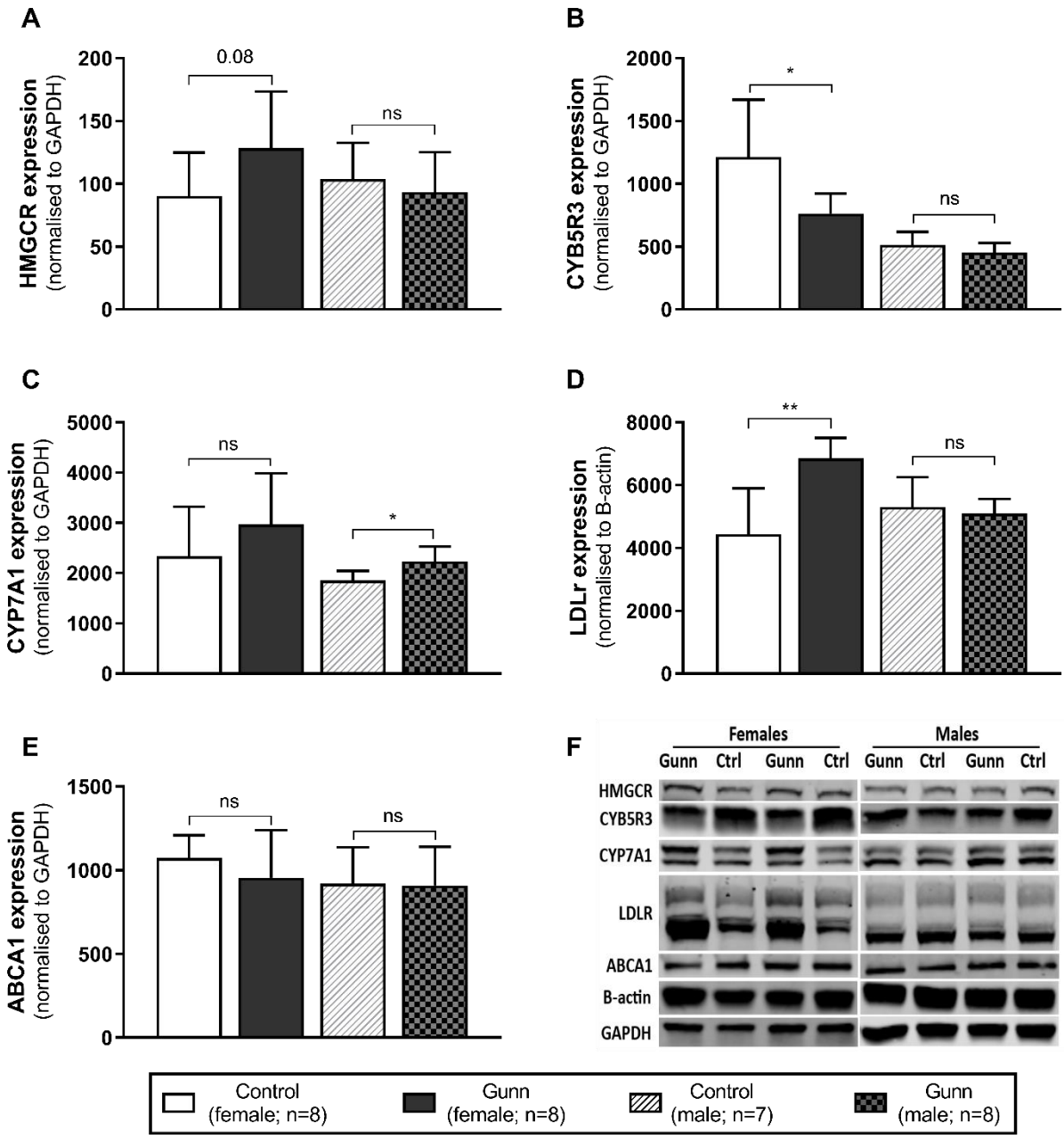

Figure 3.6. Protein expression analysis using Western blot for targets of cholesterol synthesis, transport, and breakdown in livers from adult Gunn (hyperbilirubinaemic) and control (normobilirubinaemic) rats. A-E) HMGCR, CYB5R3, CYP7A1, and ABCA1 expression normalised to GAPDH expression and LDLr expression normalised to B-actin expression. F) Cropped image that represents a single Western blot run. Abbreviations: HMGCR, 3-Hydroxy-3-methyl-glutaryl-coenzyme A reductase; CYB5R3, NADH-cytochrome b5 reductase 3; CYP7A1, Cholesterol 7 alpha-hydroxylase; LDLr, Low-Density Lipoprotein Receptor; ABCA1, ATP-binding cassette transporter; Data are presented as means (standard deviation). Significant differences are presented as P<0.05*, <0.01**, <0.001*** compared to controls of the same sex. Nonsignificant differences are indicated as “ns”.

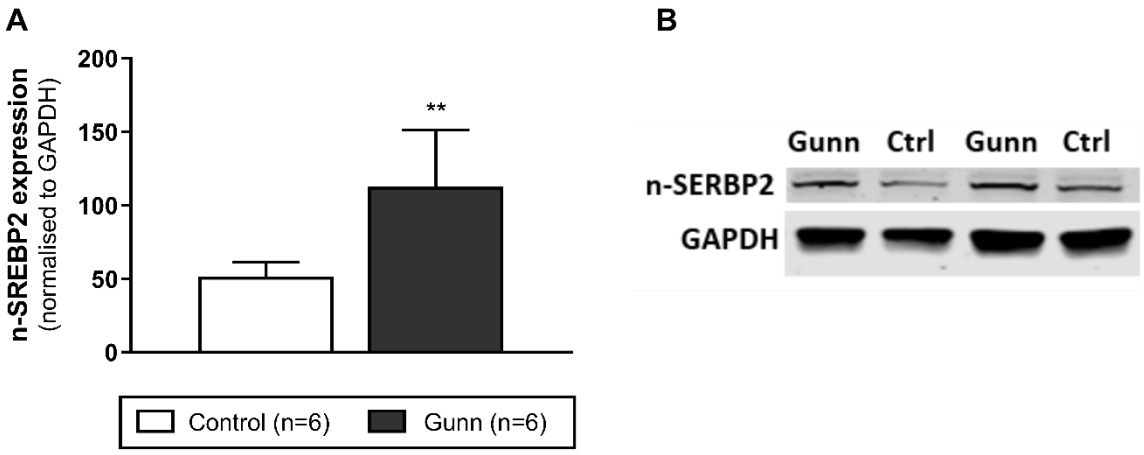

Figure 3.7. Protein expression analysis using Western blot for nuclear form of SREBP2 (n-SREBP2) in livers from adult female Gunn (hyperbilirubinaemic) and control (normobilirubinaemic) rats. A) SREBP2 expression normalised to GAPDH expression B) An example cropped image that represents a single Western blot run. Abbreviations: SREBP2, Sterol regulatory element-binding protein 2. Data are presented as means (standard deviation). Significant differences are presented as P<0.05*, <0.01**, <0.001*** compared to controls. Nonsignificant differences are indicated as “ns”.

3.4 Discussion

Hyperbilirubinaemia in humans and animals is associated with reduced circulating cholesterol concentrations, however, an explanation for this relationship remains unknown [12]. The main findings of this study included elevated fractional cholesterol synthesis, LDLr expression, and increased biliary lipid excretion in female hyperbilirubinaemic Gunn rats who demonstrated profound hypocholesterolaemia. Surprisingly, the effects of UGT1A1 impairment/hyperbilirubinaemia on lipid metabolism were consistently stronger in female animals with only minor changes observed in male Gunn rats. Increased biliary excretion of cholesterol may explain the inverse relationship between bilirubin and circulating cholesterol in hyperbilirubinaemic animals and justifies further investigation in human GS.

Female Gunn rats demonstrated a >50% reduction in serum cholesterol concentrations compared to normobilirubinaemic controls and this was explained by reductions in HDL-C, which is the dominant circulating lipoprotein in rodents [380]. These findings are congruent with previous studies that report similar reductions in female Gunn rats [246,371]. In contrast, cholesterol concentrations were not different in male rats, which is in opposition to results of Wallner et al. who reported reductions in serum cholesterol in male and female Gunn rats, albeit the effect was less pronounced in males [246]. This difference in results may be explained by the younger age of animals studied by Wallner et al. (~8 vs 16 weeks of age) [246]. In support of this explanation, male juvenile rats (3-4 weeks of age) showed a significant reduction in serum cholesterol concentrations suggesting interactions between age and sex on cholesterol concentrations. Furthermore, this is the first study to report decreased circulating phospholipids and increased bile acid concentrations specific to female Gunn rats. However, similar to cholesterol, these sex-specific effects were non-significant or reversed in juvenile Gunn rats. Therefore, these data broadly suggest that age and/or sex hormones may play an important role in various aspects of lipid metabolism in hyperbilirubinaemic rats.

The mechanisms responsible for hypocholesterolaemia were further explored by measuring expression of proteins and genes involved in cholesterol metabolism in adult rats. Hepatic LDLr expression was significantly elevated in female Gunn rats suggesting that hypocholesterolaemia may have been influenced by increased cholesterol uptake by the liver [154]. Furthermore, female Gunn rats demonstrated elevated protein expression of the nuclear form of SREBP2. SREBP2 is a master regulator of cholesterol metabolism that acts as a sterol sensing transcription factor [381]. During sterol-replete conditions, SREBP2 is retained within the membrane of the endoplasmic reticulum as part of a SREBP2-SCAP-INSIG complex. When cholesterol levels decrease, endoplasmic reticulum bound SREBP2 is cleaved and translocates to the nucleus where it transactivates genes involved in cholesterol transport and synthesis [381].

The target genes of SREBP2 that are positively regulated include HMGCR, LDLr, PMVK, 3-Hydroxy-3-methyl-glutaryl-coenzyme A synthase (HMGCS), ATP binding cassette transporter G5 (ABCG5), and ABCG8 [382]. Therefore, increased LDLr expression in female Gunn rats is consistent with greater expression of the nuclear form of SREBP2. However, the expression of other genes was not in complete agreement with increased SREBP2 expression. For example, no significant change in HMGCR or HMGCS (1.14-fold and 0.9-fold, respectively; Appendix 1, Table S3.1) gene expression occurred, while PMVK gene expression was significantly decreased (Fig. 3.5). Although gene expression of ABCG5 and ABCG8 were not measured, female Gunn rats demonstrated greater biliary cholesterol excretion indicating that the expression of these genes may be increased because they mediate export of hepatic sterols into the bile canaliculus [146].

Gene expression data was validated using protein expression for selected genes. Hepatic HMGCR protein expression was elevated (non-significantly) by ~40% in female Gunn rats ($P=0.08$; Fig. 3.6). This result was consistent with increased SREBP2 protein expression and greater fractional cholesterol synthesis also observed in female Gunn rats [127]. Therefore, increased expression in HMGCR could potentially explain elevated fractional cholesterol synthesis observed in female Gunn rats considering it is the rate-limiting enzyme of cholesterol

synthesis [130]. Surprisingly, gene expression of HMGCR was not different suggesting that increases in protein expression could be due to reduced post-translational degradation of HMGCR in female Gunn rats mediated by (non-significantly) reduced gene expression of insulin-induced gene (INSIG) proteins ($P<0.10$; Fig. 3.5B) [127,130]. Taken together, these results indicate that hepatic uptake of circulating cholesterol and cholesterol synthesis is upregulated in female Gunn rats, potentially through enhanced nuclear expression of SREBP2. This pattern of activation is a typical response to reduced hepatic cholesterol levels that aim to restore intracellular cholesterol levels as reported following statin treatment [13].

Surprisingly, there was no evidence to support reduced hepatic cholesterol concentrations in female Gunn rats, indicating that increased cholesterol synthesis and/or hepatic uptake sufficiently counterbalanced cholesterol outflow (breakdown into bile acids and biliary excretion) [127]. Indeed, this conclusion is consistent with enhanced biliary cholesterol excretion in female Gunn rats compared to controls. Female Gunn animals also demonstrated a trend towards increased biliary bile acid excretion and possessed substantially elevated circulating bile acids. The mechanisms responsible for elevated biliary lipid excretion in female Gunn rats remain unknown, however, biliary lipid excretion may be stimulated by reduced biliary excretion of bilirubin conjugates due to UGT1A1 dysfunction [12]. Several studies have examined the effects of conjugated bilirubin on the coupling of biliary lipid excretion to bile acids [383–386]. There is strong evidence to support that organic anions (including conjugated bilirubin) dissociate biliary lipid excretion from bile acids without affecting the rate of bile acid excretion [15]. For instance, Verkade et al. administered bilirubin ditaurate (BRDT), a synthetic analogue to bilirubin diglucuronide, to study the effect of bilirubin conjugates on biliary coupling of lipids to bile acids in Wistar and multidrug resistance-associated protein 2 deficient (GY) rats [385]. In both strains BRDT reduced the relative excretion of lipids (cholesterol+phospholipid) to bile acids, thus, dissociating lipid excretion from bile acids [385]. Similarly, Ayotte et al. reported that BRDT administration in Sprague-Dawley and Gunn rats profoundly decreased biliary cholesterol and phospholipid excretion by more than 50% without affecting bile flow or bile acid

excretion [383]. By administering BRDT these studies produced a model of elevated biliary bilirubin conjugate excretion, which is opposite to the Gunn rat model that has an impaired capacity to conjugate UCB and therefore excrete conjugated bilirubin. Consistent with this, exogenous UCB administration in Gunn rats does not increase excretion of bilirubin conjugates and does not lead to uncoupling of biliary lipids to bile acid excretion [383]. In contrast, UCB infusion in UGT1A1 competent animals demonstrated equivalent effectiveness as BRDT infusion in uncoupling biliary lipid excretion in Sprague-Dawley rats [383]. These data also agree with other studies that reported that the rate of biliary lipid excretion relative to bile acid excretion is specifically regulated by hydrophilic organic anions including bilirubin glucuronides [15].

In summary, strong evidence exists to support that *increased* bilirubin conjugate excretion can uncouple lipid excretion from bile acids and decrease the overall cholesterol/phospholipid output [15,383–386]. However, no studies have investigated the effect of decreased bilirubin conjugate (organic anion) excretion (as in Gunn rats) on biliary excretion. We hypothesised that decreased conjugated bilirubin excretion would lead to greater coupling of biliary lipids to bile acid excretion. In Gunn rats, the rate of biliary secretion of conjugated bilirubin is decreased by several fold compared to controls (62% and 75% decrease in female and male Gunn rats, respectively; Fig. 3.2E). In agreement with this theory, the current study presents the first evidence of increased coupling of biliary lipids to bile acid excretion in Gunn rats. Female Gunn rats demonstrated greater relative excretion of biliary lipids to bile acids with a similar non-significant trend in males (Fig. 3.2F).

Hepatic cholesterol concentrations are also affected by the rate of intestinal cholesterol absorption. Bile acids are vital for efficient cholesterol absorption and their effectiveness varies depending on their physiochemical properties [129]. Wang et al. demonstrated that the hydrophobicity index of the biliary bile acid composition (Hueman index) was strongly and positively related to intestinal cholesterol absorption (r=0.95) [151,377]. In comparison to hydrophilic bile acids (e.g. α/β-MCA species), hydrophobic species such as CA and TCA are potent

inducers of cholesterol absorption [151]. A profound decrease in absolute biliary TCA output and a minor increase in MCA excretion were documented in female Gunn rats, compared to controls. Despite greater relative ratios of MCA:TCA species, a significant change in the overall hydrophobicity index of excreted biliary bile acids did not occur (see Table 3.4). These data suggest that differences in intestinal cholesterol absorption in female Gunn rats compared to controls are unlikely to occur. Therefore, this result supports a conclusion that perturbation in cholesterol balance in female Gunn rats is more likely caused by increased secretion of biliary lipids.

Hepatic UGT1A1 is an important enzyme for 17β-estradiol conjugation and therefore excretion. UCB competes with 17β-estradiol for conjugation by UGT1A1 [16,17], with profoundly elevated UCB concentrations in Gunn rats likely to reduce UGT1A1 mediated 17β-estradiol excretion. Although circulating hormone concentrations were not measured in this study, it is possible that female Gunn rats experienced elevated levels of 17β-estradiol. The impact of oestrogen on lipid metabolism is well established in both humans and animals [387]. Studies in animals demonstrate that ovariectomy causes a substantial increase in serum cholesterol concentrations and bodyweight which are reversed by treatment with oestrogen, establishing a causal relationship of oestrogen with respect to lipid metabolism [388]. Interestingly, reduced circulating cholesterol concentrations following oestrogen treatment in rats are associated with increased LDLr expression suggesting that oestrogen induces hepatic cholesterol uptake [389]. Furthermore, oestrogen treatment in rats induces cholestasis (decreased bile flow and lipid excretion), reduces hepatic uptake of bile acids and consequently increases circulating bile acid concentrations [389]. Collectively, elevated oestrogen concentrations may potentially explain the hypocholesterolaemia, increased circulating bile acid concentrations, and enhanced LDLr expression in female Gunn rats.

In agreement with the potential effects of elevated oestrogen, female Gunn rats demonstrated reduced bodyweight, decreased serum concentrations of cholesterol and an increase in

circulating bile acid levels, and enhanced LDLr expression. However, evidence that argues against this hypothetical explanation exists because female Gunn rats had increased bile flow, cholesterol, and phospholipid excretion, whereas oestrogen treatment causes cholestasis and decreases biliary lipid excretion [389,390]. Interestingly, in both studies oestrogen treatment induced a change in bile acid composition (i.e. increase in β-MCA relative to CA) in agreement with results observed in female Gunn rats [389,390].

Considering that male animals are unlikely to experience the confounding effects of oestrogen metabolism, the effect of UGT1A1 inhibition and hyperbilirubinaemia, should be clearer in these animals. Under these conditions, effects on lipid metabolism, appeared to be milder in male Gunn rats. Male Gunn rats demonstrated a (non-significant) reduction in body mass and serum total cholesterol with increased biliary phospholipid excretion. In this circumstance, other potential mechanisms must be responsible and potentially related to bilirubin more specifically. Bilirubin is an endogenous ligand for the aryl hydrocarbon receptor (Ahr) and peroxisome proliferator-activated receptor alpha (PPARα), which are ligand-activated transcription factors that regulate lipid metabolism [10,341]. Both receptors are significantly activated at bilirubin concentrations of 50 μM, which is within the range of circulating concentrations observed in Gunn rats.

Treatment with a PPARα agonist, fenofibrate, reduces bodyweight gain and lipid concentrations in male mice fed a high fat diet which is consisted with the trends observed in male Gunn rats [391,392]. Alternatively, bilirubin could modulate lipid metabolism by binding to Ahr. Ligand activation of Ahr causes repression of several genes involved in cholesterol metabolism such as HMGCR, HMGCS, and PMVK [340]. Although the gene expression of HMGCR and HMGCS were unchanged in this study, a reduction in PMVK expression in female Gunn rats was noted. It is yet to be demonstrated whether Ahr is activated *in vivo* in hyperbilirubinaemic animal models, although, preliminary evidence shows that downstream genes of Ahr are upregulated in juvenile Gunn rats but not in adults [393]. The mechanism that explain the changes to lipid metabolism

in Gunn rats remain unknown, however, they could include bilirubin agonism of PPARα and Ahr, and/or elevated oestrogen concentrations due to UGT1A1 impairment. Future studies are required that administer PPARα/Ahr antagonists with and without ovariectomy in Gunn rats to demonstrate the importance of these receptors and of oestrogen in the regulation of lipid metabolism in hyperbilirubinaemic rats.

3.5 Limitations and future directions

The present study reports that fractional cholesterol synthesis is elevated in female Gunn rats and assumes that this rate represents the absolute rate of cholesterol synthesis. Although fractional cholesterol synthesis is generally representative of the absolute rate of cholesterol synthesis, this result can be misleading if the total cholesterol pool is different between groups [127]. Assessment of neutral (cholesterol) and acidic (bile acids) sterol faecal excretion is required to estimate the cholesterol pool [375]. In this study, absolute measures of faecal cholesterol excretion (unadjusted to bodyweight) and biliary bile acid excretion were not different between groups. These data strongly suggest that the total cholesterol pool was similar between female Gunn rats and controls, providing confidence that the measures of fractional cholesterol synthesis are likely an accurate representation of the absolute *in vivo* rate of cholesterol synthesis.

It is also essential to note the differences in lipoprotein distribution between rodents and humans. In rats, HDL constitutes the greatest lipoprotein fraction involved in plasma cholesterol transport as opposed to humans where the LDL particle is generally more abundant [127]. As such, future studies should evaluate the effects of hyperbilirubinaemia in genetic knockout models that more closely resemble human cholesterol transport such as the LDL knockout mouse model. Nonetheless, increased LDLr expression in female Gunn rats provides preliminary evidence that suggests greater LDL-mediated cholesterol clearance in hyperbilirubinaemia. Finally, profound sex-dependent effects in Gunn rats strongly suggest that sex hormones are implicated in modulating cholesterol and lipid status in UGT1A1 impairment. Therefore, future

studies should measure circulating concentrations of sex hormones and their conjugated forms in the bile of Gunn and control rats to evaluate this relationship.

3.6 Conclusion

Individuals with elevated circulating concentrations of bilirubin have reduced circulating cholesterol and are protected from CVD, however, very little is understood regarding how these affects are mediated *in vivo* [12]. This is the first study to explore the *de novo* cholesterol synthesis rate in a model of unconjugated hyperbilirubinaemia. Furthermore, this chapter provides supportive data concerning biliary lipid excretion and circulating lipid concentrations. Hypocholesterolaemia in female Gunn rats was associated with increased fractional cholesterol synthesis and enhanced hepatic LDLr expression. Additionally, female Gunn rats demonstrated increased biliary lipid excretion that is potentially responsible for depleting the circulating cholesterol pool. Consequently, enhanced biliary lipid excretion likely induces cholesterol synthesis and LDLr expression to counterbalance the cholesterol loss in hyperbilirubinaemic rats. It should be noted that sexual dimorphism in this response suggests perturbation of sex hormone metabolism in female UGT1A1 deficient Gunn rats, and therefore, it remains unclear as to whether bilirubin, per se, is responsible for these reported hypolipidaemic effects. Therefore, future studies should evaluate whether circulating oestrogen concentrations are altered in hyperbilirubinaemic animals and whether eliminating their confounding effects can reveal the true effect of bilirubin on lipid metabolism in Gunn rats.

Chapter 4: Impact of unconjugated bilirubin on mitochondrial function and body composition in the Gunn rat

The discovery of reduced bodyweight in hyperbilirubinaemic (Gunn) rats in Chapter 3 led to the investigation of body composition and bioenergetics in Chapter 4. This experimental study measured the mass of organs and skeletal muscle in addition to the total fat mass and lean mass in order to determine the body composition of hyperbilirubinaemic and normobilirubinaemic animals. Furthermore, bioenergetics were evaluated by measuring mitochondrial function of liver tissue and skeletal muscle using high-resolution respirometry and with Western Blot analysis of mitochondrial respiratory complexes and pAMPK:AMPK ratios. This the first study to comprehensively evaluate the impact of physiologically relevant bilirubin concentrations on mitochondrial function showing strong sexually dimorphic effects in hyperbilirubinaemic rats. Female hyperbilirubinaemic rats demonstrated reduced fat mass and this was associated with improved hepatic mitochondrial quality.

4.1 Introduction

Bilirubin is a breakdown product of haem catabolism and is used clinically as a diagnostic marker of liver dysfunction and blood disorders [238]. A central dogma asserts that unconjugated bilirubin (UCB) is a toxic by-product of haem catabolism due to its capacity to accumulate in specific regions of the brain, and induce oxidative stress, mitochondrial dysfunction, and apoptosis [2,256]. UCB is a tetrapyrrole in structure, and at physiological pH, exists mostly as a diacid, leading to intramolecular hydrogen bonding [238]. Consequently, UCB is hydrophobic and in the circulation is solubilised by strong binding to albumin [394]. Unbound UCB has low aqueous solubility (<70 nM)[255] and freely diffuses through cell membranes, where it accumulates within hydrophobic regions of lipid membranes, including the mitochondria [255,395].

UCB has strong affinity for lipids, which can lead to increased membrane permeability, oxidative damage, and uncoupling of the mitochondrial membrane potential [2,255]. Rodrigues, et al. [396] demonstrated that incubation of primary rat neurons with UCB induced mitochondrial swelling and membrane permeability, release of cytochrome c, and apoptosis [396,397]. Investigations with spin-labelling reported that UCB associates superficially with phospholipid bilayers from the inner mitochondrial membrane which increased membrane permeability, cytochrome c release, and induce lipid peroxidation, corroborating the prevailing notion that UCB perturbs membrane dynamics by interacting with lipids [260,398].

Under physiological conditions, a portion of the energy produced by the oxidation of dietary substrates is lost as heat due to proton leak through the inner mitochondrial membrane, known as (unregulated) mitochondrial uncoupling [72]. However, severe uncoupling of the mitochondrial membrane inhibits ATP synthesis and can lead to cell death [73]. Mild uncoupling does not affect ATP synthesis and can lead to weight loss and prevention of chronic diseases such as Type 2 Diabetes Mellitus (T2DM) [73]. Transgenic mice overexpressing uncoupling proteins such as UCP1 and UCP3 are resistant against obesity and show improved insulin

sensitivity when fed a high fat diet (HFD) [74–76]. At high concentrations, UCB causes uncoupling of the mitochondrial membrane which explains its toxic effects. However, whether physiological or mildly elevated concentrations of UCB affect mitochondrial function remains unknown and could provide a rational explanation for improved body composition and reduced risk of metabolic syndrome in individuals with increased UCB concentrations (within the normal range) [20,43,248,399].

Interestingly, individuals with Gilbert's syndrome (GS) who have mildly elevated UCB concentrations (17 – 80 μM) are protected against cardiovascular diseases (CVDs) and have reduced body mass index (BMI) compared to individuals with normal UCB levels (<17 μM serum UCB) [12,243]. Generally, the protection of GS individuals from chronic disease is attributed to the antioxidant properties of UCB [6,8,243–245]. However, few studies have explored the impact of UCB on body composition and fewer still have investigated its effect on cellular and mitochondrial metabolism *in vivo* [9,10,265].

Several clinical studies show that circulating UCB concentrations are inversely associated with BMI [242,247]. For example, women with total bilirubin (TBIL) ≥8.55 μM have significantly lower bodyweight and BMI than women with <8.55 μM TBIL. In contrast, men with TBIL ≥8.55 μM had greater bodyweight, although, BMI was comparable between groups [242]. In accordance with this study, Rodriguez et al. reported an inverse correlation between BMI and TBIL concentrations and a trend towards reduced fat mass in females with greater TBIL [247]. However, these findings are not consistent, therefore further controlled studies are required to clearly establish the impact of UCB on metabolic function [5,242,247].

Gunn rats have a congenital unconjugated hyperbilirubinaemia due to the absence of functional UDP-glucuronosyltransferase 1A1 (UGT1A1), which leads to impaired conjugation and elimination of UCB. Therefore, these animals serve as a relevant model to study the effects of unconjugated hyperbilirubinaemia on body composition and metabolism. In the present study,

we investigated whether Gunn rats had reduced bodyweight, altered body composition, and impaired skeletal muscle and hepatic mitochondrial function.

4.2 Methods

Materials:

All materials were obtained from Sigma-Aldrich (Australia) unless otherwise stated. Chemicals for high-resolution respirometry were obtained from manufacturers as recommended by Oroboros Instruments [400].

Synthesis of sodium bilirubinate

Sodium bilirubinate was synthesised in order to make UCB soluble in respiration buffer (Miro6). 2.1 molar equivalents of NaOH solution (1.5 mg mL^{-1} in ethanol) was added to UCB. The mixture was vortexed vigorously and diluted 10-fold with ethanol and evaporated in the dark under vacuum in a rotary evaporator (Maxivac; Labogene, Australia) at 21°C. The UCB content of the powder was determined to be >99% of the commercially supplied standard, using high-performance liquid chromatography photodiode array (HPLC:PDA) as previously published [346].

Animals:

Breeding pairs of heterozygote Gunn rats on a Wistar background were imported from the Rat Research and Resource Centre (Columbia, MO, USA) and bred to produce either homozygote (jaundiced) or heterozygote (normobilirubinaemic) Gunn rats. Homozygote Gunn phenotype was determined based on the presence of jaundice in the first 3 days after birth. Jaundiced Gunn rats were tagged, and their phenotype was confirmed by measuring TBIL concentrations. From herein, animals expressing hyperbilirubinaemia are phenotypically defined as “Gunn” rats while those possessing normal bilirubin levels are termed as “normobilirubinaemic controls”. Animals were housed in the G26 animal house facility at Griffith University, Gold Coast at constant temperature (20^{o}C) and humidity (60%), with a 12 hr light:dark cycle. All animals were provided a standard rodent diet (18% Protein Rodent Diet, 18% protein, 6.2% fat; TEKLAD Standard

Global, USA) and water *ad libitum.* All procedures were approved by the Griffith University Animal Ethics Research Committee (MSC/02/17/AEC) prior to experimentation.

Experimental protocol

At 10 weeks of age, animals were gradually acclimatised in metabolic cages (i.e. 2-24 hrs) before entering protocol. In total, 36 age-matched animals (~10 weeks and 5 days old) from 4 litters entered protocol in a staggered fashion. The protocol was 17 days (-1 to 15) and animals were housed in metabolic cages three times for a period of 24 hrs at a time, at day -1, 10, and 14 of the protocol. Food and water remained available *ad libitum* and was weighed before and after the animal was housed to determine food consumption. Bodyweight was recorded every 2 days from Day -1 in addition to before and after each metabolic cage day. In order to control for future therapeutic interventions additional procedures (i.p. saline and p.o. water) were conducted as described in Appendix 2 (see *Additional procedures*). Energy efficiency was calculated by subtracting the final bodyweight at day 15 from the initial bodyweight at day -1 and this value was then divided by the calories (kcal) consumed per day ($Energy\ efficiency = \frac{weight\ gained\ per\ day\ (g)}{\text{calories consumed per day (kcal)}}$). Calories consumed was calculated as an average from the 3 metabolic cage days.

Another subset of rats were bred to similar age (13-14 weeks old) and anaesthetised after an overnight fast using 50 mg kg^{-1} sodium pentobarbitone (Pharmachem, Australia) via an i.p. injection. While anaesthetised the animals were placed in a prone position and lengths were measured using a tape measurer from tip of the nose to the last sacral vertebrae. Anaesthetised animals were euthanised by removal of the heart. Blood collected from the chest cavity was centrifuged (2000 g, 10 mins, 21°C) and the serum was flash frozen and stored at -80°C for later analysis. Organs and skeletal muscle (soleus and extensor digitorum longus (EDL)) were dissected free from fat and washed in ice cold dPBS (Gibco®, United Kingdom), then patted dry, and weighed on a calibrated balance. Immediately following weighing, a section of liver tissue

was flash frozen and stored at -80°C for later analysis. Likewise, a piece of liver, EDL, and soleus were stored in Miro6 (liver) or BIOPS (muscle) as described in "*High-resolution respirometry*".

Analysis of serum biochemistry

Serum samples were thawed and analysed using the COBAS Integra® 400+ (Roche Diagnostics, Australia) for direct reacting bilirubin (BILD2), TBIL (BILT3) and albumin (ALB). All assays were calibrated with appropriate standards (CFAS) and accuracy was checked with appropriate quality controls (precinorm clinchem multi 1 (PCCC1), precinorm clinchem multi 2 (PCCC2)). All analyses were conducted in duplicate and the average of each parameter reported.

Lipid extraction

Frozen liver tissue (~100 mg) was homogenised frozen (with liquid N_2) using a mortar and pestle. Lipids were extracted with isopropyl-alcohol at a 50:1 mg:mL ratio of tissue to isopropyl-alcohol as previously published [378], with method validation presented in Appendix 4. Homogenates were vortexed vigorously and sonicated without heat for 10 mins and then centrifuged (43000 g, 10 mins, 21°C). The supernatant was collected in a separate tube and evaporated using a rotary evaporator at 35°C. Dry pellets were reconstituted in 250 µL of isopropanol and analysed for triglycerides spectrophotometrically (TRIGL, Roche Diagnostics) on the COBAS Integra 400+.

High-resolution respirometry

Liver homogenate

A small section of liver tissue was dissected from the left lateral lobe and added directly to ice-cold Miro6 buffer (280 U mL^{-1} catalase, 0.5 mM EGTA, 3 mM $MgCl_2 \cdot 6H_2O$, 60 mM K-lactobionate, 20 mM taurine, 10 mM KH_2PO_4, 20 mM HEPES, 110 mM sucrose, and 1 g L^{-1} bovine serum albumin (BSA), pH 7.1). Two to three pieces of 8-16 mg of wet-weight (Wd) of dissected liver tissue were transferred (SHREDDER Tube, Pressure BioSciences, USA) and homogenised using a PBI shredder (Shredder SG3 Kit, Pressure BioSciences, MA, USA) as previously published [401]. Using the strongest force (position 3) the tissue was shredded for 5 sec, followed by medium force (position 2) for 3 secs. The homogenate was then diluted into ice-cold Miro6 to a final

concentration of 1.3 mg tissue mL^{-1} and transferred (~2.1 mL per chamber) into the Oxygraph chambers (Oxygraph-2k; Oroboros Instruments, Austria). After O_2 flux stabilised, the substrate-uncoupler-inhibitor titration (SUIT) protocol was utilised to evaluate mitochondrial function described under "*Measurement of respiratory oxygen fluxes*".

Permeabilisation of skeletal muscle fibres

Mechanical and chemical permeabilisation of skeletal muscle was conducted as previously published [9]. Briefly, after dissection, soleus and EDL were added to BIOPS buffer (2.77 mM CaK_2EGTA, 7.23 mM K_2EGTA, 20 mM imidazole, 20 mM taurine, 50 mM MES hydrate, 0.5 mM dithiothreitol, 6.56 mM $MgCl_2\,6H_2O$, 5.77 mM Na_2ATP, 15 mM Na_2phosphocreatine, pH 7.1). 5-7 mg pieces of muscle tissue were used for mechanical isolation of muscle fibres using sharp round-end tweezers. After mechanical isolation, muscle fibres were permeabilised by adding saponin (final concentration 50 µg mL^{-1}) to the BIOPS buffer followed by gentle agitation on an orbital shaker for 30 mins on ice. Following chemical permeabilisation, tissue was washed in Miro6 for 10 mins with gentle agitation on ice. Permeabilised muscle fibres (0.7-1.5 mg Wd) were added to each Oxygraph chamber, with analysis performed in duplicates. Samples were analysed using two different conditions: first batch of animals (3 per group) were analysed at air saturation (~180 µM O_2) while the remaining animals were super-oxygenated to 400 µM O_2 concentration initially, and oxygen (O_2) concentration was maintained above 250 µM using H_2O_2 and catalase throughout measurement. Respiration parameters did not differ between methods, therefore, all results were combined for the final analysis.

Measurement of respiratory oxygen fluxes

Mitochondrial respiration measurements were conducted within 2 hrs of sample collection at 37°C using three Oxygraph units in parallel containing Miro6 buffer in each chamber. Data acquisition and analysis was conducted using 7.0 DatLab software (Oroboros Instruments, Austria). Standard carbohydrate SUIT protocol was utilised to measure the contribution of carbohydrates to the rate of mitochondrial O_2 consumption (O_2 flux) in liver tissue and skeletal

muscle from adult rats or liver tissue from normobilirubinaemic juvenile rats (3-4 weeks of age) in the absence or presence of exogenous UCB (31.3, 62.5, and 125 µM) as previously published [67]. All concentrations are represented as final concentrations. The rate of intrinsic uncoupling (LEAK state) was measured in the presence of 5 mM pyruvate, 1 mM malate and 10 mM glutamate (PMG). The maximal rate of oxidative phosphorylation (OXPHOS) through complex I (CI_P) was measured by step-wise titration with 1 mM ADP in the presence of PMG. Lack of increase in O_2 flux (<10%) after the addition of cytochrome c confirmed the integrity of the outer mitochondrial membrane. To assess CI+II convergent OXPHOS ($CI+II_P$), 10 mM succinate was added in the presence of PMG and saturating levels of ADP. The maximum O_2 flux of the electron transfer system (ETS) was measured by uncoupling O_2 flux from ATP synthesis (noncoupled state) by step-wise titration with 0.5 µM carbonyl cyanide p-trifluoromethoxyphenylhydrazone (FCCP; an extrinsic uncoupler). Noncoupled maximal respiration of complex II (CII_{ETS}) was measured in the presence of a complex I inhibitor, rotenone (0.5 µM) and residual O_2 consumption (ROX) was measured by the addition of 2.5 mM antimycin (AMA). All flux measurements were corrected for ROX and tissue mass or citrate synthase activity. Flux control ratios (RCR) were determined by adjustment to a common reference state (OXPHOS or ETS).

DEXA scan

Dual-energy X-ray absorptiometry (DEXA) (XR-36 Quickscan densitometer 4.2.4/2.3.1, software version 2.5.3a; Norland Medical Systems, Inc. USA) was conducted on a subgroup of adult Gunn and normobilirubinaemic control rats (15 weeks of age). Animals were anaesthetised using ketamine (50 mg kg^{-1}) and xylazine (3 mg kg^{-1}) mixture in a 50:30 ratio via i.p. injection and placed in a prone position in the DEXA machine. Bone mineral density (BMD), total mass, lean mass, and fat mass was collected for each animal and all scans were performed at 1.5×1.5 mm resolution at 60 mm s^{-1} in small animal mode.

Citrate Synthase

Citrate synthase (CS) activity was measured as previously published [402]. Briefly, hepatic tissue collected from Oxygraph chambers, hepatic homogenates (see Western blot analysis), or CS standard (from pig heart) were mixed with DTNB, acetyl CoA, and oxaloacetic acid in a 96-well plate, and the reaction was monitored at 412 nm in a spectrophotometer (ThermoFisher Scientific, Australia). All samples were analysed in duplicate and the average absorbance was used to calculate CS activity or the amount of CS protein using the specific activity equation #6 as previously published [402].

Western blot analysis

Frozen liver samples were homogenised by shearing tissue through 18-23G needles in CelLytic MT Cell Lysis buffer (2.5:50 mg/µL; #C3228) in the presence of protease inhibitor (#P8340) and phosphatase inhibitor (#ab201114, Abcam, USA) as per manufacturer's protocol. Tissue supernatant was generated by centrifugation (4000 g, 10 mins, 4^{o}C) and standardised based on protein concentration using the Pierce BCA Protein Assay Kit (ThermoFisher Scientific, Australia) as per manufacturer's protocol. Samples were prepared in Laemmli 2X buffer (#S3401) at 1:1 ratio and were heated for 30 mins at 37^{o}C (mitochondrial proteins) or 5 mins at 95^{o}C (AMPK), prior to loading. Proteins (10-25 µg) were separated on 12% SDS-PAGE using TGX^{TM} FastCast^{TM} gels (#1610175, Bio-Rad, Australia). After electrophoresis, proteins were transferred onto 0.45 µm polyvinylidene fluoride membranes (PVDF; #IPFL0010, Millipore, Australia) for 1-2 hrs on ice in Towbin buffer (25 mM Tris, 192 mM glycine, and 20% (v/v) methanol) or CAPS buffer (10 mM CAPS and 10% (v/v) methanol, pH 11). Following transfer, membranes were blocked with Odyssey Blocking Buffer (Millenium Science, Australia) and incubated with primary antibodies (OXPHOS, #ab110413, GAPDH, #14C10 (Cell Signaling, Australia), p-AMPK, #ab133448, AMPK, #ab80039) with gentle agitation overnight at 4^{o}C. Finally, membranes were incubated with secondary antibodies (#IRDye 680 or #IRDye 800CW, LI-COR, Australia) for 1 hr with gentle agitation at room temperature and visualised using Odyssey CLX (LI-COR). The linear range of detection was determined for each target and housekeeping (GAPDH) proteins prior to analysis,

as described in Appendix 4. Densitometry analysis of OXPHOS was normalised to GAPDH while p-AMPK was normalised as a ratio to total AMPK (Image Studio Lite version 5.2; LI-COR). Validation of the analysed target protein bands are presented in Appendix 2.

Statistical analysis

All values are expressed as mean ± (standard deviation), multiple linear regression data are presented as un-standardised regression coefficients and 95% confidence intervals. Multicollinearity in multiple linear regression was ruled out by a variance inflation factor (VIF) of less than 5. Data was tested for normality and homogeneity of variance with Kolmogorov-Smirnov and Spearman tests, respectively. Comparisons were performed between phenotype from the same sex using unpaired t-tests. When data was not normally distributed or failed equality of variance, nonparametric Mann-Whitney test and Welch's correction were used, respectively. The dose-dependent effect of UCB on mitochondrial respiration was compared using repeated measures two-way ANOVA with Bonferroni's post-hoc test comparing the effect of UCB treatment to control (vehicle) on each respiratory state (e.g. CI_P and $CI+II_P$). Statistical analysis was performed in GraphPad PRISM (v8.2) and $P<0.05$ was considered significant.

4.3 Results

Phenotype

Breeding pairs produced similar distribution of heterozygote (normobilirubinaemic) and homozygote (hyperbilirubinaemic) rats over 7 litters (Appendix 2, Table S4.1; NS). Serum TBIL concentrations were significantly greater in Gunn rats compared to controls ($P<0.001$, Table 4.1).

Body composition

A total of 16 homozygote Gunn and 27 heterozygote controls were scanned using DEXA to determine body composition (Table 4.1). Both male and female Gunn rats had significantly reduced bodyweight ($P<0.001$) and lean mass ($P<0.01$) when compared to controls (Table 4.1). Female Gunn rats had significantly reduced body length ($P<0.001$), fat mass ($P<0.05$), and liver triglyceride content ($P<0.01$) compared to female controls (Table 4.1). Male and female Gunn rats had significantly reduced soleus and EDL muscle mass compared to littermate controls ($P<0.01$; Table 4.1).

Table 4.1. TBIL concentrations and body composition of hyperbilirubinaemic and normobilirubinaemic rats.

Variable	Phenotype		P value
	Control	Gunn	
Serum TBIL (µmol L^{-1})			
• Males	2.76 (0.66)	99.8 (15.9)	**<0.001**
• Females	2.33 (1.20)	79.3 (20.6)	**<0.001**
Body length (cm)			
• Males	25.2 (1.10)	23.9 (1.15)	0.09
• Females	21.2 (0.65)	19.7 (0.58)	**<0.001**
Bodyweight (g)			
• Males	309 (17.7)	261 (37.4)	**<0.001**
• Females	176 (16.5)	150 (9.57)	**<0.001**
Lean mass (g)			
• Males	256 (18.4)	215 (32.1)	**<0.001**
• Females	160 (16.0)	140 (12.1)	**<0.01**
Fat mass (g)			
• Males	53.0 (17.7)	46.8 (19.3)	0.46
• Females	16.1 (6.65)	9.94 (5.35)	**<0.05**
Liver triglycerides (mg g^{-1})			
• Males	9.99 (3.16)	9.45 (4.38)	0.78
• Females	4.65 (1.67)	2.39 (0.92)	**<0.01**
Lean mass (% of bodyweight)			
• Males	83.0 (5.34)	82.3 (6.82)	0.79
• Females	90.9 (3.81)	93.3 (3.83)	0.18
Fat mass (% of bodyweight)			
• Males	17.0 (5.34)	17.7 (6.82)	0.79
• Females	9.13 (3.81)	6.70 (3.83)	0.18
Soleus (mg)			
• Males	175 (38.1)	134 (24.2)	**<0.05**
• Females	104 (18.1)	76.3 (11.0)	**<0.001**
EDL (mg)			
• Males	147 (20.5)	120 (10.1)	**<0.01**
• Females	89.7 (7.80)	64.0 (9.72)	**<0.001**

Note: Two different cohorts of animals were used for the parameters analysed. Cohort #1 (DEXA analysis: bodyweight, lean mass, and fat mass) constituted 27 control and 16 Gunn rats. Cohort #2 (all other parameters) constituted 18 control and 19 Gunn rats. Control group represents normobilirubinaemic heterozygote littermates. Gunn group represents hyperbilirubinaemic homozygote littermates. TBIL, total bilirubin; EDL, extensor digitorum longus. Values are represented as mean (standard deviation). All comparisons are made between phenotype within the same sex.

Organ weights

There were no significant differences in liver mass between groups (Table 4.2). Heart and lung mass were only significantly reduced (P<0.001) in female Gunn rats when compared to controls, with a trend towards reduced heart (P=0.07) and lung (P=0.14) mass in male Gunn rats (Table 4.2). Only female Gunn rats had significantly reduced kidney mass (P<0.001), however, all Gunn rats had a trend towards a reduced spleen mass (P=0.15 and P=0.05, respectively) compared to controls (Table 4.2). Additional organ masses are presented in Table 4.2. Organ masses expressed relative to bodyweight are provided in Appendix 2, Table S4.2.

Table 4.2. Organ weights of hyperbilirubinaemic and normobilirubinaemic rats.

Variable	Phenotype		P value
	Control (n=18)	Gunn (n=19)	
Liver (g)			
• Males	14.8 (3.01)	13.8 (2.79)	0.52
• Females	8.84 (1.23)	8.74 (0.91)	0.82
Heart (g)			
• Males	1.19 (0.11)	1.07 (0.13)	0.07
• Females	0.82 (0.06)	0.67 (0.06)	**<0.001**
Lungs (g)			
• Males	1.54 (0.23)	1.37 (0.19)	0.14
• Females	1.15 (0.12)	0.95 (0.08)	**<0.001**
Kidney (g)			
• Males	1.62 (0.23)	1.53 (0.22)	0.48
• Females	0.98 (0.06)	0.77 (0.04)	**<0.001**
Spleen (g)			
• Males	1.17 (0.12)	1.03 (0.13)	**0.05**
• Females	0.80 (0.10)	0.73 (0.12)	0.15
Testes (g)			
• Males	1.89 (0.20)	1.75 (0.13)	0.24

Note: Control group represents normobilirubinaemic heterozygote littermates. Gunn group represents hyperbilirubinaemic homozygote littermates. Values are represented as mean (standard deviation). All comparisons are made between phenotype within the same sex.

Multiple linear regression of organ masses

In order to differentiate the effects of the hyperbilirubinaemic phenotype (condition) from bodyweight on organ mass, multiple linear regression was conducted with organ mass as a dependent variable while bodyweight and the presence/absence of hyperbilirubinaemia were used as independent variables. In male rats, bodyweight significantly and positively predicted organ mass ($P<0.01$) while the hyperbilirubinaemic phenotype was a significant negative predictor of soleus and EDL mass ($P<0.05$, Table 4.3). In females, both bodyweight and the hyperbilirubinaemic phenotype significantly and positively predicted liver mass ($P<0.001$), however, only the hyperbilirubinaemic phenotype was a significant negative predictor of kidney mass ($P<0.01$, Table 4.3). Additionally, bodyweight was a significant positive predictor of soleus and EDL mass in females. In the second analysis, data from both sexes were combined and demonstrated that bodyweight was a significant positive predictor for the mass of all organs and skeletal muscle ($P<0.001$, Table 4.3). Conversely, the hyperbilirubinaemic phenotype was a significant positive predictor for liver and kidney mass ($P<0.001$), and a negative predictor for soleus and EDL mass ($P<0.05$, Table 4.3).

Table 4.3. Multiple linear regression of the effect of bodyweight and the hyperbilirubinaemic phenotype on organ weights and skeletal muscle.

	Independent variables		R^2	P value
	Bodyweight[a] B_1 (95% CI)	Phenotype[b] B_2 (95% CI)		
Dependent variables				
Liver (mg)				
• Males (n=14)	40.7 (32.0, 49.3)	1070 (-156, 2300)	0.91	**<0.001[a]**, 0.08[b]
• Females (n=22)	35.6 (21.0, 50.2)	2440 (1220, 3670)	0.58	**<0.001[a]**, **<0.001[b]**
• Combined (n=36)	32.0 (28.7, 35.3)	1550 (873, 2230)	0.92	**<0.001[a], <0.001[b]**
Heart (mg)				
• Males (n=14)	1.69 (1.20, 2.18)	-31.8 (-101, 37.6)	0.87	**<0.001[a]**, 0.33[b]
• Females (n=20)	0.90 (-0.39, 2.20)	-77.5 (-185, 29.9)	0.64	0.16[a], 0.15[b]
• Combined (n=34)	1.99 (1.78, 2.20)	-4.21 (-47.3, 38.8)	0.93	**<0.001[a]**, 0.84[b]
Lungs (mg)				
• Males (n=14)	2.78 (1.88, 3.68)	-34.9 (-162, 92.6)	0.84	**<0.001[a]**, 0.56[b]
• Females (n=21)	1.63 (-0.38, 3.63)	-80.6 (-253, 91.7)	0.58	0.11[a], 0.34[b]
• Combined (n=35)	2.31 (1.98, 2.64)	-43.5 (-112, 24.8)	0.88	**<0.001[a]**, 0.20[b]
Kidney (mg)				
• Males (n=14)	2.86 (1.78, 3.94)	49.9 (-104, 203)	0.77	**<0.001[a]**, 0.49[b]
• Females (n=22)	0.82 (-0.12, 1.76)	-147 (-226, -67.6)	0.85	0.08[a], **<0.01[b]**
• Combined (n=36)	3.62 (3.27, 3.96)	71.1 (0.29, 142)	0.93	**<0.001[a]**, **<0.05[b]**
Spleen (mg)				
• Males (n=14)	1.37 (0.50, 2.23)	-56.7 (-180, 66.4)	0.63	**<0.01[a]**, 0.33[b]
• Females (n=22)	1.67 (-0.45, 3.79)	49.6 (-128, 228)	0.21	0.12[a], 0.57[b]
• Combined (n=36)	1.70 (1.36, 2.04)	18.4 (-52.3, 89.1)	0.76	**<0.001[a]**, 0.60[b]
Soleus (mg)				
• Males (n=14)	0.44 (0.33, 0.54)	-15.9 (-31.1, -0.66)	0.92	**<0.001[a]**, **<0.05[b]**
• Females (n=22)	0.46 (0.24, 0.68)	5.10 (-13.3, 23.5)	0.74	**<0.001[a]**, 0.57[b]
• Combined (n=36)	0.36 (0.32, 0.40)	-9.22 (-17.9, -0.57)	0.91	**<0.001[a]**, **<0.05[b]**
EDL (mg)				
• Males (n=14)	0.19 (0.10, 0.27)	-14.9 (-27.3, -2.46)	0.81	**<0.001[a]**, **<0.05[b]**
• Females (n=22)	0.21 (0.05, 0.36)	-11.1 (-24.0, 1.85)	0.79	**<0.05[a]**, 0.09[b]
• Combined (n=36)	0.28 (0.25, 0.31)	-6.89 (-13.5, -0.33)	0.92	**<0.001[a]**, **<0.05[b]**

Note: Phenotype was entered as a dummy variable with normobilirubinaemic phenotype used as the reference group to which the hyperbilirubinaemic phenotype was compared. $B_{1\text{-}2}$ represent the un-standardised regression coefficients for bodyweight and phenotype, respectively. The "B coefficient" estimates the change in mass (mg) of the dependent variables per unit of increase in bodyweight (g) or in the presence of the hyperbilirubinaemic phenotype. CI, Confidence Interval; EDL, extensor digitorum longus. [a]Statistical significance of bodyweight as an independent predictor of organ weight P<0.05. [b]Statistical significance of phenotype as an independent predictor of organ weight P<0.05.

Energy balance

Body mass and food intake were measured over a 16-day period. Female Gunn rats gained significantly less bodyweight (P<0.01) and consumed significantly fewer calories per day compared to controls (P<0.01; Fig. 4.1 and Table 4.4). In contrast, there was no difference in body mass gain (data not shown) and food intake (Table 4.4) in male Gunn rats compared to controls. When adjusting body mass gain over calorie intake, female Gunn rats were significantly less energetically efficient compared to controls (P<0.05), however, no difference existed in males (Table 4.4).

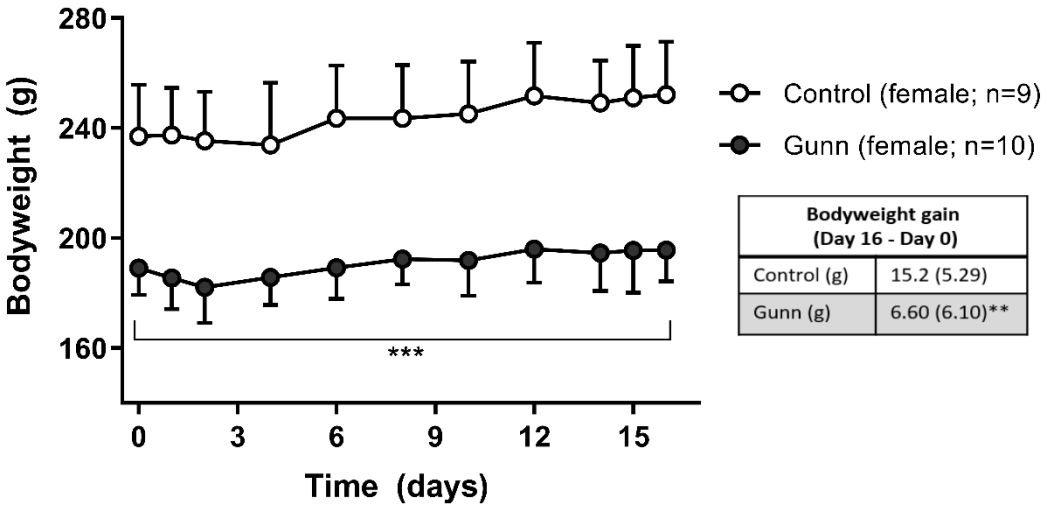

Figure 4.1. Bodyweight over a 16 day period in female Gunn (hyperbilirubinaemic) and control (normobilirubinaemic) littermates. P<0.05*, <0.01**, <0.001*** compared to control.

Table 4.4. Food intake and energy efficiency of hyperbilirubinaemic rats and their normobilirubinaemic littermates.

Variable	Phenotype		P value
	Control	Gunn	
Food Intake (kcal day^{-1})			
• Males	83.5 (14.1)	82.4 (6.78)	0.848
• Females	63.3 (6.95)	54.1 (6.38)	**<0.01**
Energy efficiency (mg kcal^{-1})			
• Males	15.6 (2.70)	17.0 (7.60)	0.65
• Females	14.9 (5.10)	8.09 (5.75)	**<0.05**

Note: Control and Gunn groups represent normobilirubinaemic heterozygote and hyperbilirubinaemic homozygote littermates, respectively. Values are represented as mean (standard deviation). Statistical comparisons are made between phenotypes within the same sex.

Mitochondrial function

Given that reduced energetic efficiency was reported in female Gunn rats, the effect of UCB on mitochondrial function was investigated. Exogenous UCB was added to control (normobilirubinaemic) liver tissue and the dose-dependent effect of UCB on mitochondrial function was assessed. At the highest concentration (125 µM), UCB significantly inhibited LEAK, CI and CI+II OXPHOS when compared to control ($P<0.001$ and $P<0.05$, respectively; Fig. 4.2A). Furthermore, 31.3 and 125 µM UCB significantly inhibited CI+II ETS and CII ETS compared to control ($P<0.01$ and $P<0.001$, respectively; Fig. 4.2A). The ratio of CI+II OXPHOS to ETS was significantly reduced only by 31.3 and 62.5 µM UCB compared to control ($P<0.05$ and $P<0.01$, respectively; Fig. 4.2C).

To assess whether similar effects of *in vitro* UCB were recapitulated in hyperbilirubinaemic Gunn rats, mitochondrial function was assessed in fresh liver tissue. No significant change in O_2 flux (LEAK, OXPHOS, or ETS) existed between Gunn rats and controls, when normalised to liver mass or citrate synthase activity (Fig. 4.3 and 4.4). However, CI+II OXPHOS relative to ETS was significantly increased in female Gunn rats compared to controls ($P<0.05$; Fig. 4.3B).

In addition to the liver, skeletal muscle importantly contributes to energy expenditure and is a major individual determinant of basal metabolic rate (BMR). The O_2 flux of intact soleus and EDL permeabilised muscle fibres was assessed in order to evaluate mitochondrial function, in predominantly slow twitch and fast twitch muscle fibres, respectively [403]. There was no difference in O_2 flux (LEAK, OXPHOS, or ETS) between Gunn and control rats for soleus or EDL (Fig. 4.5 and 4.6). As ETS was not different to CI+II OXPHOS, CI+II OXPHOS was used as a reference state to calculate FCRs. FCRs were not significantly different across groups in soleus or EDL (Fig. 4.5 and 4.6).

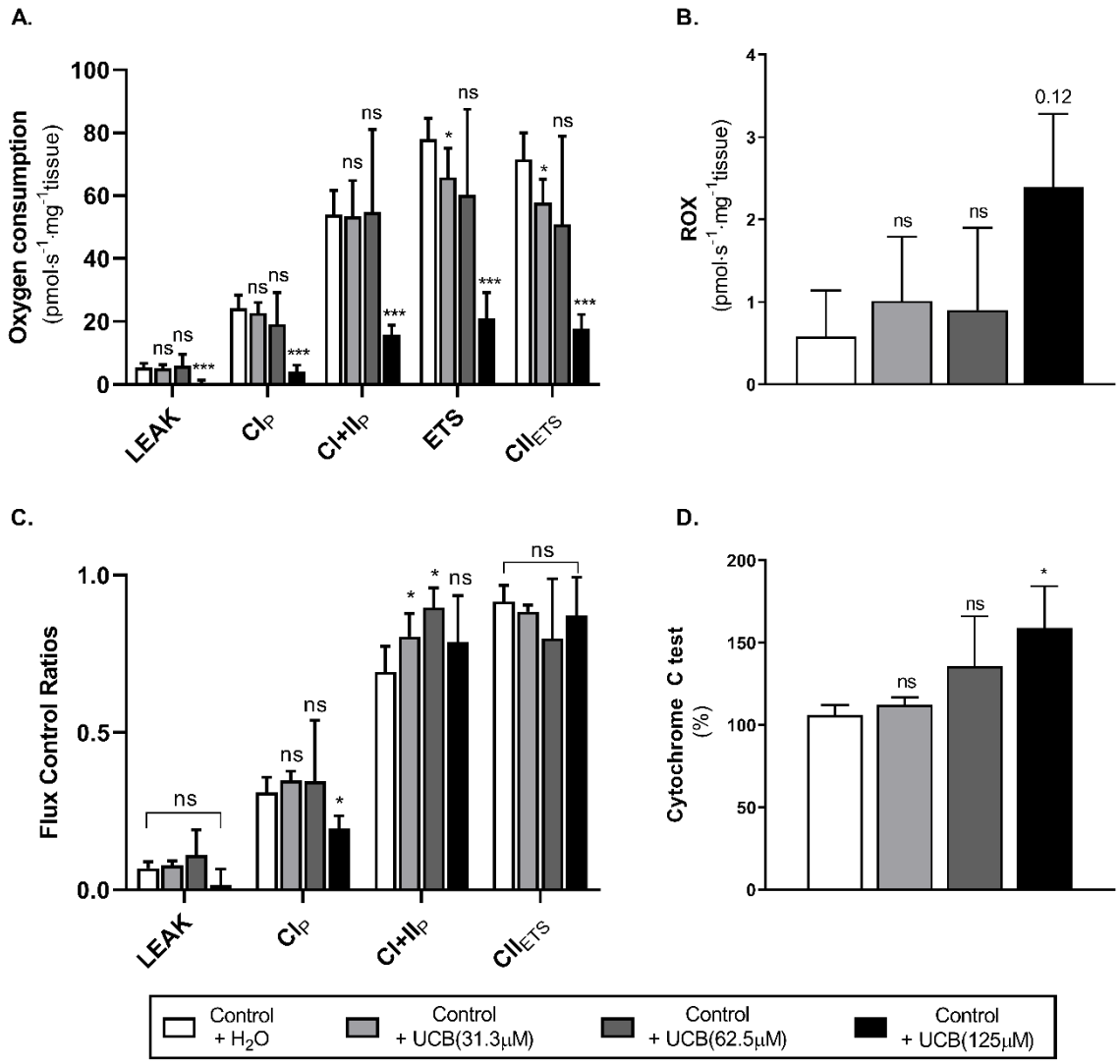

Figure 4.2. Effect of exogenous UCB on mitochondrial function in juvenile control (normobilirubinaemic) liver tissue (n=5). Mitochondrial respiratory states are identified as intrinsic uncoupling measured in the absence of ADP (LEAK), OXPHOS capacity measured at saturating levels of ADP (CI_P and $CI+II_P$) and noncoupled respiratory capacity (ETS and CII_{ETS}). A and B) The rate of respiratory states evaluated based on O_2 consumption per mass of tissue at varying UCB concentrations. C) Respiratory states expressed relative to a common reference state (ETS). D) Evaluating mitochondrial outer membrane integrity by the addition of cytochrome c, represented as % change in O_2 consumption relative to before cytochrome c addition. CI, CII, mitochondrial respiratory chain Complex I and Complex II, respectively; ETS, electron transfer system; ROX, residual O_2 consumption; UCB, unconjugated bilirubin. P<0.05*, <0.01**, <0.001*** compared to control+H_2O. ns: non-significant.

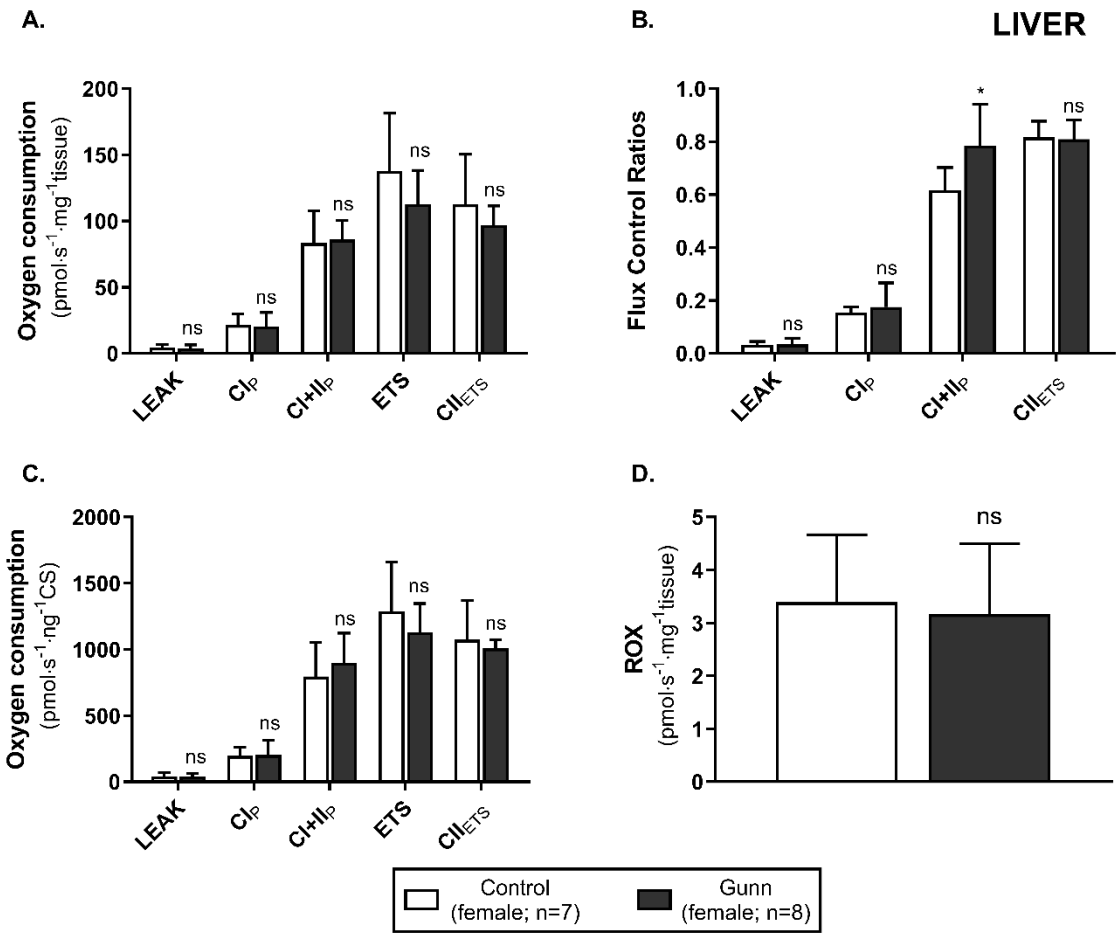

Figure 4.3. Mitochondrial function in adult female Gunn (hyperbilirubinaemic) and control (normobilirubinaemic) liver tissue. Mitochondrial respiratory states are identified as intrinsic uncoupling measured in the absence of ADP (LEAK), OXPHOS capacity measured at saturating levels of ADP (CI_P and $CI+II_P$) and noncoupled respiratory capacity (ETS and CII_{ETS}). A and D) The rate of respiratory states evaluated based on O_2 consumption per mass of tissue. B) Respiratory states expressed relative to a common reference state (ETS). C) The rate of respiratory states evaluated based on O_2 consumption per protein of citrate synthase. CI, CII, mitochondrial respiratory chain Complex I and Complex II, respectively; ETS, electron transfer system; ROX, residual O_2 consumption. P<0.05*, <0.01**, <0.001*** compared to control. ns: non-significant.

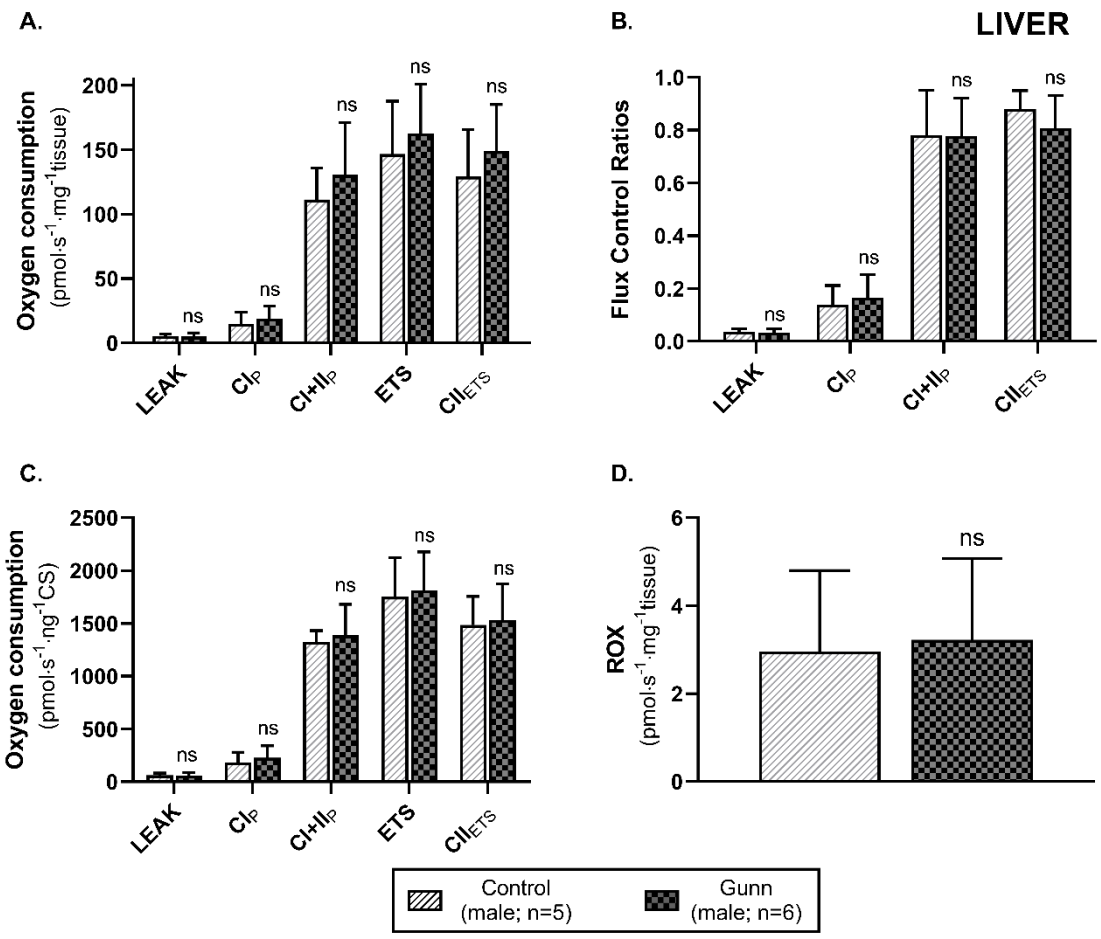

Figure 4.4. Mitochondrial function in adult male Gunn (hyperbilirubinaemic) and control (normobilirubinaemic) liver tissue. Mitochondrial respiratory states are identified as intrinsic uncoupling measured in the absence of ADP (LEAK), OXPHOS capacity measured at saturating levels of ADP (CI_P and $CI+II_P$) and noncoupled respiratory capacity (ETS and CII_{ETS}). A and D) Respiratory states evaluated based on O_2 consumption per mass of tissue. B) The rate of respiratory states expressed relative to a common reference state (ETS). C) The rate of respiratory states evaluated based on O_2 consumption per protein of citrate synthase. CI, CII, mitochondrial respiratory chain Complex I and Complex II, respectively; ETS, electron transfer system; ROX, residual O_2 consumption. P<0.05*, <0.01**, <0.001*** compared to control. ns: non-significant.

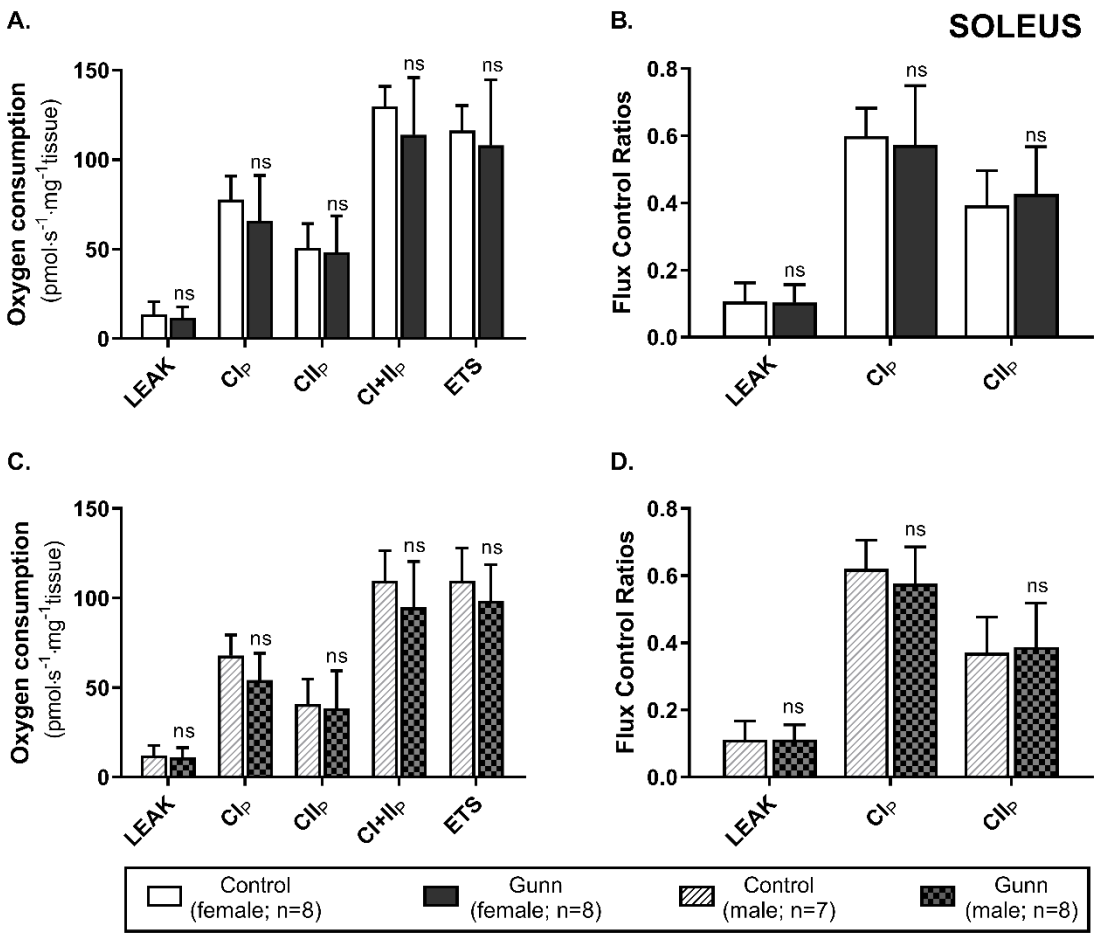

Figure 4.5. Mitochondrial function in adult female (A and B) and male (C and D) Gunn (hyperbilirubinaemic) and control (normobilirubinaemic) permeabilised soleus fibres. Mitochondrial respiratory states are identified as intrinsic uncoupling measured in the absence of ADP (LEAK), OXPHOS capacity measured at saturating levels of ADP (CI_P, CII_P, and $CI+II_P$) and noncoupled respiratory capacity (ETS). A and C) The rate of respiratory states evaluated based on O_2 consumption per mass of tissue. B and D) Respiratory states expressed relative to a common reference state ($CI+II_P$). CI, CII, mitochondrial respiratory chain Complex I and Complex II, respectively; ETS, electron transfer system; P<0.05*, <0.01**, <0.001*** compared to control. ns: non-significant.

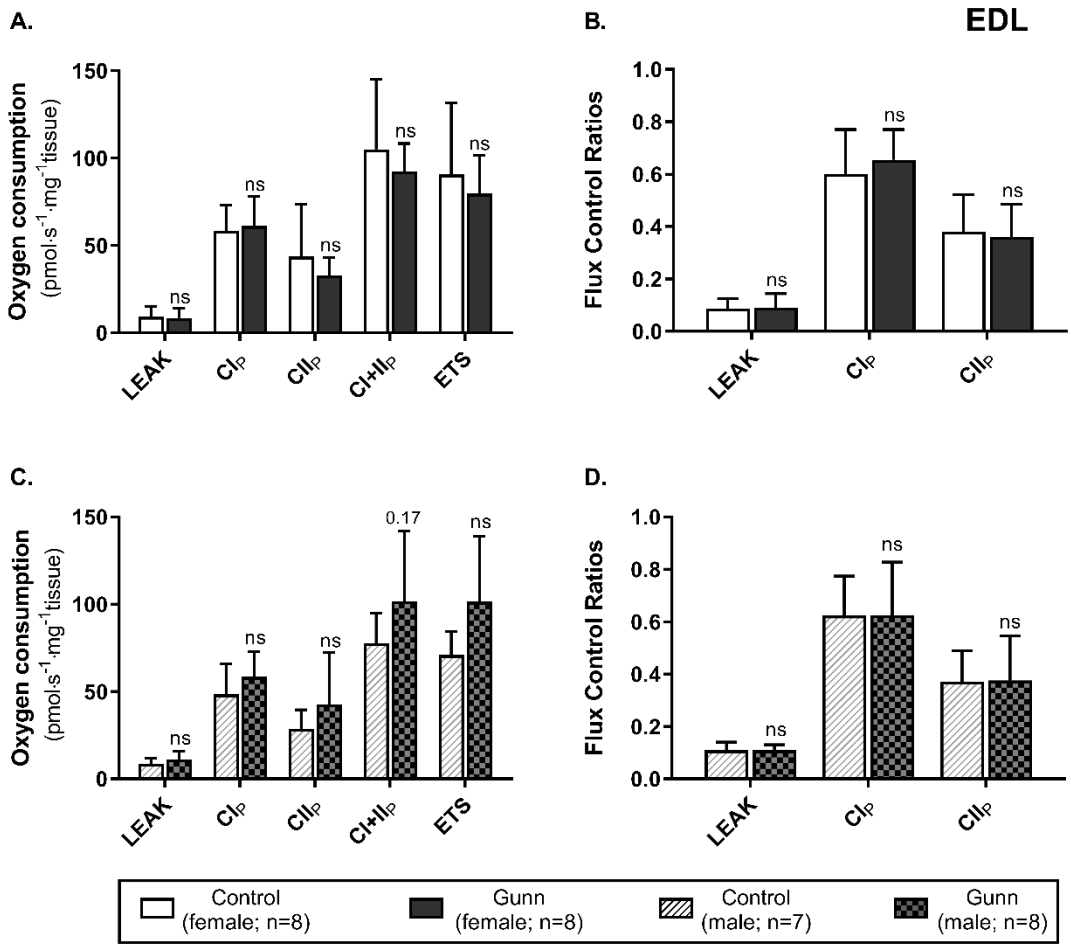

Figure 4.6. Mitochondrial function in adult female (A and B) and male (C and D) Gunn (hyperbilirubinaemic) and control (normobilirubinaemic) permeabilised EDL fibres. Mitochondrial respiratory states are identified as intrinsic uncoupling measured in the absence of ADP (LEAK), OXPHOS capacity measured at saturating levels of ADP (CI_P, CII_P, and $CI+II_P$) and noncoupled respiratory capacity (ETS). A and C) The rate of respiratory states evaluated based on O_2 consumption per mass of tissue. B and D) Respiratory states expressed relative to a common reference state ($CI+II_P$). CI, CII, mitochondrial respiratory chain Complex I and Complex II, respectively; ETS, electron transfer system; EDL, Extensor digitorum longus. P<0.05*, <0.01**, <0.001*** compared to control. ns: non-significant.

Female Gunn rats have improved mitochondrial quality

Finally, hepatic mitochondrial quantity and quality were evaluated by measuring protein expression of mitochondrial respiratory complexes using Western Blot. There was significantly greater expression of complex IV in female Gunn rats when compared to controls ($P<0.01$; Fig. 4.7D). No significant differences in the expression of all complexes were noted in male Gunn versus control rats (Fig. 4.7).

Citrate synthase activity was measured as a crude indicator of mitochondrial density in liver homogenates of adult Gunn and control rats. There were no differences in citrate synthase activity between groups (Fig. 4.8A). Phosphorylated AMP-activated protein kinase (pAMPK) relative to total AMPK was measured as an indirect marker of the AMP to ATP ratios and the energetic state of liver tissue. Ratios of pAMPK:AMPK were unchanged across groups (Fig. 4.8B).

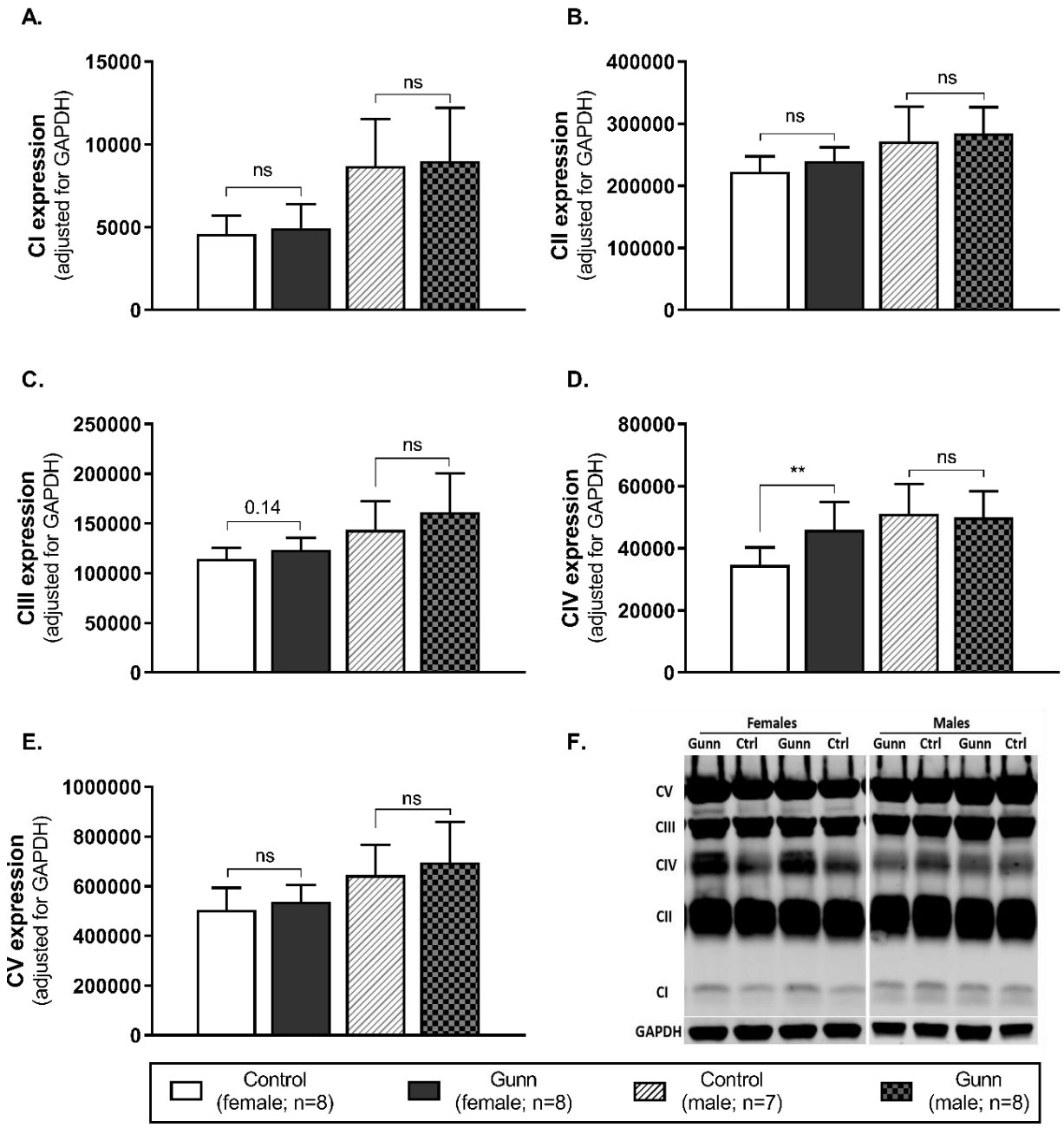

Figure 4.7. Mitochondrial quality and density assessed by Western blot in adult Gunn (hyperbilirubinaemic) and control (normobilirubinaemic) liver tissue. A-E) Protein extracts from liver tissue were investigated for CI-V protein expression adjusted for a loading control (GAPDH). F) Example Western blot analysis of mitochondrial complexes. CI-V, mitochondrial respiratory chain Complex I-V. P<0.05*, <0.01**, <0.001*** compared to control. ns: non-significant.

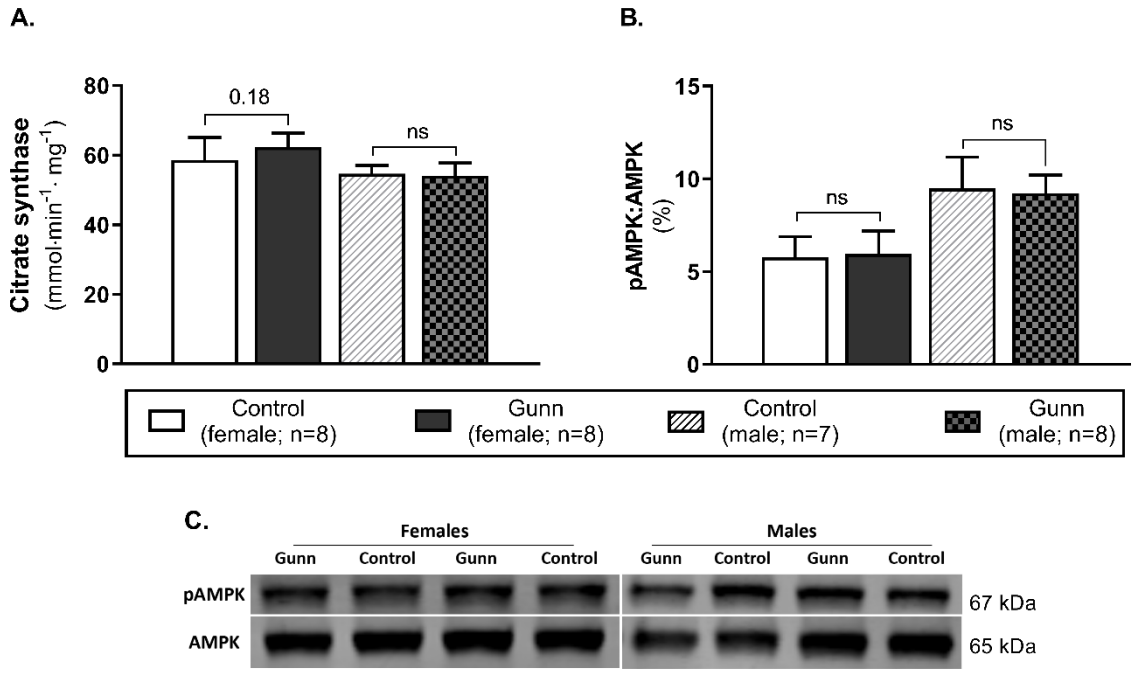

Figure 4.8. Hepatic mitochondrial density measured by citrate synthase activity and energetic state assessed using pAMPK:AMPK ratios in adult Gunn (hyperbilirubinaemic) and control (normobilirubinaemic) liver tissue. A) Citrate synthase activity measured in protein extracts from liver tissue standardised for total protein. B) Phosphorylated AMPK expression over total AMPK measured using Western blot. AMPK, AMP-activated protein kinase; pAMPK, phosphorylated AMPK. P<0.05*, <0.01**, <0.001*** compared to control. ns: non-significant.

4.4 Discussion

This study presents the first comprehensive evaluation of mitochondrial function and body composition in an animal model of benign hyperbilirubinaemia. Greater hepatic CI+II OXPHOS FCR and increased CIV expression was observed in female Gunn rats, suggesting an improvement in mitochondrial quality. These findings occurred in association with reduced bodyweight and fat mass in female Gunn rats. In contrast, exogenous addition of UCB inhibited mitochondrial function, thus, the changes in mitochondrial quality observed in female Gunn rats may be a compensatory mechanism that beneficially impacts body composition. The main findings of this study were most prominent in the female sex, indicating that the physiological impact of hyperbilirubinaemia or UGT1A1 impairment has a sexually dimorphic nature.

Hyperbilirubinaemic Gunn rats have previously been shown to have reduced body mass compared to controls [246,371,404]. We sought to determine whether fat and or lean mass was responsible for this difference and revealed significantly reduced lean mass in male and female Gunn rats compared to normobilirubinaemic littermates (controls). However, significant reductions in fat mass and body length were only observed in female Gunn rats. Excess body fat relative to bodyweight (fat mass (%)) increases the risk of CVD and is positively correlated with fasting plasma glucose, total cholesterol, and triglycerides [405]. Female Gunn rats demonstrated a notable, albeit not significant, 26% reduction in fat mass (%) compared to controls (see Table 4.1).

Stec et al. examined the effect of UCB treatment on body composition in male normobilirubinaemic mice fed a HFD [10]. After a week of UCB treatment, mice had reduced bodyweight and fat mass (%), and greater lean mass (%) [10]. Interestingly, the study reported that UCB is an endogenous agonist of peroxisome proliferator-activated receptor alpha (PPARα) and the lipid-reducing effects of UCB were abolished in PPARα knockout mice. Recently, these findings were corroborated in male mice with chronic hyperbilirubinaemia that consumed a HFD. These animals demonstrated reduced bodyweight, fat mass (%), liver triglycerides, and

greater lean mass (%) when compared to normobilirubinaemic controls and this was associated with enhanced PPARα activation [11]. Therefore, these studies suggest that UCB is an endogenous regulator of fat metabolism and support the present results of reduced fat mass in a rat model of hyperbilirubinaemia. Surprisingly, reduced adiposity was only observed in female Gunn rats (Table 4.1). Pharmacological activation of PPARα is attenuated in ovary intact animals, thus, greater lipid reductions would be expected in *male* Gunn rats if UCB activates PPARα [372]. As such, these results cannot be explained through UCB-mediated PPARα activation and argue that a more complex mechanism of action is responsible for the phenotype observed in female Gunn rats.

BMR contributes ~65% of daily energy expenditure, which is proportional to lean mass and its composition [406]. Lean mass is primarily comprised of skeletal muscle and organs, with organs responsible for a much larger fraction of BMR (70-90% organs vs 13-20% skeletal muscle) [407–409]. In mice, the liver alone accounts for 50% of BMR while constituting only 6.2% of bodyweight [409]. Although, female Gunn rats had significantly reduced organ masses (Table 4.2), they had greater organ to lean mass ratios compared to controls (Appendix 2, Fig. S4.1). Considering that organs are more metabolically active than other forms of lean mass, it is plausible that BMR relative to bodyweight is greater in female Gunn rats [407–409]. Greater BMR would explain the reduced energetic efficiency and decreased bodyweight in female Gunn rats (see Table 4.1 and 4.4). Interestingly, Hinds et al. reported that the daily rate of O_2 consumption (VO_2) was not different in male hyperbilirubinaemic mice compared to controls, however, it remains to be investigated in female hyperbilirubinaemic animals [11].

A unique finding in this study was that organ masses differed disproportionately in female Gunn and control rats. For example, female Gunn rat organs were generally lighter than controls, however, when corrected for bodyweight were significantly increased in Gunn animals (Table 4.2 and Appendix 2, Table S4.2). Toxicity studies show that the relationship of organ mass to bodyweight is not linear for every organ, thus, correction for bodyweight can introduce error

and misrepresent the effect of the condition/treatment on organ masses [410]. To avoid this problem, we applied multiple linear regression to separate the effects of bodyweight from phenotype on organ masses. This analysis revealed that liver mass increased 2.44 g and kidney mass decreased 0.15 g with the Gunn female phenotype, independent of bodyweight (Table 4.3). This is the first study to demonstrate an association of hyperbilirubinaemia/UGT1A1 impairment with organ masses. Greater voluntary physical activity is another possible reason for the leaner phenotype in Gunn rats. This conclusion is supported by data showing that 3-4 month old male Gunn rats had reduced bodyweight and travelled 23-160% more distance compared to normobilirubinaemic littermates [411]. However, a lack of measurements on the resting energy expenditure in Gunn rats precludes the ability to determine the cause of reduced bodyweight in these animals.

In order to explore the possibility of greater BMR we investigated mitochondrial function in several tissues. UCB has traditionally been described as toxic to mitochondria because it uncouples oxidative phosphorylation and induces membrane permeabilisation [260,396–398,412]. For instance, 20-40 µM of UCB reduced state 3 (submaximal oxidative phosphorylation) respiration by 50% with a corresponding increase in the rate of uncoupled mitochondrial (LEAK) respiration via CI and CII in isolated rat mitochondria [412]. In the present study exogenous UCB addition to control liver tissue induced dose-dependent inhibition of ETS, and inhibited OXPHOS at 125 µM UCB (see Fig. 4.2A). Furthermore, 125 µM UCB affected the membrane integrity of mitochondria, as demonstrated by a 59% increase in O_2 flux with cytochrome c addition (Fig. 4.2D). This is consistent with previous studies that show that UCB increases mitochondrial membrane permeability and induces release of cytochrome c [260,396,413].

Surprisingly, the rate of LEAK respiration was not affected by UCB, nor was OXPHOS inhibited at concentrations less than 125 µM (Fig. 4.2A). This is contrary to previous studies that demonstrate an uncoupling effect of UCB on respiration and inhibition of oxidative

phosphorylation in the presence of 10-100 µM UCB [253,412]. The inconsistency in findings may be explained by the concentration of albumin used in experimental models, as albumin avidly binds UCB and limits its diffusion into mitochondria [43]. For example, in the absence of albumin, UCB induces mitochondrial uncoupling, however, it has no effect on mitochondrial function at 1:1 UCB:albumin molar ratios [253,412]. This study used a final albumin concentration of 15 µM (1 g L^{-1}) indicating that significant mitochondrial dysfunction was induced above a 8:1 UCB:albumin ratio (125 µM UCB).

The impact of UCB on mitochondrial function has been investigated extensively *in vitro*. However, few studies have evaluated mitochondrial function in hyperbilirubinaemic animals and these investigations report inconsistent results [263–265]. Celier et al. showed comparable state 3 respiration and respiratory control ratios (RCR) between male Gunn and Wistar control rats (8 weeks of age) in isolated hepatic mitochondria. This is in opposition to the results of Fritz-Niggli who reported reductions in P/O ratios in male and female Gunn rats compared to Sprague-Dawley controls in isolated hepatic mitochondria [263,264]. It is important to note that the serum bilirubin concentrations of the Gunn rats from Fritz-Niggli [264] ranged between 115-240 µM, whilst those within this study approximated 80-100 µM. These bilirubin concentrations are more likely to affect mitochondrial function and may contribute to the discrepancies between studies [414]. In stark contrast, Zelenka et al. demonstrated that O_2 flux of isolated hepatic mitochondria from aged (12-18 months old) Gunn rats was greater when compared to normobilirubinaemic siblings [265]. Discrepancies in these findings could be caused by differences in the degree of hyperbilirubinaemia, although this cannot be confirmed because bilirubin concentrations were not reported outside of Fritz-Niggli [264], methods employed, and the age of the animals studied.

In this study, there was no difference in mitochondrial respiratory capacity (relative to tissue mass or citrate synthase activity) in hepatic tissue or skeletal muscle of both sexes. However, CI+II OXPHOS relative to ETS (CI+II OXPHOS FCR) was significantly greater in hepatic tissue of

female Gunn rats and this was also reported when liver tissue of normobilirubinaemic female rats was treated with 31 or 62.5 μM exogenous UCB (see Fig. 4.2C and 4.3B). These findings could be explained by UCB-mediated perturbation of the inner mitochondrial membrane or CIV inhibition [67,260,262,396–398,412].

The rate of O_2 consumption is affected by mitochondrial density and mitochondrial quality, thus, FCRs such as OXPHOS:ETS ratios, eliminate the influence of mitochondrial density allowing the study of qualitative changes in the electron transfer pathways involved in the electron transfer system [67]. Increased CI+II OXPHOS FCR indicates that hepatic mitochondria in female Gunn rats are working closer to their maximal oxidative capacity and may indicate greater mitochondrial energy efficiency [19,67]. Increased OXPHOS respiration, without a change in ETS, reflects greater coupling of mitochondrial respiration to ATP synthesis (i.e. greater mitochondrial efficiency) and causes a reduction in reserve oxidative capacity [18,19,67,415]. Conversely, enzymatic defects in mitochondrial respiratory complexes (CI-IV), independent of ATP synthesis, limits ETS respiration and reduces reserve oxidative capacity [18,67]. Female Gunn rats demonstrated a small non-significant increase in CI+II OXPHOS and a decrease in ETS (Fig. 4.3). Therefore, these results suggest that the reason of increased hepatic CI+II OXPHOS FCR in female Gunn rats was due to a combination of improved mitochondrial efficiency and enzymatic dysfunction.

Although, a similar effect was reported when control liver tissue was treated with exogenous UCB (31 or 62.5 μM), reduction in reserve oxidative capacity in this instance was likely caused by UCB-mediated inhibition of mitochondrial respiratory complexes. Exogenous UCB treatment dose-dependently inhibited ETS causing an increase in CI+II OXPHOS FCR (Fig. 4.2A). Therefore, reduction in ETS respiration suggests that UCB inhibits activity of one or more of the mitochondrial complexes [18,67]. This conclusion is supported by a study showing that UCB inhibits CIV activity by 18-20% in liver tissue at 1:2 UCB:albumin molar ratios [262]. Since this

study employed UCB:albumin molar ratios greater than 1:2, exogenous UCB treatment likely inhibited CIV activity in liver tissue causing a reduction in ETS capacity.

To further evaluate the changes in hepatic mitochondrial quality, we measured the expression of each mitochondrial respiratory complex. Intriguingly, a significant increase in CIV expression was demonstrated in female Gunn rats. Considering that UCB can inhibit CIV activity, greater CIV expression in female Gunn rats could represent a compensatory mechanism to UCB-mediated inhibition [261,262]. Surprisingly, a similar effect was not observed in male Gunn rats suggesting that changes in CIV expression could instead involve a combination of UCB and differences in reproductive hormone concentrations. In addition to UCB, UGT1A1 is an important enzyme for 17β-estradiol conjugation and excretion through the hepatobiliary route [16,17]. Consequently, UGT1A1 impairment in female Gunn rats potentially increases oestrogen concentrations, however, this remains to be determined. Galmes-Pascual et al. demonstrated that 17β-estradiol administration in ovariectomised rats increased hepatic CIV activity and protein expression. Furthermore, incubating HepG2 cells with 17β-estradiol increases CIV expression and ATP levels compared to non-treated cells [416]. Even though no changes were observed in pAMPK:AMPK ratios, CIV expression was increased in female Gunn rats, suggesting that 17β-estradiol levels may be elevated in this animal model, and requires assessment in future studies.

4.5 Conclusion

The effect of hyperbilirubinaemia in the Gunn rat shows a strong sexually dimorphic effect on body composition and hepatic mitochondrial quality. While all Gunn rats demonstrate reduced bodyweight and lean mass compared to normobilirubinaemic controls, only females had reduced fat mass and hepatic triglyceride concentrations. Reductions in fat storage could be explained by reduced food intake, differences in lean mass constitution, or changes to hepatic mitochondrial quality. Female Gunn rats demonstrated increased hepatic CI+II OXPHOS FCR and this was associated with greater CIV expression which could have developed as an adaptive response to UCB-mediated CIV inhibition. The absence of significant effects in male Gunn rats

suggests an interaction with reproductive hormones including oestrogen and warrants further investigation.

Chapter 5: The effect of Legalon® (Silymarin) treatment on circulating bilirubin concentrations and markers of cardiovascular disease in healthy men: randomised crossover single blind placebo-controlled clinical trial

The findings of reduced circulating cholesterol concentrations and decreased adiposity in hyperbilirubinaemic animals led to investigating the impact of oral silymarin (Legalon®) supplementation on circulating bilirubin and whether this affects lipid concentrations in healthy humans. Legalon® supplementation in healthy men did not affect circulating bilirubin and lipid concentrations. However, this study provides the groundwork for future investigations to study the effects of greater doses or different formulations of silymarin.

Statement of Contribution to a Co-Authored Published Paper

This chapter is in the form of a co-authored paper currently under consideration. The bibliographic details of the co-authored published paper are:

Vidimce J, Pennell EN, Foo M, Shiels RG, Shibeeb S, Watson M, Bulmer AC. The effect of Legalon®(Silymarin) treatment on circulating bilirubin concentrations and markers of cardiovascular disease in healthy men: randomised crossover single blind clinical trial. Submitted to journal of *Complementary Therapies in Medicine*.

Appropriate acknowledgements of those who contributed to the research but did not qualify as authors are included in the paper.

My contribution to the published paper involved:

- Assisted in study design and ethical approval
- Analytical experimental design, planning, development, and validation of analytical methods
- Participant recruitment, screening and follow up,
- Participant sample acquisition and processing,
- Analytical data acquisition and statistical analysis,
- Manuscript preparation, critical review and submission

(Sign) _____ 19th of March 2020 (Date)

First Author and PhD Candidate
Josif Vidimce

(Sign) _____ 19th of March 2020 (Date)

Corresponding Author and Supervisor
Associate Professor Andrew Bulmer

The effect of Legalon® (Silymarin) treatment on circulating bilirubin concentrations and markers of cardiovascular disease in healthy men: randomised crossover single blind placebo-controlled clinical trial

Josif Vidimce[a] (J. Vidimce)[#], Evan Noel Pennell[a] (E.N. Pennell)[#], Maximillian Foo[a] (M. Foo), Ryan Graeme Shiels[a] (R.G. Shiels), Sapha Shibeeb (S. Shibeeb), Michael Watson[b] (M.J. Watson)*, and Andrew Cameron Bulmer[a] (A.C. Bulmer)*

[a] School of Medical Science, Griffith University, Gold Coast, Australia

[b] Endeavour College of Natural Health, Melbourne, Australia

[#]Contributed equally to this manuscript.

*Contributed equally to this manuscript.

Corresponding Author:

A/Prof Andrew Bulmer

School of Medical Science - Griffith University

Parklands Drive, Southport 4215

QLD Australia

E: a.bulmer@griffith.edu.au

Funding

This work was supported by an Office of Research Project Grant (20160824) provided by the Endeavour College of Natural Health. This work was also supported by the School of Medical Science Griffith University.

Keywords

- Silibinin
- Silymarin
- Unconjugated bilirubin
- Cholesterol
- Lipid
- Triglyceride
- Legalon®
- Milk Thistle

Word count: 3982

5.1 Abstract

Objectives

This clinical trial investigated the impact of silymarin (Legalon®) on circulating bilirubin concentrations, lipid status, inflammation, and antioxidant status.

Design

The study was a randomised placebo controlled single blind crossover clinical trial of healthy males (18-65 years of age).

Setting

The study was conducted at Griffith University, Gold Coast, Australia, and participants were recruited from Griffith University and Endeavour College (Gold Coast).

Interventions

Participants were randomised to Legalon® (140 mg silymarin capsules thrice daily) or placebo (3 capsules daily with mannitol) for 14 days followed by ≥4 weeks washout and crossover to the other arm.

Main outcome measures

The primary outcome was an increase of >5 µM in serum bilirubin concentrations compared to baseline, and secondary outcomes were a change in serum lipid status (cholesterol and triglycerides), inflammation (c-reactive protein), and antioxidant capacity (ferric reducing ability of plasma).

Results

A total of 17 participants were included in the final analysis. Legalon® consumption did not affect serum concentrations of unconjugated bilirubin concentrations (12.5 ± 7.63 vs 11.4 ± 4.14 µM, P=0.79), cholesterol (4.80 ± 1.00 vs 4.88 ± 1.00 mM, P=0.19), triglycerides (1.07 ± 0.63 vs 1.04 ± 0.54 mM, P=0.79), c-reactive protein (1.74 ± 1.88 vs 0.92 ± 0.87 mg L^{-1}, P=0.23) or antioxidant status (1194 ± 182 vs 1183 ± 201 mmol Fe^{2+} L^{-1}, P=0.19).

Conclusion

In this trial (ACTRN12619001296123), Legalon® did not elevate serum bilirubin concentrations and antioxidant status or decrease lipids and inflammation in healthy males. These findings question previous reports of hyperbilirubinaemia following silymarin treatment and the capacity for silymarin to affect lipids, inflammation, and antioxidant status.

5.2 Introduction

Milk thistle (S*ilybum marianum)* has been used over the past 2000 years for medicinal purposes, most recently for the treatment of hepatic diseases including hepatitis and cirrhosis [350]. The active constituents of Milk thistle comprise a mixture of three main flavonolignan compounds, silibinin, silydianin, and silychristine [351]. Extracts of Milk thistle, collectively referred to as silymarin, have demonstrated antioxidant, anti-inflammatory, antifibrotic, and hepatoprotective properties [360]. Central to hepatoprotection is the ability of silymarin to preserve cell membrane integrity and modulate the transport of xenobiotics [417–420]. Silibinin is the most abundant active constituent of silymarin and it competitively inhibits hepatic organic-anion-transporting polypeptide 1B1 (OATP1B1) and OATP1B3 [354,360]. OATP1B1 and OATP1B3 transport a wide range of xenobiotics and endogenous molecules like unconjugated bilirubin (UCB) [421].

UCB is a hydrophobic haem catabolite, which is solubilised in blood by albumin binding [43]. From the circulation, UCB is taken up by hepatocytes by sinusoidal membrane OATP1B1 and OATP1B3 and is conjugated by hepatic UDP-glucuronosyltransferase 1A1 (UGT1A1). Bilirubin conjugates are then deposited by MRP2 into the bile canaliculus [422,423]. Intriguingly, silibinin inhibits UGT1A1 and MRP2 activity in addition to OATP1B1 and OATP1B3 [234,354,424]. Therefore, silibinin has the potential to inhibit uptake, conjugation, and excretion of UCB, which explains the reports of silymarin induced hyperbilirubinemia [22,23,363]. Although UCB can be toxic at severely elevated plasma concentrations (i.e. >300 µM), mild elevations (17.1 - 90 µM), as seen in Gilbert's syndrome, may be of potential benefit [373,425,426].

Individuals with GS demonstrate decreased risk of coronary artery disease (CAD), ischemic heart disease (IHD) and atherosclerosis, culminating in reduced prevalence of all-cause mortality [241,267,281]. UCB could protect against cardiovascular disease (CVD) by imparting anti-inflammatory [282], antioxidant [8,331,427], and lipid lowering effects [12]. For instance, *in vitro* UCB is a potent scavenger of peroxyl radicals [8], peroxynitrite [427], and superoxide [331], and

protects against lipid and protein oxidation *in vivo* [7,331,428]. Furthermore, circulating UCB levels are inversely correlated with serum total cholesterol, which is an important risk factor for CVD [12]. Therefore, silymarin could have potential as a cardiovascular protective agent by elevating serum UCB concentrations. Additionally, silymarin treatment, independent of its effect on UCB concentration, has demonstrated lipid lowering [429,430], anti-oxidant [431], and anti-inflammatory properties that may assist in protecting against CVD [432,433]. However, controversy exists as to whether Legalon® can provide these benefits at the recommended dose [434,435]. Despite being sold for public consumption as an 'over the counter' liver detox supplement there is a lack of studies evaluating the potential benefits in healthy individuals.

Legalon® is a standardised preparation equivalent to 140 mg of silymarin per capsule with a maximum recommended dose of three capsules per day, totalling a dosage of 420 mg day^{-1} as indicated by the manufacturer. Therefore, this clinical trial aimed to evaluate whether oral Legalon® administration, at the recommended dosage, increases serum bilirubin concentration (primary outcome), affects inflammation, antioxidant capacity and lipid status (secondary outcome) in healthy male volunteers.

5.3 Methods

Materials

Legalon® was purchased from Flordis Pty. Ltd. (Melbourne, Australia) and placebo capsules (red gelatine capsules filled with food grade mannitol powder) were purchased from Melbourne Food Depot (Melbourne, Australia). All phlebotomy consumables were purchased from Becton Dickinson (Brisbane, Australia). HPLC-grade methanol (MeOH) was purchased from Chem-Supply (Adelaide, South Australia). Biochemistry assays were purchased from Roche Diagnostics (Sydney, Australia). All other reagents were purchased from Sigma Aldrich (Sydney, Australia) unless otherwise stated.

Study design

The study was a randomised crossover single-blind placebo-controlled clinical trial. Participants were randomly assigned at 1:1 ratio to treatment (140 mg silymarin thrice daily as Legalon® preparation) or placebo (3 capsules daily of similar weight containing mannitol) for 14 days. Participants were randomised by one of the principal investigators through sequential selection of envelopes that contained a number corresponding to the study arm. Participants were blinded to the study arm by utilising red gelatine placebo capsules, similar in appearance to Legalon® capsules. At the beginning of each study arm (V2 or V5), participants received a prepacked bottle of identical appearance labelled with their ID, containing either Legalon® or placebo capsules according to their randomisation. Participants were advised to maintain a constant lifestyle and take 3 capsules a day orally, 8 hrs apart for the duration of the study arm (2 weeks; Fig. 5.1). After successful completion of the first arm, participants underwent a washout period of 4-weeks (minimum) before beginning the second arm (Fig. 5.1). Participants were required to attend the clinic weekly in each arm (i.e. baseline (V2), week 1 (V3), and week 2 (V4)). During each visit, blood was collected and brief questionnaires regarding adverse effects and concomitant medications were undertaken. Within each arm, visits were undertaken on the same day of the week at a similar time, preceded by an overnight fast prior to blood collection.

The medication bottle was retrieved from the participants at the final visit of each arm (V4 or V7) and compliance was assessed by counting unused capsules. Participants were classified as compliant if ≥80% of capsules were taken in each arm.

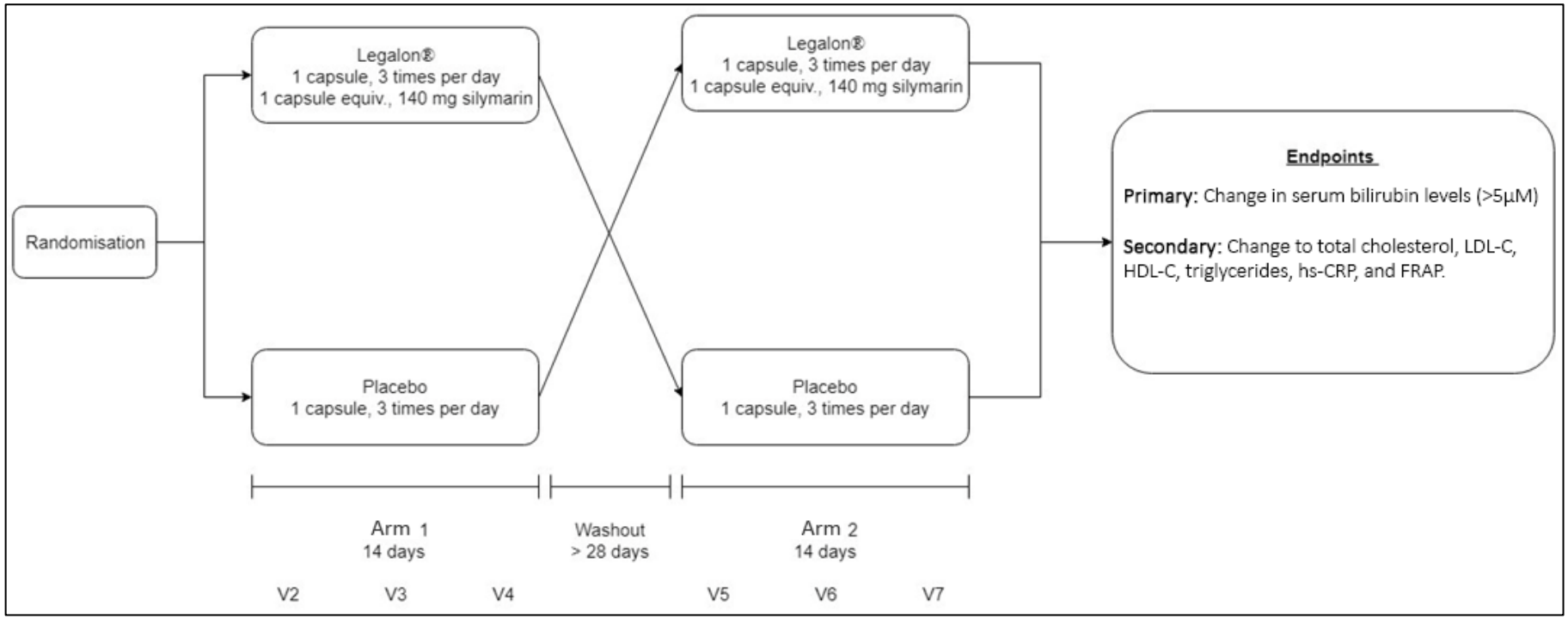

Figure 5.1. Flow diagram of the study design.

Setting and Recruitment:

The Effect of **M**ilk thistle extract (Silibinin/Legalon®) **O**n circulating uncon**J**ugated bilirubin levels and markers of **O**xidative stress and inflammation (the **MOJO** trial) was approved by the Griffith University Human Research Ethics Committee (Ref No:2017/173) and was conducted at Griffith University in Queensland, Australia. The trial is registered with the Australian New Zealand Clinical Trials Registry (ACTRN12619001296123). Participants were recruited from Griffith University (Gold Coast), Endeavour College of Natural Health (Gold Coast) and the local community, using information flyers and word of mouth. Interested individuals were provided with a participant information package that outlined the details of the study. Participants were recruited only when written consent was obtained. The target population were healthy males between 18 and 65 years of age who fit the inclusion/exclusion criteria (Table 5.1). All subjects could withdraw from the study, without penalty at any time, upon communication with the research team. In females, circulating bilirubin concentrations fluctuate with the menstrual cycle increasing intraindividual variability [436]. Therefore, only male participants were recruited in this study to eliminate the confounding effects of the menstrual cycle in females. Recruitment of females was planned in a follow up study if Legalon® treatment succeeds in meeting the primary outcome in males (i.e. increase >5 µM in circulating bilirubin following Legalon® treatment).

Assessment of eligibility (V1)

Participants' eligibility was assessed through a short interview including a medical history questionnaire and concomitant medication, weight (InnerScan® V BC-601, Tanita, Japan) and height (stadiometer) measurement, fasting blood glucose concentration, full blood count, and liver function tests. Eligible participants needed to satisfy all inclusion criteria and possess none of the exclusion criteria (Table 5.1). Blood test results were interpreted by an Australian Institute of Medical Scientists (AIMS) accredited individual. If a participant met these criteria, they were enrolled into the study and a second visit (V2) was scheduled.

Table 5.1. Inclusion and exclusion criteria for eligibility to participate in the MOJO trial

Inclusion Criteria	**Exclusion Criteria**
Adult males between the ages of 18 and 65	History of liver disease
Normal liver function tests (ALT, AST, ALP, and GGT; see Appendix 3 for normal ranges)	History of alcohol abuse
Normal full blood count results (see Appendix 3 for normal ranges)	History of type 2 diabetes
Normal fasting blood glucose concentration (3.0 – 7.7 mmol L^{-1})	History of psychological illness or condition which interferes with individual's ability to understand or comply with the requirements of the study
BMI between 18.5-29.9 kg m^{-2}	
Able to provide informed consent	

Outcomes

The primary outcome with respect to Legalon® treatment was an increase in circulating total bilirubin concentrations of >5 μM compared to baseline after 14 days of supplementation. Change in UCB is specifically reported here because UCB constitutes >95% of total bilirubin in healthy individuals [43], and due to the underlying hypothesis that Legalon inhibits hepatic uptake of UCB and conjugation by UGT1A1 [234,354,424]. All adverse events including jaundice were to be reported to the Griffith University Research Ethics Committee, however, no adverse events were noted. The secondary outcomes with respect to Legalon® treatment, were a change in lipid profile (total cholesterol, high density lipoprotein cholesterol (HDL-C), LDL-C, total cholesterol/HDL-C, and total triglycerides), inflammation (high sensitivity C reactive protein; hs-CRP) and total antioxidant capacity (ferric reducing ability of plasma; FRAP) after 14 days of treatment compared to baseline.

Blood Collection and Sample Processing

Whole blood was collected by antecubital venepuncture into Serum Plus and K_2EDTA 7.2 mg BD Vacutainers™, with the first 4 mL discarded [437]. Serum tubes were centrifuged (2000 RCF; 20 mins) and aliquots of serum were frozen in liquid nitrogen and stored at -80°C.

Full Blood Exam

A complete blood count (CBC) with differential leucocyte analysis was undertaken to ensure a normal blood cell profile for the inclusion criteria of this study (AcT5diff CP or DxH 500, Beckman Coulter, Brisbane, Australia).

Serum biochemistry

Serum samples were thawed and analysed using the Roche COBAS Integra® 400+ (Roche Diagnostics, United States) for liver function (alanine aminotransferase (ALT), aspartate aminotransferase (AST), γ-glutamyltransferase (GGT), and alkaline phosphatase (ALP)), cholesterol balance (HDL-C, LDL-C, and total cholesterol), triglycerides, albumin (ALB), glucose and hs-CRP. Total non-thiol antioxidant capacity was assessed with FRAP assay as previously published on COBAS Integra® 400+ [438]. All assays were calibrated with appropriate standards (CFAS, CFAS Lipids, CFAS Protein) and accuracy was checked with appropriate quality controls (precinorm clinchem multi 1 (PCC1), precinorm clinchem multi 2 (PCC2), Crp T control N). All parameters were measured in duplicate. Serum UCB was analysed using high-performance liquid chromatography (HPLC) (Appendix 3, methods).

Statistical analysis

This study was powered to detect >5 µM (± 3.0 µM SD) increase in circulating total bilirubin concentrations, based on a meta-analysis concluding that an increase of >5 µM bilirubin led to a clinically significant reduction in atherosclerotic risk [439]. Therefore, to detect a >5 µM (± 3.0 µM SD) increase in serum total bilirubin concentrations with a two-sided 1% significance level and power of 0.95, a sample size of 15 individuals was required while allowing for a 50% dropout using a paired t-test analysis (GPower V3.1.9.4). In total 26 male participants were recruited to

ensure that the minimum recruitment target was met. The analysis was conducted on a per-protocol basis and only individuals that satisfied the minimum compliance (≥80% of prescribed dose) and did not deviate from the protocol were included in the final analysis. All values are expressed as mean ± standard deviation (SD) or as a sum and percentage. Comparisons over time from the same participant were performed using Repeated Measures Two-Way ANOVA and Bonferroni's *post hoc* test. Chi-square analysis was performed to determine whether 14 days of Legalon® treatment increased the proportion of individuals with an increase of >5 µM in UCB in treatment versus placebo arms. Statistical analysis was performed in GraphPad PRISM (v8.2) and a $P<0.05$ was considered significant.

5.4 Results

Participants

Recruitment for the trial began in November 2017 and ended in November 2018. In the present clinical trial, 28 males were screened for inclusion, with two individuals failing to meet the inclusion criteria. From the 26 enrolled participants, two withdrew during the study period with one additional participant discontinued from the 2nd arm due to inadequate compliance to medication (<80% of compliance in 1st arm) (Fig. 5.2). From the 23 participants that completed the full trial, six participants were excluded from statistical analysis. Five were excluded based on inadequate compliance to medication and one because of a protocol violation (Fig. 5.2). The demographic characteristics of the 17 completed participants, prior to commencement, are displayed in Table 5.2. On average, the participants were young healthy males with a normal-overweight BMI and no reported comorbidities.

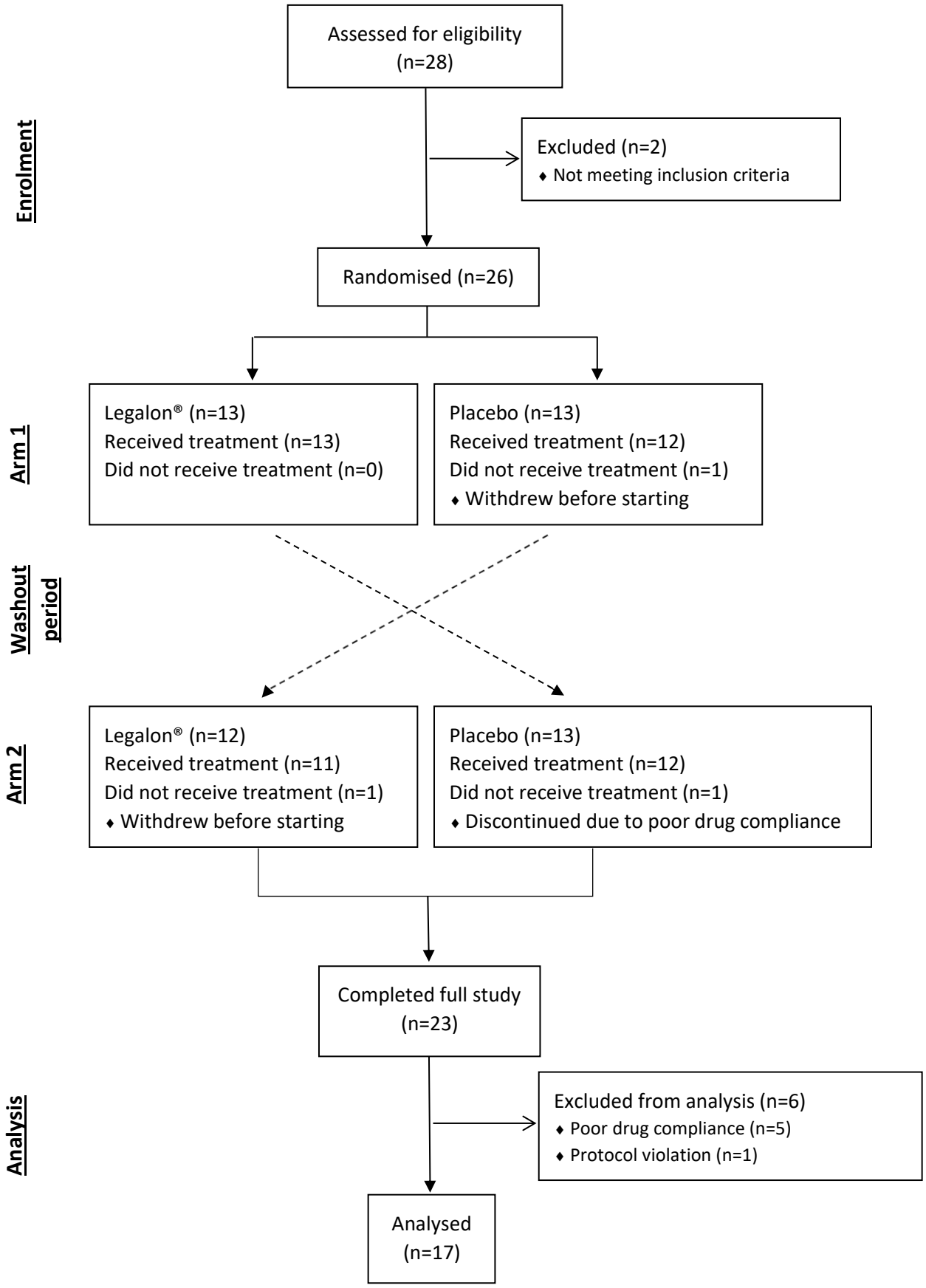

Figure 5.2. Flowchart of participants included and excluded from the MOJO study.

Table 5.2. Screening demographics, serum biochemistry and haematology parameters for completed participants.

Variable		All Participants (n=17)	Reference Range[#]
Demographics	Age (years)	31.8 (10.7)	N/A
	BMI (kg m^{-2})	24.7 (3.29)	22-26
Ethnicity			
	Caucasian	12 [70.6]	N/A
	African	1 [5.88]	N/A
	Pacific Islander	1 [5.88]	N/A
	Asian	2 [11.8]	N/A
	Middle Eastern	1 [5.88]	N/A
Serum Biochemistry			
	ALT (U L^{-1})	21.8 (14.2)	<35
	ALP (U L^{-1})	79.7 (15.2)	30-110
	AST (U L^{-1})	20.2 (7.87)	<40
	GGT (U L^{-1})	23.3 (12.6)	<50
	Fasting blood glucose (mmol L^{-1})	5.46 (0.62)	3-7.7
Complete Blood Count			
	Hb (g L^{-1})	147 (8.92)	130-170
	Hct (%)	43.0 (4.00)	40-50.0
	RBC ($\times 10^{12}$ L^{-1})	4.98 (0.45)	4.5-5.5
	WBC ($\times 10^{9}$ L^{-1})	5.23 (1.43)	4.0-10.0
	Platelets (10^{9} L^{-1})	233 (56.0)	150-400
Concomitant Medication			
	NSAIDs	2 [11.8]	N/A
	Proton Pump Inhibitors	1 [5.88]	N/A
	Antibiotics	1 [5.88]	N/A
Smokers		2 [11.8]	N/A
Compliance (%)			
	Legalon	96.2 (6.41)	N/A
	Placebo	97.2 (9.13)	N/A

Note: BMI, Body Mass Index; ALT, Alanine Aminotransferase; AST, Aspartate Aminotransferase; GGT, Gamma-Glutamyl Transferase; Hb, Haemoglobin; Hct, Hematocrit; HR, Heart rate; RBC, Red Blood Cells; WBC, White Blood Cells; PLT, Platelet count. Values are represented as mean (SD) or number [%]. [#]reference ranges obtained from The Royal College of Pathologists of Australasia (RCPA).

Primary Outcome

Serum Bilirubin Concentration

Serum UCB concentrations were not significantly affected by treatment or time (main effects: p=0.81 and p=0.79, respectively; Table 5.4). Legalon® treatment was associated with a non-significant (P=0.79) increase in UCB concentrations on day 14, with an increase of 1.1 µM in UCB compared to baseline (Fig. 5.3). Three participants (17.65%) during placebo and one participant (5.88%) during Legalon® supplementation reported an UCB increase of >5 µM compared to baseline (P=0.29, Table 5.3).

Table 5.3. Proportion of individuals that demonstrated an increase of >5 µM in UCB compared to baseline.

Treatment	> 5µM *n* (%)	≤ 5µM *n* (%)	*n*	χ^2 (df)	p value†
Placebo	3 (17.7)	14 (82.4)	17	1.13 (1)	0.287
Legalon®	1 (5.88)	16 (94.1)	17		

Note: †Chi-square test for independence.

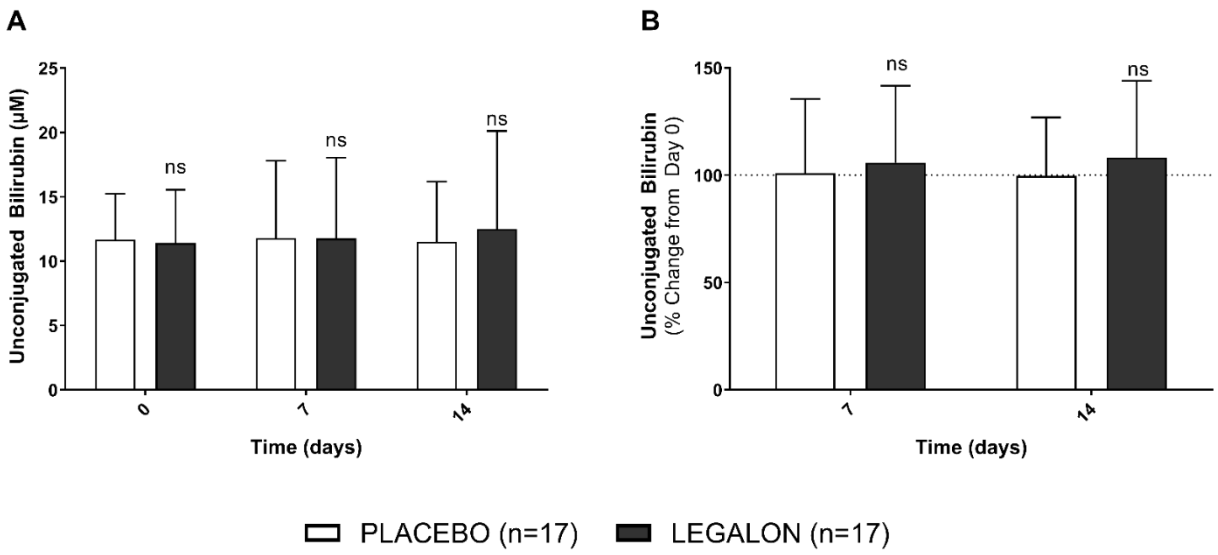

Figure 5.3. Effect of Legalon® treatment on serum unconjugated bilirubin concentration. A) Unconjugated bilirubin concentration over time in Legalon® and placebo treated groups. B) Unconjugated bilirubin concentration over time expressed as percentage (%) of baseline in Legalon® and placebo treated groups. ns, no significant difference between groups or over time (P>0.05).

Table 5.4. Biochemical parameters during Placebo and Legalon® treatment.

Parameter	Treatment	Time (days)			p value†		Post-hoc
		0	7	14	Treatment	Time	p value#
UCB (µmol L^{-1})	Placebo	11.7 (3.56)	11.8 (6.01)	11.5 (4.67)	0.82	0.79	
	Legalon®	11.4 (4.14)	11.8 (6.28)	12.5 (7.63)			
Total Cholesterol (mmol L^{-1})	Placebo	4.84 (1.11)	4.92 (1.24)	4.77 (1.17)	0.88	0.19	
	Legalon®	4.88 (1.00)	4.88 (0.99)	4.80 (1.00)			
HDL-C (mmol L^{-1})	Placebo	1.36 (0.22)	1.40 (0.26)	1.28 (0.27)	0.24	0.04*	0.09
	Legalon®	1.40 (0.28)	1.39 (0.25)	1.37 (0.26)			
LDL-C (mmol L^{-1})	Placebo	3.26 (0.97)	3.29 (1.06)	3.24 (1.02)	0.93	0.24	
	Legalon®	3.30 (0.84)	3.30 (0.87)	3.18 (0.87)			
CHOL/HDL-C	Placebo	3.61 (0.86)	3.58 (0.90)	3.96 (1.61)	0.35	0.23	
	Legalon®	3.58 (0.87)	3.59 (0.77)	3.59 (0.88)			
Triglycerides (mmol L^{-1})	Placebo	1.13 (0.54)	1.10 (0.55)	1.04 (0.53)	0.66	0.79	
	Legalon®	1.04 (0.54)	1.08 (0.48)	1.07 (0.63)			
FRAP (mmol Fe^{2+} L^{-1})	Placebo	1224 (229)	1213 (216)	1176 (254)	0.56	0.40	
	Legalon®	1183 (201)	1200 (188)	1194 (182)			
hs-CRP (mg L^{-1})	Placebo	1.17 (1.16)	1.02 (1.06)	0.98 (0.86)	0.37	0.23	
	Legalon®	0.92 (0.87)	1.06 (1.01)	1.74 (1.88)			

Note: UCB, unconjugated bilirubin; HDL-C, high-density lipoprotein cholesterol; LDL-C, low-density lipoprotein cholesterol; CHOL/HDL-C, ratio of total cholesterol over HDL cholesterol; UA, uric acid; FRAP, ferric reducing ability of plasma; hs-CRP, high sensitivity C reactive protein. Data are presented as mean (± SD). †Repeated Measures two-way ANOVA. #Bonferroni's post-hoc test comparing the treatment effect overtime against baseline. *P<0.05, statistical significance.

Secondary Outcomes

Lipid status

Total circulating total cholesterol concentrations were unaffected by treatment condition or time (main effects: p=0.88 and p=0.19, respectively; Table 5.4). Similarly, serum HDL-C concentrations were unchanged by treatment (p=0.24), however, were significantly affected by time ($p<0.05$; Table 5.4). Post-hoc analysis did not reveal a significant difference between timepoints, within condition, however, there was a trend towards reduced HDL-C concentrations at day 14 compared to day 7 in the placebo group (p=0.09; Table 5.4). Serum LDL-C levels were unaffected by treatment or time (main effects: p=0.93 and p=0.24, respectively; Table 5.4). In addition, cholesterol ratio (total cholesterol: HDL cholesterol), remained unaffected by treatment condition or time (main effects: p=0.35 and p=0.23, respectively; Table 5.4). Finally, circulating triglyceride concentrations were not significantly affected by treatment or time (main effects: p=0.66 and p=0.79, respectively; Table 5.4).

Inflammation and serum antioxidant capacity

Total serum anti-oxidant capacties as measured by the FRAP assay were not changed by treatment or time (main effects: p=0.56 and p=0.40, respectively; Fig. 5.4A). The inflammatory marker, hs-CRP, was not affected by treatment or time (main effects: p=0.37 and p=0.23, respectively; Fig. 5.4B).

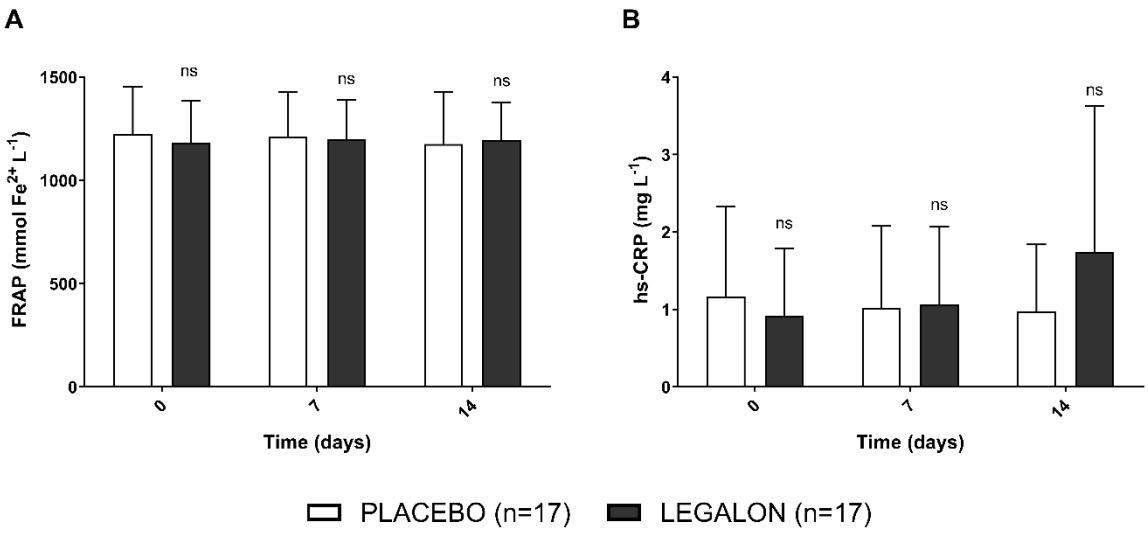

Figure 5.4. Effect of Legalon® treatment on total serum antioxidant capacity and inflammation. A) Ferric reducing ability of plasma (FRAP) over time in Legalon® and placebo treated groups. B) Serum C-reactive protein (hs-CRP) concentrations over time in Legalon® and placebo treated groups. ns, no significant difference between groups or over time (P>0.05).

Safety profile

Liver function and fasting blood glucose concentrations

Serum enzymes reflecting hepatic injury (ALT, AST, GGT, and ALP) or fasting blood glucose were not significantly changed after Legalon® or placebo supplementation (Table 5.5).

Table 5.5. Biochemical parameters of liver function and glucose during Placebo and Legalon® treatment.

Parameter	Treatment	Time (days)			p value†	
		0	7	14	Treatment	Time
ALT (U L^{-1})	Placebo	22.1 (12.9)	23.2 (14.4)	23.5 (16.5)	0.54	0.38
	Legalon®	20.4 (10.8)	21.9 (12.2)	23.5 (22.0)		
AST (U L^{-1})	Placebo	21.8 (7.77)	23.0 (10.9)	21.5 (8.84)	0.94	0.43
	Legalon®	20.5 (6.92)	20.1 (5.65)	26.0 (23.9)		
GGT (U L^{-1})	Placebo	24.2 (10.2)	24.3 (10.9)	23.5 (9.82)	0.81	0.35
	Legalon®	24.1 (11.8)	24.5 (12.4)	24.0 (11.5)		
ALP (U L^{-1})	Placebo	74.4 (15.9)	72.7 (14.7)	72.7 (14.9)	0.71	0.46
	Legalon®	73.8 (15.2)	73.7 (14.6)	74.1 (15.0)		
Fasting blood glucose (mmol L^{-1})	Placebo	5.34 (0.40)	5.47 (0.36)	5.43 (0.39)	0.54	0.84
	Legalon®	5.50 (0.40)	5.42 (0.29)	5.41 (0.29)		

Note: ALT, alanine aminotransferase; AST, aspartate aminotransferase; GGT, y-glutamyltransferase; ALP, alkaline phosphatase. Data are presented as mean (± SD). †Repeated Measures Two-way ANOVA. *P<0.05, statistical significance.

5.5 Discussion

This is the first clinical trial to investigate serum UCB concentrations, lipid status, inflammation, and serum antioxidant capacity following Legalon® administration over a period of 14 days in a healthy male population at the recommended dosage. Serum concentrations of UCB did not change following Legalon® administration. In total, three participants had an increase of >5 µM of UCB during the placebo arm, while only one participant had a similar increase during the Legalon® arm. The secondary outcomes of lipid status were not affected by Legalon® treatment, with no significant changes in serum concentrations of total cholesterol, HDL-C, LDL-C, or triglycerides. Furthermore, inflammation and serum antioxidant capacity remained unaffected by oral Legalon® administration.

Several studies demonstrate that silibinin inhibits enzymes involved in the uptake, conjugation, and excretion of UCB, which may explain the cases of hyperbilirubinemia documented with Legalon® treatment and manufacturer warnings of jaundice with Legalon® use [354,356,440]. Thus, it was hypothesised that Legalon® treatment would increase circulating UCB levels [440]. Considering that in healthy persons >95% of total circulating bilirubin exists in the unconjugated form, any change in UCB would have a significant impact on total bilirubin levels [43]. Legalon® consumption non-significantly impacted UCB concentrations and did not increase the proportion of individuals, experiencing a clinically significant increase in UCB (>5 µM).

While it was surprising that Legalon® treatment did not significantly increase UCB concentrations a subset of clinical studies have also reported no change in serum bilirubin concentrations following Legalon® administration, however, these reports were in patients with underlying pathology that could have confounded Legalon®'s effect on bilirubin concentrations [441,442]. For instance, Pares et al. studied the effects of silymarin on survival and markers of hepatic function in patients with liver cirrhosis [441]. The patients (n=125) were randomised to placebo or silymarin at a similar dose to the present study (150 mg thrice daily, orally). Two-year daily treatment with silymarin did not significantly affect total bilirubin levels compared to

baseline (39 vs 34 µM, respectively) [441]. Similarly, Ferenci et al. reported that ≥2 years of silymarin treatment (140 mg thrice daily, orally) did not significantly affect total bilirubin levels in patients with liver cirrhosis from heterogenous aetiology [442]. It is important to note that the subject population of these studies may have impacted the effectiveness of silymarin to affect UCB levels since hepatocellular dysfunction in liver cirrhosis impairs bilirubin metabolism. Thus, any inhibitory effects of silymarin on UCB metabolism may have been counteracted by an improvement in hepatic function due to silymarin induced hepatoprotection [443]. Furthermore, insufficient bioavailability of classical silymarin formulations may be ineffective at increasing UCB concentrations [360,444,445]. Indeed, more recent studies have reported significant increases in circulating bilirubin levels using preparations with greater bioavailability [22,23].

Several studies have investigated the potency of silymarin and its constituents as UGT1A1 inhibitors [355,356]. For example, incubation of various recombinant UGT enzymes in the presence of 7-Hydroxy-4-(trifluoromethyl)coumarin, demonstrated that silibinin was the most potent inhibitor of UGT1A1 with an IC_{50} of 1.4 µM [355]. Conversely, in human and rat isolated hepatic microsomes, silibinin had a notably reduced potency towards UGT1A1 inhibition, where 41.5 µM of silibinin attenuated UCB glucuronidation by 40% [356]. Interestingly, the conjugated form of silibinin (33 µg mL^{-1}) demonstrated a greater inhibition of UGT1A1 (~60% inhibition) compared to unconjugated silibinin, while other flavonolignan constituents of silymarin had no effect on UGT1A1 activity [356]. Collectively, these findings suggest that to achieve a minimum of 50% UGT1A1 inhibition, the intracellular concentration of silibinin is required to be between ~1.4 and 50 µM. These concentrations may be unattainable with Legalon® at the current dose with previous reports showing a peak silibinin concentration of ~0.37-2.8 µM after a single 120-175 mg oral silymarin supplementation [353,444,446]. Therefore, insufficient circulating silibinin concentrations could represent a potential reason for the lack of change in UCB levels in the present study. However, it should be mentioned that this conclusion does not consider that silibinin inhibits OATPs and MRP2 at lower concentrations [354].

Silibinin bioavailability increases when administered as a silibinin-phytosome formulation. Maximum serum concentrations increase to ~8.8 µM silibinin following a single 280 mg oral dose of silibinin-phytosome [360,447]. In a phase I trial assessing the pharmacokinetics and toxicity threshold of a commercial silibinin-phytosome formulation (Siliphos^{R}), 13 patients with prostate adenocarcinoma were treated with varying doses of Siliphos^{R} (2.5 to 20 g daily) [23]. At a daily dose of 13 g Siliphos^{R}, the average silibinin C_{max} was ~75 µM and 50% of courses resulted in grade 1 (17.1-25.7 µM total bilirubin) and 6% in grade 2 (25.7-51.3µM total bilirubin) hyperbilirubinaemia [23]. Conversely, at a dose of 10 g per day, 25% of courses induced grade 1 and 4% induced grade 2 hyperbilirubinaemia. Below a daily dose of 10 g, no cases of hyperbilirubinaemia were noted, indicating that 10 g of silibinin-phytosome is the minimum dose required to induce hyperbilirubinaemia in these patients [23]. The cases of hyperbilirubinaemia were characterised by an increase in total bilirubin concentrations without a corresponding change in direct bilirubin indicating that silibinin-phytosome supplementation induced unconjugated hyperbilirubinaemia, which is consistent with *in vitro* reports of silibinin-mediated inhibition of UCB conjugation [23,354–356]. Based on the evidence presented herein, a greater dose of silymarin and/or a formulation with greater oral bioavailability may be more effective at elevating circulating bilirubin concentrations [23,360,447]. Therefore, the maximal recommended oral dose of Legalon® is ineffective at increasing serum bilirubin concentrations in healthy participants.

In addition to the effects on bilirubin metabolism, silymarin also modulates lipid synthesis, uptake, and excretion [430,448–450]. Silibinin-dihemisuccinate (100 mg kg^{-1} day^{-1} i.p.) treatment for 7 days reduces biliary cholesterol excretion in male rats [448]. Similar (non-significant) trends are observed in cholecystectomised humans receiving 420 mg of silymarin orally daily [448]. The reduced biliary excretion of cholesterol is potentially related to decreased cholesterol synthesis because silibinin dose-dependently inhibits 3-hydroxy-3-methyl-glutaryl-coenzyme A reductase (HMGCR) *in vitro* with an IC_{50} of ~40 µM [448]. Further investigations in animal studies reported significant reductions in circulating cholesterol and triglyceride concentrations following

silymarin treatment in hyperlipidaemic rats, indicating that silymarin is a potentially effective lipid reducing agent [430,449,450].

Given the lipid reducing properties of silymarin in animal studies, it was hypothesised that Legalon® administration would decrease circulating cholesterol and triglyceride concentrations in humans. However, the secondary outcomes of altered lipid status were not realised following Legalon® administration. Previous studies show contradicting results on whether silymarin treatment impacts lipid status in humans [434]. For example, Mohammadi et al. conducted a meta-analysis that evaluated the overall effect of silymarin on dyslipidaemia in randomised controlled trials [434]. Aggregate analysis identified a significant reduction in total cholesterol (-0.45mM, 95% CI: -0.06, -0.83mM), LDL-C (-0.44mM, 95% CI: -0.15, -0.74mM), and triglycerides (-0.25mM, 95% CI: -0.01, -0.50mM), with a significant increase in HDL-C (0.12mM, 95% CI: 0.05-0.20mM) upon oral administration. Interestingly, after separating studies that examined silymarin in conjunction with other treatments, silymarin treatment alone did not significantly affect LDL-C and total cholesterol. Most studies were conducted in a cohort of diabetics with dyslipidaemia [434], thus, the data suggests that silymarin treatment is most effective when used as an adjunct to standard hypoglycemic therapies. The present study used silymarin as a sole treatment and reported non-significant reductions in total cholesterol (-0.08mM, 95% CI: -0.28, 0.11mM) and LDL-C (-0.12mM, 95% CI: -0.27, 0.05mM). These results are consistent with subgroup analysis of studies using silymarin as a sole treatment for dyslipidaemia [434].

Only a single study has demonstrated a beneficial effect of silymarin on lipid status in humans [434,451]. Ebrahimpour-koujan et al. explored the lipid-lowering potential of silymarin in a cohort of type 2 diabetes mellitus (T2DM) patients [451]. Patients were randomised to 140 mg thrice daily (420 mg total) of silymarin or placebo. Following 45 days of treatment, the silymarin group demonstrated significantly reduced total cholesterol, triglycerides, and LDL-C, with a significant increase in HDL-C compared to baseline. The discrepancy between these data and those reported here could be explained by the use of a different formulation of silymarin

(Livergol®) which has a greater bioavailability than Legalon® [360]. Moreover, in the present study, participants were treated for 14 days while in Ebrahimpour-koujan et al.'s patients were treated for 45 days and they had higher baseline lipid concentrations [451]. Silymarin may be more effective at reducing lipid concentrations in hyperlipidaemic patients or a longer treatment duration may be required to reduce total cholesterol and LDL-C.

Silymarin is reported to possess antioxidant and anti-inflammatory properties [431–433]. Therefore, it was hypothesised that Legalon® treatment would reduce serum concentrations of hs-CRP while increasing circulating antioxidant capacity. The secondary outcomes of reduced hs-CRP and increased antioxidant capacity were not supported in the present trial. In this study, 14 days of Legalon® treatment was associated with a (non-significant) 89% increase (16.2% decrease in placebo) in hs-CRP, and 1% increase (3.9% decrease in placebo) in circulating antioxidant capacity (FRAP). These results are in disagreement with previously published work by Ebrahimpour-koujan et al. who tested an equivalent dose of silymarin (140mg thrice per day) for 45 days in patients with T2DM and reported a 7.7% increase (1% decrease in placebo) in total antioxidant capacity (trolox equivalent antioxidant capacity) and a 28.4% decrease (vs. 47.2% increase in placebo) in hs-CRP [452]. This study also utilised the silymarin formulation with greater bioavailability (Livergol®) which would achieve greater circulating levels of silymarin constituents despite dose equivalence [360,452]. An additional reason for the differences in findings could potentially be explained by the cohorts investigated. For example, Ebrahimpour-koujan et al. recruited T2DM patients with greater baseline hs-CRP concentrations compared to the healthy cohort presented here (2.3 vs 0.9mg/L hs-CRP, respectively). Demonstration of an effect in this patient population is commensurate with the underlying pathophysiology of these diseases, which include inflammation and oxidative stress [453]. It is important to note that FRAP assesses non-thiol reducing antioxidant capacity [438] with both bilirubin and silymarin demonstrating free radical scavenging with this assay [438,454]. However, FRAP is a general measure of serum antioxidant capacity and does not assess individual antioxidant capacity and it is likely that concentrations of silymarin were insufficient to increase FRAP in this study.

Therefore, silymarin treatment as Legalon® preparation at the maximal recommended dose appears to be ineffective at affecting markers of inflammation and antioxidant capacity in the healthy range. Given that Legalon® is marketed for consumption by the general public (i.e. available over-the-counter), it was important to conduct this study to test these claims in healthy individuals.

5.6 Conclusion and Future Considerations

Significant elevations in serum UCB concentrations were not observed following Legalon® administration. Moreover, changes in lipid profile, inflammation, or antioxidant capacity were not reported following administration of Legalon® at the maximal recommended dosage in healthy males. It should be acknowledged that these findings do not preclude differing results if alternative preparations were investigated in men and/or in women. Greater increases of circulating bilirubin and/or perturbed lipid status and reduced inflammation may be realised if Siliphos® is administered, given the greater bioavailability associated with this preparation [455,456]. Future studies are required to establish a dosage regime that sufficiently elevates *in vivo* concentrations of silibinin that may increase circulating levels of bilirubin. Furthermore, the cohort studied here were healthy males screened for medical conditions that could confound results. As such additional studies are required to determine the efficacy of silymarin as a cholesterol reducing agent in a cohort of dyslipidaemic patients and as an anti-inflammatory in inflammatory conditions. Finally, an extended duration of therapy may further help evaluate the potential of silymarin as a lipid modulating agent and an anti-inflammatory compound. Collectively, the therapeutic potential of silymarin as a lipid modulator, anti-inflammatory, or antioxidant requires further investigation, however, these findings suggest that Legalon® at this dosage would not be suitable for reduction of CVD risk.

5.7 Author Contribution

AB and MW conceived the research question and with SS, finalised the study design and critically reviewed the manuscript. JV facilitated in study design, performed the biochemical analysis, analysed the data, and wrote the manuscript. EP assisted in biochemical analysis and assisted in both the writing and critical revision of the manuscript. Both JV and EP arranged participant recruitment, with assistance from MF. MF assisted with aspects of biochemical analysis. RS developed HPLC method for bilirubin quantification and assisted in analysis. All authors approved the final version and submission of this manuscript.

5.8 Acknowledgements

The authors would like to thank Zoe Ruscoe for her assistance in this clinical trial and the MOJO participants.

5.9 Funding

This work was supported by an Office of Research Project Grant (20160824) provided by the Endeavour College of Natural Health. This work was also supported by the School of Medical Science Griffith University.

5.91 Disclosure of Conflict of Interests

All other authors declare no conflict of interest.

Chapter 6: General Discussion and Future Directions

6.1 Thesis Summary and Conclusion

This thesis contains three original studies presented as a series of chapters that investigate the impact of unconjugated hyperbilirubinaemia on cholesterol metabolism, mitochondrial function, and body composition. The final experimental chapter details the results of a clinical trial that tested the effectiveness of Legalon® to increase circulating unconjugated bilirubin concentrations and decrease cholesterol concentrations in humans. This chapter will discuss the broader implications of the experimental findings considering all experimental chapters and provide recommendations for future research studies and strategies, to further develop our understanding of the field.

6.2 Introduction

The first experimental study (Chapter 3) examined the impact of congenital unconjugated hyperbilirubinaemia on cholesterol metabolism in rats deficient in UGT1A1 activity. Effects of hyperbilirubinaemia/UGT1A1 dysfunction on cholesterol synthesis, transport, and excretion in male and female animals was presented. In the same animal model, the second experimental study (Chapter 4) investigated body composition, energy balance, and mitochondrial function providing possible explanations for the leaner phenotype in female hyperbilirubinaemic animals. Finally, due to the favourable outcomes of hyperbilirubinaemia/UGT1A1 dysfunction on cholesterol metabolism and bioenergetics in rats, this thesis investigated the impact of Legalon® supplementation on circulating unconjugated bilirubin concentrations and lipid profile in humans to determine whether silymarin supplementation could induce hyperbilirubinaemia and if so, whether this would be associated with reduced cholesterol concentrations (Chapter 5).

6.3 Project Summary

The first study (Chapter 3) reports the effects of congenital unconjugated hyperbilirubinaemia on cholesterol metabolism in UGT1A1 deficient (Gunn) rats. Current understanding of the relationship between hyperbilirubinaemia and cholesterol metabolism is limited to associations

from epidemiological studies and reports of reduced circulating cholesterol concentrations in hyperbilirubinaemic animals [12]. Therefore, this chapter contains the first evidence of changes to cholesterol transport, synthesis, and biliary excretion in genetically induced unconjugated hyperbilirubinaemia. Previous studies have reported that hyperbilirubinaemic rats possess reduced circulating cholesterol concentrations [246]. Consequently, it was hypothesised that cholesterol synthesis was decreased in Gunn rats leading to reduced circulating cholesterol concentrations. Unexpectedly, increased cholesterol synthesis in female Gunn rats was reported. Statins inhibit HMGCR, the rate limiting enzyme of cholesterol synthesis, yet after chronic administration this leads to a paradoxical homeostatic increase of total body cholesterol synthesis and cellular uptake of circulating cholesterol through a negative-feedback mechanism [13]. Homeostatic counter-upregulation of HMGCR activity occurs following a reduction in intracellular cholesterol levels compensating for the loss of cholesterol [127]. This chapter reported that biliary cholesterol excretion was increased in female hyperbilirubinaemic rats and this was associated with elevated cholesterol synthesis and LDL receptor (LDLr) expression. Therefore, hypocholesterolaemia in Gunn rats could be a result of increased hepatic cholesterol uptake via LDLr. It is possible that unconjugated hyperbilirubinemia and/or UGT1A1 impairment leads to increased biliary cholesterol excretion with a subsequent increase in *de novo* synthesis and LDLr mediated cholesterol uptake ultimately reducing circulating cholesterol concentrations. While the cellular mechanisms responsible for this effect remain incompletely understood, this study strongly suggests that UGT1A1 inhibition reduces circulating cholesterol concentrations. Collectively, these findings help to explain the inverse relationship of circulating bilirubin with cholesterol concentrations reported in epidemiological studies [12]. Another interesting result included the reduction in bodyweight in Gunn rats which led to the second experimental study of this thesis.

The second study (Chapter 4) sought to determine bioenergetic changes that could potentially explain reduced bodyweight in hyperbilirubinaemic Gunn rats. The main findings of this chapter included a reduction in fat mass and lean mass in female Gunn rats that were associated with

improved hepatic mitochondrial quality. Obesity is a growing public health concern and is a risk factor for several conditions including metabolic syndrome. Despite promotion of public health intervention programs, the prevalence of obesity is expected to increase supporting the need for pharmacological treatments [28]. This study provides evidence that elevated bilirubin concentrations and/or UGT1A1 impairment are anti-obesogenic with potential to reduce fat storage. These findings are consistent with epidemiological studies that report a reduced risk of metabolic syndrome in individuals with mildly elevated bilirubin concentrations [248].

Our current understanding of the relationship between bilirubin and bodyweight/adiposity is superficial and limited to reports from epidemiological studies. Observational studies demonstrate that circulating bilirubin concentrations are inversely associated with BMI and adiposity [5,246]. However, very little is known concerning the mechanisms responsible with indirect evidence implied from studies reporting effects on mitochondria in models of bilirubin-induced neurotoxicity [2]. In these studies, bilirubin uncouples the mitochondrial membrane potential leading to reduced ATP production and cellular death/apoptosis [254,257,396,457]. Considering these reports, it was hypothesised that benign hyperbilirubinaemia would reduce bodyweight and fat mass by increasing the rate of uncoupled mitochondrial respiration without affecting maximal oxidative phosphorylation coupled to ATP synthesis (OXPHOS). This hypothesis was not supported because no change in the rate of uncoupled mitochondrial respiration in hepatic tissue or skeletal muscle occurred in Gunn rats. Conversely, the flux control ratio (FCR) of OXPHOS was greater in hepatic mitochondria in female Gunn rats. This result in female Gunn rats appears to be caused by a combination of a non-significant increase in the absolute rate of OXPHOS and a decrease in maximal noncoupled respiration (ETS) in hepatic mitochondria. Therefore, increased hepatic OXPHOS FCR in female Gunn rats potentially represents greater mitochondrial energy efficiency and/or dysfunction to one or several of the mitochondrial respiratory complexes involved in the electron transfer system (complexes I-IV).

Furthermore, female Gunn rats reported increased hepatic mitochondrial complex IV (CIV) expression. Greater OXPHOS FCR and increased CIV expression suggest an improvement to hepatic mitochondrial quality in female Gunn rats. It is not known how hyperbilirubinaemia leads to increased hepatic mitochondrial quality, however, these results could represent a compensatory adaptation to bilirubin-mediated inhibition of CIV [20,21]. Additionally, hyperbilirubinaemia may contribute to bodyweight reduction by activating PPARα, as recently demonstrated [10,11]. Fenofibrate is a clinically utilised medication to reduce triglyceride concentrations and fat stores by activating PPARα [458]. Therefore, if bilirubin induced PPARα is responsible for reduced fat stores, it could be utilised to treat adiposity if viable means to increase bilirubin could be discovered.

Surprisingly, an important sex-dependent effect of hyperbilirubinaemia/UGT1A1 dysfunction on cholesterol metabolism and bioenergetics was revealed in this thesis. In the first study, hypocholesterolaemia in male Gunn rats was modest and non-significant and this was not accompanied with changes in cholesterol synthesis, transport, or biliary excretion. Similarly, no change in fat mass or mitochondrial function in male Gunn rats was reported in study two. These findings agree with previous investigations in hyperbilirubinaemic rats that report greater reductions in circulating cholesterol levels and bodyweight in female animals [246]. However, these results are not in complete agreement with observations in human studies that show comparable reductions in circulating cholesterol concentrations and BMI in men and women with benign hyperbilirubinaemia [12]. At present the factors accounting for the discrepancy between animal and human studies in hyperbilirubinaemia remain unknown. However, a possible explanation may include that human studies do not control for contraceptive use and the proportion of post-menopausal women in case control studies.

It is well established that oestrogen reduces circulating cholesterol concentrations and regulates adiposity in animals and humans [387]. Intriguingly, *in vitro* investigations have demonstrate that bilirubin competes with oestrogen for conjugation [16,17]. Therefore, it is reasonable to

assume that UGT1A1 deficiency leads to both elevated bilirubin and oestrogen concentrations in reproductively capable women [436], leading to synergistic hypocholesterolaemic and anti-obesogenic effects. As such, post-menopausal women could be less likely to experience benefit due to substantially reduced oestrogen concentrations that are unlikely to saturate UGT1A1 activity in hyperbilirubinaemic individuals. Similarly, oral contraceptives alter the levels of circulating sex hormones and could confound the impact of UGT1A1 impairment in women [459]. These factors may explain why clear associations between bilirubin and CVD protection exist in men, but not in women [279]. These limitations were not relevant for hyperbilirubinaemic rats used in this thesis and could explain why hypocholesterolaemia and changes in bioenergetics were more profound than in humans [12]. Together, the results of this thesis suggest that pharmacological inhibition of UGT1A1 could be useful in treating hypercholesterolaemia and excessive adiposity.

Currently, a lack of clinical studies have tested the ability of pharmacological agents to impact circulating bilirubin and cholesterol concentrations in humans. Such studies would be critical to confirming whether the aforementioned relationships can be induced by mild hyperbilirubinaemia/UGT1A1 inhibition. The final study (Chapter 5) tested the effectiveness of Legalon® (silymarin) supplementation on circulating bilirubin concentrations and lipid profile. *In vitro* studies have reported that silymarin inhibits OATP transporters and UGT1A1 that are critical for hepatic uptake and conjugation of bilirubin, respectively [354–356]. It was hypothesised that silymarin supplementation (i.e. Legalon® formulation) would increase circulating bilirubin and lower cholesterol concentrations in humans. This hypothesis was not confirmed because Legalon® treatment failed to affect circulating bilirubin concentrations. Therefore, the relationship between changes in bilirubin and cholesterol could not be tested. Previous clinical trials have reported disparate results concerning the effect of silymarin on circulating bilirubin concentrations which is a likely consequence of the patient group tested, dose, and routes of administration [22,23,460,461]. Legalon® was ineffective at increasing bilirubin in this study potentially because a healthy population was recruited (with improved

hepatic function), in addition to poor bioavailability and/or an insufficient dose of silymarin (the dose used was recommended by the manufacturer). Greater silibinin concentrations could be achieved using a silibinin-phytosome formulation and this may inhibit transport/conjugation of bilirubin more effectively, leading to greater circulating bilirubin concentrations [22,23]. Furthermore, this is the first study to evaluate the impact of oral Legalon® on bilirubin and lipid status in healthy individuals [462]. Nevertheless, these findings do not preclude the possibility that greater doses of the Legalon® formulation could increase circulating bilirubin concentrations. Future studies should examine the pharmacokinetics of Legalon® administration over shorter periods using varying oral doses to determine the impact of this preparation on circulating bilirubin concentrations. Following these trials, longer supplementation studies could be conducted to study the effect on cholesterol synthesis and serum cholesterol concentrations in healthy and obese populations.

6.4 Future directions

Taken together this thesis has made several new discoveries including 1) that hypocholesterolaemia is related to increased biliary cholesterol excretion and increased hepatic LDLr expression in hyperbilirubinaemic animals 2) that reduction in bodyweight in Gunn rats is associated with reduced fat mass. This phenotype was also associated with improved hepatic mitochondrial quality in hyperbilirubinaemia 3) that the effects of hyperbilirubinaemia were sexually dimorphic and mostly reported in female Gunn rats. These findings improve our understanding of the effects of UGT1A1 dysfunction and/or unconjugated hyperbilirubinaemia on cholesterol metabolism and adiposity.

Although, this thesis documents perturbed cholesterol metabolism in Gunn rats, the underlying molecular mechanism inducing this phenomenon remains to be elucidated. Several potential explanations exist for the hypocholesterolaemia in this animal model including activation of PPARα and/or Ahr. Previous investigations report that bilirubin is an endogenous ligand of PPARα and Ahr [10,341]. Given that activation of PPARα and Ahr leads to reduced circulating

cholesterol concentrations, it is possible that they mediate the hypocholesterolaemic effects observed in Gunn rats [340,458]. Therefore, future studies in Gunn rats should assess the expression of downstream gene targets of PPARα (FGF21 and CYP4A1) [11] and Ahr (CYP1A1) [340] to confirm whether they are transcriptionally active. Additionally, these studies could be combined with parallel investigations that measure parameters of cholesterol metabolism in Gunn rats treated with inhibitors of PPARα and Ahr.

The above proposed experiments would also aid in elucidating the mechanisms of reduced fat mass and improved mitochondrial quality in hyperbilirubinaemic animals. It is well established that PPARα increases fatty acid catabolism and inhibits the fatty acid synthesis [463]. Therefore, if body composition changes are caused by enhanced PPARα activation, treatment of Gunn rats with PPARα inhibitors would decrease fat breakdown (i.e. reduced expression of genes controlling β-oxidation) and increase fatty acid synthesis (i.e. increased expression of rate-limiting enzyme, acetyl-CoA carboxylase) and confirm the involvement of PPARα [372]. An additional important experiment would include investigating the underlying cause of the profound sexual dimorphism noted in Gunn rats. Considering that UGT1A1 catalyses the conjugation of oestrogen [16,17], circulating oestrogen concentrations should be determined in female Gunn rats. A unique way to assess the potential interaction of oestrogen in UGT1A1 dysfunction would include ovariectomising Gunn and control animals to eliminate the influence of oestrogen and progesterone. Cholesterol metabolism, body composition, and mitochondrial function could then be re-evaluated to determine whether the presence of sex hormones is essential for the effects observed in female Gunn rats. Additionally, experiments could include inhibition of the oestrogen receptors (ERα and ERβ) using silencing RNA or genetic knock down with CRISPR-Cas9 in hyperbilirubinaemic animals.

Finally, future investigations should re-evaluate the effectiveness of Legalon® supplementation on circulating bilirubin concentrations at greater doses. Prior to completing this study, pharmacokinetic evaluation including dose-escalation and repeated measurements of

circulating silibinin and bilirubin concentrations could be completed to determine the minimum dose required to elevate bilirubin concentrations by >5 μM. Alternatively, a pharmacokinetics trial using different formulations of silymarin that have greater bioavailability such as silibinin-phytosome (Siliphos^{R}) [360], could be completed.

In summary, this thesis provides novel data showing that bilirubin and/or UGT1A1 inhibition is associated with reduced cholesterol concentrations and decreased weight gain. Although the underlying mechanisms regulating these effects are not yet completely understood, these studies revealed that hypocholesterolaemia occurs in tandem with elevated biliary cholesterol excretion while, the anti-obesogenic effects appear to be associated with improvement in hepatic mitochondrial quality. Importantly, these findings were more profound in the female sex. Therefore, this thesis lays the foundation for future studies to determine whether UGT1A1 impairment leads to alterations in sex hormone concentrations and whether they function synergistically with bilirubin to produce the effects reported in this thesis. Finally, to realise the clinical potential of altered bilirubin metabolism it is hoped that future studies discover a pharmacological agent that can increase bilirubin concentrations so that the effects of hyperbilirubinaemia on circulating cholesterol and cardiovascular risk can be tested in human clinical trials.

Appendices

Appendix 1 – Chapter 3: Supplementary document

Table S3.1. Hepatic gene expression of female adult Gunn (hyperbilirubinaemic; n=7) and control (normobilirubinaemic; n=8) rats. Fold change expressed relative to controls.

Gene	Fold Change	P value	Gene	Fold Change	P value
Abca1	0.89	0.46	Cyp51	0.8	0.23
Abca2	1.06	0.32	Cyp7a1	1.2	0.65
Abcg1	0.89	0.57	Cyp7b1	0.78	0.17
Akr1d1	1.1	0.48	Dhcr24	1.05	0.51
Angptl3	0.97	0.67	Dhcr7	0.92	0.44
Ankra2	0.89	0.6	Ebp	0.81	0.29
Apoa1	0.83	0.24	Fdft1	0.81	0.29
Apoa2	0.94	0.44	Fdps	0.8	0.16
Apoa4	0.87	0.32	Hdlbp	0.97	0.71
Apob	0.86	0.27	Hmgcr	1.14	0.5
Apoc1	0.92	0.31	Hmgcs1	0.9	0.49
Apoc3	0.89	0.43	Idi1	0.95	0.87
Apod	0.93	0.52	Il4	0.89	0.34
Apoe	0.89	0.46	Lcat	0.84	0.34
Apol2	0.89	0.95	Ldlrap1	0.99	0.85
Cdh13	0.9	0.52	Lep	0.87	0.7
Cel	0.91	0.82	Lipe	1.02	0.79
Cela3b	0.96	0.73	Lrp10	0.97	0.48
Cnbp	0.86	0.3	Lrp12	1	0.9
Cxcl16	0.86	0.45	Lrp1b	0.93	0.52
Cyp11a1	0.89	0.57	Lrpap1	0.86	0.3
Cyp39a1	0.94	0.77	Mbtps1	0.93	0.52

Cyp46a1	1.08	0.66	Mvd	0.93	0.65
Nr0b2	0.92	0.65	Mvk	0.98	1
Nr1h3	0.97	0.7	Prkaa2	1	0.93
Nr1h4	0.89	0.62	Prkag2	0.99	0.88
Nsdhl	0.83	0.27	RGD1564999	0.93	0.52
Olr1	0.87	0.37	Scarf1	0.92	0.31
Osbpl1a	0.92	0.28	Snx17	0.92	0.37
Osbpl5	0.9	0.52	Sorl1	1.07	0.57
Pcsk9	1.03	0.89	Srebf1	0.85	0.75
Prkaa1	0.82	0.34	Stab2	0.75	0.42
Stard3	0.97	0.55	Vldlr	0.97	0.91

Supportive evidence for *HMGCR* Western Blot

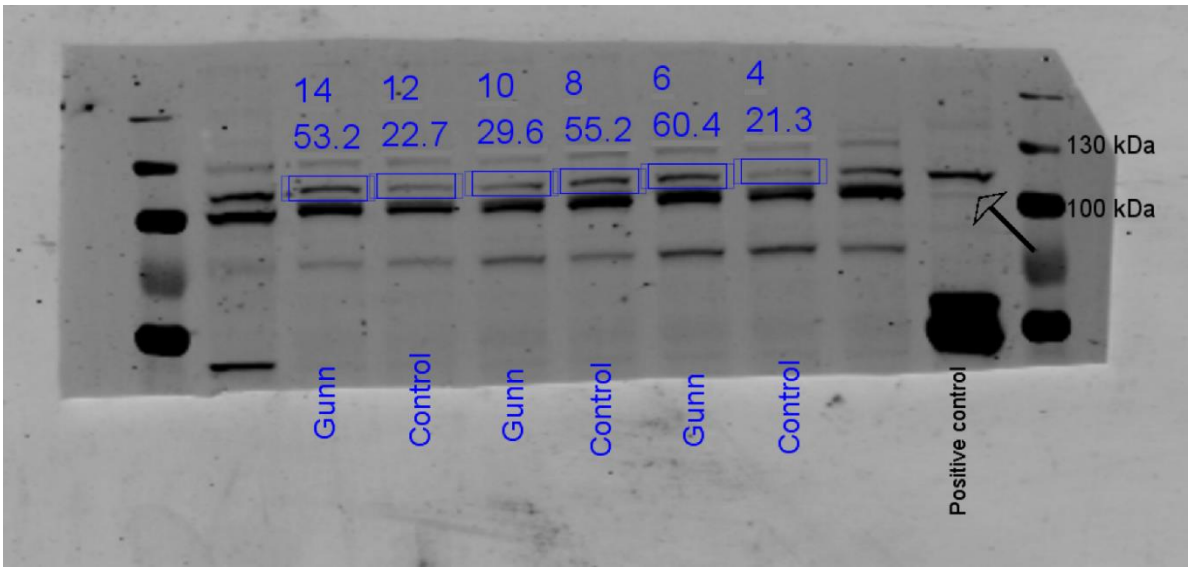

Figure S3.1. Western blot image detecting HMGCR protein. Positive control was rat brain tissue homogenate. Gunn and control represent liver tissue samples from hyperbilirubinaemic and normobilirubinaemic adult rats, respectively. Arrow points to target band region for HMGCR.

Manufacturer's predicted molecular weight of HMGCR: 97 kDa

The detected molecular weights were 100 and ~110 kDa in rat liver tissue. The positive control as per manufacturer's recommendation (rat brain homogenate) showed only a single band in that range at ~110 kDa indicating that the top band detected in liver tissue is the HMGCR protein. Therefore, HMGCR measurements in adult rat hepatic tissue was based on the top band (~110 kDa).

Supportive evidence for *CYB5R3* Western Blot

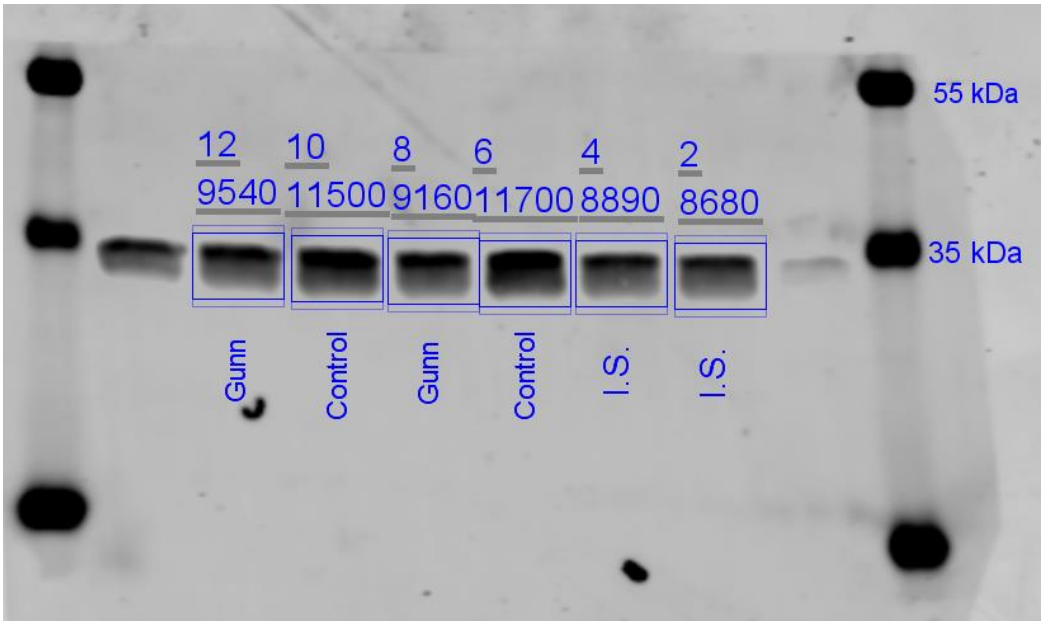

Figure S3.2. Western blot image detecting CYB5R3 protein. Gunn and control represent liver tissue samples from hyperbilirubinaemic and normobilirubinaemic adult rats, respectively.

Manufacturer's predicted molecular weight of CYB5R3: 34 kDa

The detected molecular weight in liver tissue of adult rats was ~34 kDa which is in agreement with the predicted molecular weight provided by the manufacturer. As there were no other bands detected it was concluded that this band represents CYB5R3.

Supportive evidence for *CYP7A1* Western Blot

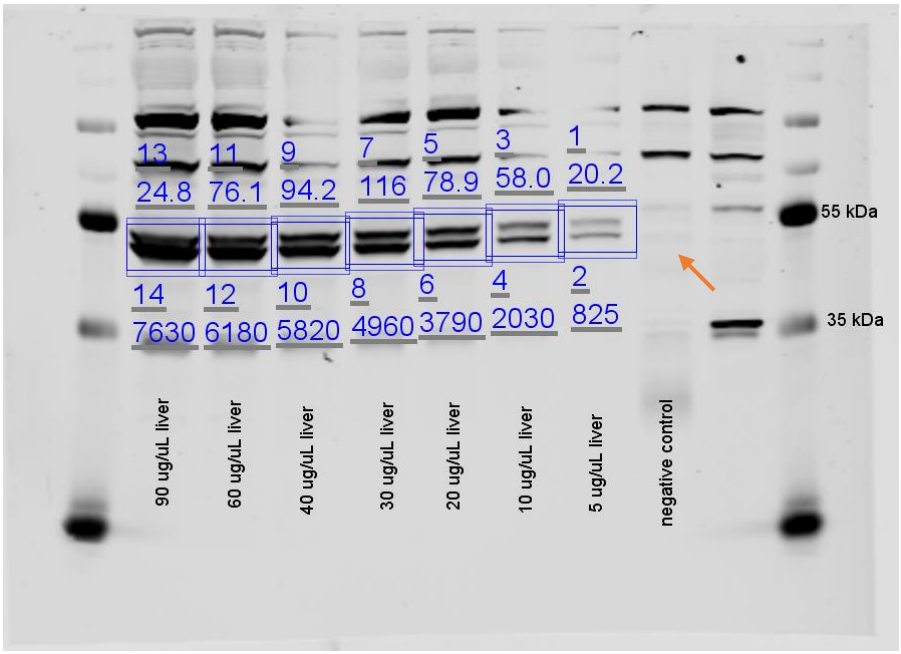

Figure S3.3. Western blot image detecting CYP7A1 protein. Rat soleus skeletal muscle was used as a negative control. Arrow points to target band region for CYP7A1 protein. Liver tissue was from adult rats.

Predicted molecular weight of CYP7A1: 58 kDa

Two bands were detected with molecular weight of ~50-54 kDa in rat liver tissue, these bands were slightly lower molecular weight compared to the predicted molecular weight. Soleus skeletal muscle was run as a negative control as per manufacturer's recommendation. Bands in the 50-54 kDa region were absent indicating that these bands represent CYP7A1. Therefore, both bands were used to analyse CYP7A1 expression in hepatic tissue of adult rats.

Supportive evidence for *LDLr* Western Blot

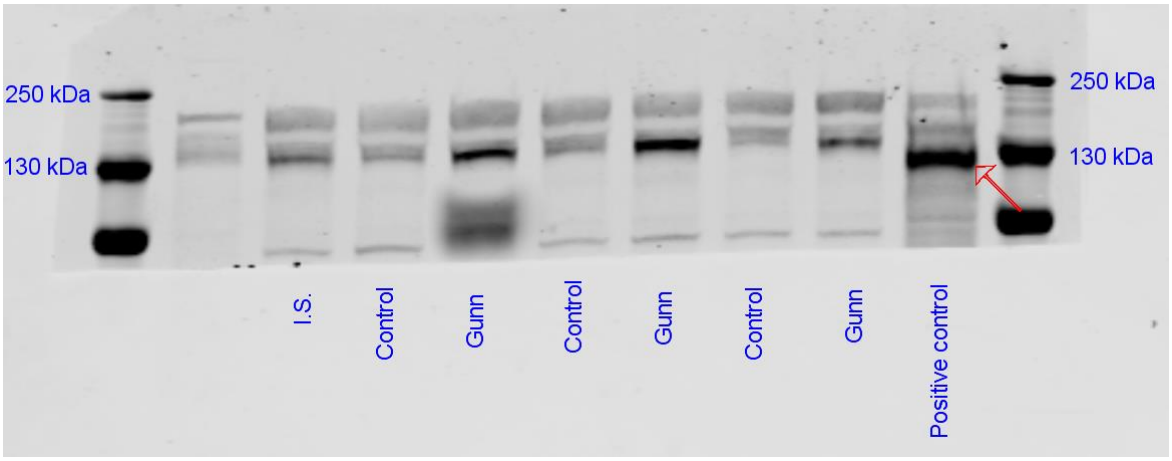

Figure S3.4. Western blot image detecting LDLr protein. Mouse liver homogenate was used as a positive control. Arrow points to target band region for LDLr protein.

Manufacturer's experimentally observed molecular weight of LDLr: 140-150 kDa

Two bands were detected with molecular weight of ~140 and ~180 kDa in rat liver tissue. The 140 kDa band was in agreement with that observed by the manufacturer. Mouse liver tissue was run as a positive control as per manufacturer's recommendation. Mouse liver tissue demonstrated two bands in similar range as that seen with rat liver tissue indicating that both bands represent LDLr protein. Therefore, both bands were used to analyse LDLr expression in hepatic tissue of adult rats.

Supportive evidence for *ABCA1* Western Blot

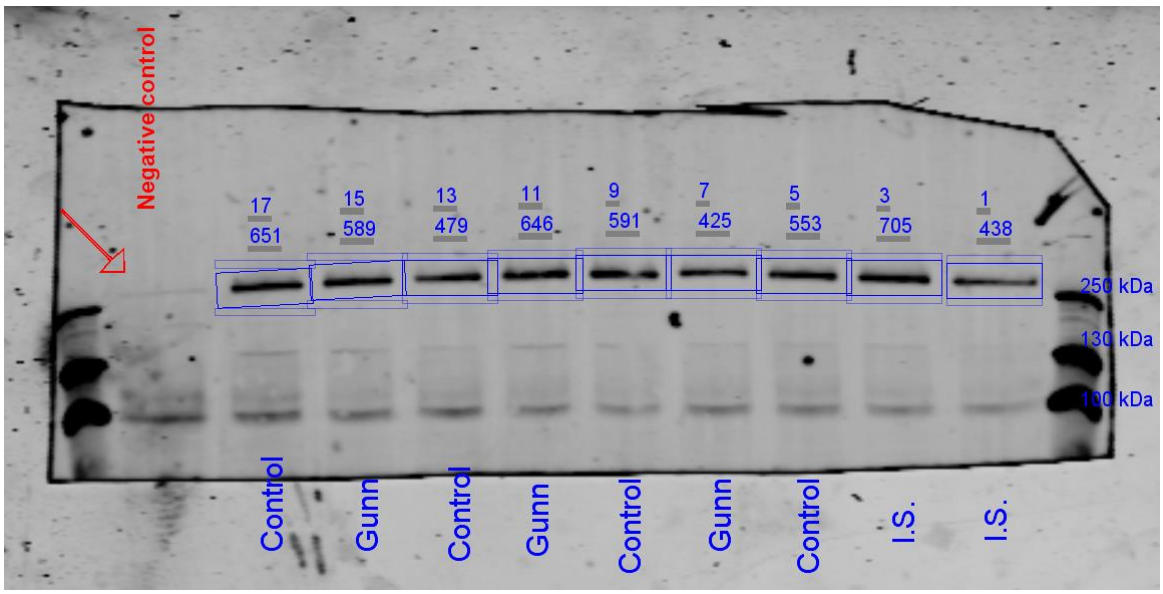

Figure S3.5. Western blot image detecting ABCA1 protein. Soleus skeletal muscle homogenate was used as a negative control. Arrow points to target band region.

Manufacturer's predicted molecular weight of ABCA1: 254 kDa

Single band was detected with molecular weight of ~254 kDa in rat liver tissue, which agreed with predicted molecular weight. Soleus skeletal muscle was run as a negative control as per manufacturer's recommendation. ~254 kDa band was absent from negative control indicating that the ~254 kDa band represents ABCA1 protein. Therefore, the ~254 kDa band was used to measure ABCA1 expression in hepatic tissue of adult rats.

Supportive evidence for *SREBP2* Western Blot

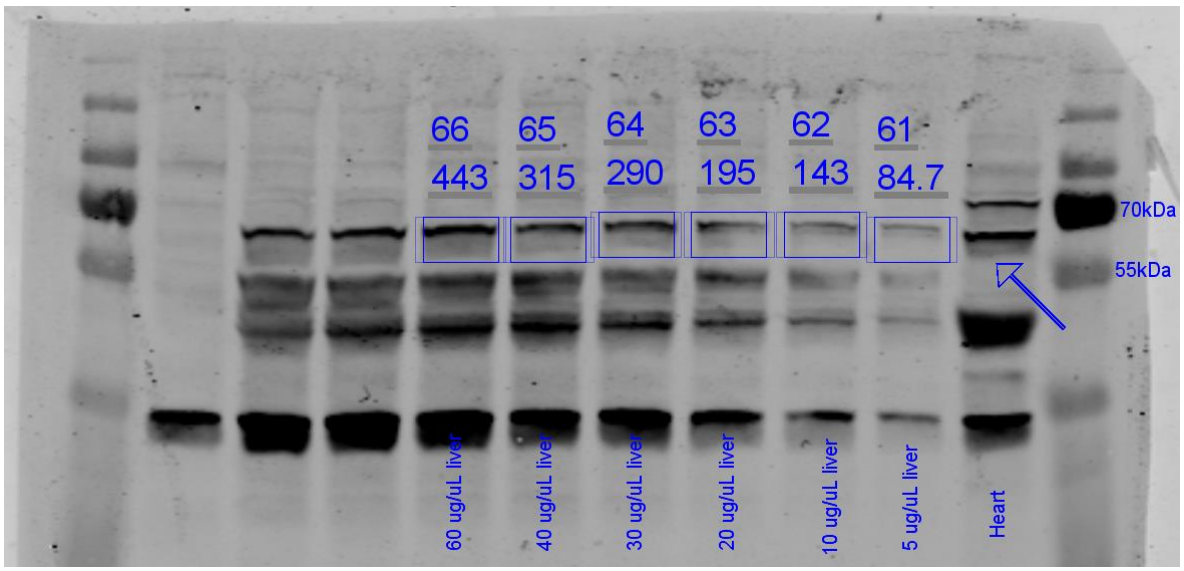

Figure S3.6. Western blot image detecting transcriptionally active form of SREBP2 protein. Arrow points to target band region. Heart (first lane) and liver tissue homogenates from adult rats were run in the western blot.

Manufacturer did not have a recommendation for the predicted molecular weight of the nuclear form of SREBP2. A study that characterised the different molecular forms of SREBP2 reported that the transcriptionally active form (nuclear form) has a molecular weight of ~70 kDa using Western blot [464]. Subsequent studies have reported similar results [465,466]. Therefore, it was concluded that bands close to 70 kDa likely represent the transcriptionally active form of SREBP2. In rat liver tissue there was one band at ~68 kDa, which was the closest to that measured previously (~70 kDa) indicating that this band is likely the transcriptionally active form of SREBP2. Based on this evidence the ~68 kDa band was used to measure the transcriptionally active SREBP2 form in liver tissue of adult rats.

Appendix 2 – Chapter 4: Supplementary document

Methods

Additional procedures:

Animals were gavaged daily with 400µL of drinking water and sterile phosphate buffered saline (Gibco®, United Kingdom) was administered every 2 days via an intraperitoneal injection from day 1 to day 15. Blood samples (approx. 1mL) were collected at Day 1 and Day 8, after a 6-7 hour fast, via tail bleed. Animals were fasted for 5-7 hrs prior to blood collection. Animals were then anaesthetised with 2-5% isofluorane (Pharmachem, Australia) in 100% oxygen via inhalation (1-2 L min^{-1}). Pedal reflexes were tested to ensure loss of pain responses. Blood was drawn via gentle massage of the tail after removal of the tail tip (1-2 mm). The first drop of blood was discarded before collecting 1 mL of blood in a 1.5 mL microtube. On the final day animals were euthanised via 50 mg kg^{-1} pentobarbitone injection (Pharmachem) and removal of the heart.

Results:

Table S4.1. Offspring distribution of homozygote and heterozygote Gunn rats

Variable	Phenotype		n	χ^2 (df)	P value†
	Het n [%]	Hom n [%]			
Offspring					
• Males	15 [21]	20 [28]	72	2.11 (3)	0.55
• Females	22 [31]	15 [21]			

Note: Het, heterozygote (normobilirubinaemic) Gunn rats; Hom, homozygote (hyperbilirubinaemic) Gunn rats. †Chi-square test for independence.

Table S4.2. Organ weights relative to bodyweight of hyperbilirubinaemic and normobilirubinaemic rats.

Variable	Phenotype		P value
	Control (n=18)	Gunn (n=19)	
Liver/Bodyweight (mg g^{-1})			
• Males	34.4 (1.98)	36.4 (2.81)	0.16
• Females	34.2 (2.99)	46.6 (3.23)	**<0.001**
Heart/Bodyweight (mg g^{-1})			
• Males	2.77 (0.20)	2.84 (0.23)	0.58
• Females	3.18 (0.34)	3.59 (0.35)	**<0.05**
Lungs/Bodyweight (mg g^{-1})			
• Males	3.60 (0.24)	3.64 (0.30)	0.8
• Females	4.46 (0.50)	5.13 (0.52)	**<0.01**
Kidney/Bodyweight (mg g^{-1})			
• Males	3.78 (0.24)	4.06 (0.42)	0.17
• Females	3.80 (0.40)	4.13 (0.32)	**<0.05**
Spleen/Bodyweight (mg g^{-1})			
• Males	2.71 (0.38)	2.74 (0.26)	0.88
• Females	3.11 (0.41)	3.90 (0.61)	**<0.01**
Testes/Bodyweight (mg g^{-1})			
• Males	4.48 (0.39)	4.75 (0.57)	0.49
Soleus/Bodyweight (mg g^{-1})			
• Males	0.40 (0.03)	0.35 (0.03)	**<0.01**
• Females	0.40 (0.04)	0.41 (0.06)	0.74
EDL/Bodyweight (mg g^{-1})			
• Males	0.34 (0.03)	0.32 (0.04)	0.42
• Females	0.35 (0.03)	0.34 (0.04)	0.66

Note: Control group represents normobilirubinaemic heterozygote littermates. Gunn group represents hyperbilirubinaemic homozygote littermates. Values are represented as mean (standard deviation). All comparisons are made between phenotype within the same sex.

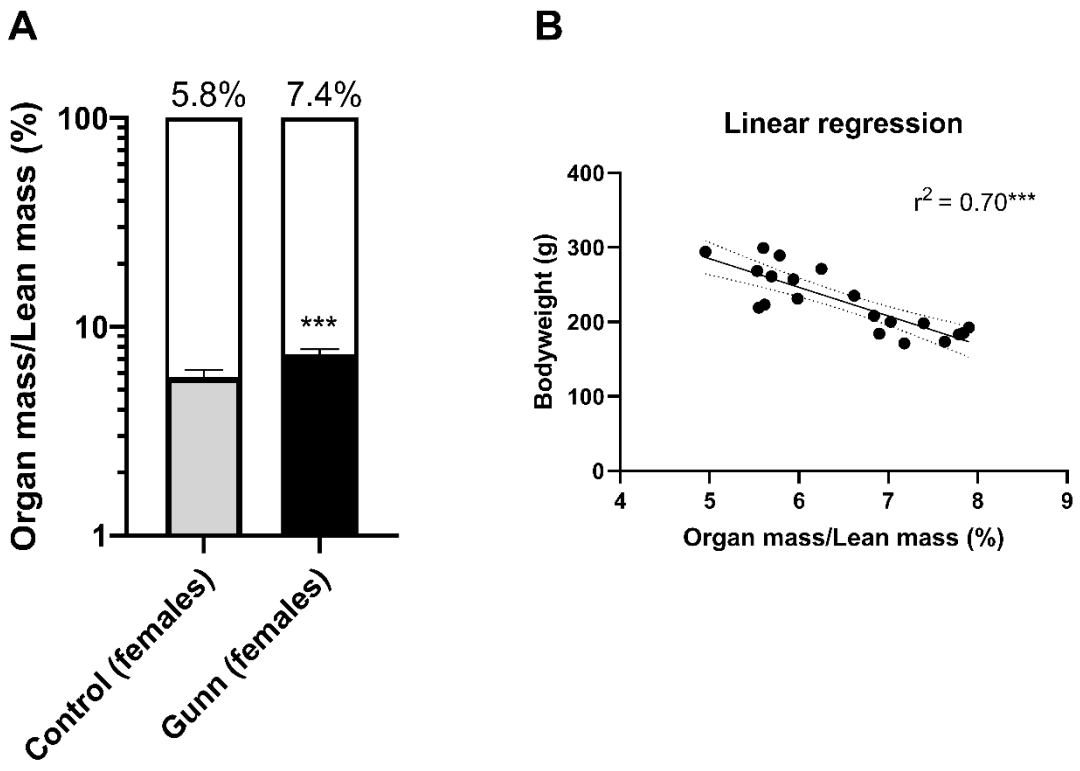

Figure S4.1. The relative proportion of organ mass to total lean mass in female hyperbilirubinaemic (Gunn) and normobilirubinaemic (control) rats (A) and the relationship of this ratio to bodyweight (B). Note: total organ mass was a sum of liver, lungs, heart, kidneys, and spleen mass. Data are presented as mean (standard deviation). P<0.05*, <0.01**, <0.001*** compared to control.

Supportive evidence for *OXPHOS* Western Blot

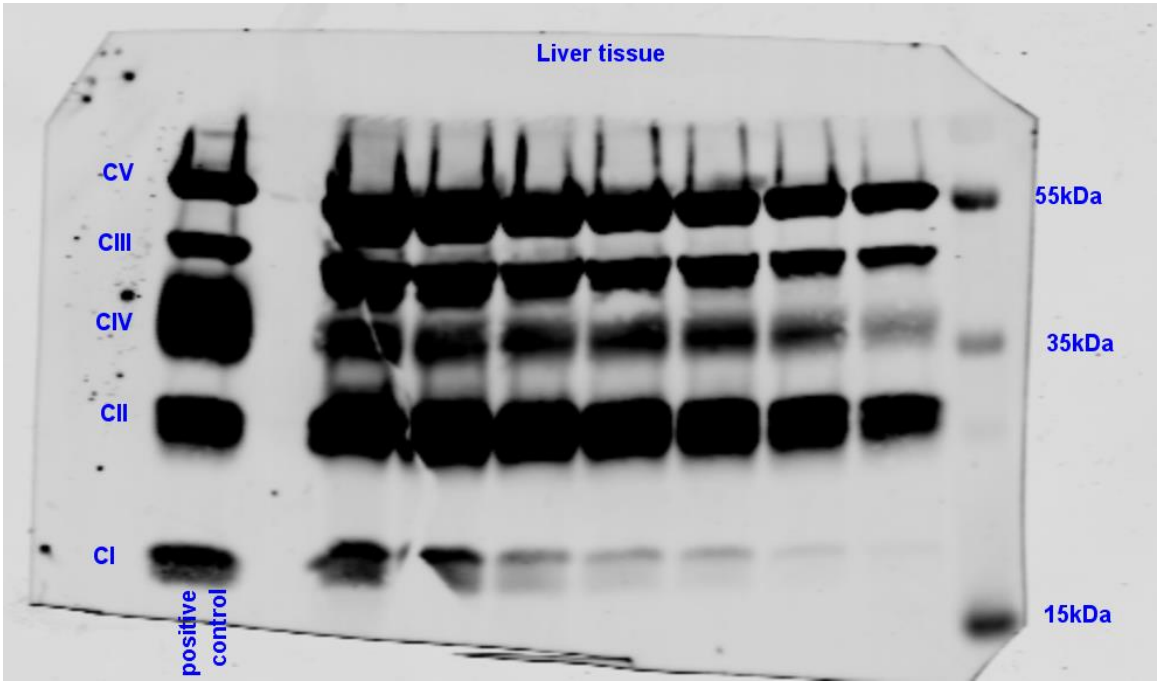

Figure S4.2. Western blot image detecting mitochondrial respiratory complexes. Isolated rat heart mitochondria were used as a positive control. Liver tissue homogenates from adult rats were run in the remaining lanes at different protein concentrations. CI-V, mitochondrial respiratory complexes I-V.

Manufacturer's experimentally documented molecular weights:

CV: ~55 kDa

CIII: ~48 kDa

CIV: ~40 kDa

CII:~30 kDa

CI: ~20 kDa

Five bands were detected from adult rat liver tissue which corresponded to mitochondrial respiratory complexes I-V (CI-V) and the molecular weights agreed with that documented by the manufacturer and by the positive control (Fig. S4.2). Therefore, the five bands as labelled in Fig. S4.2 were used to measure CI-V in liver tissue from adult rats.

Supportive evidence for *total AMPK* Western Blot

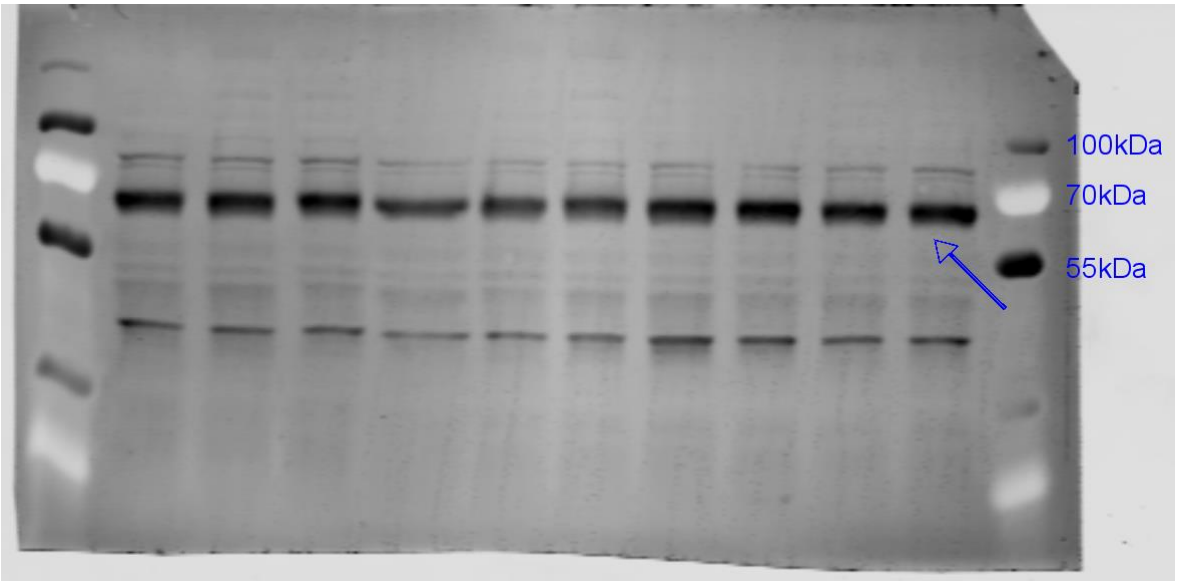

Figure S4.3. Western blot image detecting total AMPK. Liver tissue homogenates from adult hyperbilirubinaemic and normobilirubinaemic rats were run and blotted for total AMPK.

Manufacturer's predicted and experimentally determined molecular weight of AMPK: 62 kDa

Single strong band was detected at ~68 kDa which is close to that documented by the manufacturer (62 kDa). As there were no other bands in this region it was concluded that this band represented total AMPK, therefore, it was used to measure total AMPK in liver tissue of adult rats.

Supportive evidence for *phosphorylated AMPK* Western Blot

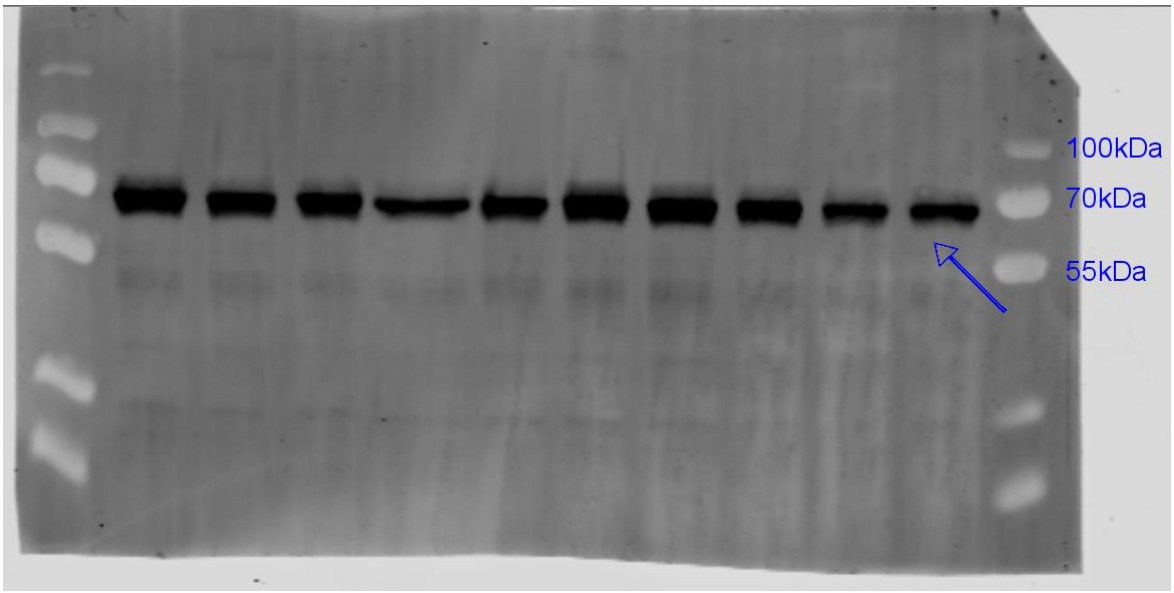

Figure S4.4. Western blot image detecting phosphorylated AMPK (pAMPK). Liver tissue homogenates from adult hyperbilirubinaemic and normobilirubinaemic rats were run and blotted for phosphorylated AMPK.

Manufacturer's predicted and experimentally determined molecular weight of pAMPK: 62-63 kDa

Single strong band was detected at ~68 kDa which is close to that documented by the manufacturer (62 kDa). As there were no other bands in this region it was concluded that this band represented pAMPK, therefore, it was used to measure pAMPK in liver tissue of adult rats.

Appendix 3 – Chapter 5: Supplementary document

Methods:

High-performance liquid chromatography (HPLC) analysis of unconjugated bilirubin

Samples were analysed for UCB via quantitative HPLC. Briefly, HPLC-PDA analysis was performed using a Shimadzu Prominence HPLC system consisting of an online degassing unit (DGU20A5R), solvent delivery unit (LC-20AT), autosampler (SIL-20 AC), column oven (CTO-20) and photo diode-array (SPD-M20A), connected in series. Separation was achieved via reverse phase C18 column (GreatSmart™ C18, 150 mm x 3 mm, 3 µm; PhaseSep Pty. Ltd., Melbourne, Australia), which was preceded by a guard column (GreatSmart™ C18, 3 µm; PhaseSep Pty. Ltd., Melbourne, Australia) and an UltraLine HPLC in-line filter (Restek, 0.5 µm; Shimadzu, Sydney, Australia), respectively. The column oven and autosampler were set to 45˚C and 12˚C, respectively, with an initial flow rate of 0.8 $mL \cdot min^{-1}$. Starting mobile phase consisted of 34% organic B (100% MeOH) and 66% aqueous A (10 mM NH_4OAc in 25% MeOH and 75% Milli-Q purified H_2O). A linear gradient was applied, reaching 95% B at 6 mins, and remaining at 95% until 9.5 mins. From 9.5 to 16 mins, the mobile phase was set to 34% B. To assist rapid equilibration, the flow rate remained at 0.8 $mL \cdot min^{-1}$ until 9.5 mins and increased to 1.3$mL \cdot min^{-1}$ at 10.2 mins remaining until 13.3 mins. Between 13.3 mins and 16 mins the flow rate was 0.8 $mL \cdot min^{-1}$. The total run time including column re-equilibration was 16 mins. UCB linearity (0.78125µM - 50µM) ($r^2 > 0.999$; Fig. S5.1) was satisfactory, with an approximated LOQ of 170 nM and a retention time of 8 mins. 160 µL of extractant was added to 40 µL of sample, vortexed and centrifuged (21 500 RCF; 10 mins). The supernatant was syringe filtered (0.22 µm, PhaseSep Pty. Ltd., Victoria, Australia) upon addition to a HPLC vial, prior to being placed in the autosampler where 10 µL was injected for analysis. The serum recovery of UCB was >80% with a %CV of <15% (Fig. S5.3).

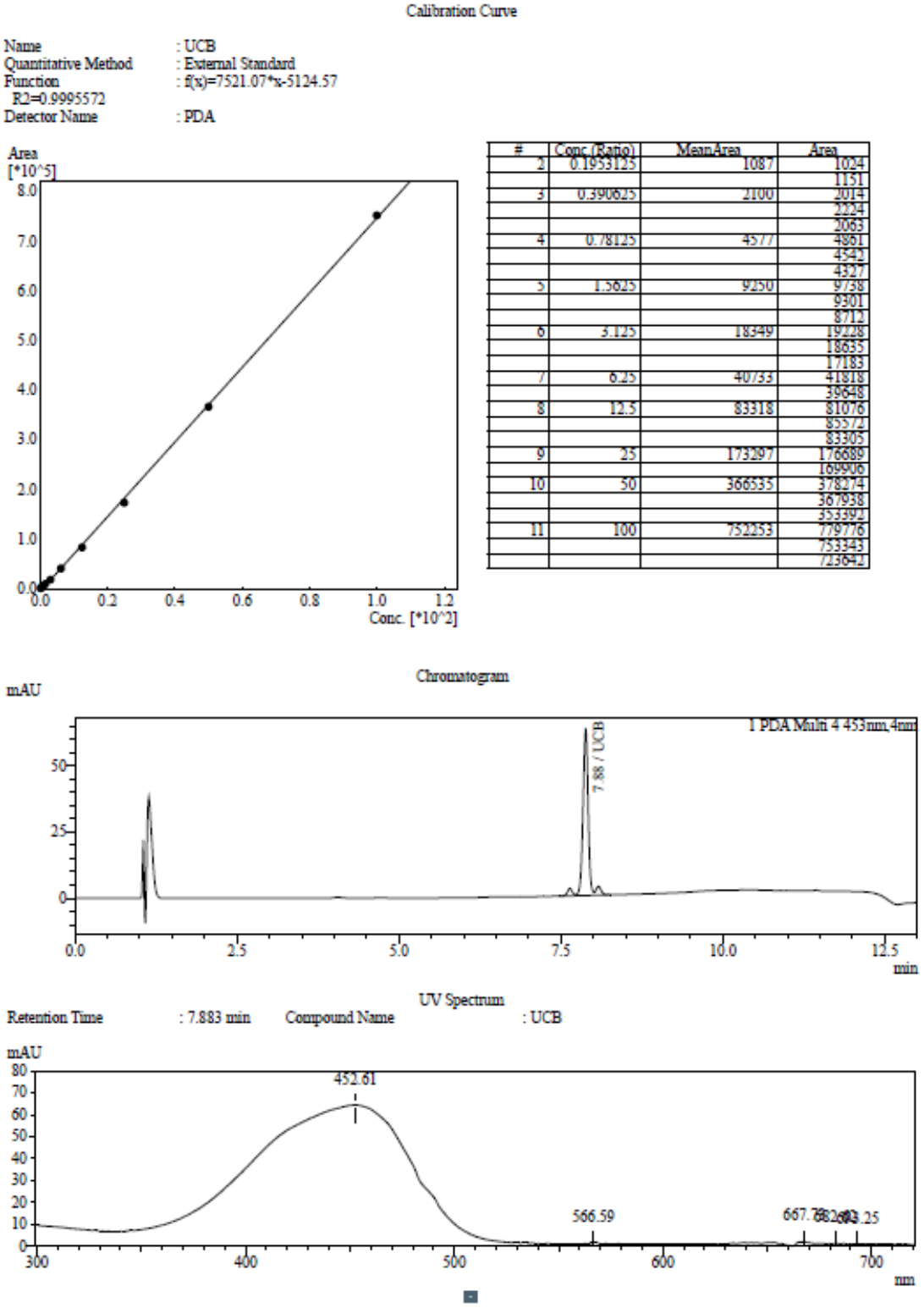

Figure. S5.1. Calibration curve with unconjugated bilirubin (UCB) on HPLC. The mean average of three runs was used to develop a calibration curve.

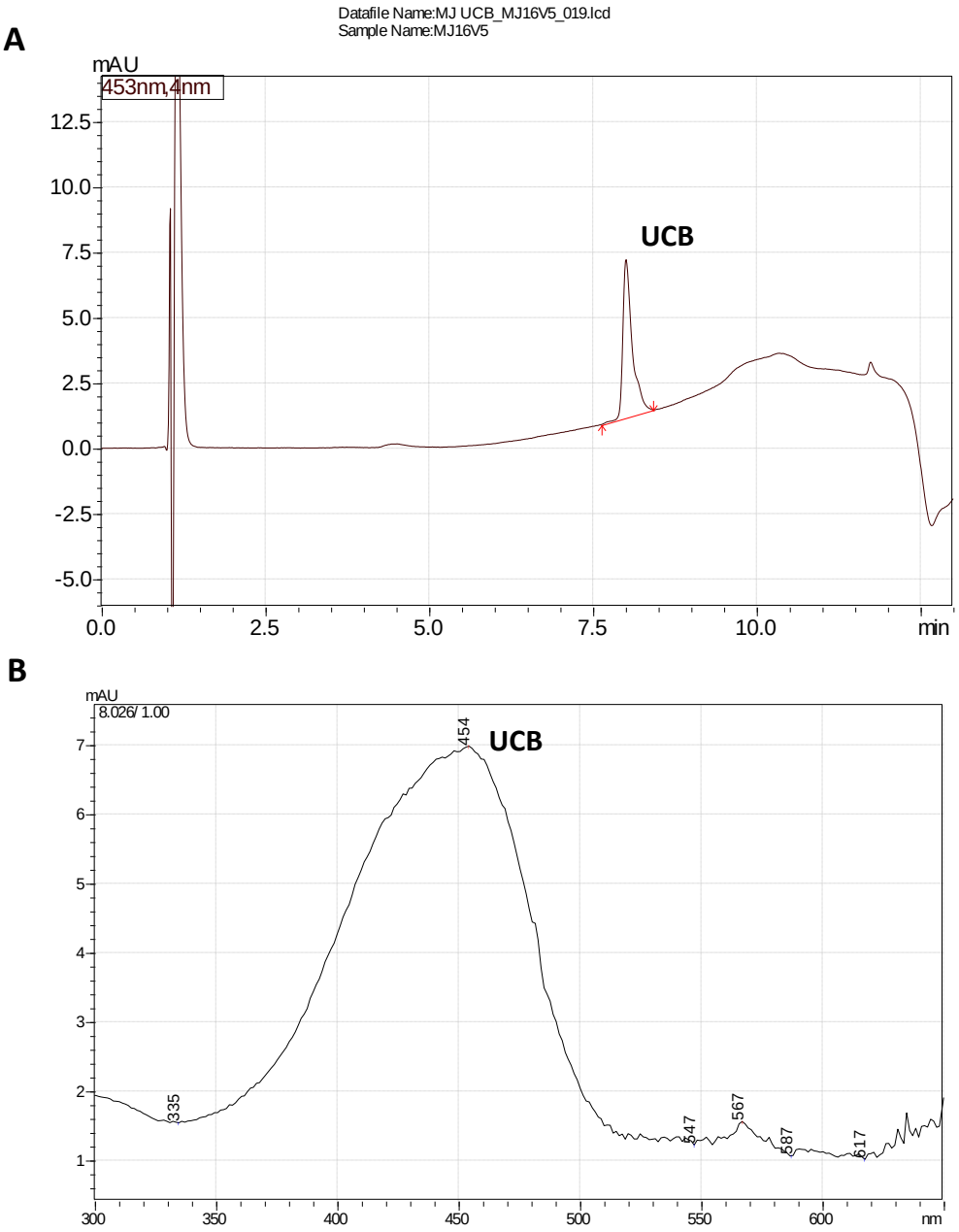

Figure S5.2. A typical chromatogram (A) of a serum sample from a participant and absorbance spectra (B) from the peak identified as unconjugated bilirubin (UCB).

A

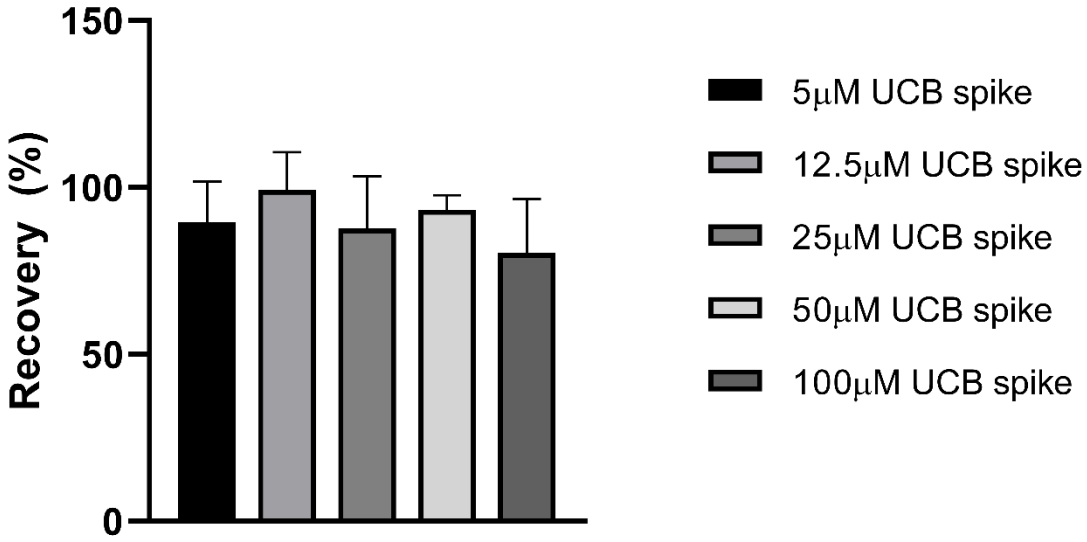

B

	5 μM spike	12.5 μM spike	25 μM spike	50 μM spike	100 μM spike
Number of values	3	3	3	3	3
Mean	89.53	99.27	87.69	93.36	80.48
Std. Deviation	12.34	11.27	15.67	4.296	16.10
Std. Error of Mean	7.125	6.505	9.049	2.480	9.294
Coefficient of variation	13.78%	11.35%	17.87%	4.601%	20.00%

Figure S5.3. Unconjugated bilirubin (UCB) recovery in human serum. A) Represents the mean (SD) recovery in percent (%) of UCB from three different human serum samples. B) Table presentation of the average recovery and the coefficient of variation (%CV) of UCB from human serum.

Normal Ranges for Baseline Blood test results

(Based on Royal College of Pathologists of Australasia)

Normal LFT:

Alanine aminotransferase (ALT) < 35U/L

Alkaline phosphatase (ALP)

Male: 17y to <19y (50–220) U/L: 19y to <22y (45–150) U/L: 22y to <120y (30–110) U/L

Female: 16y to <22y (35–140) U/L: 22y to <120y (30–110) U/L:

Aspartate aminotransferase (AST) < 40 U/L.

Gamma glutamyltransferase (GGT)

Male: < 50 U/L Female: < 30 U/L

Normal FBC

Haemoglobin: The normal haemoglobin level for adult males is 130-170 g/L, and 120-150 g/L for adult females.

Haematocrit Adult males is 40-50 per cent, and 36-46 per cent for adult females.

Red cell count: The normal red cell count for adult males is 4.5-5.5 x 10^{12}/L, and 3.8-4.8 x 10^{12}/L for adult females.

White cell count: The normal white cell count for adults is 4.0-10.0 x 10^{9}/L.

Platelet count: The normal platelet count for adults is 150-400 x 10^{9}/L.

Appendix 4 – Supplementary document for common methods used in Chapters 3 and 4

Western Blot optimisations:

For all proteins measured using Western blot the linearity of signal detection was determined. The goal of these experiments was to determine the overlapping range of linearity for both the housekeeping protein and the target protein. One example of an overlapping range of linearity is demonstrated for CYB5R3 (target protein) and GAPDH (housekeeping protein) (Fig. S6.1). CYB5R3 detection is linear with respect to total protein concentration until 30 µg/30 µL of protein, with the signal becoming saturated after this range. Conversely, the signal of GAPDH is linear throughout the measured ranges (5-60 µg/30 µL), however, the slope changes after 10 µg/ 30 µL of protein. As such, the overlapping range of linearity with a constant slope is found between the two vertically dotted red lines (10-30 µg/µL of protein). 20 µg/µL of total hepatic protein was selected for measuring hepatic CYB5R3 expression in adult rats because it was the middle concentration of the linear range.

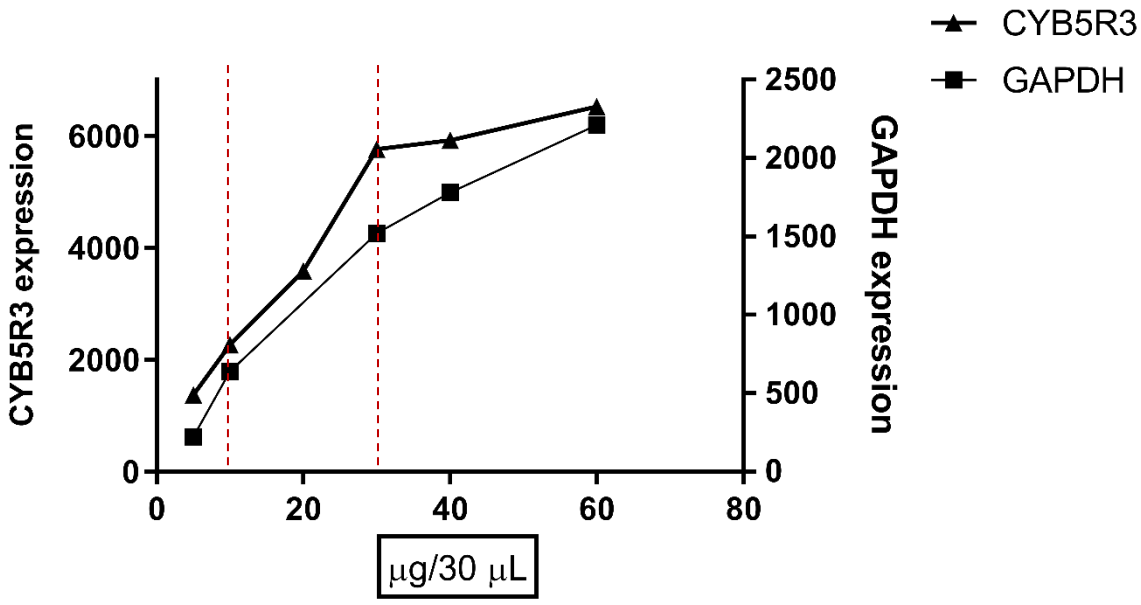

Figure S6.1. The range of linear detection for CYB5R3 and GAPDH. The x axis represents different concentrations of total protein loaded from liver homogenate. The vertical dotted red lines represent the overlapping range of linearity for target protein (CYB5R3) and housekeeping protein (GAPDH).

Lipid recovery in faeces and liver tissue:

LIVER TISSUE:

Four liver homogenates were spiked (1 mM, 3 mM, or 5 mM) with cholesterol (#C3045; Sigma Aldrich, Australia) or triglycerides (#17811; Sigma Aldrich) and the lipids were extracted with isopropyl alcohol as described in Chapters 3 and 4. Recovery for cholesterol was >78% with %CV <5%. Recovery for triglycerides was >73% with %CV <10% (Fig. S6.2).

A

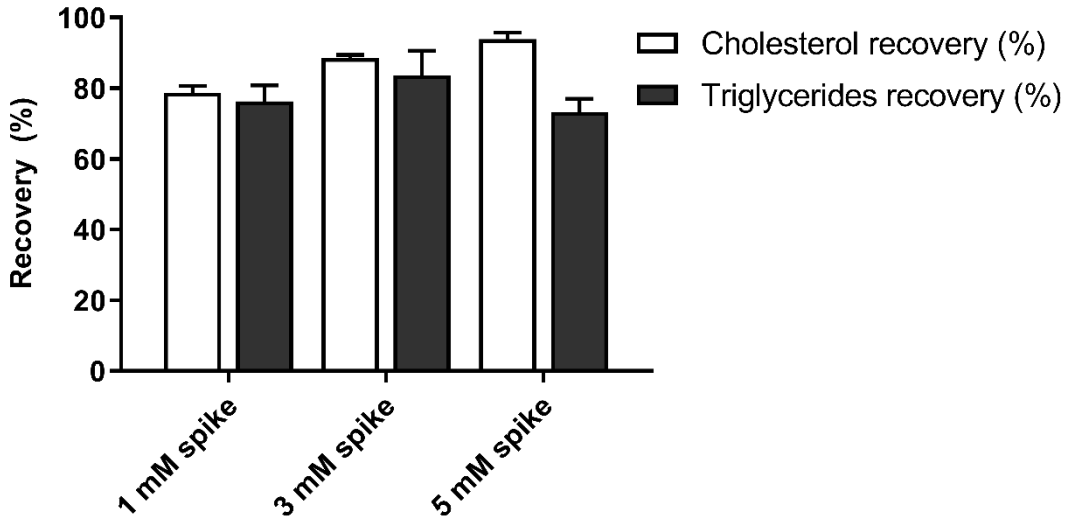

B

Cholesterol recovery (%)			Triglycerides recovery (%)		
Mean	%CV	N	Mean	%CV	N
78.773	2.404	4	76.256	6.000	4
88.573	0.985	4	83.648	8.287	4
93.913	1.990	4	73.280	5.117	4

Figure S6.2. The mean (SD) recovery of cholesterol and triglycerides (A) and the coefficient of variance (%CV) (B) from four liver homogenates.

FAECES:

Three faecal homogenates were spiked (0.5 mM or 1 mM) with cholesterol (#C3045; Sigma Aldrich, Australia) and the lipids were extracted with isopropyl alcohol as described in Chapters 3 and 4. The recovery of cholesterol was >85% with a %CV <10% (Fig. S6.3)

A

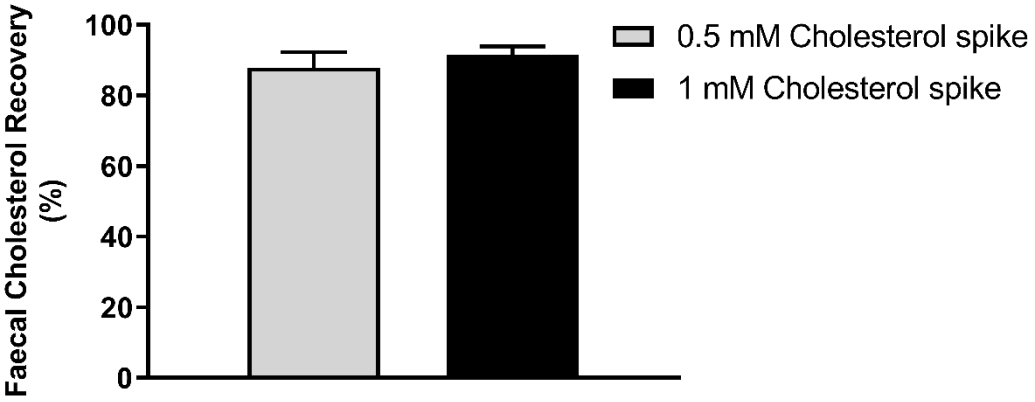

B

	0.5 mM Cholesterol spike	1 mM Cholesterol spike
Number of values	3	3
Mean	87.81	91.45
Std. Deviation	4.475	2.455
Std. Error of Mean	2.584	1.417
Coefficient of variation	5.097%	2.684%

Figure S6.3. The mean (SD) recovery of cholesterol (A) and the coefficient of variance (%CV) (B) from three faecal homogenates.

Example of solvent interference analysis:

Cholesterol standards were solubilised with 100% isopropyl alcohol and analysed using COBAS Integra 400+ as described in Chapter 3. To determine whether solvent interfered with the cholesterol measurement the same samples were diluted 10-fold in H_2O and re-analysed. There were no changes in the slope between non-diluted and diluted cholesterol standard curves, nor were the measured cholesterol concentrations different from the cholesterol standard concentrations (Figure S6.4). Therefore, it was concluded that isopropyl alcohol does not interfere with cholesterol measurement. The same validation was conducted for triglyceride measurement with not interference detected.

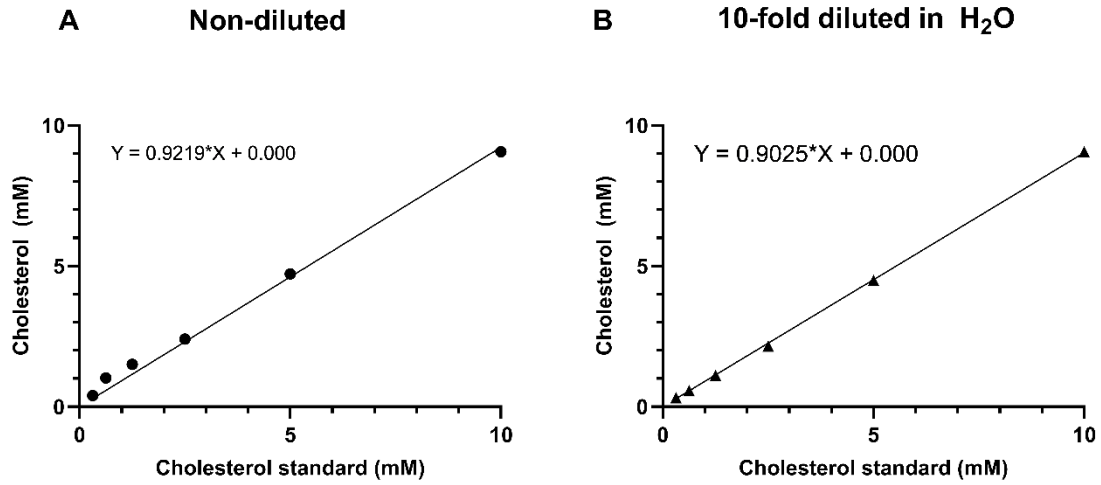

Figure S6.4. Standard curve of cholesterol solubilised in isopropyl alcohol. Non-diluted represents non-diluted cholesterol standards (A) while 10-fold diluted in H_2O represents cholesterol standards solubilised in isopropanol that were subsequently diluted 10-fold in H_2O prior to analysis (B).

References

1. Ostrow LV and JD. Bilirubin Chemistry and Metabolism; Harmful and Protective Aspects. *Curr Pharm Des* 2009;**15**:2869–83.

2. Watchko JF, Tiribelli C. Bilirubin-induced neurologic damage - Mechanisms and management approaches. *N Engl J Med* 2013;**369**:2021–30.

3. Vítek L. Bilirubin and Atherosclerotic Diseases. *Physiol Res* 2017;**66**:S11–20.

4. Vitek L, Hubacek JA, Pajak A *et al.* Association between plasma bilirubin and mortality. *Ann Hepatol* 2019;**18**:379–85.

5. Seyed Khoei N, Grindel A, Wallner M *et al.* Mild hyperbilirubinaemia as an endogenous mitigator of overweight and obesity: Implications for improved metabolic health. *Atherosclerosis* 2018;**269**:306–11.

6. Neuzil J, Stocker R. Free and albumin-bound bilirubin are efficient co-antioxidants for α-Tocopherol, inhibiting plasma and low density lipoprotein lipid peroxidation. *J Biol Chem* 1994;**269**:16712–9.

7. Boon AC, Hawkins CL, Coombes JS *et al.* Bilirubin scavenges chloramines and inhibits myeloperoxidase-induced protein/lipid oxidation in physiologically relevant hyperbilirubinemic serum. *Free Radic Biol Med* 2015;**86**:259–68.

8. Stocker R, Yamamoto Y, McDonagh AF *et al.* Bilirubin is an antioxidant of possible physiological importance. *Science* 1987;**235**:1043–6.

9. Liu J, Dong H, Zhang Y *et al.* Bilirubin Increases Insulin Sensitivity by Regulating Cholesterol Metabolism, Adipokines and PPARγ Levels. *Sci Rep* 2015;**5**:9886.

10. Stec DE, John K, Trabbic CJ *et al.* Bilirubin Binding to PPARα Inhibits Lipid Accumulation. *PLoS One* 2016;**11**:e0153427.

11. Hinds TD, Hosick PA, Chen S *et al.* Mice with hyperbilirubinemia due to Gilbert's syndrome polymorphism are resistant to hepatic steatosis by decreased serine 73 phosphorylation of PPARα. *Am J Physiol - Endocrinol Metab* 2017;**312**:E244–52.

12. Bulmer AC, Verkade HJ, Wagner KH. Bilirubin and beyond: A review of lipid status in Gilbert's syndrome and its relevance to cardiovascular disease protection. *Prog Lipid Res* 2013;**52**:193–205.

13. Schonewille M, De Boer JF, Mele L *et al.* Statins increase hepatic cholesterol synthesis and

stimulate fecal cholesterol elimination in mice. *J Lipid Res* 2016;**57**:1455–64.

14. Jakulj L, van Dijk TH, de Boer JF *et al.* Transintestinal Cholesterol Transport Is Active in Mice and Humans and Controls Ezetimibe-Induced Fecal Neutral Sterol Excretion. *Cell Metab* 2016;**24**:783–94.

15. Verkade HJ. Inhibition of biliary phospholipid and cholesterol secretion by organic anions affects bile canalicular membrane composition and fluidity. *J Gastroenterol* 2000;**35**:481–5.

16. Zhou J, Tracy TS, Remmel RP. Correlation between Bilirubin Glucuronidation and Estradiol-3-Gluronidation in the Presence of Model UDP-Glucuronosyltransferase 1A1 Substrates/Inhibitors. *Drug Metab Dispos* 2011;**39**:322–9.

17. Sambasivarao S V. Glucuronidation of the steroid enantiomers ent-17β-estradiol ent-androsterone and ent-etiocholanolone by the human UDP-glucuronosyltransferases. 2013;**18**:1199–216.

18. Lemieux H, Semsroth S, Antretter H *et al.* Mitochondrial respiratory control and early defects of oxidative phosphorylation in the failing human heart. *Int J Biochem Cell Biol* 2011;**43**:1729–38.

19. Holland OJ, Cuffe JSM, Dekker Nitert M *et al.* Placental mitochondrial adaptations in preeclampsia associated with progression to term delivery. *Cell Death Dis* 2018;**9**:1150.

20. Vaz AR, Delgado-Esteban M, Brito MA *et al.* Bilirubin selectively inhibits cytochrome c oxidase activity and induces apoptosis in immature cortical neurons: Assessment of the protective effects of glycoursodeoxycholic acid. *J Neurochem* 2010;**112**:56–65.

21. Malik S., Irwanto K., Ostrow J. *et al.* Effect of bilirubin on cytochrome c oxidase activity of mitochondria from mouse brain and liver. *BMC Res Notes* 2010;**3**:162.

22. Rendina M, D'Amato M, Castellaneta A *et al.* Antiviral activity and safety profile of silibinin in HCV patients with advanced fibrosis after liver transplantation: A randomized clinical trial. *Transpl Int* 2014;**27**:696–704.

23. Flaig TW, Gustafson DL, Su LJ *et al.* A phase I and pharmacokinetic study of silybin-phytosome in prostate cancer patients. *Invest New Drugs* 2007;**25**:139–46.

24. Mariño Z, Crespo G, D'Amato M *et al.* Intravenous silibinin monotherapy shows significant antiviral activity in HCV-infected patients in the peri-transplantation period. *J Hepatol* 2013;**58**:415–20.

25. World Health Organization. *Health in 2015 from MDGs to SDGs*. Geneva: World Health

Organization, 2015.

26. Australian Institute of Health and Welfare. *Health-Care Expenditure on Cardiovascular Diseases 2008-09*., 2014.

27. Redinger RN. The pathophysiology of obesity and its clinical manifestations. *Gastroenterol Hepatol (N Y)* 2007;**3**:856–63.

28. Chan RSM, Woo J. Prevention of overweight and obesity: how effective is the current public health approach. *Int J Environ Res Public Health* 2010;**7**:765–83.

29. VanderLaan PA, Reardon CA, Getz GS. Site Specificity of Atherosclerosis: Site-Selective Responses to Atherosclerotic Modulators. *Arterioscler Thromb Vasc Biol* 2004;**24**:12–22.

30. Gimbrone MA, García-Cardeña G. Endothelial Cell Dysfunction and the Pathobiology of Atherosclerosis. *Circ Res* 2016;**118**:620–36.

31. Williams KJ, Tabas I. The response-to-retention hypothesis of early atherogenesis. *Arterioscler Thromb Vasc Biol* 1995;**15**:551–61.

32. Tabas I, Williams KJ, Borén J. Subendothelial lipoprotein retention as the initiating process in atherosclerosis: Update and therapeutic implications. *Circulation* 2007;**116**:1832–44.

33. Tabas I, García-Cardeña G, Owens GK. Recent insights into the cellular biology of atherosclerosis. *J Cell Biol* 2015;**209**:13–22.

34. Lovren F, Teoh H, Verma S. Obesity and Atherosclerosis: Mechanistic Insights. *Can J Cardiol* 2015;**31**:177–83.

35. Trialists CT. Efficacy and safety of cholesterol-lowering treatment: Prospective meta-analysis of data from 90 056 participants in 14 randomised trials of statins. *Lancet* 2005;**366**:1267–78.

36. Insull W. The Pathology of Atherosclerosis: Plaque Development and Plaque Responses to Medical Treatment. *Am J Med* 2009;**122**:S3–14.

37. Arca M, Pigna. Treating statin-intolerant patients. *Diabetes, Metab Syndr Obes Targets Ther* 2011:155.

38. Li H, Horke S, Förstermann U. Vascular oxidative stress, nitric oxide and atherosclerosis. *Atherosclerosis* 2014;**237**:208–19.

39. Gimbrone MA, García-Cardeña G. Vascular endothelium, hemodynamics, and the pathobiology of atherosclerosis. *Cardiovasc Pathol* 2013;**22**:9–15.

40. Kriszbacher I, Koppán M, Bódis J. Inflammation, atherosclerosis, and coronary artery disease. *N Engl J Med* 2005;**353**:429–30; author reply 429-30.

41. Steinberg D, Witztum JL. Oxidized Low-Density Lipoprotein and Atherosclerosis. *Arter Thromb Vasc Biol* 2010;**30**:2311–6.

42. Lewis SJ. Prevention and Treatment of Atherosclerosis: A Practitioner's Guide for 2008. *Am J Med* 2009;**122**:S38–50.

43. Vitek L, Ostrow J. Bilirubin Chemistry and Metabolism; Harmful and Protective Aspects. *Curr Pharm Des* 2009;**15**:2869–83.

44. Kunutsor SK, Bakker SJL, Gansevoort RT *et al.* Circulating Total Bilirubin and Risk of Incident Cardiovascular Disease in the General Population. *Arterioscler Thromb Vasc Biol* 2015;**35**:716–24.

45. Flegal KM, Carroll MD, Ogden CL *et al.* Prevalence and trends in obesity among US adults, 1999-2008. *JAMA* 2010;**303**:235–41.

46. Hruby A, Hu FB. The Epidemiology of Obesity: A Big Picture. *Pharmacoeconomics* 2015;**33**:673–89.

47. Nuttall FQ. Body mass index: Obesity, BMI, and health: A critical review. *Nutr Today* 2015;**50**:117–28.

48. Lee M-J, Wu Y, Fried SK. Adipose tissue remodeling in pathophysiology of obesity. *Curr Opin Clin Nutr Metab Care* 2010;**13**:371–6.

49. Allison DB, Kaprio J, Korkeila M *et al.* The heritability of body mass index among an international sample of monozygotic twins reared apart. *Int J Obes Relat Metab Disord* 1996;**20**:501–6.

50. Wright SM, Aronne LJ. Causes of obesity. *Abdom Radiol* 2012;**37**:730–2.

51. Centers for Disease Control and Prevention (CDC). Prevalence of regular physical activity among adults--United States, 2001 and 2005. *MMWR Morb Mortal Wkly Rep* 2007;**56**:1209–12.

52. Wilding J. Are the causes of obesity primarily environmental? Yes. *BMJ* 2012;**345**:e5843–e5843.

53. Lavie CJ, Laddu D, Arena R *et al.* Healthy Weight and Obesity Prevention. *J Am Coll Cardiol* 2018;**72**:1506–31.

54. Wadden TA, Webb VL, Moran CH *et al.* Lifestyle Modification for Obesity. *Circulation* 2012;**125**:1157–70.

55. Liesa M, Shirihai OS. Mitochondrial dynamics in the regulation of nutrient utilization and energy expenditure. *Cell Metab* 2013;**17**:491–506.

56. Burtscher M. Exercise Limitations by the Oxygen Delivery and Utilization Systems in Aging and Disease: Coordinated Adaptation and Deadaptation of the Lung-Heart Muscle Axis - A Mini-Review. *Gerontology* 2013;**59**:289–96.

57. Myers J, Prakash M, Froelicher V *et al.* Exercise Capacity and Mortality among Men Referred for Exercise Testing. *N Engl J Med* 2002;**346**:793–801.

58. Wei M, Kampert JB, Barlow CE *et al.* Relationship between low cardiorespiratory fitness and mortality in normal-weight, overweight, and obese men. *JAMA* 1999;**282**:1547–53.

59. Mustelin L, Pietila KH, Rissanen A *et al.* Acquired obesity and poor physical fitness impair expression of genes of mitochondrial oxidative phosphorylation in monozygotic twins discordant for obesity. *Am J Physiol Metab* 2020:E148–54.

60. Auwerx J. Improving metabolism by increasing energy expenditure. *Nat Med* 2006;**12**:44–5.

61. Phielix E, Meex R, Moonen-Kornips E *et al.* Exercise training increases mitochondrial content and ex vivo mitochondrial function similarly in patients with type 2 diabetes and in control individuals. *Diabetologia* 2010;**53**:1714–21.

62. Meex RCR, Schrauwen-Hinderling VB, Moonen-Kornips E *et al.* Restoration of Muscle Mitochondrial Function and Metabolic Flexibility in Type 2 Diabetes by Exercise Training Is Paralleled by Increased Myocellular Fat Storage and Improved Insulin Sensitivity. *Diabetes* 2010;**59**:572–9.

63. Stephenson EJ, Hawley JA. Mitochondrial function in metabolic health: A genetic and environmental tug of war. *Biochim Biophys Acta - Gen Subj* 2014;**1840**:1285–94.

64. Campbell M, Farrell S, McDougal O. *Biochemistry*. 9th ed. Brooks Cole, 2017.

65. Watmough NJ, Frerman FE. The electron transfer flavoprotein: Ubiquinone oxidoreductases. *Biochim Biophys Acta - Bioenerg* 2010;**1797**:1910–6.

66. Mráček T, Drahota Z, Houštěk J. The function and the role of the mitochondrial glycerol-3-phosphate dehydrogenase in mammalian tissues. *Biochim Biophys Acta - Bioenerg* 2013;**1827**:401–10.

67. Gnaiger E. *Mitochondrial Pathways and Respiratory Control An Introduction to OXPHOS Analysis*., 2014.

68. Berry BJ, Trewin AJ, Amitrano AM *et al.* Use the Protonmotive Force: Mitochondrial Uncoupling and Reactive Oxygen Species. *J Mol Biol* 2018;**430**:3873–91.

69. Divakaruni AS, Brand MD. The Regulation and Physiology of Mitochondrial Proton Leak. *Physiology* 2011;**26**:192–205.

70. Rolfe DFS, Brand MD. Contribution of mitochondrial proton leak to skeletal muscle respiration and to standard metabolic rate. *Am J Physiol Physiol* 1996;**271**:C1380–9.

71. Brand MD. The efficiency and plasticity of mitochondrial energy transduction. *Biochem Soc Trans* 2005;**33**:897.

72. Divakaruni AS, Brand MD. The regulation and physiology of mitochondrial proton leak. *Physiology (Bethesda)* 2011;**26**:192–205.

73. Busiello RA, Savarese S, Lombardi A. Mitochondrial uncoupling proteins and energy metabolism. *Front Physiol* 2015;**6**:36.

74. Keipert S, Ost M, Chadt A *et al.* Skeletal muscle uncoupling-induced longevity in mice is linked to increased substrate metabolism and induction of the endogenous antioxidant defense system. *Am J Physiol Metab* 2013;**304**:E495–506.

75. Ost M, Werner F, Dokas J *et al.* Activation of AMPKα2 Is Not Crucial for Mitochondrial Uncoupling-Induced Metabolic Effects but Required to Maintain Skeletal Muscle Integrity. Eckel J (ed.). *PLoS One* 2014;**9**:e94689.

76. Costford SR, Chaudhry SN, Salkhordeh M *et al.* Effects of the presence, absence, and overexpression of uncoupling protein-3 on adiposity and fuel metabolism in congenic mice. *Am J Physiol - Endocrinol Metab* 2006;**290**:1304–12.

77. Childress ES, Alexopoulos SJ, Hoehn KL *et al.* Small Molecule Mitochondrial Uncouplers and Their Therapeutic Potential. *J Med Chem* 2018;**61**:4641–55.

78. Perry RJ, Zhang D, Zhang XM *et al.* Controlled-release mitochondrial protonophore reverses diabetes and protonophore reverses diabetes and steatohepatitis in rats. *Science (80-)* 2015;**347**:1253–6.

79. Gnaiger E. Capacity of oxidative phosphorylation in human skeletal muscle: new perspectives of mitochondrial physiology. *Int J Biochem Cell Biol* 2009;**41**:1837–45.

80. Weibel ER, Taylor CR, Hoppeler H. The concept of symmorphosis: a testable hypothesis of structure-function relationship. *Proc Natl Acad Sci* 1991;**88**:10357–61.

81. Huertas JR, Casuso RA, Agustín PH *et al.* Stay Fit, Stay Young: Mitochondria in Movement: The Role of Exercise in the New Mitochondrial Paradigm. *Oxid Med Cell Longev* 2019;**2019**:1–18.

82. Hood DA, Tryon LD, Carter HN *et al.* Unravelling the mechanisms regulating muscle mitochondrial biogenesis. *Biochem J* 2016;**473**:2295–314.

83. Yun JW. Possible anti-obesity therapeutics from nature – A review. *Phytochemistry* 2010;**71**:1625–41.

84. Marieb NE, Hoenhn K. *Human Anatomy and Physiology*. 9th ed. Beauparlant S (ed.). Glenview: Pearson Education, 2013.

85. Mann DL, Zipes DP, Libby P *et al. Braunwald's Heart Disease: A Textbook of Cardiovascular Medicine*. Elsevier Health Sciences, 2014.

86. Glagov S, Zarins C, Giddens DP *et al.* Hemodynamics and atherosclerosis. Insights and perspectives gained from studies of human arteries. *Arch Pathol Lab Med* 1988;**112**:1018–31.

87. Boulanger CM. Endothelium. *Arterioscler Thromb Vasc Biol* 2016;**36**:e26–31.

88. Bennett MR, Sinha S, Owens GK. Vascular Smooth Muscle Cells in Atherosclerosis. *Circ Res* 2016;**118**:692–702.

89. Ross R. The pathogenesis of atherosclerosis: a perspective for the 1990s. *Nature* 1993;**362**:801–9.

90. Stary H, Chandler A, Glagov S *et al.* AHA Medical / Scientific Statement Special Report A Definition of Initial , Fatty Streak , and Intermediate Lesions of Atherosclerosis. *Circulation* 1994;**89**:2462–78.

91. Fuster V, Moreno PR, Fayad ZA *et al.* Atherothrombosis and high-risk plaque: Part I: Evolving concepts. *J Am Coll Cardiol* 2005;**46**:937–54.

92. Malek AM. Hemodynamic Shear Stress and Its Role in Atherosclerosis. *Jama* 1999;**282**:2035.

93. Davies PF. Flow-Mediated Mechanotransduction. *Physiol Rev* 1995;**75**:519–60.

94. Fledderus JO, Boon RA, Volger OL *et al.* KLF2 primes the antioxidant transcription factor Nrf2 for activation in endothelial cells. *Arterioscler Thromb Vasc Biol* 2008;**28**:1339–46.

95. Khalil MF, Wagner WD, Goldberg IJ. Molecular interactions leading to lipoprotein retention and the initiation of atherosclerosis. *Arterioscler Thromb Vasc Biol* 2004;**24**:2211–8.

96. Williams KJ. Arterial wall chondroitin sulfate proteoglycans: diverse molecules with distinct roles in lipoprotein retention and atherogenesis. *Curr Opin Lipidol* 2001;**12**:477–87.

97. Moore KJ, Tabas I. Macrophages in the Pathogenesis of Atherosclerosis. *Cell* 2011;**145**:341–55.

98. Blankenberg S, Barbaux S, Tiret L. Adhesion molecules and atherosclerosis. *Atherosclerosis* 2003;**170**:191–203.

99. Frei B, Stocker R, Ames BN. Antioxidant defenses and lipid peroxidation in human blood plasma. *Proc Natl Acad Sci U S A* 1988;**85**:9748–52.

100. Stocker R, Keaney JF. Role of oxidative modifications in atherosclerosis. *Physiol Rev* 2004;**84**:1381–478.

101. Ross R. The pathogenesis of atherosclerosis: a perspective for the 1990s. *Nature* 1993;**362**:801–9.

102. Tabas I. Consequences and therapeutic implications of macrophage apoptosis in atherosclerosis: The importance of lesion stage and phagocytic efficiency. *Arterioscler Thromb Vasc Biol* 2005;**25**:2255–64.

103. Gordon S, Martinez FO. Alternative activation of macrophages: Mechanism and functions. *Immunity* 2010;**32**:593–604.

104. Yuan Y, Li P, Ye J. Lipid homeostasis and the formation of macrophage-derived foam cells in atherosclerosis. *Protein Cell* 2012;**3**:173–81.

105. Ouimet M, Marcel YL. Regulation of lipid droplet cholesterol efflux from macrophage foam cells. *Arterioscler Thromb Vasc Biol* 2012;**32**:575–81.

106. Tabas I. Macrophage death and defective inflammation resolution in atherosclerosis. *Nat Rev Immunol* 2010;**10**:36–46.

107. Peluso I, Morabito G, Urban L *et al.* Oxidative stress in atherosclerosis development: the central role of LDL and oxidative burst. *Endocr Metab Immune Disord Drug Targets* 2012;**12**:351–60.

108. Arai S, Shelton JM, Chen M *et al.* A role for the apoptosis inhibitory factor AIM/Spα/Api6 in atherosclerosis development. *Cell Metab* 2005;**1**:201–13.

109. Hasson CJ, Caldwell GE, Emmerik REA Van. Reduced Macrophage Apoptosis Is Associated With Accelerated Atherosclerosis in Low-Density Lipoprotein Receptor-Null Mice. *Motor Control* 2009;**27**:590–609.

110. Boesten LSM, Zadelaar ASM, van Nieuwkoop A *et al.* Macrophage p53 controls macrophage death in atherosclerotic lesions of apolipoprotein E deficient mice. *Atherosclerosis* 2009;**207**:399–404.

111. Babaev VR, Chew JD, Ding L *et al.* Macrophage EP4 Deficiency Increases Apoptosis and Suppresses Early Atherosclerosis. *Cell Metab* 2008;**8**:492–501.

112. Wang BY, Ho HK, Lin PS *et al.* Regression of atherosclerosis: role of nitric oxide and apoptosis. *Circulation* 1999;**99**:1236–41.

113. Henson PM, Bratton DL, Fadok VA. Apoptotic cell removal. *Curr Biol* 2001;**11**:795–805.

114. Virmani R, Virmani R, Kolodgie FD *et al.* Lessons From Sudden Coronary Death. *Arterioscler Thromb* 2000:1262–75.

115. VIRMANI R, BURKE AP, KOLODGIE FD *et al.* Vulnerable Plaque: The Pathology of Unstable Coronary Lesions. *J Interv Cardiol* 2002;**15**:439–46.

116. Virmani R, Burke AP, Farb A *et al.* Pathology of the Vulnerable Plaque. *J Am Coll Cardiol* 2006;**47**:C13–8.

117. Virmani R, Burke AP, Farb A. Sudden cardiac death. *Cardiovasc Pathol* 2001;**10**:211–8.

118. Viles-Gonzalez JF, Fuster V, Badimon JJ. Atherothrombosis: A widespread disease with unpredictable and life-threatening consequences. *Eur Heart J* 2004;**25**:1197–207.

119. Meijboom WB, Van Mieghem CAG, van Pelt N *et al.* Comprehensive Assessment of Coronary Artery Stenoses. Computed Tomography Coronary Angiography Versus Conventional Coronary Angiography and Correlation With Fractional Flow Reserve in Patients With Stable Angina. *J Am Coll Cardiol* 2008;**52**:636–43.

120. Ikonen E. Cellular cholesterol trafficking and compartmentalization. *Nat Rev Mol Cell Biol* 2008;**9**:125–38.

121. Hu J, Zhang Z, Shen WJ *et al.* Cellular cholesterol delivery, intracellular processing and utilization for biosynthesis of steroid hormones. *Nutr Metab* 2010;**7**:7–9.

122. Imaizumi K. Diet and Atherosclerosis in Apolipoprotein E- Deficient Mice. 2017;**8451**, DOI: 10.1271/bbb.110059.

123. Gotto AM. Cholesterol intake and serum cholesterol level. *N Engl J Med* 1991;**324**:912–3.

124. Yokogoshi H, Oda H. Dietary taurine enhances cholesterol degradation and reduces serum and liver cholesterol concentrations in rats fed a high-cholesterol diet. *Amino Acids* 2002;**23**:433–9.

125. Grundy SM. Absorption and metabolism of dietary cholesterol. *Annu Rev Nutr* 1983;**3**:71–96.

126. Lecerf JM, De Lorgeril M. Dietary cholesterol: From physiology to cardiovascular risk. *Br J Nutr* 2011;**106**:6–14.

127. Van Der Wulp MYM, Verkade HJ, Groen AK. Regulation of cholesterol homeostasis. *Mol Cell Endocrinol* 2013;**368**:1–16.

128. Monte MJ, Marin JJG, Antelo A *et al.* Bile acids: Chemistry, physiology, and pathophysiology. *World J Gastroenterol* 2009;**15**:804–16.

129. de Boer JF, Kuipers F, Groen AK. Cholesterol Transport Revisited: A New Turbo Mechanism to Drive Cholesterol Excretion. *Trends Endocrinol Metab* 2018;**29**:123–33.

130. DeBose-Boyd RA. Feedback regulation of cholesterol synthesis: sterol-accelerated ubiquitination and degradation of HMG CoA reductase. *Cell Res* 2008;**18**:609–21.

131. Burg JS, Espenshade PJ. Regulation of HMG-CoA reductase in mammals and yeast. *Prog Lipid Res* 2011;**50**:403–10.

132. Horton JD, Goldstein JL, Brown MS. SREBPs: activators of the complete program of cholesterol and fatty acid synthesis in the liver. *J Clin Invest* 2002;**109**:1125–31.

133. Hughes AL, Todd BL, Espenshade PJ. SREBP pathway responds to sterols and functions as an oxygen sensor in fission yeast. *Cell* 2005;**120**:831–42.

134. Shimano H, Sato R. SREBP-regulated lipid metabolism: convergent physiology — divergent pathophysiology. *Nat Rev Endocrinol* 2017;**13**:710–30.

135. Brown AJ, Sun L, Feramisco JD *et al.* Cholesterol Addition to ER Membranes Alters Conformation of SCAP, the SREBP Escort Protein that Regulates Cholesterol Metabolism. *Mol Cell* 2002;**10**:237–45.

136. Radhakrishnan A, Ikeda Y, Kwon HJ *et al.* Sterol-regulated transport of SREBPs from endoplasmic reticulum to Golgi: Oxysterols block transport by binding to Insig. *Proc Natl Acad Sci* 2007;**104**:6511–8.

137. Gong Y, Lee JN, Lee PCW *et al.* Sterol-regulated ubiquitination and degradation of Insig-1 creates a convergent mechanism for feedback control of cholesterol synthesis and uptake. *Cell Metab* 2006;**3**:15–24.

138. Shin D-J, Osborne TF. Thyroid Hormone Regulation and Cholesterol Metabolism Are Connected through Sterol Regulatory Element-binding Protein-2 (SREBP-2). *J Biol Chem* 2003;**278**:34114–8.

139. Sato R, Inoue J, Kawabe Y *et al.* Sterol-dependent Transcriptional Regulation of Sterol Regulatory Element-binding Protein-2. *J Biol Chem* 1996;**271**:26461–4.

140. Jo Y, DeBose-Boyd RA. Control of cholesterol synthesis through regulated ER-associated degradation of HMG CoA reductase. *Crit Rev Biochem Mol Biol* 2010;**45**:185–98.

141. Engelking LJ, Liang G, Hammer RE *et al.* Schoenheimer effect explained - feedback regulation of cholesterol synthesis in mice mediated by Insig proteins. *J Clin Invest* 2005;**115**:2489–98.

142. Mihaylova MM, Shaw RJ. The AMPK signalling pathway coordinates cell growth, autophagy and metabolism. *Nat Cell Biol* 2011;**13**:1016–23.

143. Afonso MS, Machado RM, Lavrador M *et al.* Molecular Pathways Underlying Cholesterol Homeostasis. *Nutrients* 2018;**10**:760.

144. Gazzerro P, Proto MC, Gangemi G *et al.* Pharmacological Actions of Statins: A Critical Appraisal in the Management of Cancer. Gottesman MM (ed.). *Pharmacol Rev* 2012;**64**:102–46.

145. Grundy SM. Does Dietary Cholesterol Matter? *Curr Atheroscler Rep* 2016;**18**:68.

146. Boyer JL. Bile formation and secretion. *Compr Physiol* 2013;**3**:1035–78.

147. Hernell O, Staggers JE, Carey MC. Physical-chemical behavior of dietary and biliary lipids during intestinal digestion and absorption. 2. Phase analysis and aggregation states of luminal lipids during duodenal fat digestion in healthy adult human beings. *Biochemistry* 1990;**29**:2041–56.

148. Cohen DE, Leonard MR. Immobilized artificial membrane chromatography: A rapid and accurate HPLC method for predicting bile salt-membrane interactions. *J Lipid Res* 1995;**36**:2251–60.

149. Cohen DE, Leighton LS, Carey MC. Bile salt hydrophobicity controls vesicle secretion rates and transformations in native bile. *Am J Physiol Liver Physiol* 1992;**263**:G386–95.

150. Xu Y, Li F, Zalzala M *et al.* Farnesoid X receptor activation increases reverse cholesterol transport by modulating bile acid composition and cholesterol absorption in mice. *Hepatology* 2016;**64**:1072–85.

151. Wang DQH, Tazuma S, Cohen DE *et al.* Feeding natural hydrophilic bile acids inhibits intestinal cholesterol absorption: Studies in the gallstone-susceptible mouse. *Am J Physiol - Gastrointest Liver Physiol* 2003;**285**:494–502.

152. Garcia-Calvo M, Lisnock J, Bull HG *et al.* The target of ezetimibe is Niemann-Pick C1-Like 1 (NPC1L1). *Proc Natl Acad Sci* 2005;**102**:8132–7.

153. Altmann SW. Niemann-Pick C1 Like 1 Protein Is Critical for Intestinal Cholesterol Absorption. *Science (80-)* 2004;**303**:1201–4.

154. Daniels TF, Killinger KM, Michal JJ *et al.* Lipoproteins, cholesterol homeostasis and cardiac health. *Int J Biol Sci* 2009;**5**:474–88.

155. Davidson NO, Shelness GS. Apolipoprotein B: mRNA Editing, Lipoprotein Assembly, and Presecretory Degradation. *Annu Rev Nutr* 2000;**20**:169–93.

156. Baggio G, Manzato E, Gabelli C *et al.* Apolipoprotein C-II deficiency syndrome. Clinical features, lipoprotein characterization, lipase activity, and correction of hypertriglyceridemia after apolipoprotein C-II administration in two affected patients. *J Clin Invest* 1986;**77**:520–7.

157. Actis Dato V, Chiabrando G. The Role of Low-Density Lipoprotein Receptor-Related Protein 1 in Lipid Metabolism, Glucose Homeostasis and Inflammation. *Int J Mol Sci* 2018;**19**:1780.

158. Stanford KI, Bishop JR, Foley EM *et al.* Syndecan-1 is the primary heparan sulfate proteoglycan mediating hepatic clearance of triglyceride-rich lipoproteins in mice. *J Clin Invest* 2009;**119**:3236–45.

159. Foley EM, Gordts PLSM, Stanford KI *et al.* Hepatic Remnant Lipoprotein Clearance by Heparan Sulfate Proteoglycans and Low-Density Lipoprotein Receptors Depend on Dietary Conditions in Mice. *Arterioscler Thromb Vasc Biol* 2013;**33**:2065–74.

160. Rasmussen KL. Plasma levels of apolipoprotein E, APOE genotype and risk of dementia and ischemic heart disease: A review. *Atherosclerosis* 2016;**255**:145–55.

161. Tiwari S, Siddiqi SA. Intracellular Trafficking and Secretion of VLDL. *Arterioscler Thromb Vasc Biol* 2012;**32**:1079–86.

162. Sundaram M, Yao Z. Recent progress in understanding protein and lipid factors affecting

hepatic VLDL assembly and secretion. *Nutr Metab (Lond)* 2010;**7**:35.

163. Olofsson SO, Stillemark-Billton P, Asp L. Intracellular assembly of VLDL: Two major steps in separate cell compartments. *Trends Cardiovasc Med* 2000;**10**:338–45.

164. Barter PJ, Brewer HB, Chapman MJ *et al.* Cholesteryl ester transfer protein: a novel target for raising HDL and inhibiting atherosclerosis. *Arterioscler Thromb Vasc Biol* 2003;**23**:160–7.

165. Ladu MJ, Reardon C, Van Eldik L *et al.* Lipoproteins in the central nervous system. *Ann N Y Acad Sci* 2000;**903**:167–75.

166. Spady D. Hepatic Clearance of Plasma Low Density Lipoproteins. *Semin Liver Dis* 1992;**12**:373–85.

167. Ouimet M, Barrett TJ, Fisher EA. HDL and reverse cholesterol transport: Basic mechanisms and their roles in vascular health and disease. *Circ Res* 2019;**124**:1505–18.

168. Shen W-J, Azhar S, Kraemer FB. SR-B1: A Unique Multifunctional Receptor for Cholesterol Influx and Efflux. *Annu Rev Physiol* 2018;**80**:95–116.

169. Lewis GF, Rader DJ. New insights into the regulation of HDL metabolism and reverse cholesterol transport. *Circ Res* 2005;**96**:1221–32.

170. Phillips MC. Molecular Mechanisms of Cellular Cholesterol Efflux. *J Biol Chem* 2014;**289**:24020–9.

171. Oram JF. Tangier disease and ABCA1. *Biochim Biophys Acta - Mol Cell Biol Lipids* 2000;**1529**:321–30.

172. Timmins JM, Timmins JM, Lee J *et al.* Targeted inactivation of hepatic Abca1 causes profound hypoalphalipoproteinemia and kidney hypercatabolism of apoA-I. *J Clin Invest* 2005;**115**:1333–42.

173. Boadu E, Bilbey NJ, Francis GA. Cellular cholesterol substrate pools for adenosine-triphosphate cassette transporter A1-dependent high-density lipoprotein formation. *Curr Opin Lipidol* 2008;**19**:270–6.

174. Tarling E. Expanding roles of ABCG1 and sterol transport. *Curr Opin Lipidol* 2013;**24**:138–46.

175. Gelissen IC, Harris M, Rye K-A *et al.* ABCA1 and ABCG1 Synergize to Mediate Cholesterol Export to ApoA-I. *Arterioscler Thromb Vasc Biol* 2006;**26**:534–40.

176. Vaughan AM, Oram JF. ABCA1 and ABCG1 or ABCG4 act sequentially to remove cellular

cholesterol and generate cholesterol-rich HDL. *J Lipid Res* 2006;**47**:2433–43.

177. Voloshyna I, Reiss AB. The ABC transporters in lipid flux and atherosclerosis. *Prog Lipid Res* 2011;**50**:213–24.

178. Moore KJ, Rayner KJ, Suárez Y *et al.* The Role of MicroRNAs in Cholesterol Efflux and Hepatic Lipid Metabolism. *Annu Rev Nutr* 2011;**31**:49–63.

179. Zhang W, Yancey PG, Su YR *et al.* Inactivation of Macrophage Scavenger Receptor Class B Type I Promotes Atherosclerotic Lesion Development in Apolipoprotein E–Deficient Mice. *Circulation* 2003;**108**:2258–63.

180. Kozarsky KF, Donahee MH, Glick JM *et al.* Gene Transfer and Hepatic Overexpression of the HDL Receptor SR-BI Reduces Atherosclerosis in the Cholesterol-Fed LDL Receptor–Deficient Mouse. *Arterioscler Thromb Vasc Biol* 2000;**20**:721–7.

181. Acton S, Rigotti A, Landschulz KT *et al.* Identification of scavenger receptor SR-BI as a high density lipoprotein receptor. *Science* 1996;**271**:518–20.

182. Neculai D, Schwake M, Ravichandran M *et al.* Structure of LIMP-2 provides functional insights with implications for SR-BI and CD36. *Nature* 2013;**504**:172–6.

183. Thuahnai ST, Lund-Katz S, Williams DL *et al.* Scavenger Receptor Class B, Type I-mediated Uptake of Various Lipids into Cells. *J Biol Chem* 2001;**276**:43801–8.

184. Lopez D, McLean MP. Sterol Regulatory Element-Binding Protein-1a Binds to cis Elements in the Promoter of the Rat High Density Lipoprotein Receptor SR-BI Gene1. *Endocrinology* 1999;**140**:5669–81.

185. Lopez D, McLean MP. Activation of the rat scavenger receptor class B type I gene by PPARα. *Mol Cell Endocrinol* 2006;**251**:67–77.

186. Schoonjans K, Annicotte J, Huby T *et al.* Liver receptor homolog 1 controls the expression of the scavenger receptor class B type I. *EMBO Rep* 2002;**3**:1181–7.

187. Lopez D, Sanchez MD, Shea-Eaton W *et al.* Estrogen activates the high-density lipoprotein receptor gene via binding to estrogen response elements and interaction with sterol regulatory element binding protein-1A. *Endocrinology* 2002;**143**:2155–68.

188. ZHOU L, LI C, GAO L *et al.* High-density lipoprotein synthesis and metabolism (Review). *Mol Med Rep* 2015;**12**:4015–21.

189. Van Der Velde AE, Brufau G, Groen AK. Transintestinal cholesterol efflux. *Curr Opin Lipidol*

2010;**21**:167–71.

190. van der Veen JN, van Dijk TH, Vrins CLJ *et al.* Activation of the liver X receptor stimulates trans-intestinal excretion of plasma cholesterol. *J Biol Chem* 2009;**284**:19211–9.

191. Temel RE, Sawyer JK, Yu L *et al.* Biliary sterol secretion is not required for macrophage reverse cholesterol transport. *Cell Metab* 2010;**12**:96–102.

192. Temel RE, Brown JM. Biliary and nonbiliary contributions to reverse cholesterol transport. *Curr Opin Lipidol* 2012;**23**:85–90.

193. Dietschy JM. Central nervous system: cholesterol turnover, brain development and neurodegeneration. *Biol Chem* 2009;**390**:287–93.

194. Ioannou GN. The Role of Cholesterol in the Pathogenesis of NASH. *Trends Endocrinol Metab* 2016;**27**:84–95.

195. Oude Elferink RPJ, Groen AK. Mechanisms of biliary lipid secretion and their role in lipid homeostasis. *Semin Liver Dis* 2000;**20**:293–305.

196. Shamburek RD, Schwartz CC. Selective composition of biliary phosphatidylcholines is affected by secretion rate but not by bile acid hydrophobicity. *J Lipid Res* 1993;**34**:1833–42.

197. Wang R, Chen H-L, Liu L *et al.* Compensatory role of P-glycoproteins in knockout mice lacking the bile salt export pump. *Hepatology* 2009;**50**:948–56.

198. Vrins C, Vink E, Vandenberghe KE *et al.* The sterol transporting heterodimer ABCG5/ABCG8 requires bile salts to mediate cholesterol efflux. *FEBS Lett* 2007;**581**:4616–20.

199. Yu L, Hammer RE, Li-Hawkins J *et al.* Disruption of Abcg5 and Abcg8 in mice reveals their crucial role in biliary cholesterol secretion. *Proc Natl Acad Sci* 2002;**99**:16237–42.

200. Elferink RPJO, Paulusma CC, Groen AK. Hepatocanalicular Transport Defects: Pathophysiologic Mechanisms of Rare Diseases. *Gastroenterology* 2006;**130**:908–25.

201. Oude Elferink RP, Ottenhoff R, van Wijland M *et al.* Regulation of biliary lipid secretion by mdr2 P-glycoprotein in the mouse. *J Clin Invest* 1995;**95**:31–8.

202. Smit JJM, Groen K, Mel CAAM *et al.* Homozygous disruption of the murine MDR2 P-glycoprotein gene leads to a complete absence of phospholipid from bile and to liver disease. *Cell* 1993;**75**:451–62.

203. Fickert P, Wagner M. Biliary bile acids in hepatobiliary injury – What is the link? *J Hepatol* 2017;**67**:619–31.

204. Calkin AC, Tontonoz P. Transcriptional integration of metabolism by the nuclear sterol-activated receptors LXR and FXR. *Nat Rev Mol Cell Biol* 2012;**13**:213–24.

205. Yamanashi Y, Takada T, Yoshikado T *et al.* NPC2 regulates biliary cholesterol secretion via stimulation of ABCG5/G8-mediated cholesterol transport. *Gastroenterology* 2011;**140**:1664–74.

206. Yamanashi Y, Takada T, Shoda JI *et al.* Novel function of Niemann-Pick C1-like 1 as a negative regulator of Niemann-Pick C2 protein. *Hepatology* 2012;**55**:953–64.

207. Bosner MS, Lange LG, Stenson WF *et al.* Percent cholesterol absorption in normal women and men quantified with dual stable isotopic tracers and negative ion mass spectrometry. *J Lipid Res* 1999;**40**:302–8.

208. Dawson PA. Role of the Intestinal Bile Acid Transporters in Bile Acid and Drug Disposition. *Handbook of Experimental Pharmacology*. Vol 201. 2011, 169–203.

209. Chiang JYL. Bile acid metabolism and signaling. *Compr Physiol* 2013;**3**:1191–212.

210. Russell DW. The Enzymes, Regulation, and Genetics of Bile Acid Synthesis. *Annu Rev Biochem* 2003;**72**:137–74.

211. Javitt NB. 25R,26-Hydroxycholesterol revisited: synthesis, metabolism, and biologic roles. *J Lipid Res* 2002;**43**:665–70.

212. Ren S, Hylemon PB, Marques D *et al.* Overexpression of cholesterol transporter StAR increasesin vivo rates of bile acid synthesis in the rat and mouse. *Hepatology* 2004;**40**:910–7.

213. Pandak WM, Ren S, Marques D *et al.* Transport of Cholesterol into Mitochondria Is Rate-limiting for Bile Acid Synthesis via the Alternative Pathway in Primary Rat Hepatocytes. *J Biol Chem* 2002;**277**:48158–64.

214. Takahashi S, Fukami T, Masuo Y *et al.* Cyp2c70 is responsible for the species difference in bile acid metabolism between mice and humans. *J Lipid Res* 2016;**57**:2130–7.

215. Peet DJ, Turley SD, Ma W *et al.* Cholesterol and Bile Acid Metabolism Are Impaired in Mice Lacking the Nuclear Oxysterol Receptor LXRα. *Cell* 1998;**93**:693–704.

216. Agellon LB, Drover VAB, Cheema SK *et al.* Dietary Cholesterol Fails to Stimulate the Human Cholesterol 7α-Hydroxylase Gene (CYP7A1) in Transgenic Mice. *J Biol Chem* 2002;**277**:20131–4.

217. Chen JY, Levy-Wilson B, Goodart S *et al.* Mice Expressing the Human CYP7A1 Gene in the

Mouse CYP7A1 Knock-out Background Lack Induction of CYP7A1 Expression by Cholesterol Feeding and Have Increased Hypercholesterolemia When Fed a High Fat Diet. *J Biol Chem* 2002;**277**:42588–95.

218. Pandak WM, Vlahcevic ZR, Chiang JYL *et al.* Bile acid synthesis. VI. Regulation of cholesterol 7 alpha-hydroxylase by taurocholate and mevalonate. *J Lipid Res* 1992;**33**:659–68.

219. Post SM, Duez H, Gervois PP *et al.* Fibrates Suppress Bile Acid Synthesis via Peroxisome Proliferator–Activated Receptor-α–Mediated Downregulation of Cholesterol 7α-Hydroxylase and Sterol 27-Hydroxylase Expression. *Arterioscler Thromb Vasc Biol* 2001;**21**:1840–5.

220. Chiang JYL, Li T. Regulation of bile acid and cholesterol metabolism by PPARs. *PPAR Res* 2009;**2009**, DOI: 10.1155/2009/501739.

221. PATEL DD, KNIGHT BL, SOUTAR AK *et al.* The effect of peroxisome-proliferator-activated receptor-α on the activity of the cholesterol 7α-hydroxylase gene. *Biochem J* 2000;**351**:747.

222. Lammel Lindemann JA, Angajala A, Engler DA *et al.* Thyroid hormone induction of human cholesterol 7 alpha-hydroxylase (Cyp7a1) in vitro. *Mol Cell Endocrinol* 2014;**388**:32–40.

223. Sauter G, Weiss M, Hoermann R. Cholesterol 7α-Hydroxylase Activity in Hypothyroidism and Hyperthyroidism in Humans. *Horm Metab Res* 1997;**29**:176–9.

224. Ness GC, Lopez D. Transcriptional regulation of rat hepatic low-density lipoprotein receptor and cholesterol 7α Hydroxylase by thyroid hormone. *Arch Biochem Biophys* 1995;**323**:404–8.

225. Grefhorst A, Verkade HJ, Groen AK. The TICE Pathway: Mechanisms and Lipid-Lowering Therapies. *Methodist Debakey Cardiovasc J* 2019;**15**:70–6.

226. van der Velde AE, Vrins CLJ, van den Oever K *et al.* Direct Intestinal Cholesterol Secretion Contributes Significantly to Total Fecal Neutral Sterol Excretion in Mice. *Gastroenterology* 2007;**133**:967–75.

227. BANDSMA RHJ, STELLAARD F, VONK JR *et al.* Contribution of newly synthesized cholesterol to rat plasma and bile determined by mass isotopomer distribution analysis: bile-salt flux promotes secretion of newly synthesized cholesterol into bile. *Biochem J* 1998;**329**:699–703.

228. Kruit JK, Plösch T, Havinga R *et al.* Increased fecal neutral sterol loss upon liver X receptor activation is independent of biliary sterol secretion in mice. *Gastroenterology* 2005;**128**:147–56.

229. Temel RE, Tang W, Ma Y *et al.* Hepatic Niemann-Pick C1–like 1 regulates biliary cholesterol concentration and is a target of ezetimibe. *J Clin Invest* 2007;**117**:1968–78.

230. Vrins CLJ, Ottenhoff R, Van Den Oever K *et al.* Trans-intestinal cholesterol efflux is not mediated through high density lipoprotein. *J Lipid Res* 2012;**53**:2017–23.

231. Le May C, Berger JM, Lespine A *et al.* Transintestinal Cholesterol Excretion Is an Active Metabolic Process Modulated by PCSK9 and Statin Involving ABCB1. *Arterioscler Thromb Vasc Biol* 2013;**33**:1484–93.

232. de Boer JF, Schonewille M, Boesjes M *et al.* Intestinal Farnesoid X Receptor Controls Transintestinal Cholesterol Excretion in Mice. *Gastroenterology* 2017;**152**:1126-1138.e6.

233. Jakulj L, Vissers MN, van Roomen CP *et al.* Ezetimibe stimulates faecal neutral sterol excretion depending on abcg8 function in mice. *FEBS Lett* 2010;**584**:3625–8.

234. Wang X, Chowdhury JR, Chowdhury NR. Bilirubin metabolism: Applied physiology. *Curr Paediatr* 2006;**16**:70–4.

235. Shemin D, Rittenberg D. The life span of the human red blood cell. *J Biol Chem* 1946;**166**:627–36.

236. Maines DM. Overview of heme degradation pathway. *Curr Protoc Toxicol* 2001, DOI: 10.1002/0471140856.tx0901s00.

237. Kamisako T, Kobayashi Y, Takeuchi K *et al.* Recent advances in bilirubin metabolism research: The molecular mechanism of hepatocyte bilirubin transport and its clinical relevance. *J Gastroenterol* 2000;**35**:659–64.

238. Fevery J. Bilirubin in clinical practice: A review. *Liver Int* 2008;**28**:592–605.

239. Van Es H, Bout A, Liu J *et al.* Assignment of the human UDP glucuronosyltransferase gene (UGT1A1) to chromosome region 2q37. *Cytogenet Cell Genet* 1993;**63**:114–6.

240. Tiribelli C, Ostrow JD. Intestinal flora and bilirubin. *J Hepatol* 2005;**42**:170–2.

241. Lin JP, O'Donnell CJ, Schwaiger JP *et al.* Association between the UGT1A1*28 allele, bilirubin levels, and coronary heart disease in the Framingham Heart Study. *Circulation* 2006;**114**:1476–81.

242. Temme EH, Zhang J, Schouten EG *et al.* Serum bilirubin and 10-year mortality risk in a Belgian population. *Canc Causes Contr* 2001;**12**:887–94.

243. Bulmer AC, Bakrania B, Du Toit EF *et al.* Bilirubin acts as a multipotent guardian of

cardiovascular integrity: More than just a radical idea. *Am J Physiol - Hear Circ Physiol* 2018;**315**:H429–47.

244. Bakrania B, Du Toit EF, Wagner KH *et al.* Pre- or post-ischemic bilirubin ditaurate treatment reduces oxidative tissue damage and improves cardiac function. *Int J Cardiol* 2016;**202**:27–33.

245. Shiels RG, Vidimce J, Pearson AG *et al.* Unprecedented Microbial Conversion of Biliverdin into Bilirubin-10-sulfonate. *Sci Rep* 2019;**9**:1–10.

246. Wallner M, Marculescu R, Doberer D *et al.* Protection from age-related increase in lipid biomarkers and inflammation contributes to cardiovascular protection in Gilbert's syndrome. *Clin Sci* 2013;**125**:257–64.

247. Rodrigues C, Costa E, Vieira E *et al.* Bilirubin dependence on UGT1A1 polymorphisms, hemoglobin, fasting time and body mass index. *Am J Med Sci* 2012;**343**:114–8.

248. Vítek L. The Role of Bilirubin in Diabetes, Metabolic Syndrome, and Cardiovascular Diseases. *Front Pharmacol* 2012;**3**:1–7.

249. Choi SH, Yun KE, Choi HJ. Relationships between serum total bilirubin levels and metabolic syndrome in Korean adults. *Nutr Metab Cardiovasc Dis* 2013;**23**:31–7.

250. Lin L-Y, Kuo H-K, Hwang J-J *et al.* Serum bilirubin is inversely associated with insulin resistance and metabolic syndrome among children and adolescents. *Atherosclerosis* 2009;**203**:563–8.

251. Stojanov M, Stefanovic A, Dzingalasevic G *et al.* Total bilirubin in young men and women: Association with risk markers for cardiovascular diseases. *Clin Biochem* 2013;**46**:1516–9.

252. Chang J-L, Bigler J, Schwarz Y *et al.* UGT1A1 Polymorphism Is Associated with Serum Bilirubin Concentrations in a Randomized, Controlled, Fruit and Vegetable Feeding Trial. *J Nutr* 2007;**137**:890–7.

253. Mustafa MG, Cowger ML, King TE. Effects of bilirubin on mitochondrial reactions. *J Biol Chem* 1969;**244**:6403–14.

254. Rodrigues CMP, Solá S, Silva RFM *et al.* Aging confers different sensitivity to the neurotoxic properties of unconjugated bilirubin. *Pediatr Res* 2002;**51**:112–8.

255. Ostrow JD, Pascolo L, Brites D *et al.* Molecular basis of bilirubin-induced neurotoxicity. *Trends Mol Med* 2004;**10**:65–70.

256. Rodrigues CMP, Solá S, Brites D. Bilirubin induces apoptosis via the mitochondrial pathway in developing rat brain neurons. *Hepatology* 2002;**35**:1186–95.

257. Keshavan P, Schwemberger SJ, Smith DLH *et al.* Unconjugated bilirubin induces apoptosis in colon cancer cells by triggering mitochondrial depolarization. *Int J cancer* 2004;**112**:433–45.

258. Zucker SD, Storch J, Zeidel ML *et al.* Mechanism of the spontaneous transfer of unconjugated bilirubin between small unilamellar phosphatidylcholine vesicles. *Biochemistry* 1992;**31**:3184–92.

259. Brito MA, Brondino CD, Moura JJG *et al.* Effects of Bilirubin Molecular Species on Membrane Dynamic Properties of Human Erythrocyte Membranes: A Spin Label Electron Paramagnetic Resonance Spectroscopy Study. *Arch Biochem Biophys* 2001;**387**:57–65.

260. Rodrigues CMP, Solá S, Brito MA *et al.* Bilirubin directly disrupts membrane lipid polarity and fluidity, protein order, and redox status in rat mitochondria. *J Hepatol* 2002;**36**:335–41.

261. Vaz AR, Delgado-Esteban M, Brito MA *et al.* Bilirubin selectively inhibits cytochrome c oxidase activity and induces apoptosis in immature cortical neurons: assessment of the protective effects of glycoursodeoxycholic acid. *J Neurochem* 2010;**112**:56–65.

262. Malik SG, Irwanto KA, Ostrow JD *et al.* Effect of bilirubin on cytochrome c oxidase activity of mitochondria from mouse brain and liver. *BMC Res Notes* 2010;**3**:162.

263. Celier C, Francois D, Marsac C *et al.* Impairment of mitochondrial 5-aminolevulinic acid synthase activity in Gunn rat liver. *Biochem Pharmacol* 1992;**44**:1465–7.

264. Fritz-Niggli H. Inhibited Oxidative Phosphorylation in Rat Liver Mitochondria of Congenitally Jaundiced Gunn Rats and the Protective Action of Hydroxyethylrutosides Against Bilirubin-induced Uncoupling. *Med exp* 1968;**18**:239–46.

265. Zelenka J, Dvořák A, Alán L *et al.* Hyperbilirubinemia Protects against Aging-Associated Inflammation and Metabolic Deterioration. *Oxid Med Cell Longev* 2016;**2016**:1–10.

266. Schwertner H a, Jackson WG, Tolan G. Association of low serum concentration of bilirubin with increased risk of coronary artery disease. *Clin Chem* 1994;**40**:18–23.

267. Hopkins PN, Wu LL, Hunt SC *et al.* Higher Serum Bilirubin Is Associated With Decreased Risk for Early Familial Coronary Artery Disease. *Arterioscler Thromb Vasc Biol* 1996;**16**:250 LP – 255.

268. Hunt SC, Kronenberg F, Eckfeldt JH *et al.* Association of plasma bilirubin with coronary heart disease and segregation of bilirubin as a major gene trait: The NHLBI family heart study.

Atherosclerosis 2001;**154**:747–54.

269. Endler G, Hamwi A, Sunder Plassmann R *et al.* Is low serum bilirubin an independent risk factor for coronary artery disease in men but not in women? *Clin Chem* 2003;**49**:1201–4.

270. Nolting PRWDS, Kusters DM, Hutten B a *et al.* Serum bilirubin levels in familial hypercholesterolemia: a new risk marker for cardiovascular disease? *J Lipid Res* 2011;**52**:1755–9.

271. Amor AJ, Ortega E, Perea V *et al.* Relationship between total serum bilirubin levels and carotid and femoral atherosclerosis in familial dyslipidemia. *Arterioscler Thromb Vasc Biol* 2017;**37**:2356–63.

272. Xu J, Zou MH. Molecular insights and therapeutic targets for diabetic endothelial dysfunction. *Circulation* 2009;**120**:1266–86.

273. Ishizaka N, Ishizaka Y, Takahashi E *et al.* High Serum Bilirubin Level Is Inversely Associated With the Presence of Carotid Plaque. *Stroke* 2001;**32**:580 LP – 583.

274. Erdogan D, Gullu H, Yildirim E *et al.* Low serum bilirubin levels are independently and inversely related to impaired flow-mediated vasodilation and increased carotid intima-media thickness in both men and women. *Atherosclerosis* 2006;**184**:431–7.

275. Zhong K, Wang X, Ma X *et al.* Association between serum bilirubin and asymptomatic intracranial atherosclerosis: results from a population-based study. *Neurol Sci* 2020, DOI: 10.1007/s10072-020-04268-x.

276. Dekker D, Dorresteijn MJ, Pijnenburg M *et al.* The bilirubin-increasing drug atazanavir improves endothelial function in patients with type 2 diabetes mellitus. *Arterioscler Thromb Vasc Biol* 2011;**31**:458–63.

277. Breimer LH, Wannamethee G, Ebrahim S *et al.* Serum bilirubin and risk of ischemic heart disease in middle-aged British men. *Clin Chem* 1995;**41**:1504–8.

278. Troughton JA, Woodside J V, Young IS *et al.* Bilirubin and coronary heart disease risk in the Prospective Epidemiological Study of Myocardial Infarction (PRIME). *Eur Soc Cardiol* 2007.

279. Djousse L, Levy D, Cupples L a *et al.* Total serum bilirubin and risk of cardiovascular disease in the Framingham offspring study. *Am J Cardiol* 2001;**87**:1196–200; A4, 7.

280. Concepts C, Targher G, Day CP *et al.* Risk of Cardiovascular Disease in Patients with Nonalcoholic Fatty Liver Disease. 2010:1341–50.

281. Novotný L, Vítek L. Inverse relationship between serum bilirubin and atherosclerosis in men: a meta-analysis of published studies. *Exp Biol Med* 2003;**228**:568–71.

282. Jangi S, Otterbein L, Robson S. The molecular basis for the immunomodulatory activities of unconjugated bilirubin. *Int J Biochem Cell Biol* 2013;**45**:2843–51.

283. Mazzone GL, Rigato I, Ostrow JD *et al.* Bilirubin inhibits the TNFalpha-related induction of three endothelial adhesion molecules. *Biochem Biophys Res Commun* 2009;**386**:338–44.

284. Li Y, Zhao S. Effects of serum bilirubin on lipoproteins. *Hunan Yi Ke Da Xue Xue Bao* 1998;**23**:578–80.

285. Peyton KJ, Shebib AR, Azam M a *et al.* Bilirubin inhibits neointima formation and vascular smooth muscle cell proliferation and migration. *Front Pharmacol* 2012;**3**:48.

286. Nakagami T, Toyomura K, Kinoshita T *et al.* A beneficial role of bile pigments as an endogenous tissue protector: Anti-complement effects of biliverdin and conjugated bilirubin. *BBA - Gen Subj* 1993;**1158**:189–93.

287. Mazzone GL, Rigato I, Ostrow JD *et al.* Bilirubin effect on endothelial adhesion molecules expression is mediated by the NF-kappaB signaling pathway. *Biosci Trends* 2009;**3**:151–7.

288. Mancuso C, Pani G, Calabrese V. Bilirubin: an endogenous scavenger of nitric oxide and reactive nitrogen species. *Redox Rep* 2006;**11**:207–13.

289. Arriaga SM, Mottino AD, Almará AM. Inhibitory effect of bilirubin on complement-mediated hemolysis. *Biochim Biophys Acta - Gen Subj* 1999;**1473**:329–36.

290. Stocker R. Antioxidant activities of bile pigments. *Antioxid Redox Signal* 2004;**6**:841–9.

291. Hammerman C, Goldschmidt D, Caplan MS *et al.* Protective effect of bilirubin in ischemia-reperfusion injury in the rat intestine. *J Pediatr Gastroenterol Nutr* 2002;**35**:344–9.

292. Adin CAC, Croker BPB, Agarwal A. Protective effects of exogenous bilirubin on ischemia-reperfusion injury in the isolated, perfused rat kidney. *Am J Physiol Renal Physiol* 2005;**0126**:778–84.

293. Bakrania B, Du Toit E, Headrick J *et al.* Bilirubin loading of the heart: a novel treatment for ischemia-reperfusion injury (667.5). *FASEB J* 2014;**28**.

294. Boon A-C, Lam AK, Gopalan V *et al.* Endogenously elevated bilirubin modulates kidney function and protects from circulating oxidative stress in a rat model of adenine-induced kidney failure. *Sci Rep* 2015;**5**:15482.

295. Kadl A, Pontiller J, Exner M *et al.* Single Bolus Injection of Bilirubin Improves the Clinical Outcome in a Mouse Model of Endotoxemia. *Shock* 2007;**28**:582–8.

296. Liu J, Wang L, Tian XY *et al.* Unconjugated bilirubin mediates heme oxygenase-1-induced vascular benefits in diabetic mice. *Diabetes* 2015;**64**:1564–75.

297. Dong H, Huang H, Yun X *et al.* Bilirubin increases insulin sensitivity in leptin-receptor deficient and diet-induced obese mice through suppression of ER stress and chronic inflammation. *Endocrinology* 2014;**155**:818–28.

298. Kirkby K, Baylis C, Agarwal A *et al.* Intravenous bilirubin provides incomplete protection against renal ischemia-reperfusion injury in vivo. *Am J Physiol Renal Physiol* 2007;**292**:F888–94.

299. Stec DE, Storm M V., Pruett BE *et al.* Antihypertensive actions of moderate hyperbilirubinemia: Role of superoxide inhibition. *Am J Hypertens* 2013;**26**:918–23.

300. Andria B, Bracco A, Attanasio C *et al.* Biliverdin Protects against Liver Ischemia Reperfusion Injury in Swine. *PLoS One* 2013;**8**:1–8.

301. Ikeda N, Inoguchi T, Sonoda N *et al.* Biliverdin protects against the deterioration of glucose tolerance in db/db mice. *Diabetologia* 2011;**54**:2183–91.

302. Stocker R, Perrella MA. Heme oxygenase-1: A novel drug target for atherosclerotic diseases? *Circulation* 2006;**114**:2178–89.

303. Araujo JA, Zhang M, Yin F. Heme oxygenase-1, oxidation, inflammation, and atherosclerosis. *Front Pharmacol* 2012;**3 JUL**:1–17.

304. Paine A, Eiz-Vesper B, Blasczyk R *et al.* Signaling to heme oxygenase-1 and its anti-inflammatory therapeutic potential. *Biochem Pharmacol* 2010;**80**:1895–903.

305. Vítek L, Schwertner H a. The Heme Catabolic Pathway and its Protective Effects on Oxidative Stress-Mediated Diseases. *Adv Clin Chem* 2007;**43**:1–57.

306. Lundvig DMS, Immenschuh S, Wagener FADTG. Heme oxygenase, inflammation, and fibrosis: The good, the bad, and the ugly? *Front Pharmacol* 2012;**3 MAY**:1–14.

307. Ishikawa K, Sugawara D, Wang Xp *et al.* Heme oxygenase-1 inhibits atherosclerotic lesion formation in ldl-receptor knockout mice. *Circ Res* 2001;**88**:506–12.

308. Cheng C, Noordeloos AM, Jeney V *et al.* Heme oxygenase 1 determines atherosclerotic lesion progression into a vulnerable plaque. *Circulation* 2009;**119**:3017–27.

309. Ayer A, Zarjou A, Agarwa A *et al.* Heme oxygenases in cardiovascular health and disease.

Physiol Rev 2016;**96**:1449–508.

310. Burton GW, Ingold KU. Vitamin E: application of the principles of physical organic chemistry to the exploration of its structure and function. *Acc Chem Res* 1986;**19**:194–201.

311. Kato Y, Shimazu M, Kondo M *et al.* Bilirubin rinse: A simple protectant against the rat liver graft injury mimicking heme oxygenase-1 preconditioning. *Hepatology* 2003;**38**:364–73.

312. Fondevila C, Shen X-D, Tsuchiyashi S *et al.* Biliverdin therapy protects rat livers from ischemia and reperfusion injury. *Hepatology* 2004;**40**:1333–41.

313. Clark JE, Foresti R, Sarathchandra P *et al.* Heme oxygenase-1-derived bilirubin ameliorates postischemic myocardial dysfunction. *Am J Physiol Hear Circ Physiol* 2000;**278**:H643-51.

314. Bakrania B, Du Toit EF, Ashton KJ *et al.* Hyperbilirubinemia modulates myocardial function, aortic ejection, and ischemic stress resistance in the Gunn rat. *Am J Physiol Heart Circ Physiol* 2014;**307**:H1142-9.

315. Sarady-Andrews JK, Liu F, Gallo D *et al.* Biliverdin administration protects against endotoxin-induced acute lung injury in rats. *Am J Physiol Lung Cell Mol Physiol* 2005;**289**:L1131-7.

316. Bisht K, Wegiel B, Tampe J *et al.* Biliverdin modulates the expression of C5aR in response to endotoxin in part via mTOR signaling. *Biochem Biophys Res Commun* 2014;**449**:94–9.

317. Bisht K, Tampe J, Shing C *et al.* Endogenous Tetrapyrroles Influence Leukocyte Responses to Lipopolysaccharide in Human Blood: Pre-Clinical Evidence Demonstrating the Anti-Inflammatory Potential of Biliverdin. *J Clin Cell Immunol* 2014;**5**:1000218.

318. Wegiel B, Baty CJ, Gallo D *et al.* Cell surface biliverdin reductase mediates biliverdin-induced anti-inflammatory effects via phosphatidylinositol 3-kinase and Akt. *J Biol Chem* 2009;**284**:21369–78.

319. Fujii M, Inoguchi T, Sasaki S *et al.* Bilirubin and biliverdin protect rodents against diabetic nephropathy by downregulating NAD(P)H oxidase. *Kidney Int* 2010;**78**:905–19.

320. Vogel ME, Idelman G, Konaniah ES *et al.* Bilirubin prevents atherosclerotic lesion formation in low-density lipoprotein receptor-deficient mice by inhibiting endothelial VCAM-1 and ICAM-1 signaling. *J Am Heart Assoc* 2017;**6**:1–19.

321. Kosaka J, Morimatsu H, Takahashi T *et al.* Effects of Biliverdin Administration on Acute Lung Injury Induced by Hemorrhagic Shock and Resuscitation in Rats. *PLoS One* 2013;**8**:1–9.

322. Pell VR, Chouchani ET, Murphy MP *et al.* Moving forwards by blocking back-flow the yin and yang of MI therapy. *Circ Res* 2016;**118**:898–906.

323. Hayashi S, Takamiya R, Yamaguchi T *et al.* Induction of Heme Oxygenase-1 Suppresses Venular Leukocyte Adhesion Elicited by Oxidative Stress. *Circ Res* 1999;**85**.

324. Ishikawa K, Navab M, Leitinger N *et al.* Induction of heme oxygenase-1 inhibits the monocyte transmigration induced by mildly oxidized LDL. *J Clin Invest* 1997;**100**:1209–16.

325. Ollinger R, Yamashita K, Bilban M *et al.* Bilirubin and biliverdin treatment of atherosclerotic diseases. *Cell Cycle* 2007;**6**:39–43.

326. Konior A, Schramm A, Czesnikiewicz-Guzik M *et al.* NADPH oxidases in vascular pathology. *Antioxid Redox Signal* 2014;**20**:2794–814.

327. Li H, Förstermann U. Uncoupling of endothelial NO synthase in atherosclerosis and vascular disease. *Curr Opin Pharmacol* 2013;**13**:161–7.

328. Kwak JY, Takeshige K, Cheung BS *et al.* Bilirubin inhibits the activation of superoxide-producing NADPH oxidase in a neutrophil cell-free system. *Biochim Biophys Acta (BBA)/Protein Struct Mol* 1991;**1076**:369–73.

329. Nakamura H, Uetani Y, Komura M *et al.* Inhibitory action of bilirubin on superoxide production by polymorphonuclear leukocytes. *Biol Neonate* 1987:273–8.

330. Iwanaga M, Nakagawara A, Matsuo S *et al.* Impaired polymorphonuclear leukocyte function in biliary atresia:Role of bilirubin and bile acids. *J Pediatr Surg* 1987;**22**:967–72.

331. Vasavda C, Kothari R, Malla AP *et al.* Bilirubin Links Heme Metabolism to Neuroprotection by Scavenging Superoxide. *Cell Chem Biol* 2019;**26**:1450-1460.e7.

332. Pflueger A, Croatt AJ, Peterson TE *et al.* The hyperbilirubinemic Gunn rat is resistant to the pressor effects of angiotensin II. *Am J Physiol Renal Physiol* 2005;**288**:F552-8.

333. Vera T, Stec DE. Moderate hyperbilirubinemia improves renal hemodynamics in ANG II-dependent hypertension. *Am J Physiol Regul Integr Comp Physiol* 2010;**299**:R1044-9.

334. Radi R. Oxygen radicals, nitric oxide, and peroxynitrite: Redox pathways in molecular medicine. *Proc Natl Acad Sci U S A* 2018;**115**:5839–48.

335. Mancuso C, Bonsignore A, Di Stasio E *et al.* Bilirubin and S-nitrosothiols interaction: Evidence for a possible role of bilirubin as a scavenger of nitric oxide. *Biochem Pharmacol* 2003;**66**:2355–63.

336. Kawamura K, Ishikawa K, Wada Y *et al.* Bilirubin from heme oxygenase-1 attenuates vascular endothelial activation and dysfunction. *Arterioscler Thromb Vasc Biol* 2005;**25**:155–60.

337. Nakayama M, Takahashi K, Komaru T *et al.* Increased Expression of Heme Oxygenase-1 and Bilirubin Accumulation in Foam Cells of Rabbit Atherosclerotic Lesions. *Arter Thromb Vasc Biol* 2001;**21**:1012–373.

338. Keshavan P, Deem TL, Schwemberger SJ *et al.* Unconjugated Bilirubin Inhibits VCAM-1-Mediated Transendothelial Leukocyte Migration. *J Immunol* 2005;**174**:3709–18.

339. Ollinger R, Bilban M, Erat A *et al.* A natural inhibitor of vascular smooth muscle cell proliferation. *Circulation* 2005;**112**:1030–9.

340. Tanos R, Patel RD, Murray IA *et al.* Aryl hydrocarbon receptor regulates the cholesterol biosynthetic pathway in a dioxin response element-independent manner. *Hepatology* 2012;**55**:1994–2004.

341. Phelan D, Winter GM, Rogers WJ *et al.* Activation of the Ah receptor signal transduction pathway by bilirubin and biliverdin. *Arch Biochem Biophys* 1998;**357**:155–63.

342. Grygiel-Górniak B. Peroxisome proliferator-activated receptors and their ligands: nutritional and clinical implications--a review. *Nutr J* 2014;**13**:17.

343. König B, Koch A, Spielmann J *et al.* Activation of PPARα lowers synthesis and concentration of cholesterol by reduction of nuclear SREBP-2. *Biochem Pharmacol* 2007;**73**:574–85.

344. Wegiel B, Otterbein LE. Go green: The anti-inflammatory effects of biliverdin reductase. *Front Pharmacol* 2012;**3 MAR**:1–8.

345. Baranano DE, Rao M, Ferris CD *et al.* Biliverdin reductase: a major physiologic cytoprotectant. *Proc Natl Acad Sci U S A* 2002;**99**:16093–8.

346. Bulmer AC, Coombes JS, Blanchfield JT *et al.* Bile pigment pharmacokinetics and absorption in the rat: Therapeutic potential for enteral administration. *Br J Pharmacol* 2011;**164**:1857–70.

347. Dekker D, Dorresteijn MJ, Welzen MEB *et al.* Parenteral bilirubin in healthy volunteers: a reintroduction in translational research. *Br J Clin Pharmacol* 2018;**84**:268–79.

348. Zhang D, Chando TJ, Everett DW *et al.* IN VITRO INHIBITION OF UDP GLUCURONOSYLTRANSFERASES BY ATAZANAVIR AND OTHER HIV PROTEASE INHIBITORS AND THE RELATIONSHIP OF THIS PROPERTY TO IN VIVO BILIRUBIN GLUCURONIDATION. *Drug Metab*

Dispos 2005;**33**:1729–39.

349. Zucker SD, Qin X, Rouster SD *et al.* Mechanism of indinavir-induced hyperbilirubinemia. *Proc Natl Acad Sci* 2001;**98**:12671–6.

350. Gazak R, Walterova D, Kren V. Silybin and Silymarin - New and Emerging Applications in Medicine. *Curr Med Chem* 2007;**14**:315–38.

351. Vargas-Mendoza N, Madrigal-Santillán E, Morales-González Á *et al.* Hepatoprotective effect of silymarin. *World J Hepatol* 2014;**6**:144–9.

352. Reddy KR, Belle SH, Fried MW *et al.* Rationale, challenges, and participants in a Phase II trial of a botanical product for chronic hepatitis C. *Clinical Trials*. 2012.

353. Zhu HJ, Brinda BJ, Chavin KD *et al.* An assessment of pharmacokinetics and antioxidant activity of free silymarin flavonolignans in healthy volunteers: A dose escalation study. *Drug Metab Dispos* 2013;**41**:1679–85.

354. Wlcek K, Koller F, Ferenci P *et al.* Hepatocellular organic anion-transporting polypeptides (OATPs) and multidrug resistance-Associated protein 2 (MRP2) are inhibited by silibinin. *Drug Metab Dispos* 2013;**41**:1522–8.

355. Sridar C, Goosen TC, Kent UM *et al.* Silybin inactivates cytochromes P450 3A4 and 2C9 and inhibits major hepatic glucuronosyltransferases. *Drug Metab Dispos* 2004;**32**:587–94.

356. D'Andrea V, Pérez LM, Sánchez Pozzi EJ. Inhibition of rat liver UDP-glucuronosyltransferase by silymarin and the metabolite silibinin-glucuronide. *Life Sci* 2005;**77**:683–92.

357. Mengs U, Torsten Pohl R-, Mitchell T. Legalon® SIL: The Antidote of Choice in Patients with Acute Hepatotoxicity from Amatoxin Poisoning. *Curr Pharm Biotechnol* 2012;**13**:1964–70.

358. Vogel G, Temme I. Curative antagonism of phalloidin induced liver damage with silymarin as a model of an antihepatotoxic therapy. *Arzneimittelforschung* 1969;**19**:613–5.

359. Schriewer H, Lohmann J, Rauen HM. The effect of silybin-dihemisuccinate on regulation disorders in phospholipid metabolism in acute galactosamine intoxication in the rat. *Arzneimittelforschung* 1975;**25**:1582–5.

360. Bijak M. Silybin, a Major Bioactive Component of Milk Thistle (Silybum marianum L. Gaernt.) — Chemistry, Bioavailability, and Metabolism. *Molecules* 2017;**22**:1–11.

361. Miranda SR, Jin KL, Brouwer KLR *et al.* Hepatic metabolism and biliary excretion of

silymarin flavonolignans in isolated perfused rat livers: Role of multidrug resistance-associated protein 2 (Abcc2). *Drug Metab Dispos* 2008;**36**:2219–26.

362. Togawa T, Mizuochi T, Sugiura T *et al.* Clinical, Pathologic, and Genetic Features of Neonatal Dubin-Johnson Syndrome: A Multicenter Study in Japan. *J Pediatr* 2018;**196**:161-167.e1.

363. Rutter K, Scherzer TM, Beinhardt S *et al.* Intravenous silibinin as "rescue treatment" for on-treatment non-responders to pegylated interferon/ribavirin combination therapy. *Antivir Ther* 2011;**16**:1327–33.

364. Rutter K, Scherzer TM, Beinhardt S *et al.* Intravenous silibinin as "rescue treatment" for on-treatment non-responders to pegylated interferon/ribavirin combination therapy. *Antivir Ther* 2011;**16**:1327–33.

365. Mariño Z, Crespo G, D'Amato M *et al.* Intravenous silibinin monotherapy shows significant antiviral activity in HCV-infected patients in the peri-transplantation period. *J Hepatol* 2013, DOI: 10.1016/j.jhep.2012.09.034.

366. Rendina M, D'Amato M, Castellaneta A *et al.* Antiviral activity and safety profile of silibinin in HCV patients with advanced fibrosis after liver transplantation: A randomized clinical trial. *Transpl Int* 2014;**27**:696–704.

367. Roos K, Lohmann V, Stremmel W *et al. First Case Description of a Quadruple Therapy with Silibinin, Telaprevir, Ribavirin and PegIFNα2a in a Liver Transplanted Patient with Chronic Hepatitis C Virus Infection*., 2013.

368. Najera I, McCown M, Leveque V *et al.* 951 SILIBININ INHIBITS HCV REPLICATION IN VITRO. *J Hepatol* 2009, DOI: 10.1016/s0168-8278(09)60953-3.

369. Horsfall LJ, Nazareth I, Pereira SP *et al.* Gilbert's syndrome and the risk of death: A population-based cohort study. *J Gastroenterol Hepatol* 2013;**28**:1643–7.

370. Bulmer AC, Blanchfield JT, Toth I *et al.* Improved resistance to serum oxidation in Gilbert's syndrome: A mechanism for cardiovascular protection. *Atherosclerosis* 2008;**199**:390–6.

371. Boon AC, Hawkins CL, Bisht K *et al.* Reduced circulating oxidized LDL is associated with hypocholesterolemia and enhanced thiol status in Gilbert syndrome. *Free Radic Biol Med* 2012;**52**:2120–7.

372. Yoon M. The role of PPARα in lipid metabolism and obesity: Focusing on the effects of estrogen on PPARα actions. *Pharmacol Res* 2009;**60**:151–9.

373. Strassburg CP. Hyperbilirubinemia syndromes (Gilbert-Meulengracht, Crigler-Najjar, Dubin-Johnson, and Rotor syndrome). *Best Pract Res Clin Gastroenterol* 2010;**24**:555–71.

374. Iyanagilg T, Watanabey T, Uchiyamay Y. The 3-Methylcholanthrene-inducible UDP-glucuronosyltransferase Deficiency in the Hyperbilirubinemic Rat (Gunn Rat) Is Caused by a -1 Frameshift Mutation *. *J Biol Chem* 1989;**264**:21302–7.

375. Ronda OAHO, van Dijk TH, Verkade HJ *et al.* Measurement of Intestinal and Peripheral Cholesterol Fluxes by a Dual-Tracer Balance Method. *Curr Protoc Mouse Biol* 2016;**6**:408–34.

376. Glass DC, Gray CN. Estimating mean exposures from censored data: exposure to benzene in the Australian petroleum industry. *Ann Occup Hyg* 2001;**45**:275–82.

377. Heuman DM, Hylemon PB, Vlahcevic ZR. Regulation of bile acid synthesis. III. Correlation between biliary bile salt hydrophobicity index and the activities of enzymes regulating cholesterol and bile acid synthesis in the rat. *J Lipid Res* 1989;**30**:1161–71.

378. Hsun-Wei Huang T, Peng G, Qian Li G *et al.* Salacia oblonga root improves postprandial hyperlipidemia and hepatic steatosis in Zucker diabetic fatty rats: Activation of PPAR-α. *Toxicol Appl Pharmacol* 2006;**210**:225–35.

379. Ashton KJ, Tupicoff A, Williams-Pritchard G *et al.* Unique Transcriptional Profile of Sustained Ligand-Activated Preconditioning in Pre- and Post-Ischemic Myocardium. Kukreja R (ed.). *PLoS One* 2013;**8**:e72278.

380. Camus MC, Chapman MJ, Forgez P *et al.* Distribution and characterization of the serum lipoproteins and apoproteins in the mouse, Mus musculus. *J Lipid Res* 1983;**24**:1210–28.

381. Eberlé D, Hegarty B, Bossard P *et al.* SREBP transcription factors: Master regulators of lipid homeostasis. *Biochimie* 2004;**86**:839–48.

382. Horton JD, Shah NA, Warrington JA *et al.* Combined analysis of oligonucleotide microarray data from transgenic and knockout mice identifies direct SREBP target genes. *Proc Natl Acad Sci U S A* 2003;**100**:12027–32.

383. Ayotte P, Plaa GL. Biliary excretion in Sprague-Dawley and Gunn rats during manganese-bilirubin-induced cholestasis. *Hepatology* 1988;**8**:1069–78.

384. Kajihara T, Tazuma S, Yamashita G *et al.* Effects of bilirubin ditaurate on biliary secretion of proteins arid lipids: Influence on the hepatic vesicle transport system. *J Gastroenterol Hepatol* 1999;**14**:578–82.

385. Verkade HJ, Havinga R, Gerding A *et al.* Mechanism of bile acid-induced biliary lipid

secretion in the rat: Effect of conjugated bilirubin. *Am J Physiol - Gastrointest Liver Physiol* 1993;**264**, DOI: 10.1152/ajpgi.1993.264.3.g462.

386. Kajihara T, Tazuma S, Yamashita G *et al.* Bilirubin overload modulates bile canalicular membrane fluidity in rats: Association with disproportionate reduction of biliary lipid secretion. *J Gastroenterol* 2000;**35**:450–5.

387. Palmisano BT, Zhu L, Stafford JM. Role of estrogens in the regulation of liver lipid metabolism. *Adv Exp Med Biol* 2017;**1043**:227–56.

388. Zhu L, Brown WC, Cai Q *et al.* Estrogen treatment after ovariectomy protects against fatty liver and may improve pathway-selective insulin resistance. *Diabetes* 2013;**62**:424–34.

389. Koopen NR, Post SM, Wolters H *et al.* Differential effects of 17α-ethinylestradiol on the neutral and acidic pathways of bile salt synthesis in the rat. *J Lipid Res* 1999;**40**:100–8.

390. Yamamoto Y, Moore R, Hess HA *et al.* Estrogen receptor α mediates 17α-ethynylestradiol causing hepatotoxicity. *J Biol Chem* 2006;**281**:16625–31.

391. Yoon M, Jeong S, Nicol JC *et al.* Fenofibrate regulates obesity and lipid metabolism with sexual dimorphism. *Exp Mol Med* 2002;**34**:481–8.

392. Jeong S, Yoon M. Inhibition of the actions of peroxisome proliferator-activated receptor a on obesity by estrogen. *Obesity* 2007;**15**:1430–40.

393. Kapitulnik J, Gonzalez JF. Marked endogenous activation of the CYP1A1 and CYP1A2 genes in the congenitally jaundiced Gunn rat. *Mol Pharmacol* 1993;**43**:722–5.

394. Rolf B, Stern L. Introduction: bilirubin encephalopathy - the preventive role of bilirubin binding to albumin. *Crit Rev Clin Lab Sci* 1980;**11**:307–99.

395. Mustafa MG, King TE. Binding of Bilirubin with Lipid. *J Biol Chem* 1970;**245**:1084–9.

396. Rodrigues CM, Solá S, Silva R *et al.* Bilirubin and amyloid-beta peptide induce cytochrome c release through mitochondrial membrane permeabilization. *Mol Med* 2000;**6**:936–46.

397. Jiang X, Wang X. Cytochrome C -Mediated Apoptosis . *Annu Rev Biochem* 2004;**73**:87–106.

398. Zucker SD, Storch J, Zeidel ML *et al.* Mechanism of the spontaneous transfer of unconjugated bilirubin between small unilamellar phosphatidylcholine vesicles. *Biochemistry* 1992;**31**:3184–92.

399. Pennell EN, Shiels R, Vidimce J *et al.* The impact of bilirubin ditaurate on platelet quality

during storage. *Platelets* 2019:1–13.

400. Fontana-Ayoub M, Fasching M, Gnaiger E. Selected media and chemicals for respirometry with mitochondrial preparations. *Mitochondr Physiol Netw* 2016;**03.02**:1–10.

401. Larsen S, Kraunsøe R, Gram M *et al.* The best approach: Homogenization or manual permeabilization of human skeletal muscle fibers for respirometry? *Anal Biochem* 2014;**446**:64–8.

402. Eigentler A, Draxl A, Wiethüchter A. Laboratory protocol: citrate synthase a mitochondrial marker enzyme. *Mitochondrial Physiol Netw* 2015;**04**:1–11.

403. Okumura N, Hashida-Okumura A, Kita K *et al.* Proteomic analysis of slow- and fast-twitch skeletal muscles. *Proteomics* 2005;**5**:2896–906.

404. Fu YY, Kang KJ, Ahn JM *et al.* Hyperbilirubinemia Reduces the Streptozotocin-Induced Pancreatic Damage through Attenuating the Oxidative Stress in the Gunn Rat. *Tohoku J Exp Med* 2010;**222**:265–73.

405. Zeng Q, Dong SY, Sun XN *et al.* Percent body fat is a better predictor of cardiovascular risk factors than body mass index. *Brazilian J Med Biol Res* 2012;**45**:591–600.

406. Dulloo AG, Jacquet J, Solinas G *et al.* Body composition phenotypes in pathways to obesity and the metabolic syndrome. *Int J Obes* 2010;**34**:S4–17.

407. Holliday MA, Potter D, Jarrah A *et al.* The relation of metabolic rate to body weight and organ size. *Pediatr Res* 1967;**1**:185–95.

408. Even PC, Rolland V, Roseau S *et al.* Prediction of basal metabolism from organ size in the rat: Relationship to strain, feeding, age, and obesity. *Am J Physiol - Regul Integr Comp Physiol* 2001;**280**:1887–96.

409. Kummitha CM, Kalhan SC, Saidel GM *et al.* Relating tissue/organ energy expenditure to metabolic fluxes in mouse and human: Experimental data integrated with mathematical modeling. *Physiol Rep* 2014;**2**:1–20.

410. Bailey SA, Zidell RH, Perry RW. Relationships Between Organ Weight and Body/Brain Weight in the Rat: What Is the Best Analytical Endpoint? *Toxicol Pathol* 2004;**32**:448–66.

411. Stanford JA, Shuler JM, Fowler SC *et al.* Hyperactivity in the Gunn rat model of neonatal jaundice: Age-related attenuation and emergence of gait deficits. *Pediatr Res* 2015;**77**:434–9.

412. Noir BA, Boveris A, Pereira AMG *et al.* Bilirubin: a multi-site inhibitor of mitochondrial

respiration. *FEBS Lett* 1972;**27**.

413. Naveenkumar SK, Thushara RM, Sundaram MS *et al.* Unconjugated Bilirubin exerts Pro-Apoptotic Effect on Platelets via p38-MAPK activation. *Sci Rep* 2015;**5**:1–16.

414. Rossi F, Francese M, Iodice RM *et al.* Inherited disorders of bilirubin metabolism. *Minerva Pediatr* 2005;**57**:53–63.

415. Greggio C, Jha P, Kulkarni SS *et al.* Enhanced Respiratory Chain Supercomplex Formation in Response to Exercise in Human Skeletal Muscle. *Cell Metab* 2017;**25**:301–11.

416. Galmés-Pascual BM, Nadal-Casellas A, Bauza-Thorbrügge M *et al.* 17β-estradiol improves hepatic mitochondrial biogenesis and function through PGC1B. *J Endocrinol* 2017;**232**:297–308.

417. Anthony KP, Saleh MA. Free radical scavenging and antioxidant activities of silymarin components. *Antioxidants* 2013;**2**:398–407.

418. Farghali H, Kameniková L, Hynie S *et al.* Silymarin effects on intracellular calcium and cytotoxicity: A study in perfused rat hepatocytes after oxidative stress injury. *Pharmacol Res* 2000;**41**:231–7.

419. Valenzuela A, Guerra R. Protective effect of the flavonoid silybin dihemisuccinate on the toxicity of phenylhydrazine on rat liver. *FEBS Lett* 1985;**181**:291–4.

420. Valenzuela A, Garrido A. Biochemical bases of the pharmacological action of the flavonoid silymarin and of its structural isomer silibinin. *Biol Res* 1994;**27**:105–12.

421. Zamek-Gliszczynski MJ, Hoffmaster KA, Nezasa KI *et al.* Integration of hepatic drug transporters and phase II metabolizing enzymes: Mechanisms of hepatic excretion of sulfate, glucuronide, and glutathione metabolites. *Eur J Pharm Sci* 2006;**27**:447–86.

422. Čvorović J, Passamonti S. Membrane Transporters for Bilirubin and Its Conjugates: A Systematic Review. *Front Pharmacol* 2017;**8**:887.

423. Fujiwara R, Mathias H, Elke S *et al.* Systemic regulation of bilirubin homeostasis: Potential benefits of hyperbilirubinemia. *Hepatology* 2017;**67**:1609–19.

424. Zuber R, Modrianský M, Dvořák Z *et al.* Effect of silybin and its congeners on human liver microsomal cytochrome P450 activities. *Phyther Res* 2002;**16**:632–8.

425. Bulmer AC, Bakrania B, Du Toit EF *et al.* Bilirubin acts as a multipotent guardian of cardiovascular integrity: More than just a radical idea. *Am J Physiol - Hear Circ Physiol*

2018;**315**:H429–47.

426. Wallner M, Bulmer AC, Mölzer C *et al.* Haem catabolism: A novel modulator of inflammation in Gilbert's syndrome. *Eur J Clin Invest* 2013;**43**:912–9.

427. Kaur H, Hughes MN, Green CJ *et al.* Interaction of bilirubin and biliverdin with reactive nitrogen species. *FEBS Lett* 2003;**543**:113–9.

428. Tapan S, Karadurmus N, Dogru T *et al.* Decreased small dense LDL levels in Gilbert's syndrome. *Clin Biochem* 2011;**44**:300–3.

429. Skottova N, Krecman V, Vana P *et al.* Effect of Silymarin and Silibinin-Phosphatidylcholine Complex on Plasma and Lipoprotein Cholesterol, and Oxidation of Ldl in Rats Fed on High Cholesterol Diet Supplemented With Currant Oil. *Biomed Pap* 2000;**144**:55–8.

430. Krečman V, Škottová N, Walterová D *et al.* Silymarin inhibits the development of diet-induced hypercholesterolemia in rats. *Planta Med* 1998;**64**:138–42.

431. Surai PF. Silymarin as a natural antioxidant: An overview of the current evidence and perspectives. *Antioxidants* 2015;**4**:204–47.

432. Trappoliere M, Caligiuri A, Schmid M *et al.* Silybin, a component of sylimarin, exerts anti-inflammatory and anti-fibrogenic effects on human hepatic stellate cells. *J Hepatol* 2009;**50**:1102–11.

433. Wu CH, Huang SM, Yen GC. Silymarin: A novel antioxidant with antiglycation and antiinflammatory properties in vitro and in vivo. *Antioxidants Redox Signal* 2011;**14**:353–66.

434. Mohammadi H, Hadi A, Arab A *et al.* Effects of silymarin supplementation on blood lipids: A systematic review and meta-analysis of clinical trials. *Phyther Res* 2019;**33**:871–80.

435. Ebrahimpour Koujan S, Gargari BP, Mobasseri M *et al.* Effects of Silybum marianum (L.) Gaertn. (silymarin) extract supplementation on antioxidant status and hs-CRP in patients with type 2 diabetes mellitus: A randomized, triple-blind, placebo-controlled clinical trial. *Phytomedicine* 2015;**22**:290–6.

436. Yamaguchi K, Okuda K, Yonemitsu H *et al.* Cyclic Premenstrual Unconjugated Hyperbilirubinemia. Report of two cases. *Ann Intern Med* 1975;**83**:514–7.

437. Taylor ML, Misso NLA, Stewart GA *et al.* Differential expression of platelet activation markers in aspirin-sensitive asthmatics and normal subjects. *Clin Exp Allergy* 1996;**26**:202–15.

438. Benzie IFF, Strain JJ. The Ferric Reducing Ability of Plasma (FRAP) as a Measure of

"Antioxidant Power": The FRAP assay. *Anal Biochem* 1996;**239**:70–6.

439. Novotný L, Vítek L. Inverse Relationship Between Serum Bilirubin and Atherosclerosis in Men: A Meta-Analysis of Published Studies. *Exp Biol Med* 2003;**228**:568–71.

440. Šuk J, Jašprová J, Biedermann D *et al.* Isolated Silymarin Flavonoids Increase Systemic and Hepatic Bilirubin Concentrations and Lower Lipoperoxidation in Mice. *Oxid Med Cell Longev* 2019;**2019**:1–12.

441. Parés A, Planas R, Torres M *et al.* Effects of silymarin in alcoholic patients with cirrhosis of the liver: Results of a controlled, double-blind, randomized and multicenter trial. *J Hepatol* 1998;**28**:615–21.

442. Ferenci P, Dragosics B, Dittrich H *et al.* Randomized controlled trial of silymarin treatment in patients with cirrhosis of the liver. *J Hepatol* 1989;**9**:105–13.

443. Newsome PN, Cramb R, Davison SM *et al.* Guidelines on the management of abnormal liver blood tests. *Gut* 2018;**67**:6–19.

444. Poruba M, Kazdová L, Oliyarnyk O *et al.* Improvement bioavailability of silymarin ameliorates severe dyslipidemia associated with metabolic syndrome. *Xenobiotica* 2015;**45**:751–6.

445. Méndez-Sánchez N, Dibildox-Martinez M, Sosa-Noguera J *et al.* Superior silybin bioavailability of silybin-phosphatidylcholine complex in oily-medium soft-gel capsules versus conventional silymarin tablets in healthy volunteers. *BMC Pharmacol Toxicol* 2019;**20**:5.

446. Kim YC, Kim EJ, Lee ED *et al.* Comparative bioavailability of silibinin in healthy male volunteers. *Int J Clin Pharmacol Ther* 2003;**41**:593–6.

447. Awasthi R, Kulkarni GT, Pawar VK. Phytosomes: An approach to increase the bioavailability of plant extracts. *Int J Pharm Pharm Sci* 2011;**3**:1–3.

448. Nassuato G, Iemmolo RM, Strazzabosco M *et al.* Effect of Silibinin on biliary lipid composition experimental and clinical study. *J Hepatol* 1991;**12**:290–5.

449. Rui YC. Advances in pharmacological studies of silymarin. *Mem Inst Oswaldo Cruz* 1991;**86**:79–85.

450. Sobolová L, Škottová N, Večeřa R *et al.* Effect of silymarin and its polyphenolic fraction on cholesterol absorption in rats. *Pharmacol Res* 2006;**53**:104–12.

451. Ebrahimpour-koujan S, Gargari BP, Mobasseri M *et al.* Lower glycemic indices and lipid

profile among type 2 diabetes mellitus patients who received novel dose of Silybum marianum (L.) Gaertn. (silymarin) extract supplement: A Triple-blinded randomized controlled clinical trial. *Phytomedicine* 2018;**44**:39–44.

452. Ebrahimpour Koujan S, Gargari BP, Mobasseri M *et al.* Effects of Silybum marianum (L.) Gaertn. (silymarin) extract supplementation on antioxidant status and hs-CRP in patients with type 2 diabetes mellitus: A randomized, triple-blind, placebo-controlled clinical trial. *Phytomedicine* 2015;**22**:290–6.

453. Keane KN, Cruzat VF, Carlessi R *et al.* Molecular Events Linking Oxidative Stress and Inflammation to Insulin Resistance and β -Cell Dysfunction. *Oxid Med Cell Longev* 2015;**2015**:1–15.

454. Farjad E, Sc M, Momeni HR *et al.* Silymarin Ameliorates Oxidative Stress and Enhances Antioxidant Defense System Capacity in Cadmium-Treated Mice. *Cell J* 2018;**20**:422–6.

455. Kidd P, Head K. A review of the bioavailability and clinical efficacy of milk thistle phytosome: A silybin-phosphatidylcholine complex (Siliphos??). *Altern Med Rev* 2005;**10**:193–203.

456. Kim YC, Kim EJ, Lee ED *et al.* Comparative bioavailability of silibinin in healthy male volunteers. *Int J Clin Pharmacol Ther* 2003;**41**:593–6.

457. Rodrigues CMP, Solá S, Brites D. Bilirubin induces apoptosis via the mitochondrial pathway in developing rat brain neurons. *Hepatology* 2002;**35**:1186–95.

458. Yoon M. The role of PPARα in lipid metabolism and obesity: Focusing on the effects of estrogen on PPARα actions. *Pharmacol Res* 2009;**60**:151–9.

459. Wiegratz I, Kutschera E, Lee JH *et al.* Effect of four different oral contraceptives on various sex hormones and serum-binding globulins. *Contraception* 2003;**67**:25–32.

460. Velussi M, Maria A, Monte A De *et al.* Long-term (12 months) treatment with an anti-oxidant drug (silymarin) is effective on hyperinsulinemia, exogenous insulin need and malondialdehyde levels in cirrhotic diabetic patients. 2001:1–9.

461. Salmi HA, Sarna S. Effect of silymarin on chemical, functional, and morphological alterations of the liver: A double-blind controlled study. *Scand J Gastroenterol* 1982;**17**:517–21.

462. Schrieber SJ, Wen Z, Vourvahis M *et al.* The Pharmacokinetics of Silymarin Is Altered in Patients with Hepatitis C Virus and Nonalcoholic Fatty Liver Disease and Correlates with Plasma

Caspase-3/7 Activity. *Drug Metab Dispos* 2008;**36**:1909–16.

463. Yoon M. PPAR in obesity: Sex difference and estrogen involvement. *PPAR Res* 2010;**2010**, DOI: 10.1155/2010/584296.

464. Sakai J, Duncan EA, Rawson RB *et al.* Sterol-regulated release of SREBP-2 from cell membranes requires two sequential cleavages, one within a transmembrane segment. *Cell* 1996;**85**:1037–46.

465. Bjune K, Sundvold H, Leren TP *et al.* MK-2206, an allosteric inhibitor of AKT, stimulates LDLR expression and LDL uptake: A potential hypocholesterolemic agent. *Atherosclerosis* 2018;**276**:28–38.

466. López-Soldado I, Avella M, Botham KM. Suppression of VLDL secretion by cultured hepatocytes incubated with chylomicron remnants enriched in n−3 polyunsaturated fatty acids is regulated by hepatic nuclear factor-4α. *Biochim Biophys Acta - Mol Cell Biol Lipids* 2009;**1791**:1181–9.